SCUOLA DI DOTTORATO
UNIVERSITÀ DEGLI STUDI DI MILANO-BICOCCA

Dipartimento di / Department of
Materials Science

Dottorato di Ricerca in / PhD program **Materials Science and Nanotechnology**
Ciclo / Cycle **XXXVIII**

Curriculum in (se presente / if it is)

TITOLO TESI / THESIS TITLE

Myopia and Myopia Progression: Validation of Measurement Methods and Longitudinal/Cross-Sectional Assessment of Refraction, Axial length, and Near-Work Effects

Cognome / Surname **Obaid** Nome / Name **Aziza MS**

Matricola / Registration number **906934**

Tutore / Tutor: **Prof.ssa Anna Galli**

Supervisor: **Prof.ssa Silvia Tavazzi**

Coordinatore / Coordinator: **Prof. Francesco Montalenti**

ANNO ACCADEMICO / ACADEMIC YEAR 2024/2025

Abstract:

Introduction & Aim

Myopia is increasing worldwide and it can lead to sight-threatening complications, creating a need for accurate and clinically realistic measurement tools to monitor progression and related ocular changes. This thesis aimed to compare objective optical refraction techniques based on near-infrared retinal reflection with standard subjective refraction, to evaluate the effect of increasing pupil size on objective refraction outputs and higher-order aberration–related metrics and to apply these techniques to the assessment of myopia-related risk factors. These included longitudinal changes in refractive error and axial length, axial-length percentile tracking, near-work effects, and cross-sectional peripheral refraction patterns.

Methods

This work combined method-validation, experimental, and longitudinal/cross-sectional analyses. Objective refraction obtained with open-field and closed-field aberrometer and open-field autorefractors was compared with subjective refraction. Additional analyses evaluated the effect of computational pupil enlargement from 3 to 6 mm on refraction and spherical aberration. These validated methods were then applied to longitudinal axial-length monitoring, near-work experiments, choroidal thickness assessment, and peripheral refraction analysis in children and adults.

Results

At a 3-mm pupil size, objective refraction methods showed some between-method differences but strong correlations with subjective refraction, particularly for open-field aberrometry (OFA) and open-field autorefractors (OFAUTO) in young subjects (Spearman's rho: subjective–OFA 0.96; subjective–OFAUTO 0.95; all $p<0.001$), with no evidence of proportional bias in Bland–Altman analyses. Monocular and binocular measurements were generally comparable for spherical equivalent (M), and any statistically detected differences were clinically negligible.

When pupil size increased (3–6 mm), within-method comparisons showed no significant change in spherical equivalent refraction across pupil sizes, indicating that pupil enlargement did not substantially alter refraction results within the same device. For spherical aberration (described by

the coefficient C4,0 of the Zernike expansion of the wavefront error function), paired comparisons also remained non-significant after Bonferroni correction ($p<0.0167$), suggesting stability of C4,0 across pupil sizes for both OFA and closed field aberrometer (CFA).

In the longitudinal component, axial-length percentile tracking identified meaningful variability in growth trajectories: over 0→18 months, a high-risk shift (≥10 percentiles) was observed in 15.8% of female children and 20.8% of male children in one eye, and in 10.5% and 25%, respectively, in the fellow eye, while older groups remained mostly stable. Acute near work (10 minutes at 33 cm) did not produce significant changes in central spherical equivalent, and overall near-task effects were subtle. Choroidal responses were location-dependent and not always detectable after short exposure, while peripheral refraction showed a consistent pattern of relative peripheral myopia compared with the central reference in both children and adults, varying by meridian and eccentricity.

Conclusion

The findings show that interpretation of myopia-related measures depends strongly on measurement method and testing conditions. Open-field objective refraction was reliable under non-cycloplegic conditions and appeared less affected by accommodation-related bias than closed-field measurements. Computational pupil enlargement from 3 to 6 mm did not materially alter spherical equivalent or spherical aberration under the tested conditions. Longitudinal results support axial length, especially when interpreted using age-referenced percentiles, as a sensitive tool for monitoring pediatric growth trajectories. The location-dependent behavior of choroidal thickness and peripheral refraction further indicates that retinal eccentricity and protocol design are important for interpreting peripheral and biometric parameters. Overall, these findings support standardized, clinically realistic measurement protocols for myopia research and monitoring, and provide a basis for future studies on physiological pupil dilation, longer near-work exposure, and pediatric progression risk.

Keywords

Myopia, ocular axial length, optical objective eye refraction, near work, choroidal thickness, peripheral eye refraction, open field ocular aberrometry, pupil size.

Sommario

Introduzione e obiettivi

La miopia è in aumento a livello mondiale e può portare a complicanze potenzialmente in grado di compromettere la vista, rendendo necessari strumenti di misura accurati e clinicamente realistici per monitorarne la progressione e i cambiamenti oculari correlati. Questa tesi si è proposta di confrontare tecniche di refrazione oggettiva basate sulla riflessione retinica nel vicino infrarosso con la refrazione soggettiva standard, di valutare l'effetto dell'aumento del diametro pupillare sui parametri della refrazione oggettiva e sulle metriche correlate alle aberrazioni di ordine superiore, e di applicare tali tecniche alla valutazione dei fattori di rischio associati alla miopia. Tra questi rientrano le variazioni longitudinali dell'errore refrattivo e della lunghezza assiale, il monitoraggio della lunghezza assiale basato sui percentili, gli effetti del lavoro da vicino e i pattern della refrazione periferica in analisi trasversali.

Metodi

Il presente lavoro ha combinato analisi di validazione metodologica, studi sperimentali e analisi longitudinali e trasversali. La refrazione oggettiva ottenuta mediante aberrometri open-field e closed-field e autorefrattometri open-field è stata confrontata con la refrazione soggettiva. Ulteriori analisi hanno valutato l'effetto dell'ampliamento computazionale del diametro pupillare da 3 a 6 mm sulla refrazione e sull'aberrazione sferica. Questi metodi validati sono stati successivamente applicati al monitoraggio longitudinale della lunghezza assiale, a esperimenti sul lavoro da vicino, alla valutazione dello spessore coroideale e all'analisi della refrazione periferica in bambini e adulti.

Risultati

Con un diametro pupillare di 3 mm, i metodi di refrazione oggettiva hanno mostrato alcune differenze tra metodi, ma forti correlazioni con la refrazione soggettiva, in particolare per l'aberrometria open-field (OFA) e per gli autorefrattometri open-field (OFAUTO) nei soggetti giovani (rho di Spearman: soggettiva–OFA 0,96; soggettiva–OFAUTO 0,95; tutti $p<0,001$), senza evidenza di bias proporzionale nelle analisi di Bland–Altman. Le misurazioni monoculari e

binoculari sono risultate generalmente comparabili per l'equivalente sferico (M), e le eventuali differenze statisticamente significative sono state ritenute clinicamente trascurabili.

Quando il diametro pupillare è aumentato da 3 a 6 mm, i confronti intra-metodo non hanno mostrato variazioni significative della refrazione equivalente sferica tra i diversi diametri pupillari, indicando che tale ampliamento non ha modificato in modo sostanziale i risultati refrattivi all'interno dello stesso strumento. Per l'aberrazione sferica, descritta dal coefficiente C4,0 dell'espansione di Zernike della funzione di errore del fronte d'onda, anche i confronti appaiati sono rimasti non significativi dopo correzione di Bonferroni ($p<0,0167$), suggerendo una stabilità di C4,0 rispetto al diametro pupillare sia per OFA sia per l'aberrometro closed-field (CFA).

Nella componente longitudinale, il monitoraggio della lunghezza assiale basato sui percentili ha identificato una variabilità significativa nelle traiettorie di crescita: tra baseline e 18 mesi, uno spostamento classificato come ad alto rischio (≥10 percentili) è stato osservato nel 15,8% delle bambine e nel 20,8% dei bambini in un occhio, e rispettivamente nel 10,5% e nel 25% nell'occhio controlaterale, mentre i gruppi di età maggiore sono rimasti per lo più stabili. Il lavoro da vicino acuto (10 minuti a 33 cm) non ha prodotto variazioni significative dell'equivalente sferico centrale e, nel complesso, gli effetti del compito da vicino sono risultati modesti. Le risposte coroideali si sono dimostrate dipendenti dalla sede di misurazione e non sempre rilevabili dopo una breve esposizione, mentre la refrazione periferica ha mostrato un pattern coerente di miopia periferica relativa rispetto al riferimento centrale sia nei bambini sia negli adulti, con entità variabile a seconda del meridiano e dell'eccentricità.

Conclusioni

I risultati mostrano che l'interpretazione delle misure correlate alla miopia dipende in modo rilevante dal metodo di misura e dalle condizioni di esame. La refrazione oggettiva open-field si è dimostrata affidabile in condizioni non cicloplegiche ed è risultata meno influenzata dal bias legato all'accomodazione rispetto alle misurazioni closed-field. L'ampliamento computazionale del diametro pupillare da 3 a 6 mm non ha modificato in modo sostanziale né l'equivalente sferico né l'aberrazione sferica nelle condizioni analizzate. I risultati longitudinali supportano l'utilità della lunghezza assiale, soprattutto se interpretata mediante percentili specifici per età, come strumento sensibile per il monitoraggio delle traiettorie di crescita in età pediatrica. L'andamento dipendente

dalla sede di misurazione dello spessore coroideale e della refrazione periferica indica inoltre che l'eccentricità retinica e il protocollo di misura sono elementi fondamentali per interpretare correttamente i parametri periferici e biometrici. Nel complesso, questi risultati supportano l'uso di protocolli di misura standardizzati e clinicamente realistici nella ricerca e nel monitoraggio della miopia, e forniscono una base per futuri studi sulla dilatazione pupillare fisiologica, su esposizioni più prolungate al lavoro da vicino e sul rischio di progressione miopica in età pediatrica.

Parole chiave

Miopia, lunghezza assiale, refrazione oggettiva, lavoro da vicino, spessore coroideale, refrazione periferica, aberrometria open-field, diametro pupillare.

To my family, who have been my Rock wherever I am...

To the unexpected hardships that reshaped me in the hardest of ways...

To the coincidences that turned strangers into a home away from home...

To the Mercy of GOD that carried me through it all.

Table of Contents

List of Figures

List of Tables

Chapter 1. Background and literature review

1.1 The Growing Problem of Myopia

Studies estimate that myopia and high myopia prevalence will show a significant increase worldwide, affecting 5 billion people (50% of the world population) and one billion people (10 % of the world population), respectively, by 2050 [1]. This increase in prevalence rates is shown more in Asia, but also in Europe and North America [2]. The younger the age of myopia onset, the higher the risk factor for myopia progression and therefore the higher the risk for myopia-related complications to arise, children (6-7 years old) who have at least -1.25 myopia are at higher risk for faster progression when compared to older children [2], [3].

There are many myopia-related complications including macular degeneration, cataract, retinal detachment, and glaucoma which are particularly important because they can lead to vision impairment, and the risk of these conditions generally increases as myopia becomes more severe. [4]. However, although the individual risk of complications is higher in high myopia, low-to-moderate myopia is far more common, therefore, the overall population burden (the absolute number of cases) of myopia-related complications can still be substantial even among people with lower levels of myopia[5]. The number of people with vision loss resulting from high myopia would increase 7 times from 2000 to 2050, and myopia would become a leading cause of permanent blindness worldwide [1]. These complications can significantly reduce the quality of life by impairing day to day functioning, participation in school or work, and increasing dependence on optical correction [1], [6]. At a population level, these individual impacts translate into an economic burden through the direct costs of vision correction and follow-up care, as well as indirect costs such as productivity loss [6], [7].

This rapid increase in myopia prevalence led to an increase in research to try to determine the causes, mechanisms and predisposing factors that can lead to myopia onset and progression and greatly set the need for comprehensive eye care services including refractive services, monitoring myopia onset and progression and preventing myopia-related ocular complications and vision loss among people with high myopia.

1.2 Visual Mechanisms in Myopia Development

1.2.1 Accommodation lag, near vision and hyperopic defocus

Accommodation is the process of the eye changing its optical power to maintain the image focused on the retina when viewing near objects [8], [9]. Under normal viewing conditions, the accommodative response closely matches the stimulus demand. The accommodative demand is inversely related to object distance, however, an important factor to be taken into consideration is the accuracy in the response, in many individuals the response can be insufficient, leading to what is called accommodative lag [10], [11]. This lag results in the image being focused behind the retina (hyperopic retinal defocus) Figure 1. 1. Refractive errors have long been associated with the eye's ability to respond accurately during accommodation, and the response frequently lags behind the demand when the visual task requires a greater accommodative effort. This causes a hyperopic blur on the retina, which is thought to cause myopia by sending signals that encourage the eye to get longer [3], [12].

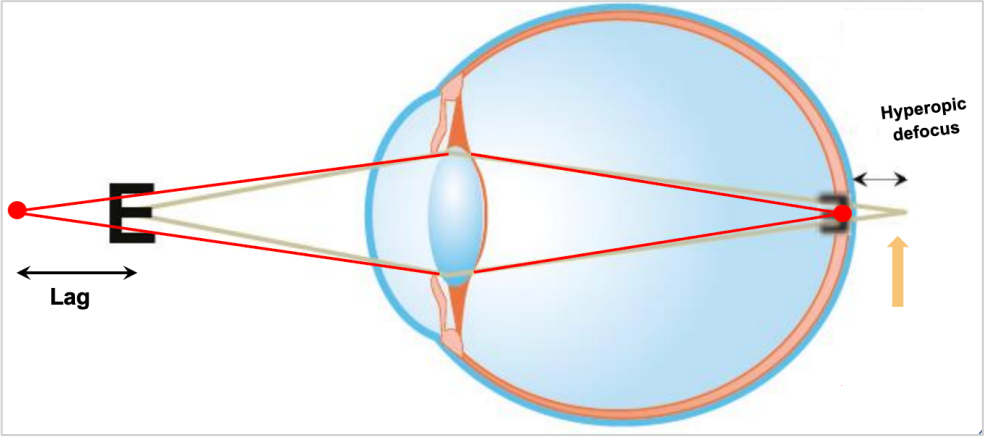

Figure 1. 1 Schematic illustration of accommodative lag during near viewing. When the accommodative response is insufficient relative to the stimulus demand, the image is focused behind the retina, resulting in hyperopic retinal defocus[13].

Evidence from animal and primate models supported the accommodation lag hypothesis and its biological possibility, it explained that optical defocus can directly affect eye growth. The exposure

to hyperopic defocus (when the image falls behind the retinal photoreceptors) induces axial elongation, while myopic defocus (when the image falls in front of the retinal photoreceptors) suppresses it [14], [15], [16]. According to this, the retina may be able to recognize the defocus sign and start biochemical reactions that involve neurotransmitters that affect ocular growth and scleral remodeling, including dopamine and retinoic acid [17], [18]. In the case of consistent hyperopic defocus brought by an accommodative lag during near work it may serve as a myopiagenic signal, encouraging the eye to gradually elongate.

There are conflicting results regarding the relationship between accommodative lag and myopia progression. It has been reported that there is a relationship between high accommodative demand, due to prolonged near work, and myopia development [19], [20], [21], [22], [23], [24], the presence of accommodative lag extended over time can represent a potential myopiagenic factor. Epidemiological studies have shown a correlation between time spent in near work and the outcome and progression of myopia[20], [24], [25], [26]. The main findings of a 2023 systematic review and meta-analysis of 78 studies confirmed that near work exposure, including occupational exposure in adults, could be associated with myopia. The likelihood of developing myopia increases by approximately 31% in children and 21% in adults among those engaged in prolonged near work [27].

Moreover, The International Myopia Institute review notes that “larger lags associated with high accommodative demand produce hyperopic defocus at the fovea, providing a stimulus for the eye to grow longer and become myopic”. It has been reported that sustained high accommodative demand, such as that experienced during prolonged near work, may contribute to myopia development.[10]

However, this accommodative lag hypothesis has been opposed by longitudinal human data and several studies failed to find a link between accommodative lag and myopia progression. The Collaborative Longitudinal Evaluation of Ethnicity and Refractive Error (CLEERE) study found that accommodative lag was increased after myopia onset and not before, this may suggest that accommodative lag may be a result and not a cause for myopia progression [28]. A following CLEERE analysis of more than 500 children also found no association between lag magnitude and

the annual rate of refractive change in subjects who already had myopia [29]. Similarly, a randomized Correction of Myopia Evaluation Trial (COMET) and its follow-ups confirmed that reducing lag with progressive addition lenses (PALs) produced only a small (clinically insignificant) slowing of myopia, in children with both high accommodative lag and near esophoria [30], [31], [32].

Moreover, other longitudinal studies supported these null findings, Rosenfield, Desai & Portello (2002) [33] found that newly developing myopes did not show a reduction in accommodative response, and that stable myopes showed the largest lags. Koomson et al. (2016) [11] reported no relationship between lag and myopia progression in Ghanaian schoolchildren, and that axial elongation occurred independently of lag magnitude.

The contradictions between studies investigating accommodative lag and myopia progression can possibly be explained by differences in the measurement techniques that were used. Older [14], [15], [16] research often used subjective retinoscopy methods, such as the Monocular Estimation Method (MEM) or Nott retinoscopy, which rely on the examiner's judgment and can vary with illumination, different targets, and examiner experience [34], [35]. More recent studies [11], [28], [30], [32] have used objective techniques, including open field autorefractors and aberrometers, which provide greater repeatability and allow for natural binocular viewing. However, even among objective instruments, differences in accommodative stimulus demand [36], target type [37], and viewing conditions [28] can produce variable lag magnitudes. For example, lag values increase with higher accommodative demands or smaller target sizes and are typically smaller under binocular than monocular viewing conditions. Moreover, closed-field autorefractors, which restrict viewing to an internal fixation target, may overestimate lag by suppressing proximal and vergence cues [38], [39]. Therefore, differences in the methods used in these studies, combined with variations in participant age, refractive errors, and environmental exposure, probably contributed to the inconsistent conclusions regarding the role of accommodative lag in myopia development

Overall, accommodative lag and its resultant hyperopic retinal defocus represent a possible mechanism linking near work to myopia development. While animal and theoretical models provide strong support for defocus-driven axial elongation, human data remain inconsistent.

Variability in age, measurement techniques, viewing conditions likely contribute to the contradictory findings across studies. This methodological variability limits direct comparison across studies and highlights the need for more standardized, repeatable approaches when evaluating accommodative behavior in relation to myopia.

1.2.2 Accommodative instability and transient fluctuations in the axial length.

Many studies have investigated the effect of accommodation on axial length measurement in different populations and methods. Results often vary depending on how the experiment was set up, factors like the level of accommodative stimulus [40], the type of visual target [37], how long the stimulus was presented [41], and whether changes in lens thickness were accounted for in the measurements [42].

In general, studies using modern optical biometers have shown that accommodation causes a small but measurable increase in axial length (within minutes), usually close to the resolution of the instrument (or the order of approximately 10-20 micrometers), in both emmetropic and myopic eyes [40], [43], [44], [45]. It is important to note that older studies that reported larger elongations during accommodation often did not correct for lens-thickness changes, which means part of the observed elongation may have been optical rather than structural [44], [45], [46]. Several studies have also shown that after near task exposure for 30 or 60 minutes the eye does not return immediately to its baseline length once accommodation stops. Instead, a short recovery period occurs before axial length returns to its previous value, typically within 10 minutes, although this recovery can be slower in myopic eyes (up to 30 minutes)[40], [41], [47], [48].It has been hypothesized in these studies that subjects who experience greater transient variation in axial length during accommodation may be more prone to long-term myopic progression.

Laughton et al. also investigated the idea of the ocular biomechanics changing with age. They noticed a sharp reduction in the magnitude and inter-subjects' variability of accommodation induced axial elongation after the age of 43 [42].Their earlier work [49] studies this effect on young adults in longitudinal study where they reported structural stiffening over time among adult years. This is also supported by a recent 2025 study which found that accommodative accuracy

shifts with age even in mid-adulthood [50].This suggests that while the eye continues to go through slow biometric changes with age, the accommodation response is reduced, possibly due to stiffening of posterior ocular tissues [51], [52].

Accommodative induced axial length changes are small and can be temporary, but they are highly sensitive to how the experiment is conducted. Differences in instruments, stimulus demand and the timing of post-task measurements make comparisons across studies difficult and may partly explain the mixed findings. More standardized protocols and different measurement approaches are needed to clarify whether these transient fluctuations have meaningful implications for long-term myopia progression.

1.2.3 Binocular Vision and Accommodation-Convergence Interaction in Myopia

An important factor to consider in myopia development is binocular vision and its connection to the accommodation and vergence system [53] as these interactions may function differently in myopes [54]. Accommodation and vergence usually work together to maintain a clear single image when individuals focus on near objects, this interaction usually happens in the right amount to keep the vision comfortable and stable specially during sustained near tasks such as reading or using screens [37], [53], [54], [55].

However, studies show that myopes tend to have a lower accommodative gain (more accommodation lag) compared to emmetropes [56], [57], this means that their accommodation response is weaker than the demand. Also, they often demonstrate higher accommodative convergence/ accommodation (AC/A) ratios [10], [54], [58], [59], [60] which drifts toward near esophoria [10], [28] suggesting a stronger convergence response compared to the amount of accommodation. These studies revealed that this indicates that myopes rely less on binocular feedback to control accommodation and more on blur cues. At the same time, myopes show reduced sensitivity to image blur (reduced sensitivity to differentiate between small differences)[61], [62] and reduced stereoacuity (depth of focus) compared to emmetropes [63] this can lead to a weak accommodative response and more accommodation lag during near tasks [64], [65], this means that myopes system initially prefers convergence over accommodation.

Consistent with this, myopic subjects also tend to have greater positive fusional vergence (base-in)[60], [66] and a different pattern of long-term visual adaptation compared to emmetropes. Normally, the eye relies on the vergence system to change and help stabilize the eye alignment to reduce the strain over time, but in myopes, the adaptation happened more in the accommodation system rather than the vergence system [10], [60], this can explain why they might still have slight esophoria after prolonged near task. As a result, myopes depend on the blur cues to keep the image clear, and since they have reduced sensitivity to image blur, this can lead to a more accommodative lag and visual fatigue during prolonged near tasks.

While these binocular characteristics are not examined directly in the present thesis, they provide important physiological context for understanding accommodative behavior during near tasks. They highlight the relevance of measurement conditions that preserve natural viewing and binocular cues when assessing accommodation and refractive responses in myopia research.

1.2.4 Choroidal thickness measurement and transient choroid thinning in response to defocus or near work.

The choroid is a vascular and pigmented layer in the eye between the sclera and Bruch's membrane that plays the role of providing oxygen and nutrients to the outer retina[18], [67], it regulates ocular temperature and helps with waste removal [68]. Beyond these roles, the choroid is very elastic[67], and it shows rapid thickness changes within minutes to hours[69], [70], This dynamic behavior suggests an active role in the ocular growth and the refractive adaptation to visual demands.

Choroidal thickness (CT) is defined as the vertical distance from the outer border of the retinal pigment epithelium (RPE) or Bruch's membrane to the choroid–scleral interface[71], [72]. In clinical practice, optical coherence tomography (OCT) is the most used method to measure this thickness According to a 2021 review by Xie et al [73]. OCT is a non-invasive imaging technique that uses low coherence interferometry to produce cross-sectional (OCT B-scans) images of ocular tissues with high level resolution (micrometers), it uses light from a broadband source that splits into a sample beam, which is directed toward the retina and choroid, and a reference beam, that is reflected by a mirror [74], [75]. The interference between both these returning beams transfers

optical path differences, which are processed by Fourier transformation to produce depth resolved reflectivity profiles[76].

Traditional time-domain OCT was limited by low acquisition speed and insufficient penetration to the posterior choroid, which lead to the development of spectral-domain OCT (SD-OCT), that replaced the movement of the reference mirror with a spectrometer that increased the speed and axial resolution (5–7 μm). After that the Enhanced Depth Imaging (EDI) was available which enhanced the visualization of deep choroid layers [77], [78]. More recently, the swept-source OCT (SS-OCT) has become available, It uses a narrow band laser (1050–1060 nm) that allows for a faster acquisition rates (>100,000 A-scans) and deeper light penetration through the RPE, this gives a clearer definition of the choroid–sclera interface [79], [80]. When Comparing choroidal thickness measurements obtained with both techniques, SD-OCT (particularly when using enhanced depth imaging (EDI)) gave slightly higher choroidal thickness values than SS-OCT across macular regions[81], [82], [83], [84], the differences in these studies were largely credited to the difference in light source wavelength, axial resolution and segmentation algorithms. On the other hand, the SS-OCT provides a deeper penetration and more visualization of the choroid–sclera interface[82], [85], [86], [87]. Despite these differences, both devices showed strong correlations and high inter-device agreement, suggesting that they can be used interchangeably but with caution, especially when comparing data in diseased eyes and when relying on automated segmentation, this accuracy may decline [81], [82], [84].

The most common OCT based CT measurement methods are the manual measurement method and automated segmentation method [73] . In the manual method, clinicians usually use the cross-sectional OCT B-scans built-in tools to mark the RPE/Bruch's membrane boundary and the choroid–scleral boundary [72], [88], usually at the sub-foveal point or also at certain nasal and temporal points at 500 μm and 1000 μm away from the fovea [72], [89], [90]. This method is still widely used due to its simplicity and because many earlier studies used it[72], [88], [91], [92], [93]. However, the manual choroidal segmentation is time consuming and highly subjective, which can lead to inconsistencies between graders[92]. It also highly depends on image quality and can be prone to human error, especially at the choroid–sclera interface when the boundary is blurred [92], [93].

Recently, notable progress has been made in the automated segmentation of the choroid using OCT, which reduced the reliance on the manual caliper measurement. Deep learning segmentation and convolutional neural network models has been used and showed a strong agreement with the manual segmentation in research settings (ICCs > 0.90) [91], [94], [95]. However, some limitations remain, segmentation of the choroid–scleral interface can still be challenging when the image quality is poor, and the boundary is not very clear [96], [97]. Also, it was noted that the accuracy is lower in eyes with very thick or very thin choroids or extreme axial lengths [91], [94], [98]. Moreover, many of the used algorithms remain research tools rather than being fully integrated into the commercial OCT platforms [93]. Although the automated segmentation shows promise in improving repeatability and efficiency[99], [100], larger datasets and further validation are still needed before it can be used in clinical settings.

Advances in CT measurement techniques have made it possible to study the physiological significance of these thickness changes and their potential role in ocular growth regulation. In animal models first (Troilo et al., 2019) and then in humans [70], [101], [102], [103], [104], it has been shown that hypermetropic retinal defocus reduces the thickness of the choroid. If this transient change persists, it can lead to ocular elongation at the level of the scleral fibrous structures which would become irreversible, leading to the development of myopia [16]. For example, one study reported that after 60 minutes of myopic defocus the sub-foveal choroid thickened by +8 ± 11 μm, whereas hyperopic defocus caused a −4 ± 11 μm thinning [47]. Studies also shown that the choroidal thickness is affected by the changes in the spherical equivalent refraction (SER), for example, Zhu et al. (2024)[105] reported that each 1-diopter decrease in SER was associated with a 13 μm reduction in sub foveal CT. In addition to these refractive changes, CT also shows spatial variation, it was thinner nasally than temporally across the posterior pole [91], [106], [107].

This thinning has also been linked to near task demands, suggesting that the choroid (and possibly the sclera) thins in response to sustained accommodation or image blur from defocus [104], [106]. These dynamic changes suggest that the choroid is more than a passive vascular structure, it may act as a biomechanical buffer, adjusting its volume to modify the retina's position relative to the focal plane, thereby playing a role in the emmetropisation process and ocular growth regulation.

Studying the transient response of the choroid in relation to hyperopic defocus/ accommodative lag could increase understanding of the relationship between the two phenomena in causing future myopia. The attention has been placed on the choroid and its contribution on the transient variations of the axial length, as the reduction in choroidal thickness, rather than a mechanical consequence in response to ciliary muscle contraction, seems to represent a related feedback response of accommodation, where the choroidal thinning (or thickening) can be seen as a mechanism to compensate for a defocus, shifting the plane image in order to obtain a focused image on the retina and possibly serving as an early biomarker of myopia progression [43], [70], [107], [108]

Although several studies have reported transient choroidal changes in response to retinal defocus, the long-term implications of these fluctuations on eye growth and myopia development remain uncertain[67]. There is a need to study the contribution of the choroid on the regulation of eye growth and to identify those myopia genetic factors that lead to transient thinning. It is, in fact, still unclear how much the long-term variation of the thickness of the choroid during or following the accommodation can contribute to the development of myopia and more long-term human studies are necessary to clarify its mechanisms[90].

Future longitudinal studies that combine high resolution OCT imaging with genetic and biological data are needed to determine whether choroidal thickness changes represent a factor or a response or serve as a biomarker in the development and progression of myopia.

1.3 Measuring Accommodation, Refractive Error and Aberrations

Refraction measurement plays a major role when evaluating and correcting refractive errors and accurate and reliable measurement techniques are required to prescribe appropriate corrective lenses and to evaluate the effectiveness of refractive treatments. Subjective refraction is considered the gold standard for assessing refractive error and accommodative function for over 200 years [109], [110], [111], [112]. Traditionally, this technique includes adjusting the refractive correction based on the patient's responses to achieve the best corrected visual acuity (BCVA)[36], [109], [113]. However, subjective refraction results usually show variations based on clinicians' experience, test conditions and other factors, such as vertex distance, this can reduce repeatability and the validity of the results[109], [111]. Studies on subjective refraction[109], [114], [115], [116] emphasized that with the subjective refraction as the gold standard, other objective methods should also be employed to provide good comfortable vision and patient contentment.

Many devices have been developed to provide objective measurements of refraction without relying on the patient's response. Autorefractors are the most common devices to be used in ophthalmic and optometric practice as a starting point for subjective refraction, they offer a fast, reliable automated assessment of refractive status [110], [117], [118], [119]. Together with auto lensometers and phoropters, they form a complete automated subjective refraction [120], [121].

Objective devices are not alternatives for subjective refraction, as they can either overestimate or underestimate refractive errors[110], [122] these instruments also operate under specific optical and viewing conditions such as monocular closed-field designs, internal fixation targets, and controlled illumination and fixation distances, which can affect accommodation and measurement accuracy [38], [123]. Similarly, subjective refraction can make overestimations in the accommodative amplitude due to changes in depth of focus and pupil size [124], [125], [126], [127]. When we combine the methods, however, they provide complementary measurements, and they are both important to ensure accurate and reliable assessment of refractive error across different instruments and study populations [109], [110].

Nevertheless, both subjective refraction and autorefractors only measure lower-order aberrations, sphere (defocus) and astigmatism [120], [128]. Optical image quality at the retina can also be reduced by higher-order aberrations like coma and spherical aberration [127], [129], that lead to

the development of the wavefront aberrometers. They possess the ability to measure a wide range of aberrations including lower and higher order aberrations, and the corresponding effect on refraction [130], [131], [132]. Validation studies on aberrometers report mean differences below 0.25 D and ICC values above 0.95 when compared with standard autorefractors, indicating that these differences are not clinically significant [38], [133], [134], [135], [136].

The most common autorefractors and aberrometers used in the market are the closed-field designs, in these devices, the fixation target is viewed internally. Studies have shown that this configuration can trigger proximal accommodation and produce a type of myopia known as instrument myopia [137], [138]. Such limitations can reduce the ecological validity of their measurements specially when evaluating accommodation, binocular vision or peripheral refraction.

The latest advances in the field are the open field aberrometers and open field autorefractors. These state-of-the-art techniques offer the distinct advantage of accurately measuring both refractive errors and higher-order aberrations under real-world environmental conditions, which provides ecological validity and accuracy in evaluating visual performance under natural conditions [117], [119], [128]. Conversely, open field autorefractors produce less instrumental myopia than that of conventional autorefractors, making them useful for both clinical screening and research [38], [119], [139].

Despite the limited availability of models and the lack of comprehensive data on reliability studies, open field aberrometers show a very promising ability to accurately assess accommodation and astigmatism [133], [138], [140], [141].They are discussed in detail in the next section.

1.4 Aberrometers: Principles and Types

1.4.1 Principles of aberrometry

In recent years, aberrometer technology has advanced significantly and it increased our understanding of the visual system and the way we diagnose and correct visual aberrations. It is a powerful diagnostic tool that provides insights into optical aberrations by analyzing the wavefront of light as it travels in the eye [142]. This technique enables clinicians and researchers to understand the nuances of vision and to fit precise solutions for individual patients.

Optical aberrations occur when an optical system creates an image that deviates from the one expected for an ideal optical system, resulting in image imperfection. These aberrations emerge because the behavior of light rays deviates from the principles ideal optical systems and when with larger pupil diameters, the human eye does not function as a flawless optical system [143]. Many factors are influenced by the presence of aberrations in the eye's optical system, including contrast sensitivity, near and distance vision, performance under light and dark conditions, and the brain's interpretation of the input from the sensory apparatus. [144] .

The primary optical anomalies of the eye can be categorized into two main groups, low-order aberrations, which encompass conditions like defocus (myopia, hyperopia) and regular astigmatism, and high-order aberrations, which includes factors such as spherical aberration, distortion, coma, oblique astigmatism, as well as other higher-order aberration [145]. Only in the late 20th century, wavefront sensors were developed to allow routine estimation of these high-ocular aberrations.
When the actual wavefront is ahead of the ideal wavefront, the wave aberration is considered positive, and if the actual wavefront lags behind the ideal one, the wave aberration is negative. The wave aberration function is typically minute and is commonly quantified in micrometers (μm) or as a fraction of wavelengths [145].

There are two methods available for measuring the localized deviations of rays in the pupil plane by the eye's optical system, known as outgoing and ingoing light aberrometry. In ingoing light aberrometry, a bundle of parallel rays emitted by a near-infrared (NIR) light source enters the eye through the pupil, and the transverse ray deviation is determined relative to a reference ray entering

parallel to the line of sight at the same pupil location. The deviation of the considered ray on the retina can be measured using a standard ophthalmoscope system, which is why ingoing light aberrometers are sometimes referred to as retinal imaging aberrometers. This method assumes uniform retinal reflection, so retinal inhomogeneities or irregular surface shape may affect the measurement. In outgoing light aberrometry, a near-infrared (NIR) light source is used to create a fundus reflex. It can be regarded as a secondary point source for a bundle of test rays. The deflection of rays in the pupil plane is then analyzed with respect to a non-deflected ray that is parallel to the line of sight. Most commercial aberrometers work according to this principle and use a Hartmann–Shack wavefront sensor as the key measurement component for determination of local transverse ray deviations [146], [147].

1.4.2 The importance of open-field systems

Aberrometers can also be categorized according to the field of view of the subjects, as closed field and open field aberrometers. There are widely available devices of commercially aberrometers including Hartmann-Shack Aberrometer [147], Tscherning Aberrometer, COAS (Customized Optical Aberration System) and others. In closed field systems, the fixation target is integrated within the device, meaning that subjects view an internal image at a short distance. The closed field design can stimulate accommodation and lead to slightly more myopia in the measurements [39], [119].

On the other hand, open field systems allow the subject to fixate on a real distant target placed outside the instrument, which minimizing instrument-induced accommodation and allow a more natural viewing conditions [38], [137], [148], [149]. The main difference between the two systems lies in whether the fixation target is presented internally (closed-field) or externally (open-field), which directly influences the degree of accommodative demand and the ecological validity of the measurement. These systems may also enable a broader assessment of the eye's optical performance, as some devices can capture wavefront data from a wider pupil area or over peripheral visual angles, depending on the optical design [150], [151]. Open-field designs usually rely on outgoing-light aberrometry principles like Hartmann–Shack sensors, where light reflected from the retina is analyzed to derive local wavefront slopes [147].

1.4.3 Open field systems applications

Open-field aberrometers are designed to minimize accommodation induced by instrument proximity, a limitation commonly associated with closed-field systems. By allowing binocular viewing of a real, distant fixation target through an open window, these systems reduce accommodative responses that are driven by internal targets and better approximate natural viewing conditions [152], [153]

Therefore, open-field aberrometers have been widely applied to the objective assessment of accommodative behavior under near-viewing conditions. Binocular Hartmann–Shack systems have been used to measure real-time changes in spherical equivalent and pupil response in patients with intermittent exotropia and accommodative spasm, demonstrating their ability to capture excessive or unstable accommodation without cycloplegia [140], [154]. Open-field binocular aberrometry has also been applied to the assessment of binocular fusion maintenance (BFM) using virtual reality stimuli, where it showed higher diagnostic accuracy for visual fatigue compared with conventional subjective measures such as fusional vergence and near point of convergence [155], [156].

The Hartmann–Shack aberrometer open field technique was also used in pre-presbyopic subjects to assess accommodation and compare between the subjective and objective methods [125]. Although this study was done monocularly to eliminate vergence accommodation, it's important to note that in everyday life, we use both eyes simultaneously, the ability of the open-field devices to measure binocular accommodation makes their results more realistic and relevant to everyday visual conditions.

Beyond accommodation, open-field Shack–Hartmann systems such as the COAS-HD VR have enabled precise off-axis and peripheral refraction measurements. Studies in emmetropic and myopic eyes reported fast, repeatable peripheral measurements and a quadratic increase in higher-order aberrations from the fovea toward the periphery, with accommodation affecting relative peripheral refraction differently in myopes and emmetropes [157], [158]. Comparisons with open view autorefractors showed similar central and peripheral defocus at small pupil sizes, while larger pupils revealed systematic differences, particularly under conditions involving multifocal optics

[128], [159]. These capabilities have been applied to evaluate how progressive and single-vision lenses alter peripheral defocus in myopic children[160], [161].

In clinical practice, correcting peripheral refraction matters even more for patients relying on off-axis vision due to central visual field loss, [162], [163] studies validated a rapid approach to off-axis refraction and showed that correcting as little as 1.50 D of peripheral astigmatism can improve low-contrast acuity by one line, it also found that dynamic contrast sensitivity benefits at 7.5 Hz for low spatial frequencies with appropriate off-axis correction in central field loss, highlighting the value of fully correcting peripheral errors. Together, these studies highlight the importance of open field systems as a technique choice when studying and correcting peripheral refraction.

Across pediatric and adult populations, multiple open-field aberrometry devices have demonstrated acceptable agreement and repeatability for refractive error and higher-order aberration measurements when compared with subjective refraction, cycloplegic autorefraction, and established wavefront devices [127], [136], [141], [164]. Integrated open-field systems combining Hartmann–Shack sensing with double-pass techniques further extends these applications by enabling simultaneous assessment of optical aberrations and intraocular scattering [136].

Taken together, these applications demonstrate that the open field systems provide a uniquely suitable method for investigating accommodation, binocular vision, and peripheral refraction under conditions that closely resemble natural viewing. However, the diversity of experimental designs, viewing conditions, and analytical approaches across studies highlights the need for methodologically consistent protocols when applying these techniques to refractive error research.

1.5 Thesis Aim and Objectives

The general aim of this thesis is to strengthen the evaluation of myopia and myopia-related change by linking objective measurement with clinically relevant interpretation of both functional (refraction, accommodation, aberrations) and structural (axial length, choroidal thickness) ocular parameters using both cross-sectional and longitudinal data. From an optical measurement perspective, these outcomes are treated as optical estimates derived from specific instruments and measurement conditions, where factors such as pupil size (aperture), viewing conditions (open vs closed field), alignment, fixation and accommodation can influence the values that are recorded and how small changes are detected.

This aim is addressed through two objectives:

1. Methods validation and agreement: the aim was to assess the reliability and clinical relevance of objective refraction by comparing open-field and closed-field systems with subjective refraction under controlled viewing conditions, and by determining how key analysis factors (particularly pupil size as an optical aperture) influence agreement and aberration-related metrics.

2. Application to study myopia-related risk factors: the aim was to apply the validated measurement strategy to characterize myopia-related measurements across time and across retinal location by integrating refractive and biometric outcomes, including longitudinal axial-length trajectories, central and peripheral spherical equivalent refraction, near-work responses and choroidal thickness assessment.

1.6 References

[1] Holden BA, Fricke TR, Wilson DA, Jong M, Naidoo KS, Sankaridurg P, et al. Global prevalence of myopia and high myopia and temporal trends from 2000 through 2050. Ophthalmology 2016;123(5):1036–42. https://doi.org/10.1016/j.ophtha.2016.01.006.

[2] Grzybowski A, Kanclerz P, Tsubota K, Lanca C, Saw SM. A review on the epidemiology of myopia in school children worldwide. BMC Ophthalmol 2020;20:27. https://doi.org/10.1186/s12886-019-1220-0.

[3] Hyman LG, Gwiazda J, Hussein M, Norton TT, Wang Y, Marsh-Tootle W, et al. Relationship of age, sex, and ethnicity with myopia progression and axial elongation in the Correction of Myopia Evaluation Trial. Arch Ophthalmol 2005;123(7):977–87. https://doi.org/10.1001/archopht.123.7.977

[4] Ohno-Matsui K, Spaide RF, Yannuzzi LA. Pathologic Myopia. 2nd ed. Berlin: Springer-Verlag; 2014.

[5] Bullimore MA, Richdale K. Myopia Control 2020: Where are we and where are we heading? Ophthalmic Physiol Opt 2020;40(3):254–270. https://doi.org/10.1111/opo.12686.

[6] Fricke TR et al., "Global cost of correcting vision impairment from uncorrected refractive error," Bull World Health Organ 2012;90(10):728–38. https://doi.org/10.2471/BLT.12.104034.

[7] Naidoo KS et al., "Potential lost productivity resulting from the global burden of myopia," Ophthalmology 2019;126(3):338–46. https://doi.org/10.1016/j.ophtha.2018.10.029.

[8] Bharadwaj SR. "Ocular accommodation: the autofocus mechanism of the human eye," Annu Rev Vis Sci 2025;26:49. https://doi.org/10.1146/annurev-vision-110623.

[9] de Jong PTVM. "The quest for the human ocular accommodation mechanism," Acta Ophthalmol 2020;98(1):98–104. https://doi.org/10.1111/aos.14194.

[10] Logan NS et al., "IMI accommodation and binocular vision in myopia development and progression," Invest Ophthalmol Vis Sci 2021;62(5):4. https://doi.org/10.1167/iovs.62.5.4.

[11] Koomson NY, Amedo AO, Opoku-Boadi S, Amponsah A, Kyei S, Ankamah-Lomotey S. Relationship between reduced accommodative lag and myopia progression. Optom Vis Sci 2016;93(7):683–691. https://doi.org/10.1097/OPX.0000000000000863.

[12] Gwiazda JE et al., "Accommodation and related risk factors associated with myopia progression," Invest Ophthalmol Vis Sci 2004;45(7):2143–51. https://doi.org/10.1167/iovs.03-1306.

[13] Drobe B, Yeo AC, Paillé D, Koh P. Myopia and Effective Management Solutions. Points de Vue – International Review of Ophthalmic Optics. 2016;73(Autumn):56–65.

[14] Irving EL, Callender MG, Sivak JG. "Inducing ametropias in hatchling chicks by defocus–aperture effects and cylindrical lenses," Vision Res 1995;35(9):1165–74. https://doi.org/10.1016/0042-6989(94)00235-E.

[15] Smith EL III, Hung LF. "The role of optical defocus in regulating refractive development in infant monkeys," Vision Res 1999;39(8):1415–35. https://doi.org/10.1016/S0042-6989(98)00229-6.

[16] Troilo D et al., "IMI report on experimental models of emmetropization and myopia," Invest Ophthalmol Vis Sci 2019;60(3):M31–M88. https://doi.org/10.1167/iovs.18-25967.

[17] Wallman J, Winawer J. "Homeostasis of eye growth and the question of myopia," Neuron 2004;43(3):447–68. https://doi.org/10.1016/j.neuron.2004.08.008.

[18] Nickla DL, Wallman J. "The multifunctional choroid," Prog Retin Eye Res 2010;29(2):144–68. https://doi.org/10.1016/j.preteyeres.2009.12.002.

[19] Smith EL III, Hung LF, Harwerth RS. Developmental visual system anomalies and the limits of emmetropization. Ophthalmic Physiol Opt 1999;19(2):90–102. https://doi.org/10.1046/j.1475-1313.1999.00429.x

[20] Mutti DO et al., "Parental myopia, near work, school achievement, and children's refractive error," Invest Ophthalmol Vis Sci 2002;43(12):3633–40.

[21] Saw SM et al., "Incidence and progression of myopia in Singaporean school children," Invest Ophthalmol Vis Sci 2005;46(1):51–57. https://doi.org/10.1167/iovs.04-0565.

[22] Pärssinen O et al., "Progression of myopia from childhood to adulthood," Acta Ophthalmol 2014;92(8):730–39. https://doi.org/10.1111/aos.12387.

[23] Chamberlain P et al., "Axial length targets for myopia control," Ophthalmic Physiol Opt 2021;41(3):523–31. https://doi.org/10.1111/opo.12812.

[24] Czepita D, Mojsa A, Ustianowska M, Czepita M, Lachowicz E. Reading, writing, working on a computer or watching television, and myopia. Klin Oczna. 2010;112(10–12):293–295

[25] Ip JM et al., "Role of near work in myopia," Invest Ophthalmol Vis Sci 2008;49(7):2903–10. https://doi.org/10.1167/iovs.07-0804.

[26] Enthoven CA et al., "Smartphone use and refractive error," Ophthalmology 2021;128(12):1681–88. https://doi.org/10.1016/j.ophtha.2021.06.016.

[27] Dutheil F et al., “Myopia and near work: meta-analysis,” Int J Environ Res Public Health 2023;20(1):875. https://doi.org/10.3390/ijerph20010875.

[28] Mutti DO et al., “Accommodative lag before and after onset of myopia,” Invest Ophthalmol Vis Sci 2006;47(3):837–46. https://doi.org/10.1167/iovs.05-0888.

[29] Berntsen DA et al., “Accommodative lag and myopia progression,” Vision Res 2011;51(9):1039–46. https://doi.org/10.1016/j.visres.2011.02.016.

[30] Gwiazda J et al., “Five-year results from COMET,” Invest Ophthalmol Vis Sci 2006;47(13):4689–96. https://doi.org/10.1167/iovs.06-0568.

[31] Gwiazda J et al., “Progressive addition lenses vs single vision lenses,” Invest Ophthalmol Vis Sci 2003;44(4):1492–1500. https://doi.org/10.1167/iovs.02-0816.

[32] Berntsen DA et al., “Randomized trial of progressive addition lenses,” Invest Ophthalmol Vis Sci 2012;53(2):640–49. https://doi.org/10.1167/iovs.11-7769.

[33] Rosenfield M, Desai R, Portello JK. Do progressing myopes show reduced accommodative responses? Optom Vis Sci 2002;79(4):268–73. https://doi.org/10.1097/00006324-200204000-00005.

[34] Bakaraju RC, Yeotikar NS, Rao VS. Accommodative lag versus different stimuli. J Mod Opt 2007;54(9):1299–1305. https://doi.org/10.1080/09500340600855296

[35] Manny RE et al., “Accommodative lag by autorefraction,” Optom Vis Sci 2009;86(3):233–43. https://doi.org/10.1097/OPX.0b013e318197180c.

[36] Mallen EAH et al., “Clinical evaluation of Shin-Nippon SRW-5000,” Ophthalmic Physiol Opt 2015;35(6):622–27. https://doi.org/10.1111/opo.12254.

[37] Rosenfield M, Gilmartin B. Myopia and Nearwork. Oxford: Butterworth-Heinemann; 1998.

[38] Carracedo G, Carpena-Torres C, Batres L, Serramito M, Gonzalez-Bergaz A. Comparison of two wavefront autorefractors: binocular open-field versus monocular closed-field. J Ophthalmol 2020;2020:8580471. https://doi.org/10.1155/2020/8580471.

[39] Nagra M, Akhtar A, Huntjens B, Campbell P. Open versus closed view autorefraction in young adults. J Optom 2021;14(1):86–91. https://doi.org/10.1016/j.optom.2020.06.007.

[40] Mallen EAH, Kashyap P, Hampson KM. Transient axial length change during the accommodation response in young adults. Invest Ophthalmol Vis Sci 2006;47(3):1251–54. https://doi.org/10.1167/iovs.05-1086.

[41] Woodman EC, Read SA, Collins MJ. Axial length and choroidal thickness changes accompanying prolonged accommodation in myopes and emmetropes. Vision Res 2012;72:34–41. https://doi.org/10.1016/j.visres.2012.09.009.

[42] Laughton DS, Sheppard AL, Mallen EAH, Read SA, Davies LN. Does transient increase in axial length during accommodation attenuate with age? Clin Exp Optom 2017;100(6):676–82. https://doi.org/10.1111/cxo.12533.

[43] Read SA, Collins MJ, Woodman EC, Cheong SH. Axial length changes during accommodation in myopes and emmetropes. Vision Res 2010;50(13):1278–85. https://doi.org/10.1016/j.visres.2010.02.001.

[44] O'Donoghue L, Saunders KJ, Anderson RS. Effect of accommodation on axial length measurement in myopes and emmetropes. Invest Ophthalmol Vis Sci 2005;46(13):5591 (ARVO Abstract).

[45] Schmetterer L, Hitzenberger C. Eye elongation during accommodation in humans: differences between emmetropes and myopes. Vision Res 1998;38(12):1931–39. https://doi.org/10.1016/S0042-6989(97)00227-6

[46] Shum PJT, Ko LS, Ng CL, Lin SL. A biometric study of ocular changes during accommodation. Am J Ophthalmol 1993;115(1):76–81. https://doi.org/10.1016/S0002-9394(14)73528-7.

[47] Delshad S, Collins MJ, Read SA, Vincent SJ. The time course of onset and recovery of axial length changes in response to imposed defocus. Sci Rep 2020;10(1):65151. https://doi.org/10.1038/s41598-020-65151-5.

[48] Chakraborty R, Read SA, Collins MJ. Monocular myopic defocus and daily changes in axial length and choroidal thickness of human eyes. Exp Eye Res 2012;103:47–54. https://doi.org/10.1016/j.exer.2012.08.002.

[49] Laughton DS, Sheppard AL, Davies LN. A longitudinal study of accommodative changes in biometry during incipient presbyopia. Ophthalmic Physiol Opt 2016;36(1):33–42. https://doi.org/10.1111/opo.12242.

[50] Arcas-Carbonell M, Orduna-Hospital E, Oliete-Lorente S, Mechó-García M, Fernández-Espinosa G, Sanchez-Cano A. Structural and functional analysis of the eye according to the accommodation-age relationship. Vision Res 2025;230:108596. https://doi.org/10.1016/j.visres.2025.108596.

[51] Ebneter A, Wagels B, Zinkernagel MS. Non-invasive biometric assessment of ocular rigidity in glaucoma patients and controls. Eye (Lond) 2009;23(3):606–11. https://doi.org/10.1038/eye.2008.47.

[52] Croft MA, Nork MT, McDonald JP, Katz A, Lütjen-Drecoll E, Kaufman PL. Accommodative movements of the vitreous membrane, choroid, and sclera in young and presbyopic human and nonhuman primate eyes. Invest Ophthalmol Vis Sci 2013;54(7):5049–58. https://doi.org/10.1167/iovs.12-10847.

[53] Hoffman DM, Banks MS. Focus information is used to interpret binocular images. J Vis 2010;10(5):13. https://doi.org/10.1167/10.5.13.

[54] Gwiazda J, Thorn F, Held R. Accommodation, accommodative convergence, and response AC/A ratios before onset of myopia in children. Optom Vis Sci 2005;82(4):273–8. https://doi.org/10.1097/01.opx.0000156313.57876.4a

[55] Schor CM. A dynamic model of cross-coupling between accommodation and convergence: simulations of step and frequency responses. Optom Vis Sci 1992;69(4):258–69. https://doi.org/10.1097/00006324-199204000-00002.

[56] Huang CT, Satou T, Niida T. Effect of pupil size and binocular viewing on accommodative gain in emmetropia and myopia. J Binocul Vis Ocul Motil 2020;70(3):103–108. https://doi.org/10.1080/2576117X.2020.1780878.

[57] Mutti DO et al., "The response AC/A ratio before and after the onset of myopia," Invest Ophthalmol Vis Sci 2017;58(3):1594–602. https://doi.org/10.1167/iovs.16-19093.

[58] Mutti DO, Jones LA, Moeschberger ML, Zadnik K. AC/A ratio, age, and refractive error in children. Invest Ophthalmol Vis Sci 2000;41(9):2466–71. https://doi.org/10.1167/iovs.41.9.2466

[59] Gwiazda J, Grice K, Thorn F. Response AC/A ratios are elevated in myopic children. Ophthalmic Physiol Opt 1999;19(2):173–79. https://doi.org/10.1046/j.1475-1313.1999.00437.x.

[60] Sreenivasan V, Irving EL, Bobier WR. Effect of heterophoria type and myopia on accommodative and vergence responses during sustained near activity in children. Vision Res 2012;57:9–17. https://doi.org/10.1016/j.visres.2012.01.011.

[61] Maiello G, Walker L, Bex PJ, Vera-Diaz FA. Blur perception throughout the visual field in myopia and emmetropia. J Vis 2017;17(5):3. https://doi.org/10.1167/17.5.3.

[62] Labhishetty V, Chakraborty A, Bobier WR. Is blur sensitivity altered in children with progressive myopia? Vision Res 2019;154:142–53. https://doi.org/10.1016/j.visres.2018.11.002.

[63] Vera-Diaz FA, Bex PJ, Ferreira A, Kosovicheva A. Binocular temporal visual processing in myopia. J Vis 2018;18(11):17. https://doi.org/10.1167/18.11.17.

[64] Mather G. The use of image blur as a depth cue. Perception 1997;26(9):1147–58. https://doi.org/10.1068/p261147.

[65] Mather G, Smith DRR. Blur discrimination and its relation to blur-mediated depth perception. Perception 2002;31(10):1211–19. https://doi.org/10.1068/p3254.

[66] Jorge J, Borges de Almeida J, Parafita MA. Binocular vision changes in university students: a 3-year longitudinal study. Optom Vis Sci. 2008 Oct;85(10):E999–E1006. https://doi.org/10.1097/OPX.0b013e3181890d35

[67] Ostrin LA et al., IMI — the dynamic choroid: new insights, challenges, and potential significance for human myopia. Invest Ophthalmol Vis Sci 2023;64(6):4. https://doi.org/10.1167/iovs.64.6.4.

[68] Zhang W, Kaser-Eichberger A, Fan W, Platzl C, Schrödl F, Heindl LM. The structure and function of the human choroid. Ann Anat 2024;258:152239. https://doi.org/10.1016/j.aanat.2024.152239.

[69] Wang D et al., Optical defocus rapidly changes choroidal thickness in schoolchildren. PLoS One 2016;11(8):e0161535. https://doi.org/10.1371/journal.pone.0161535.

[70] Liu Y, Wang L, Xu Y, Pang Z, Mu G. The influence of the choroid on the onset and development of myopia: perspectives of choroidal thickness and blood flow. Acta Ophthalmol 2021;99(3):e397–e405. https://doi.org/10.1111/aos.14773.

[71] Lee CO et al., Comparison of choroidal thickness measurements between spectral-domain and swept-source OCT in children. Sci Rep 2021;11(1):92980. https://doi.org/10.1038/s41598-021-92980-9.

[72] Yamashita T et al., Repeatability and reproducibility of subfoveal choroidal thickness in normal Japanese eyes using different SD-OCT devices. Invest Ophthalmol Vis Sci 2012;53(3):1102–07. https://doi.org/10.1167/iovs.11-8836.

[73] Xie R, Qiu B, Chhablani J, Zhang X. Evaluation of choroidal thickness using optical coherence tomography: a review. Front Med 2021;8:783519. https://doi.org/10.3389/fmed.2021.783519.

[74] Hee MR et al., Optical coherence tomography of the human retina. Arch Ophthalmol 1995;113(3):325–32. https://doi.org/10.1001/archopht.1995.01100030081025.

[75] Huang D et al., Optical coherence tomography. Science 1991;254(5035):1178–81. https://doi.org/10.1126/science.1957169.

[76] Wu L, Alpizar-Alvarez N. Choroidal imaging by spectral-domain OCT. Taiwan J Ophthalmol 2013;3(1):3–10. https://doi.org/10.1016/j.tjo.2013.01.003.

[77] Margolis R, Spaide RF. A pilot study of enhanced depth imaging OCT of the choroid in normal eyes. Am J Ophthalmol 2009;147(5):811–15. https://doi.org/10.1016/j.ajo.2008.12.008.

[78] Spaide RF, Koizumi H, Pozonni MC. Enhanced depth imaging spectral-domain OCT. Am J Ophthalmol 2008;146(4):496–500. https://doi.org/10.1016/j.ajo.2008.05.032.

[79] Srinivasan VJ et al., Ultrahigh-speed OCT for 3D imaging of the retina and optic nerve head. Invest Ophthalmol Vis Sci 2008;49(11):5103–10. https://doi.org/10.1167/iovs.08-2127.

[80] Zheng F et al., Advances in swept-source OCT and OCT angiography. Asia Pac Opt Rev 2023;11:000–000 (in press). https://doi.org/10.1016/j.aopr.2022.10.005.

[81] Tan CS, Cheong KX, Lim LW, Sadda SR. Comparison of macular choroidal thickness from swept-source and spectral-domain OCT. Br J Ophthalmol 2016;100(7):995–99. https://doi.org/10.1136/bjophthalmol-2015-307541.

[82] Zafar S, Siddiqui MAR, Shahzad R. Comparison of choroidal thickness measurements between spectral-domain and swept-source OCT in normal and diseased eyes. Clin Ophthalmol 2016;10:2271–76. https://doi.org/10.2147/OPTH.S117022.

[83] Philip AM et al., Choroidal thickness maps from spectral domain and swept source OCT: algorithmic versus ground truth annotation. Br J Ophthalmol 2016;100(10):1372–76. https://doi.org/10.1136/bjophthalmol-2015-307985.

[84] Pinilla I et al., Choroidal differences between spectral and swept-source domain technologies. Curr Eye Res 2021;46(2):239–47. https://doi.org/10.1080/02713683.2020.1795883.

[85] Copete S et al., Direct comparison of spectral-domain and swept-source OCT in measurement of choroidal thickness in normal eyes. Br J Ophthalmol 2014;98(3):334–38. https://doi.org/10.1136/bjophthalmol-2013-303904.

[86] Choudhry N, Golding J, Manry MW, Rao RC. Ultra-widefield steering-based spectral-domain OCT imaging of the retinal periphery. Ophthalmology 2016;123(6):1368–74. https://doi.org/10.1016/j.ophtha.2016.01.045.

[87] Yeu E, Berdahl JP, Gupta PK, Patterson M. Sensitivity and specificity of SS-OCT for detecting macular pathologies vs SD-OCT. J Cataract Refract Surg 2024;50(5):481–85. https://doi.org/10.1097/j.jcrs.0000000000001394.

[88] Hamzah F, Shinojima A, Mori R, Yuzawa M. Choroidal thickness measurement by enhanced depth imaging and swept-source OCT in central serous chorioretinopathy. BMC Ophthalmol 2014;14:145. https://doi.org/10.1186/1471-2415-14-145.

[89] Asmussen A, Smith BS, Møller F, Jakobsen TM. Repeatability and inter-observer variation of choroidal thickness measurements in myopic Danish children aged 6–14 years. Acta Ophthalmol 2022;100(1):74–81. https://doi.org/10.1111/aos.14890.

[90] Muhiddin HS et al., Choroidal thickness in correlation with axial length and myopia degree. Vision (Basel) 2022;6(1):16. https://doi.org/10.3390/vision6010016.

[91] Lim ZW et al., Comparison of manual and AI-automated choroidal thickness segmentation in myopic adults. Eye Vis (Lond) 2024;11(1):2. https://doi.org/10.1186/s40662-024-00385-2.

[92] Branchini L et al., Reproducibility of choroidal thickness measurements across three spectral domain OCT systems. Ophthalmology 2012;119(1):119–23. https://doi.org/10.1016/j.ophtha.2011.07.002.

[93] Saeidian J et al., Segmentation of choroidal area in OCT images using transfer learning-based neural network: focus on diabetic retinopathy. BMC Med Imaging 2024;24:14592. https://doi.org/10.1186/s12880-024-01459-2.

[94] Li M et al., Choroid automatic segmentation and thickness quantification in highly myopic patients. Ann Transl Med 2022;10(11):620. https://doi.org/10.21037/atm-21-6736.

[95] Bellemo V et al., Optical coherence tomography choroidal enhancement using generative deep learning. NPJ Digit Med 2024;7:1119. https://doi.org/10.1038/s41746-024-01119-3.

[96] Masood S et al., Automatic choroid layer segmentation using deep learning on OCT images. Sci Rep 2019;9:39795. https://doi.org/10.1038/s41598-019-39795-x.

[97] Hsia WP, Tse SL, Chang CJ, Huang YL. Automatic segmentation of choroid layer using deep learning on spectral OCT. Appl Sci 2021;11(12):5488. https://doi.org/10.3390/app11125488.

[98] Chen HJ et al., Application of AI and deep learning for choroid segmentation in myopia. Transl Vis Sci Technol 2022;11(2):38. https://doi.org/10.1167/tvst.11.2.38.

[99] Sah RP et al., Deep learning-based segmentation of OCT images for choroidal thickness. J Optom 2025;18(2):556. https://doi.org/10.1016/j.optom.2025.100556.

[100] Selvam A et al., Artificial intelligence in choroid through OCT: comprehensive review. Artif Intell Rev 2025;58(4):11067-9. https://doi.org/10.1007/s10462-024-11067-9.

[101] Delshad S, Collins MJ, Read SA, Vincent SJ. Effects of brief periods of clear vision on defocus-mediated axial length and choroidal thickness changes. Ophthalmic Physiol Opt 2021;41(4):932–40. https://doi.org/10.1111/opo.12833.

[102] Kobia-Acquah E, Flitcroft DI, Martinez Hernandez G, Loskutova E, Loughman J. Relationship between choroidal thickness, axial length, and degree of myopia in European children. Invest Ophthalmol Vis Sci. 2021;62(8):ARVO E-Abstract 1386

[103] Shao L, Zhao HQ, Zhang RH, Zhou WD, Wei WB. Distribution and associated factors of choroidal thickness in highly myopic eyes: a real-world study based on a Chinese population. Eye (Lond) 2025;39(1):102–108. https://doi.org/10.1038/s41433-024-03383-9.

[104] Aldakhil S. The effect of optical defocus on the choroidal thickness: a review. Open Ophthalmol J 2021;15(1):283–287. https://doi.org/10.2174/1874364102115010283.

[105] Zhu S, et al. The relationship between accommodative and binocular function with myopia progression in myopic children undergoing orthokeratology. Contact Lens Anterior Eye 2024;47(3):102171. https://doi.org/10.1016/j.clae.2024.102171.

[106] Meng QY, et al. Choroidal thickness, myopia, and myopia control interventions in children: a meta-analysis and systematic review. Int J Ophthalmol 2023;16(3):453–464. https://doi.org/10.18240/ijo.2023.03.17.

[107] Yang X, Zhang J, Liang Y. Correlation between choroidal thickness and the degree of myopia. Technol Health Care 2024;32(6):5065–5080. https://doi.org/10.3233/THC-240761.

[108] Chiang STH, Phillips JR, Backhouse S. Effect of retinal image defocus on the thickness of the human choroid. Ophthalmic Physiol Opt 2015;35(4):405–413. https://doi.org/10.1111/opo.12218.

[109] Elliott DB. What is the appropriate gold standard test for refractive error? Ophthalmic Physiol Opt 2017;37:115–117. https://doi.org/10.1111/opo.12360.

[110] Kozlov Y, et al. Subjective versus objective refraction in healthy young adults. BMC Ophthalmol 2024;24(1):3340. https://doi.org/10.1186/s12886-024-03340-w.

[111] Rodriguez-Lopez V, Dorronsoro C. Beyond traditional subjective refraction. Curr Opin Ophthalmol 2022. https://doi.org/10.1097/ICU.0000000000000834.

[112] Billson AS. Subjective and objective refraction compared. Br J Physiol Opt 1954;11(2):107–118.

[113] Davies LN, Mallen EAH, Wolffsohn JS, Gilmartin B. Clinical evaluation of the Shin-Nippon NVision-K 5001/Grand Seiko WR-5100K autorefractor. *Optom Vis Sci.* 2003 Apr;80(4):320–324. https://doi.org/10.1097/00006324-200304000-00011

[114] Miller AD, Kris MJ, Griffiths AC. Effect of small focal errors on vision. Optom Vis Sci 1997;74(7):521–526. https://doi.org/10.1097/00006324-199707000-00020.

[115] Atchison DA, Schmid KL, Edwards KP, Muller SM, Robotham J. The effect of under- and over-refractive correction on visual performance and spectacle lens acceptance. Ophthalmic Physiol Opt 2001;21(4):255–261. https://doi.org/10.1046/j.1475-1313.2001.00588.x.

[116] Carpena-Torres C, Batres L, Serramito M, Carracedo G. Repeatability of subjective refraction in different age groups. Photonics 2024;11(7):634. https://doi.org/10.3390/photonics11070634.

[117] Guo R, Shi L, Xu K, Hong D. Clinical evaluation of autorefraction and subjective refraction with and without cycloplegia in Chinese school-aged children: a cross-sectional study. Transl Pediatr 2022;11(6):933–946. https://doi.org/10.21037/tp-22-226.

[118] Wang Y, et al. Emmetropia deviation in autorefraction compared to subjective refraction result in patients after corneal refractive surgery. BMC Ophthalmol 2025;25(1):4292. https://doi.org/10.1186/s12886-025-04292-5.

[119] Noya-Padin V, Nores-Palmas N, Sabucedo-Villamarin B, Giraldez MJ, Yebra-Pimentel E, Pena-Verdeal H. Comparing close-field and open-field autorefractometry and subjective refraction. J Clin Med 2025;14(16):5680. https://doi.org/10.3390/jcm14165680.

[120] Otero C, Aldaba M, Pujol J. Clinical evaluation of an automated subjective refraction method implemented in a computer-controlled motorized phoropter. J Optom 2019;12(2):74–83. https://doi.org/10.1016/j.optom.2018.09.001.

[121] Carracedo G, et al. Accuracy and precision of automated subjective refraction in young hyperopes under cycloplegia. J Optom 2023;16(4):252–260. https://doi.org/10.1016/j.optom.2023.03.001.

[122] Choong YF, Chen AH, Goh PP. A comparison of autorefraction and subjective refraction with and without cycloplegia in primary school children. Am J Ophthalmol 2006;142(1):68–74. https://doi.org/10.1016/j.ajo.2006.01.084.

[123] Venkataraman AP, Brautaset R, Domínguez-Vicent A. Effect of six different autorefractor designs on the precision and accuracy of refractive error measurement. PLoS One 2022;17(11):e0278269. https://doi.org/10.1371/journal.pone.0278269.

[124] Dhallu SK, et al. Factors influencing pseudo-accommodation: the difference between subjectively reported range of clear focus and objectively measured accommodation range. Vision (Basel) 2019;3(3):34. https://doi.org/10.3390/vision3030034.

[125] Hirota M, Morimoto T, Miyoshi T, Fujikado T. Simultaneous measurement of objective and subjective accommodation in response to step stimulation. Invest Ophthalmol Vis Sci 2020;61(13):38. https://doi.org/10.1167/iovs.61.13.38.

[126] Win-Hall DM, Glasser A. Objective accommodation measurements in prepresbyopic eyes using an autorefractor and an aberrometer. J Cataract Refract Surg 2008;34(5):774–784. https://doi.org/10.1016/j.jcrs.2007.12.033.

[127] Vasudevan B, Fisher B, Case B, Lam P, Wayman J. Progression of lower and higher-order aberrations: a longitudinal study. BMC Ophthalmol 2015;15:11. https://doi.org/10.1186/1471-2415-15-11.

[128] Demir P, Macedo AF, Chakraborty R, Baskaran K. Comparison of an open-view autorefractor with an open-view aberrometer in determining peripheral refraction in children. J Optom 2023;16(1):20–29. https://doi.org/10.1016/j.optom.2021.12.002.

[129] Hughes RPJ, Read SA, Collins MJ, Vincent SJ. Higher-order aberrations and retinal image quality during short-term accommodation in myopic and non-myopic children. Ophthalmic Physiol Opt 2023;43(4):827–841. https://doi.org/10.1111/opo.13146.

[130] Carracedo G, Carpena-Torres C, Serramito M, Batres-Valderas L, Gonzalez-Bergaz A. Comparison between aberrometry-based binocular refraction and subjective refraction. Transl Vis Sci Technol 2018;7(4):11. https://doi.org/10.1167/tvst.7.4.11.

[131] Carracedo G, Carpena-Torres C, Pastrana C, Privado-Aroco A, Serramito M, Batres L. Repeatability of aberrometry-based automated subjective refraction in healthy and keratoconus subjects. J Ophthalmol 2020;2020:4831298. https://doi.org/10.1155/2020/4831298.

[132] Maeda N. Clinical applications of wavefront aberrometry: a review. Clin Exp Ophthalmol 2009;37:118–129. https://doi.org/10.1111/j.1442-9071.2009.02005.x.

[133] Bhatt UK, et al. Design and validity of a miniaturized open-field aberrometer. J Cataract Refract Surg 2013;39(1):36–40. https://doi.org/10.1016/j.jcrs.2012.08.052.

[134] Nguyen MT, Berntsen DA. Aberrometry repeatability and agreement with autorefraction. Optom Vis Sci 2017;94(9):886–893. https://doi.org/10.1097/OPX.0000000000001107.

[135] Rao DP, et al. Validation of a simple-to-use, affordable, portable wavefront aberrometry-based autorefractometer in adults: a prospective study. BMC Ophthalmol 2022;22(1):2684. https://doi.org/10.1186/s12886-022-02684-5.

[136] Gabriel C, Klaproth OK, Titke C, Baumeister M, Bühren J, Kohnen T. Repeatability of topographic and aberrometric measurements at different accommodative states using a combined topographer and open-view aberrometer. J Cataract Refract Surg 2015;41(4):806–811. https://doi.org/10.1016/j.jcrs.2014.07.037.

[137] Mallen EAH, Wolffsohn JS, Gilmartin B, Tsujimura S. Clinical evaluation of the Shin-Nippon SRW-5000 autorefractor in adults. Ophthalmic Physiol Opt 2001;21(2):101–107. https://doi.org/10.1046/j.1475-1313.2001.00585.x.

[138] Yamaguchi T, et al. Validity of a miniaturised open-field aberrometer with surgical application. Invest Ophthalmol Vis Sci 2012;53(14):8673–8678. https://doi.org/10.1167/iovs.12-11093.

[139] Pedersen HR, Svarverud E, Hagen LA, Gilson SJ, Baraas RC. Comparing ocular biometry and autorefraction measurements from the Myopia Master with the IOLMaster 700 and the Huvitz HRK-8000A autorefractor. Ophthalmic Physiol Opt 2023;43(3):410–417. https://doi.org/10.1111/opo.13101.

[140] Kanda H, Kobayashi M, Mihashi T, Morimoto T, Nishida K, Fujikado T. Serial measurements of accommodation by open-field Hartmann-Shack wavefront aberrometer in eyes with accommodative spasm. Jpn J Ophthalmol 2012;56(6):617–623. https://doi.org/10.1007/s10384-012-0187-7.

[141] Harvey EM, Miller JM, Schwiegerling J. Utility of an open-field Shack-Hartmann aberrometer for measurement of refractive error in infants and young children. J AAPOS 2013;17(5):494–500. https://doi.org/10.1016/j.jaapos.2013.05.015.

[142] Vacalebre M, et al. Advanced optical wavefront technologies to improve patient quality of vision and meet clinical requests. Polymers (Basel) 2022;14(23):5321. https://doi.org/10.3390/polym14235321.

[143] Bădescu VS, Barac R, Schmitzer S, Tataru C. The influence of optical aberrations in refractive surgery. J Optom 2015;8(3):143–53. https://doi.org/10.1016/j.optom.2014.12.001.

[144] Holladay JT. Quality of vision: essential optics for the cataract and refractive surgeon. Thorofare (NJ): Slack Incorporated; 2006.

[145] Atchison DA. Recent advances in representation of monochromatic aberrations of human eyes. Clin Exp Optom 2004;87(3):138–148. https://doi.org/10.1111/j.1444-0938.2004.tb03166.x.

[146] Christy J, Parab A. Aberrometry in ophthalmology and its applications in cataract surgery. TNOA J Ophthalmic Sci Res 2023;61(1):32. https://doi.org/10.4103/tjosr.tjosr_125_22.

[147] Kaschke M, Rill MS. Optical devices in ophthalmology and optometry. Oxford: Butterworth-Heinemann; 2014.

[148] Carracedo G, et al. Effect of wavefront autorefractor design on cycloplegic refraction in young hyperopes: monocular vs binocular. Photonics 2025;12(8):765. https://doi.org/10.3390/photonics12080765.

[149] Wolffsohn JS, et al. IMI—Clinical myopia control trials and instrumentation report. Invest Ophthalmol Vis Sci 2019;60:M132–M160. https://doi.org/10.1167/iovs.18-25955.

[150] Zhao Y, Li S, Fang F. Validation of widefield aberrometer for global peripheral aberration scanning. Measurement 2024;227:114304. https://doi.org/10.1016/j.measurement.2024.114304.

[151] Pusti D, Degre Kendrick C, Wu Y, Ji Q, Jung HW, Yoon G. Widefield wavefront sensor for multidirectional peripheral retinal scanning. Biomed Opt Express 2023;14(8):4190. https://doi.org/10.1364/BOE.491412.

[152] Wei LT. Design and validation of a scanning Shack-Hartmann aberrometer for measurements of the eye over a wide field of view. Opt Express 2010;18(2):1134–1143. https://doi.org/10.1364/OE.18.001134.

[153] Lundström L, Unsbo P, Gustafsson J. Off-axis wavefront measurements for optical correction in eccentric viewing. J Biomed Opt 2005;10(3):034002. https://doi.org/10.1117/1.1920587.

[154] Morimoto T, Kanda H, Hirota M, Nishida K, Fujikado T. Insufficient accommodation during binocular near viewing in eyes with intermittent exotropia. Jpn J Ophthalmol 2020;64(1):77–85. https://doi.org/10.1007/s10384-019-00695-2.

[155] Hirota M, et al. Comparison of visual fatigue caused by head-mounted display for virtual reality and two-dimensional display using objective and subjective evaluation. Ergonomics 2019;62(6):759–766. https://doi.org/10.1080/00140139.2019.1582805.

[156] Hirota M, et al. Objective evaluation of visual fatigue using binocular fusion maintenance. Transl Vis Sci Technol 2018;7(2):9. https://doi.org/10.1167/tvst.7.2.9.

[157] Lundström L, Mira-Agudelo A, Artal P. Peripheral optical errors and their change with accommodation differ between emmetropic and myopic eyes. J Vis 2009;9(6):17. https://doi.org/10.1167/9.6.17.

[158] Baskaran K, Theagarayan B, Carius S, Gustafsson J. Repeatability of peripheral aberrations in young emmetropes. Optom Vis Sci. 2010 Oct;87(10):751–759. https://doi.org/10.1097/OPX.0b013e3181f36336

[159] Bakaraju RC, Fedtke C, Ehrmann K, Ho A. Comparing the relative peripheral refraction effect of single vision and multifocal contact lenses measured using an autorefractor and an aberrometer: a pilot study. J Optom 2015;8(3):206–218. https://doi.org/10.1016/j.optom.2015.01.005.

[160] Berntsen DA, Mutti DO, Zadnik K. Study of theories about myopia progression (STAMP): design and baseline data. Optom Vis Sci 2010;87(7):482–93. https://doi.org/10.1097/OPX.0b013e3181e6f0d0

[161] Berntsen DA, Barr CD, Mutti DO, Zadnik K. Peripheral defocus and myopia progression in myopic children randomly assigned to wear single vision and progressive addition lenses. Invest Ophthalmol Vis Sci 2013;54(8):5761–5770. https://doi.org/10.1167/iovs.13-11904.

162] Lewis P, Baskaran K, Rosén R, Lundström L, Unsbo P, Gustafsson J. Objectively determined refraction improves peripheral vision. Optom Vis Sci. 2014;91(7):740–746. https://doi.org/10.1097/OPX.0000000000000301

[163] Lewis P, Venkataraman AP, Lundström L. Contrast sensitivity in eyes with central scotoma: effect of stimulus drift. Optom Vis Sci 2018;95(4):354–361. https://doi.org/10.1097/OPX.0000000000001195.

[164] Gil A, et al. Assessment of the QuickSee wavefront autorefractor for characterizing refractive errors in school-age children. PLoS One 2020;15(10):e0240933. https://doi.org/10.1371/journal.pone.0240933

Chapter 2. Open-field and closed-field aberrometry to measure ocular refraction: a prospective semi-randomized crossover study.

2.1 Introduction

Objective and subjective methods to assess ocular refraction play a crucial role in the decision-making process that brings to the optical prescription. The subjective refraction, which requires the patient's involvement and expert clinicians, is considered the "gold standard" assessment when an optical prescription needs to be released [1–3]. It has been further suggested that a preferable approach, might be to consider patient satisfaction with the subjective prescription as the gold standard.[4] Indeed, new methods and techniques have been traditionally compared to subjective refraction as a reference [5–14]. This also applies to the so-called objective methods. Objective refraction assessment, especially by new automated instruments, is increasing its clinical role, and not only as starting point of the subjective refraction [2,4]. Various procedures/techniques are available which can be clinically performed to get an objective refraction: retinoscopy, and automated procedure such as autorefractometry, aberrometry, and photo-video refractometry.[15]

Ocular aberrometers rely on different approaches, using either ingoing devices such as laser ray tracing and Tscherning aberrometers, or more commonly, outgoing methods such as the one based on the Hartmann–Shack sensor.[16–18]. In the case of outgoing aberrometers, such as those used in this study, light enters the eye and is reflected back from the fundus. In an ideal eye, the light rays that emerge from the eye are considered parallel and an undistorted plane wavefront would be formed. However, in human eyes, the information that reaches the detector of the instrument depends on ocular aberrations and it is possible to measure on a detector the deviations of the outgoing wavefront from the reference ideal plane through the so called wavefront error (W) in each point of the entrance pupil plane of the eye. These methods allow to determine a "wavefront refraction", defined as the process of deriving a conventional spherocylindrical prescription from the wavefront error measurements by considering the amount and type of aberrations present in the eye.[3] However, there are several ways (i.e. different mathematical approach) to convert an

aberration map into a spherocylindrical prescription, each with different level of accuracy and precision.[19]

Different wavefront expansion basis functions have been used to describe W. The most used are Zernike polynomials with coefficients c_n^m where m is the meridional frequency and n is the radial order. These polynomials are used to fit the wavefront slopes, and specific Zernike coefficients are calculated to obtain the best fit for W. By assuming that the wavefront is approximated by a spherocylindrical surface in the entrance pupil plane, these coefficients can then be converted into the power vector notation (M, J0, and J45) through the Zernike equations (Equation 2. 1, Equation 2. 2 and Equation 2. 3) that use only second-order Zernike coefficients). Finally, these components can be easily transformed into spherocylindrical notation.[15]

$$M = \frac{-c_2^0 4\sqrt{3}}{r^2}$$

Equation 2. 1 Zernike formula to derive the M component (in dioptres, D) of the power vector from defocus coefficient c_2^0 (in µm), where r is the radius of the entrance pupil in mm

$$J_0 = \frac{-c_2^2 2\sqrt{6}}{r^2}$$

Equation 2. 2 Zernike formula to derive the value of J0 component (in D) of the power vector from c_2^2 coefficient (in µm), where r is the radius of the entrance pupil in mm

$$J_{45} = \frac{-c_2^{-2} 2\sqrt{6}}{r^2}$$

Equation 2. 3 Zernike formula to derive the value of J45 component (in D) of the power vector from c_2^{-2} coefficient (in µm), where r is the radius of the entrance pupil in mm

Aberrometers, which are now widely used in clinical practice,[20] can be categorized based on the subject's field of view into closed-field and open-field devices.[21] Typically, in the closed-field aberrometers the subjects fixates monocularly on a virtual target located inside the device, whereas in the open-field systems the subjects can binocularly look at a real target placed at a distance determined by the examiner/clinician, through an open aperture. Since in closed-field devices the virtual target inside the instrument might ignite a false proximity of the target even if it is optically displayed at infinitive,[22] a built-in fogging technique is implemented to relax accommodation.[23,24] Conversely, the open-field devices offer the distinct advantage of making measurements in a real-world environmental condition: the fixation target is in the real space and is looked binocularly, eventually eliminating the accommodation elicited by the target proximity.

Mixed results about the accuracy and repeatability of aberrometers in determining wavefront refraction are available. As far as concern closed-field aberrometry, in several studies, the agreement of wavefront refraction with subjective refraction resulted clinically good both in adult and paediatric population [11,13,14,25–27], though other studies have found differences higher than 0.25 D [28–31]. Despite the limited availability of commercialized models and the fact that many studies have been carried out on prototypes, open-field aberrometry has showed very promising ability to accurately assess refraction in comparison with subjective refraction, autorefractometry, and closed-field aberrometry.[21,27,32–36] Repeatability of wavefront refraction achieved by closed-field and open-field aberrometers resulted generally good [11,12,14,21,25,28,29,32,37] However, some aspects still need to be better understood. For example, it is possible that different factors, acting in opposite directions, may contribute, in some cases, to making the results obtained with one technique similar to those obtained with another one. Among these factors are the potential accommodation of the subject being examined, possible contributions from spherical and/or other aberrations, differences associated with the choice of the object-point distance conjugated with the retinal image during the measurement, as well as other factors. Recently, a new generation of closed-field aberrometers based on pyramidal wavefront sensor (PWS) technology has been introduced.[38–41] However, limited evidence is available about the reliability of these instruments in providing wavefront refraction[42]. Moreover, an open-field instrument based on the same PWS technology was made available raising further

interest in evaluating its reliability in assessing wavefront refraction compared with closed-field aberrometer with the same technology.

This study aimed to evaluate the agreement in assessing non-cycloplegic spherocylindrical refraction between an open-field and a closed-field PWS aberrometer, an open-field autorefractometer, and the subjective refraction. The comparison was conducted in two distinct groups: young adults and presbyopes. This allowed to evaluate whether the need to control accommodation might influence measurements outcomes. Furthermore, in the case of open-field devices, refraction was measured under both monocular and binocular viewing conditions to explore the effect of binocularity on refraction assessment.

2.2 Methods

2.2.1 Study Design

A prospective, semi-randomized, crossover study was conducted.

2.2.2 Participants

Fifty participants (mean age: 38.3 ± 16.6 years, range 18.0 - 78.9, 17 males and 33 females) were enrolled in the study on a voluntary basis (the SD reflects the spread of ages in the sample). The participants were enrolled to create two different groups, hereafter referred as “Old group” (n=23; mean age: 54.7 ± 8.5 years, range 45.5 - 78.9, 8 males and 15 females) and “Young group” (n=27; mean age: 24.3 ± 3.7 years, range 18.0 – 36.2, 9 males and 18 females) according to the inclusion criteria reported in Table 2. 1.

To calculate the necessary sample size to make paired comparisons *(in a repeated-measures design)*, a priori analysis was performed by the G*Power software (version 3.1.9.4). The mean and the standard deviation of the distribution of the refractive measurements (M component of the power vector notation) performed both with aberrometers (closed-field and open-field) and subjective procedure collected in the COMiB Research Centre in preliminary studies were used. Using the correlation between these repeated measures, the effect size resulted equal to 0.63. Having fixed the first type error α at 0.05, the power 1-β power at 0.80, for a two-tailed comparison, the sample size was equal to 23 (eyes) considering the non-parametric statistics (Wilcoxon Test).

All participants provided a written informed consent, and all procedures were conformed to the Declaration of Helsinki and were approved by the Ethical Committee of the University of Milano-Bicocca (Approval number: 0020067-UOR:003406, January 19th, 2024).

Table 2. 1 Inclusion Criteria for Subjects enrolled in the study (BCVA: best corrected visual acuity; logMAR: Logarithm base 10 of the minimum angle of resolution expressed in arcminutes; SER: spherical equivalent refraction; D: diopters).

Inclusion criteria
Age between 18 (Young Group) and 38 years or over 50 years (Old Group).
Absence of any known ocular pathology and not being subjected to refractive surgery or ocular drug treatment.
Absence of any known general pathology.
Not taking any ocular or systemic medication known to affect the ocular refraction.
BCVA better than 0.1 logMAR.
Monocular BCVA difference between the two eyes not exceeding 0.2 logMAR.
SER between +6.00D and -6.00D.
Willingness to participate in the study.

2.2.3 Devices/techniques

According to the procedure reported in the next section, three different objective devices/techniques (a closed-field aberrometer, an open-field aberrometer, and an open-field autorefractor) and a subjective procedure were used to perform refraction on the same participants.
- Closed-field aberrometer (CFA): the device used was the Osiris (CSO, Florence, Italy), which is based on PWS technology.[38,39] This system employs a four-faced pyramid wavefront sensor positioned at the focal plane of the optical system with its tip aligned to the optical axis to generate four sub-pupil images. Intensity differences among these images reflect the local slope of the wavefront as it exits the eye, providing wavefront gradients in horizontal and vertical orthogonal directions. The device utilizes an LED source with an emission wavelength centered at 850 nm. Its sensor offers superior resolution compared to commercial alternatives, capturing up to 45,000 data points for a maximum pupil diameter of 9.0 mm, equivalent to a spatial resolution of 41 μm, with a sampling rate of 33 Hz. The measurable range extends from −25.0 and +15.0 D for spherical

power, and from 0.0 to 10.0 D for cylindrical power, with supported pupil diameters ranging from 2.0 to 9.0 mm.

- Open-field aberrometer (OFA): this device was a prototype (CSO, Florence, Italy) representing the developmental version of the production-equivalent series. It is based on the same PWS technology as the CFA Osiris, described above.

- Open-field autorefractor (OFAUTO): this device was the WAM5500 GrandSeiko (Grand Seiko Co. Ltd., Hiroshima, Japan); an open-field autorefractor and keratometer. The range of measurements is ±22 D sphere and ±10 D cylinder in increments of 0.01, 0.12, or 0.25 D for power, and 1 degree for cylinder axis.[43]

-Subjective refraction: it was performed by two "senior" optometrists (randomly assigned to the participants) who were strictly aligned about the procedure performed (see below) using a phoropter while the stimuli to carry out the exam were displayed on an LCD screen at 4.5 m of distance.

2.2.4 Procedure

All measurements were performed in non-cycloplegic conditions, in both eyes, in the same clinic, following the procedure outlined in the flow chart reported in Figure 2. 1. The measurements with the three objective refraction devices (CFA, OFA, OFAUTO) were performed in a random order with 5-minute interval between them. For each single objective procedure, the measurements were collected for both right (RE) and left (LE) eye in a random order. Only in the case of OFA and OFAUTO, the measurements were also performed both monocularly (with the contralateral eye occluded with a plastic rigid patch) and binocularly with both eyes open, always in a random order. The OFA and OFAUTO were performed while the participants were asked to look at a Maltese cross at 6.0 meters distance. Objective measurements were considered valid only when fixation errors or eye misalignments (such as improper centering and focusing on the subject's pupil), blinking, etc., were absent and a minimum pupil size of 3 mm was achieved for both the open-field and the closed-field aberrometers. If any of these conditions were not met, the corresponding data were discarded and the measurements repeated. The components of the power vector (M, J0, and J45) were deduced for a pupil diameter of 3 mm for CFA and OFA. The final refraction was taken at the ocular vertex and the components of the power vector (M, J0, and J45) were achieved. [44] Subjective refraction was always performed at the end of all objective procedures, but

operators were masked compared to the previous procedures. The subjective refraction procedure included two phases: a monocular phase to identify initial Maximum Plus to Maximum Visual Acuity (MPMVA), refining cylinder axis and power by crossed cylinder, cylinder power search, and a second MPMVA. The binocular phase involved a dissociation procedure by Risley Prisms, binocular balancing and the duochrome test.[45]. Stimuli to carry out the subjective exam were displayed on an LCD screen at 4.5 m of distance. Subjective refraction values were recalculated at the ocular vertex from the measurements achieved at the end of all procedures, accounting for the vertex distance of the phoropter. All the procedures were performed at the same light condition, the illuminance at cornea level (with the device switched off) were similar (150±30 lux, as measured by HT307 luxmeter; HTItalia, Faenza, Italy).

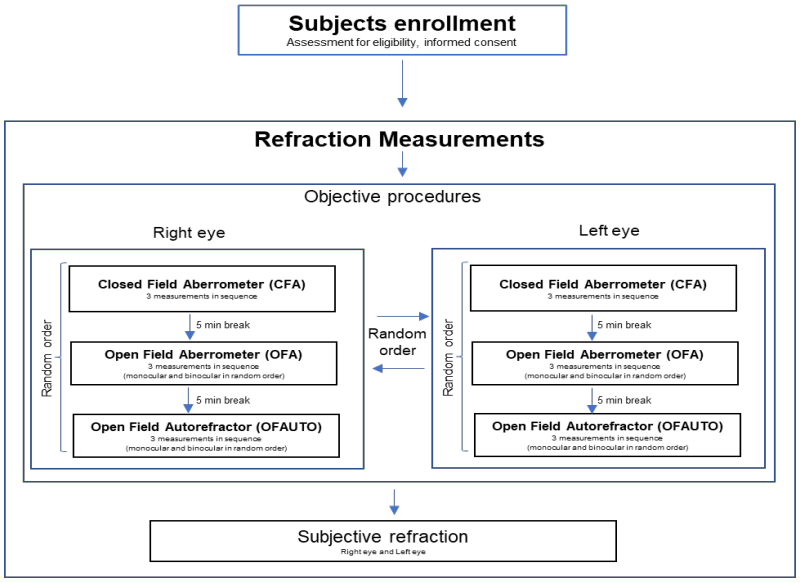

Figure 2. 1 Flow diagram of the study design

2.3 Data analysis

Data analyses were carried out separately for the RE and LE to avoid statistical issue,[46] as well as for the three components of the power vector (M, J0, and J45). Looking at the difference between the several procedures and considering the possible difference between the two groups of participants (Old Group and Young group), a two-way ANOVA (for each component of the power vector) with the four procedures of measurement (CFA, OFA, OFAUTO, and subjective refraction) as repeated measure and the two groups (Old and Young) as a between factor was carried out. In case of significance, a post-hoc analysis (Tukey test) was performed with Bonferroni adjustment applied to correct for multiple comparisons. The Spearman correlation coefficient was calculated for each pair of measurements. Additionally, Bland–Altman plots were used to assess the difference between each objective refraction procedure and subjective refraction as a function of the mean of the two measurements.[47] The presence of a proportional bias in the Bland–Altman plots was explored by examining the correlation between the average and the difference between the two measurements (objective and subjective). As far as concern the reliability, a series of different coefficients were calculated on the three measures carried out for each procedure. The coefficients of precision (CP), and repeatability (CR), and the Intraclass Correlation Coefficient (ICC) were worked out. CP was calculated as 1.96 * sw (sw is the within-subjects standard deviation for repeated measures). CR was calculated as $1.96*\sqrt{\{sw\^2\}*2}$ that is the value under

which it would be the difference between two measurements in the 95% of probability. ICC was based on single measurement, absolute agreement, two-way mixed effects model. Statistical analyses were performed with SPSS version 29.0.1 (IBM SPSS Statistics, USA).

2.4 Results

Although data analyses were carried out for the three components of the power vector (M, J0, and J45), the results presented below are limited to the M component. The results of J0 and J45 showed poor clinical implications due to small differences between the procedures; therefore, the full outcomes for J0 and J45 are reported only in the supplementary materials.

2.4.1 Agreement among the different refraction procedures

Descriptive statistics for M are reported in Table 2. 2 (RE) and Table 2. 3 (LE). The comparisons between the instruments were performed on the M mean data of CFA monocular, OFA monocular, OFAUTO monocular, and subjective procedure for right eye and left eye separately. These data set for both eyes and groups (Old and Young) did not result normally distributed (Shapiro–Wilk test; $p < 0.005$) except for the distribution of the 3rd reading of CFA in the right eye of Young group that resulted normally distributed.

Table 2. 2 Mean, standard deviation (SD), median, and interquartile range (IQR) of M values of the right eye achieved in the four procedures (for OFA and OFAUTO both in monocular and binocular conditions) for the Old Group (n = 23), and the Young Group (n = 27). The three repeated measurements and average for right eye are reported for CFA, OFA, and OFAUTO whereas in the case of subjective refraction only the final measure is reported.

	Old group (n=23)				**Young Group (n=27)**			
	First Reading Mean ± SD; Median (IQ Range) (D)	**Second Reading Mean ± SD; Median (IQ Range) (D)**	**Third Reading Mean ± SD; Median (IQ Range) (D)**	**Average Reading Mean ± SD; Median (IQ Range) (D)**	**First Reading Mean ± SD; Median (IQ Range) (D)**	**Second Reading Mean ± SD; Median (IQ Range) (D)**	**Third Reading Mean ± SD; Median (IQ Range) (D)**	**Average Reading Mean ± SD; Median (IQ Range) (D)**
CFA	-0.25 ± 2.13; 0.07 (1.75)	-0.25 ± 2.13; 0.08 (1.72)	-0.25 ± 2.14; 0.07 (1.74)	-0.25 ± 2.14; 0.07 (1.72)	-1.26 ± 1.61; -1.06 (2.75)	-1.23 ± 1.57; -0.93 (2.79)	-1.19 ± 1.60; -1.06 (2.81)	-1.23 ± 1.59; -0.95 (2.78)
OFA (Mono)	-0.30 ± 2.16; 0.16 (2.13)	-0.28 ± 2.17; 0.19 (2.16)	-0.29 ± 2.16; 0.18 (2.07)	-0.29 ± 2.16; 0.17 (2.12)	-0.64 ± 1.36; -0.07 (1.95)	-0.65 ± 1.34; 0.04 (1.90)	-0.64 ± 1.35; 0.05 (1.90)	-0.65 ± 1.35; 0.05 (1.91)
OFA (Bino)	-0.24 ± 2.13; 0.27 (2.00)	-0.27 ± 2.15; 0.30 (2.08)	-0.26 ± 2.13; 0.28 (1.99)	-0.26 ± 2.14; 0.28 (2.02)	-0.61 ± 1.38; 0.05 (1.89)	-0.60 ± 1.38; 0.04 (1.88)	-0.61 ± 1.36; 0,06 (1.88)	-0.61 ± 1.38; 0.07 (1.88)
OFAUTO (Mono)	-0.52 ± 2.15; -0.07 (1.51)	-0.48 ± 2.16; -0.03 (1.52)	-0.49 ± 2.15; 0.03 (1.54)	-0.50 ± 2.15; -0.02 (1.52)	-0.79 ± 1.45; -0.15 (1.82)	-0.77 ± 1.48; -0.31 (1.82)	-0.80 ± 1.45; -0.31 (1.81)	-0.79 ± 1.46; -0.28 (1.85)
OFAUTO (Bino)	-0.49 ± 2.12; -0.04 (1.73)	-0.47 ± 2.15; 0.02 (1.75)	-0.46 ± 2.14; -0.01 (1.80)	-0.47 ± 2.14; -0.01 (1.76)	-0.79 ± 1.39; -0.20 (1.89)	-0.74 ± 1.39; -0.12 (1.86)	-0.74 ± 1.38; -0.20 (1.86)	-0.76 ± 1.39; -0.19 (1.87)
Subjective Procedure	_____	_____	_____	-0.86 ± 2.13; -0.50 (1.49)	_____	_____	_____	-1.02 ± 1.42; -0.37 (1.95)

Table 2. 3 Mean, standard deviation (SD), median, and interquartile range (IQR) of M values of the left eye achieved in the four procedures (for OFA and OFAUTO both in monocular and binocular conditions) for the Old Group (n = 23), and the Young Group (n = 27). The three repeated measurements and average for left eye are reported for CFA, OFA, and OFAUTO whereas in the case of subjective refraction only the final measure is reported.

	Old group (n=23)				**Young Group (n=27)**			
	First Reading Mean ± SD; Median (IQ Range) (D)	**Second Reading Mean ± SD; Median (IQ Range) (D)**	**Third Reading Mean ± SD; Median (IQ Range) (D)**	**Average Reading Mean ± SD; Median (IQ Range) (D)**	**First Reading Mean ± SD; Median (IQ Range) (D)**	**Second Reading Mean ± SD; Median (IQ Range) (D)**	**Third Reading Mean ± SD; Median (IQ Range) (D)**	**Average Reading Mean ± SD; Median (IQ Range) (D)**
CFA	-0.39 ± 2.25; 0.17 (2.38)	-0.39 ± 2.26; 0.20 (2.39)	-0.38 ± 2.26; 0.20 (2.35)	-0.39 ± 2.26; 0.22 (2.37)	-1.10 ± 1.76; -0.64 (3.10)	-1.07 ± 1.72; -0.59 (3.21)	-1.04 ± 1.70; -0.62 (3.19)	-1.07 ± 1.73; -0.63 (3.11)
OFA (Mono)	-0.42 ± 2.26; 0.19 (2.19)	-0.40 ± 2.28; 0.35 (2.16)	-0.41 ± 2.27; 0.34 (2.17)	-0.41 ± 2.27; 0.34 (2.16)	-0.52 ± 1.42; 0.08 (1.89)	-0.55 ± 1.39; 0.12 (1.88)	-0.54 ± 1.41; 0.09 (1.90)	-0.54 ± 1.40; 0.10 (1.89)
OFA (Bino)	-0.39 ± 2.27; 0.37 (2.08)	-0.44 ± 2.30; 0.34 (2.68)	-0.43 ± 2.29; 0.37 (2.71)	-0.42 ± 2.28; 0.36 (2.36)	-0.46 ± 1.39; 0.08 (1.93)	-0.46 ± 1.40; 0.07 (1.91)	-0.47 ± 1.42; 0.06 (1.88)	-0.46 ± 1.40; 0.06 (1.91)
OFAUTO (Mono)	-0.59 ± 2.27; 0.06 (2.54)	-0.58 ± 2.26; 0.09 (2.48)	-0.57 ± 2.28; 0.10 (2.56)	-0.58 ± 2.27; 0.08 (2.57)	-0.81 ± 1.43; -0.20 (1.87)	-0.77 ± 1.42; -0.11 (1.88)	-0.75 ± 1.45; -0.04 (1.92)	-0.78 ± 1.43; -0.13 (1.92)
OFAUTO (Bino)	-0.61 ± 2.27; 0.03 (2.29)	-0.59 ± 2.28; 0.06 (2.23)	-0.57 ± 2.29; 0.05 (2.38)	-0.59 ± 2.28; 0.05 (2.34)	-0.71 ± 1.42; 0.01 (1.83)	-0.69 ± 1.44; 0.06 (1.80)	-0.70 ± 1.44; 0.06 (1.77)	-0.70 ± 1.43; 0.04 (1.80)
Subjective Procedure	_____	_____	_____	-0.99 ± 2.27; -0.37 (3.07)	_____	_____	_____	-1.03 ± 1.44; -0.37 (1.95)

The two-way ANOVA, run for the M component of the power vector (Figure 2. 2) in the right eye, showed a main effect of procedure (within the subjects) ($F_{(3,144)}$= 6.84; Greenhouse-Geisser correction: p = 0.007), with an effect of group was not significant ($F_{(1,48)}$= 0.82; p = 0.37), whereas interaction resulted significant; ($F_{(3,144)}$ = 5.80; Greenhouse-Geisser correction: p = 0.01). Separate post-hoc analyses (Tukey test with Bonferroni correction) for the right eye showed a significant difference for these comparisons: for the Old group, between OFA and OFAUTO (p=0.035), OFA and subjective (p<0.001), and OFAUTO and subjective (p<0.001); whereas in the Young group between OFA and subjective (p<0.001) and OFAUTO and subjective (p=0.018). A similar scenario was found in the case of M (Figure 2. 3), for the left eye. The main effect of procedure (within the subjects) was present ($F_{(3,144)}$= 9.83; Greenhouse-Geisser correction: p<0.001), the effect of group was not significant ($F_{(1,48)}$= 0.25; p = 0.62), whereas interaction resulted significant; ($F_{(3,144)}$ = 4.29; Greenhouse-Geisser correction: p = 0.03). Separate post-hoc analyses (Tukey test with Bonferroni correction) for the left eye showed a significant difference for three comparisons in the Old group: between OFA and OFAUTO (p=0.03), OFA and subjective (p<0.001), and OFAUTO and subjective (p=0.006). Also, in the Young group three comparisons resulted

significant: between OFA and OFAUTO ($p<0.001$), OFA and subjective ($p=0.02$) and OFAUTO and subjective ($p=0.04$).

In Figure 2. 4 a and b are reported the scatterplots between right eye M values achieved with subjective refraction versus objective procedures for the Old group and the Young group respectively. In Figure 2. 5 a and b are reported the scatterplots between left eye M values achieved with subjective refraction versus objective procedures in the Old group and Young group respectively. In the right eye (Old group), a significant correlation was found between the M value measured with subjective refraction and the objective methods: Spearman's Rho resulted 0.91, 0.98, and 0.98 ($p<0.001$), for the relations subjective-CFA, subjective-OFA, and subjective-OFAUTO respectively. Also, in the right eye of the Young group a significant correlation was found between the M value measured with subjective refraction and the objective methods: Spearman's Rho resulted 0.61, 0.97, and 0.96 ($p<0.001$), for the relations subjective-CFA, subjective-OFA, and subjective-OFAUTO respectively.

Similarly, in the left eye (Old group), a significant correlation was found between the M value measured with subjective refraction and the objective methods: Spearman's Rho resulted 0.99, 0.99, and 0.99 (all $ps<0.001$), for the relations subjective-CFA, subjective-OFA, and subjective-OFAUTO respectively. Also, for the Young group a significant correlation was found between the M value measured with subjective refraction and the objective methods: Spearman's Rho resulted 0.69 ($p<0.001$), 0.96 ($p<0.001$), and 0.95 ($p<0.001$), for the relations subjective-CFA, subjective-OFA, and subjective-OFAUTO respectively.

No Bland–Altman plots of the relationship between M values achieved by subjective refraction and the objective procedures (CFA, OFA, and OFAUTO) in the right eye both for the Old group, (Figure 2. 6 a, b, and c respectively) and the Young group (Figure 2. 7 a, b, and c) as well as in the left eye, for the Old group (Figure 2. 8 a, b, and c) and the Young group (Figure 2. 9 a, b, and c) showed any proportional bias

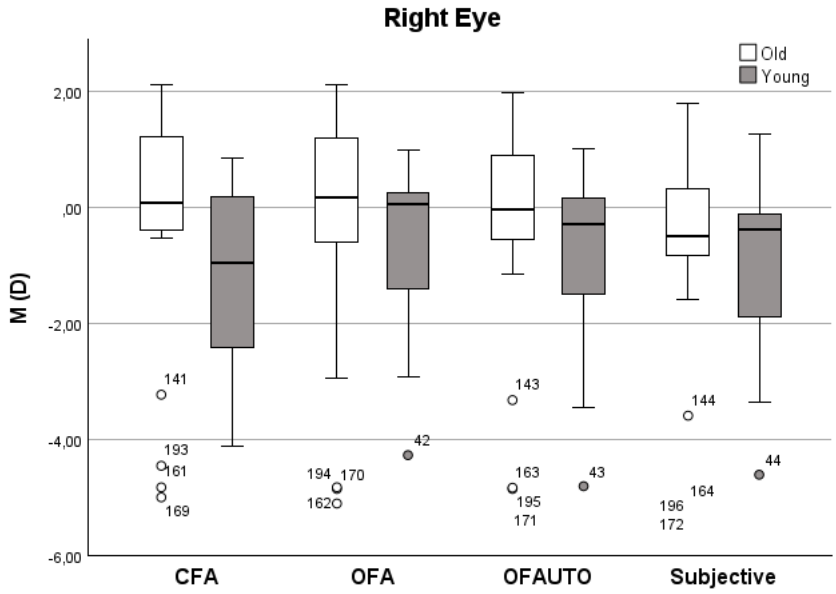

Figure 2. 2 Box and whisker plot of the M values in the right eye achieved in the four procedures for the Old Group (n = 23), and the Young Group (n = 27) respectively. CFA: Closed-field aberrometer; OFA: Open-field aberrometer; OFAUTO: Open-field autorefractor; Subjective: subjective refraction.

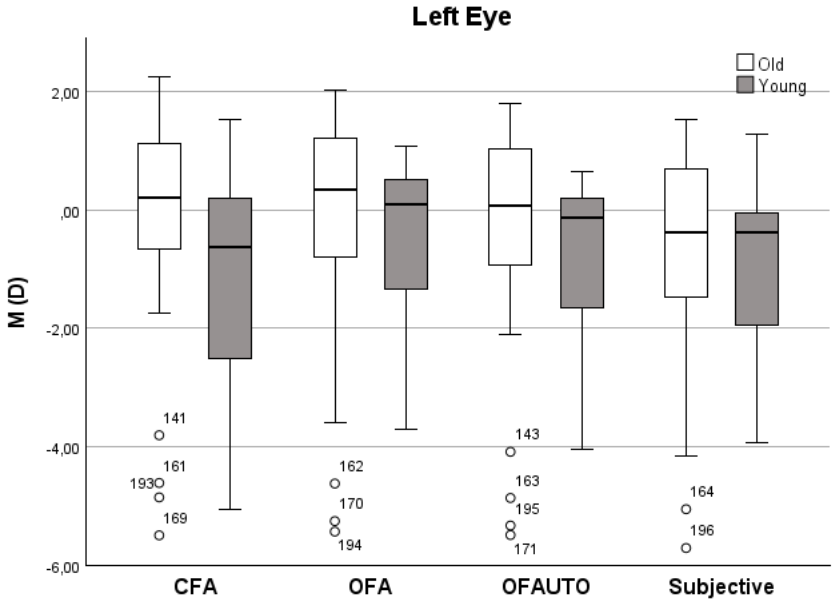

Figure 2. 3 Box and whisker plot of the M values in the left eye achieved in the four procedures for the Old Group (n = 23), and the Young Group (n = 27) respectively. CFA: Closed-field aberrometer; OFA: Open-field aberrometer; OFAUTO: Open-field autorefractor; Subjective: subjective refraction.

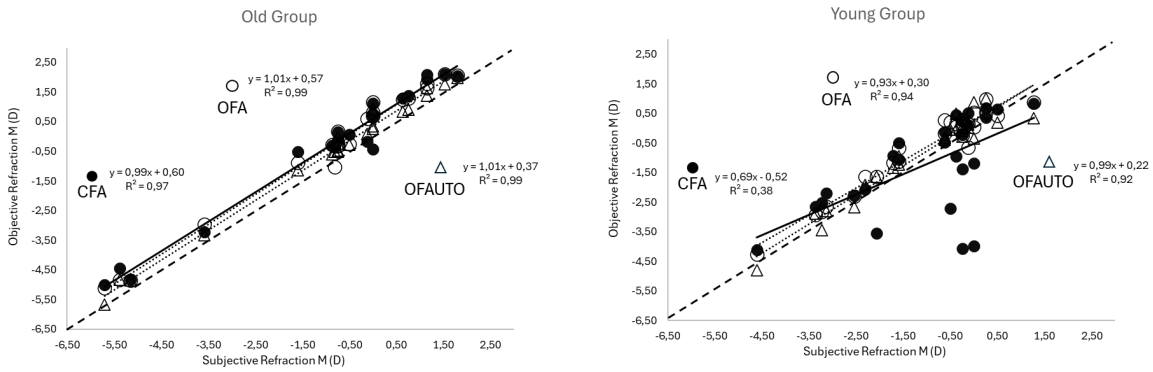

a) *b)*

Figure 2. 4 scatterplot between M values achieved with subjective refraction versus objective procedures in the right eye for the Old Group (N=23) (a) and the Young Group (N=27) (b) respectively.

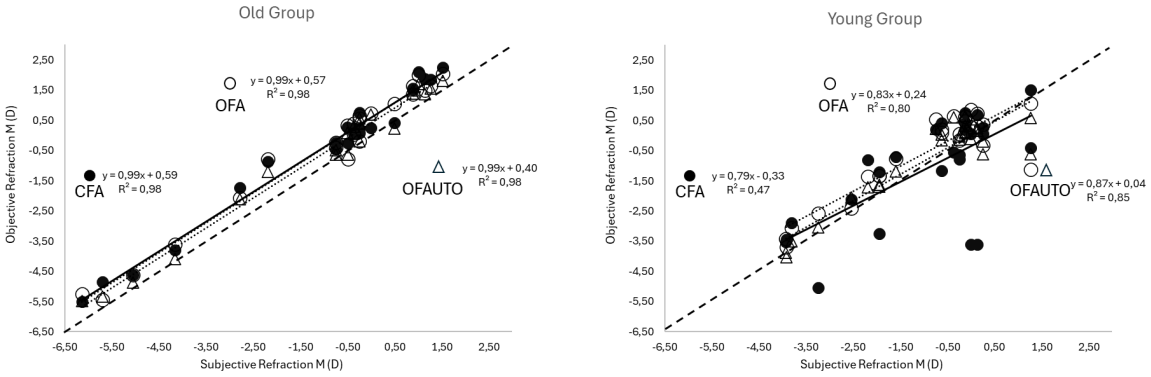

a) *b)*

Figure 2. 5 scatterplot between M values achieved with subjective refraction versus objective procedures in the left eye for the Old Group (N=23) (a) and the Young Group (N=27) (b) respectively

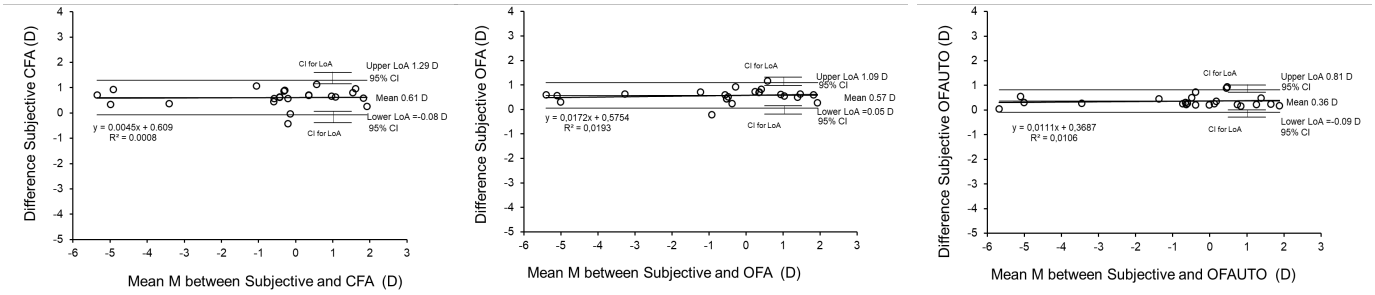

a) *b)* *c)*

Figure 2. 6 Bland–Altman plot for the relationship between M values achieved with subjective refraction and objective procedures on the right eye of the Old Group (N=23): CFA (a), OFA (b), and OFAUTO (c). The Spearman Rho coefficients between the mean and the difference of M values achieved with subjective and objective refraction resulted 0.04, 0.13, and -0.13 for CFA, OFA and OFAUTO respectively (all n.s.). The limits of agreement (LoA) were calculated as mean of difference ± 1.96 SD of difference (D).

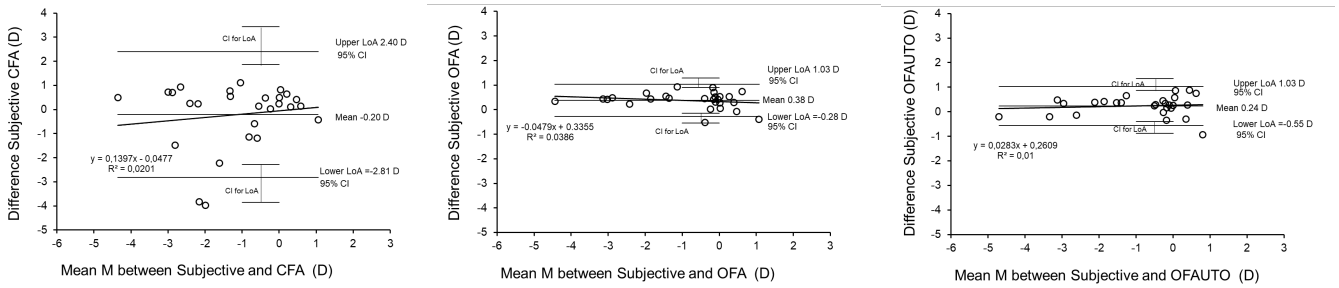

a) *b)* *c)*

Figure 2. 7 Bland–Altman plot for the relationship between M values achieved with subjective refraction and objective procedures on the right eye of the Young Group (N=27): CFA (a), OFA (b), and OFAUTO (c). Spearman Rho coefficients between the mean and the difference of M values achieved with subjective and objective refraction resulted -0.08, -0.16, and 0.07 for CFA, OFA and OFAUTO respectively (all n.s.). The limits of agreement (LoA) were calculated as mean of difference ± 1.96 SD of difference (D).

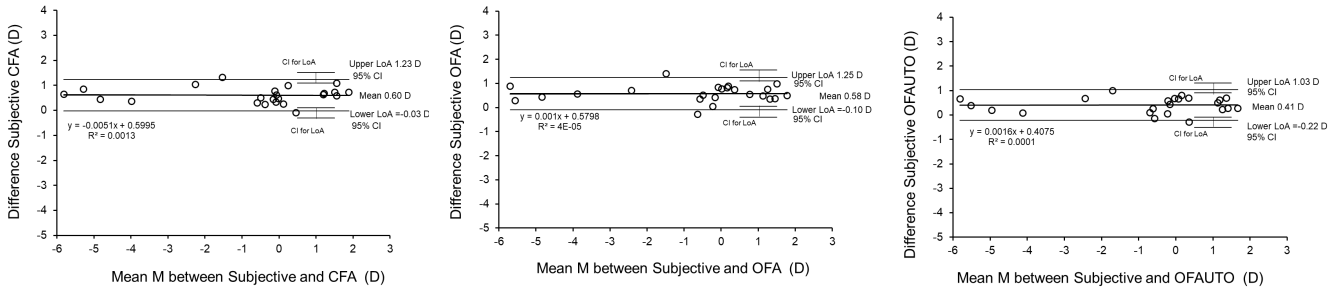

a) *b)* *c)*

Figure 2. 8 Bland–Altman plot for the relationship between M values achieved with subjective refraction and objective procedures on the left eye of the Old Group (N=23): CFA (a), OFA (b), and OFAUTO (c). Spearman Rho coefficients between the mean and the difference of M values achieved with subjective and objective refraction resulted 0.08, 0.10, and 0.09 for CFA, OFA and OFAUTO respectively (all n.s.). The limits of agreement (LoA) were calculated as mean of difference ± 1.96 SD of difference (D).

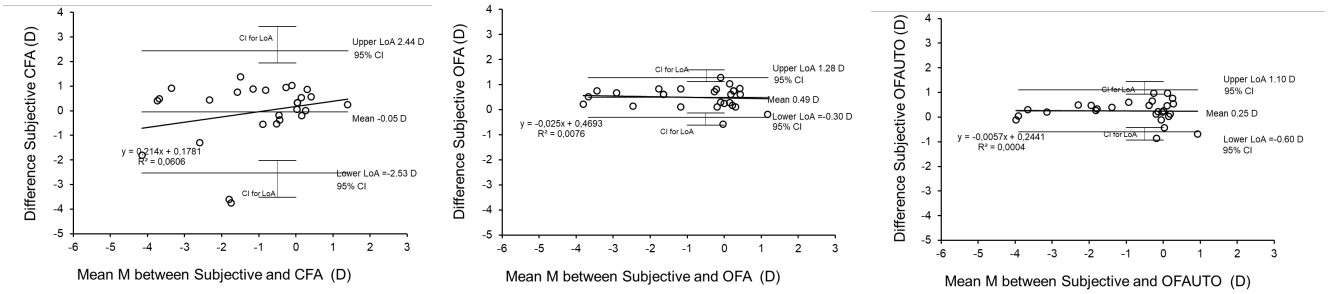

a) *b)* *c)*

Figure 2. 9 Bland–Altman plot for the relationship between M values achieved with subjective refraction and objective procedures on the left eye of the Young Group (N=27): CFA (a), OFA (b), and OFAUTO (c). Spearman Rho coefficients between the mean and the difference of M values achieved with subjective and objective refraction resulted 0.14, -0.05, and -0.04 for CFA, OFA and OFAUTO respectively (all n.s.). The limits of agreement (LoA) were calculated as mean of difference ± 1.96 SD of difference (D).

2.4.2 Mono vs Bino: M component

No statistically significant differences were found between monocular and binocular measurements of the M component of the power vector for the OFA and OFAUTO devices in the right eye of either Old or Young group (all Wilcoxon tests: n.s.). Similar results were observed for the left eye, except for the comparison between monocular and binocular measurements obtained with the OFAUTO in the Young group, which showed a significantly different (Wilcoxon test=288; p=0.02). However, this difference was considered clinically negligible (see Table 2. 3).

2.4.3 Reliability of the different refraction procedures: M component

In Table 2. 4 and Table 2. 5 are shown the CP, CR, and ICC calculated for the value M achieved in the three repeated measures for each procedure separately for the Old and the Young group in the right and left eye respectively. All the reliability coefficients worked out for all procedures were extraordinarily high in the case of old group in both eyes, with a certain reduction in reliability for the binocular measures achieved by OFA on the left eye. In the Young group the reliability of M measures is slightly reduced compared to the Old group with an important drop for CFA in both eyes.

Table 2. 4 CP, CR, and ICC calculated for the value M achieved in the right eye from the three repeated measures for each procedure separately for the old group (n = 23), and Young (n = 27). * <0.001

	Old group (n=23)			Young Group (n=27)		
	CP	**CR**	**ICC (95% CI)**	**CP**	**CR**	**ICC (95% CI)**
CFA	0.06	0.09	1.000* (1.000-1.000)	0.36	0.50	0-987* (0.976-0.994)
OFA (Mono)	0.07	0.09	1.000* (1.000-1.000)	0.09	0.13	0.999* (0.998-0.999)
OFA (Bino)	0.09	0.13	0.999* (0.999-1.000)	0.10	0.14	0.999* (0.998-0.999)
OFAUTO (Mono)	0.07	0.10	1.000* (0.999 -1.000)	0.19	0.27	0.996* (0.992-0.998)
OFAUTO (Bino)	0.09	0.13	1.000* (0.999-1.000)	0.13	0.19	0.998* (0.995-0.999)

Table 2. 5 CP, CR, and ICC calculated for the value M achieved in the left eye from the three repeated measures for each procedure separately for the old group (n = 23), and Young (n = 27). * <0.001

	Old group (n=23)			Young Group (n=27)		
	CP	**CR**	**ICC (95% CI)**	**CP**	**CR**	**ICC (95% CI)**
CFA	0.06	0.08	1.000* (1.000-1.000)	0.21	0.29	0.996* (0.993-0.998)
OFA (Mono)	0.11	0.15	0.999* (0.999-1.000)	0.12	0.17	0.998* (0.997-0.999)
OFA (Bino)	0.24	0.33	0-997* (0.994-0.999)	0.13	0.19	0.998* (0.996-0.999)
OFAUTO (Mono)	0.08	0.11	1.000* (0.999 -1.000)	0.14	0.19	0.998* (0.995-0.999)
OFAUTO (Bino)	0.09	0.12	1.000* (0.999 -1.000)	0.10	0.15	0.999* (0.997-0.999)

2.5 Discussion

Refractive measurement is an important part of optometric and ophthalmological clinical practice. The need for refractive services is globally increasing to deal with vision impairment resulting from uncorrected refractive error.[48] Objective refraction can help clinicians in feeding this need, to improve the speed of measurement to ignite the subjective refraction that is still considered the gold standard to prescribe optical correction[1–3], and eventually, in the future time, supplant completely subjective clinician refraction.[4] It is clear that such a scenario depends on the validity and repeatability of the automated procedure of objective refraction, which is why new automated instruments are studied in this sense.[5–14]. Aberrometers are sophisticated instruments, generally more expensive than autorefractometers, which are designed to measure high-order aberrations of the ocular system, but which also provide the possibility of obtaining measurements of spherocylindrical refraction. The present study looked at a pyramidal wavefront-based aberrometer, available both with a closed-field and open-field version (CFA and OFA), in determining the non-cycloplegic spherocylindrical refraction in healthy subjects. The study was conducted in a group of young people and a group of presbyopic people, to evaluate differences in spherocylindrical refraction (accuracy and reliability) measured by the instruments in groups where the need to control accommodation is different. Moreover, the evaluation made on open-field and closed-field devices offered the opportunity to evaluate the effect of binocularity on refraction assessment.

2.5.1 Accuracy of the pyramidal wavefront-based open-field and closed field aberrometry

The accuracy was evaluated by looking at the level of agreement of the wavefront-based objective technique with the subjective refraction. A further comparison was made with the open-field autorefractor (OFAUTO) which is considered as point of reference for this technology in the field: the Grand Seik.[43].

The first point to be discussed concerns the comparison between open-field and closed-field conditions. In the literature, there are several studies in which a more myopic value is found when using closed-field instruments compared to open-field methods. A negative M shift was found by Carracedo et al[21] for a monocular closed-field wavefront autorefractor (VX110; Luneau Technology; Chartres, France) in comparison to a binocular open-field wavefront autorefractor. Also, Zhu et al[31] found a myopic M shift using a Wavefront Supported Custom Ablation (Zeiss, Jena, Germany) closed-field aberrometer in comparison to manifest subject refraction. Also with some closed-field autorefractors (Retinomax K plus 2; Nikon Corp, Japan and Canon RK10; Canon, Japan, Nidek ARK700-A; Nidek Inc. Japan), it has been found a negative shift of non-cycloplegic refraction compared to subjective refraction and open-field autorefractor (Grand Seiko WR-5100 Shin-Nippon, Japan).[6,49] Compared to previous studies, a key advantage of the present work is that the only instrumental difference between OFA and CFA lies in the open-field versus closed-field condition. All other instrumental characteristics are identical, as both use the same technology produced by the same manufacturer. Consistent with previously reported findings in the literature, the data and statistical analyses from this study show that, in the specific case of young subjects, CFA yields more negative M values compared to OFA. It is likely that, during the CFA measurement, an accommodative response was ignited in the young group of participants for a reduction/failure of the efficacy of the fogging system that should limit the “instrument myopia”.[50] This wouldn’t be the case with open-field devices that should minimize accommodation response by measuring the refraction during the fixation of a target displayed at a far distance. Further support for this interpretation is provided by the greater variability observed in CFA measurements in the young group, both in comparison with presbyopic subjects and with the other methods used in the same young participants. This pattern is reasonably attributable to poorer control of accommodation under closed-field conditions.

A further point to discuss is the comparison between OFA and OFAUTO. The comparison between monocular results highlighted in the post-hoc analyses showed some significant differences though clinically limited (always lower than 0.25 D for both age groups and both eyes). Similar findings emerged from the same comparison when measurements were taken with both eyes open.

Concerning the comparison between the OFA technique and the gold standard method, namely subjective refraction, both young and presbyopic subjects show more positive M values with OFA when compared to subjective refraction—that is, less myopia is found with OFA. It should be noted that the pupil size at which the measurement is taken may play a role. Indeed, the measurements conducted in this study followed typical clinical procedures used in optometric practice. Although pupil size was not measured during the subjective refraction procedure, it is reasonable to assume—especially for the younger group—that the pupil diameter was typically larger during subjective testing than during the OFA measurement, where it was fixed at 3 mm. A larger pupil may be associated with an increase of the detected myopia (lower M) due to the eye's positive spherical aberration.[51] It would be interesting to study how M OFA values change as a function of pupil size; however, such an analysis was not conducted in this work. It is also worth noting that the OFA technique is an outgoing method, in which the emerging wavefront is compared to an ideal plane wavefront (zero vergence of light rays). In contrast, the subjective technique was conducted to find the correction at 4.5 meters, thus inducing a difference in the vergence of the incident light at the ocular plane equal to about 0.22 D compared to OFA. This vergence difference is typically negligible in optometric practice and was not treated here as a systematic error, as it falls well within the typical human depth of focus[52]. If it were to be considered, it would likely result in an even more negative value of M as determined by the subjective method. Attributing the difference between OFA and subjective refraction to difficulties in controlling accommodation also seems unlikely, as any effect of accommodation should be evident only in young subjects.

2.5.2 Monocular-Binocular Agreement in the open field devices.

Another finding of the present study was the comparison between the refraction measured by open-field devices in monocular and binocular conditions. It is well known that the accommodative system is naturally coupled with the binocular system and this interaction has been described in the interactive static model.[22] In theory, binocular refraction allows to perform refraction measurement in more "ecological conditions"; for example, no accommodation would be induced by perceived proximity. However, the perceived proximity should be also avoided in monocular conditions since the participant can look through the "open window" over the instrument, in the real environment. Moreover, considering the very far distance of fixation used in the present study during both the open-field procedures (6 m), the effect of binocularity should not introduce a big difference in the vergence response with minimum effect on the refraction. The results of the present study in terms of M vector (but also for J0 and J45; see the supplementary materials) confirmed the absence of any significant difference between monocular and binocular measurements in both groups. Therefore, in both open-field instruments (OFA and OFAUTO), the accommodative response is under control also for the Young group in non-cycloplegic conditions, contrary to what happened for the CFA.

2.5.3 Reliability

In this study, all the measurements were repeated three times to allow a repeatability assessment. The CP, and CR, worked out on the M component in the Old group of both eyes were extraordinarily good and very similar in the case of CFA, OFA mono, OFAUTO mono and bino (Table 2. 4 and Table 2. 5). Conversely, for the Young group, it is possible to spot a general slight reduction in consistency between the three measures (coefficients increased) of OFA and OFAUTO procedures, and a more sensitive drop in the case of CFA. Once again, it is possible to think that the non-cycloplegic measurement in young participants did not guarantee consistent control of accommodation. The ICC was excellent for both eyes in both groups (Old and Young). The peak repeatability performances achieved with OFA mono were in agreement with the best performances achieved for other open-field instruments such as the binocular open-field wavefront autorefractor studied by Carracedo et al[21], the Aston miniaturized open field aberrometer,[32]

the open-field COAS-HDVR aberrometer (Wavefront sciences, Albuquerque, NM)[36], the Shin-Nippon NVision-K5001[36], and open-view binocular handheld aberrometer (QuickSee)[27].

2.5.4 Limitations

The first limitation of the present study is represented by the inclusion limited to healthy participants. Usually, aberrometry is an investigation procedure very useful in the characterization of eyes with high-order aberrations, but in such cases, the accuracy of spherocylindrical refraction might be poorer than the one observed in this study. It has been demonstrated that in the case of manipulation of the cornea by refractive surgery or orthokeratology, the disparity between objective and subjective refraction can be increased.[4]
A second limitation is that patients were enrolled with a spherical equivalent refraction between +6.00D and -6.00D: actually, the sphere was comprised between -6.00 D and +2.00 D, and the cylinder was not higher than 2.00 D. This means that the outcomes cannot be automatically extended beyond these borders.
The absence of a detailed investigation into the variation of results with pupil size constitutes an additional limitation, highlighting the need for further research in this area.

2.6 Conclusion

This study investigated the accuracy and reliability of a pyramidal wavefront sensor based aberrometer, in both closed-field (CFA) and open-field (OFA) configurations, in assessing non-cycloplegic spherocylindrical refraction. The comparison included a commercially available open field autorefractor (OFAUTO) and standard subjective refraction as the clinical reference.

In younger participants, CFA showed a more myopic shift in refraction values compared to OFA, likely due to accommodative activation. This highlights the challenge of accommodation control in non-cycloplegic conditions for closed-field systems. Both OFA and OFAUTO showed high reliability, with repeatability coefficients and ICC values indicating excellent measurement consistency. Binocular versus monocular measurements in the open-field devices yielded no clinically significant differences, reinforcing the robustness of measurements under both

conditions. OFA tended to produce slightly more hyperopic values compared to subjective refraction, this may be tentatively attributed to differences in pupil size.

Overall, the OFA and OFAUTO performed well across age groups and demonstrated strong potential for clinical adoption, especially in scenarios requiring rapid, repeatable, and less examiner-dependent refractive assessments.

2.7 References

[1] Elliott DB. What is the appropriate gold standard test for refractive error? Ophthalmic Physiol Opt 2017;37:115–7. https://doi.org/10.1111/opo.12360.

[2] Atchison DA. Objective refraction. In: Rosenfield M, Logan N, editors. Optom. Sci. Tech. Clin. Manag., Elsevier Health Sciences.; 2009.

[3] Thibos LN, Himebaugh N l., Coe CD. Wavefront refraction. In: Benjamin WJ, editor. Borish's Clin. Refract., Elsevier Health Sciences.; 2006.

[4] Bullimore M. Will the auto-refractor ever replace the optometrist? Ophthalmic Physiol Opt 2000;20:S4–5. https://doi.org/10.1016/s0275-5408(99)00081-2.

[5] Davies LN, Mallen EAH, Wolffsohn JS, Gilmartin B. Clinical evaluation of the Shin-Nippon NVision-K 5001/Grand Seiko WR-5100K autorefractor. Optom Vis Sci 2003;80:320–4. https://doi.org/10.1097/00006324-200304000-00011.

[6] Choong YF, Chen AH, Goh PP. A Comparison of Autorefraction and Subjective Refraction With and Without Cycloplegia in Primary School Children. Am J Ophthalmol 2006;142:68–74. https://doi.org/10.1016/j.ajo.2006.01.084.

[7] Kemchoknatee P, Sunlakaviset P, Khieokhoen N, Srisombut T, Tangon D. A Comparison of Autorefraction and Subjective Refraction in an Academic Optometry Clinic. Cureus 2023;15. https://doi.org/10.7759/cureus.37448.

[8] Mallen EAH, Wolffsohn JS, Gilmartin B, Tsujimura S. Clinical evaluation of the Shin-Nippon SRW-5000 autorefractor in adults. Ophthalmic Physiol Opt 2001;21:101–7. https://doi.org/10.1046/j.1475-1313.2001.00585.x.

[9] Kinge B. Clinical evaluation of the Allergan Humphrey 500 autorefractor and the Nidek AR-1000 autorefractor. Br J Ophthalmol 1996;80:35–9. https://doi.org/10.1136/bjo.80.1.35.

[10] Wolffsohn JS, Davies LN, Naroo SA, Buckhurst PJ, Gibson GA, Gupta N, et al. Evaluation of an open-field autorefractor's ability to measure refraction and hence potential to assess objective accommodation in pseudophakes. Br J Ophthalmol 2011;95:498–501. https://doi.org/10.1136/bjo.2010.185009.

[11] Shneor E, Millodot M, Avraham O, Amar S, Gordon-Shaag A. Clinical evaluation of the L80 autorefractometer. Clin Exp Optom 2012;95:66–71. https://doi.org/10.1111/j.1444-0938.2011.00644.x.

[12] Pesudovs K, Parker KE, Cheng H, Applegate RA. The precision of wavefront refraction compared to subjective refraction and autorefraction. Optom Vis Sci 2007;84:387–92. https://doi.org/10.1097/OPX.0b013e31804f81a9.

[13] Rao DP, Negiloni K, Gurunathan S, Velkumar S, Sivaraman A, Baig AU, et al. Validation of a simple-to-use, affordable, portable, wavefront aberrometry-based auto refractometer in the adult population: A prospective study. BMC Ophthalmol 2022;22. https://doi.org/10.1186/s12886-022-02684-5.

[14] Gordon-Shaag A, Piñero DP, Kahloun C, Markov D, Parnes T, Gantz L, et al. Validation of refraction and anterior segment parameters by a new multi-diagnostic platform (VX120). J Optom 2018;11:242–51. https://doi.org/10.1016/j.optom.2017.12.003.

[15] Kaschke M, Donnerhacke KH, Rill MS. Optical Devices in Ophthalmology and Optometry: Technology, Design Principles and Clinical Applications. vol. 9783527410. 2014. https://doi.org/10.1002/9783527648962.

[16] Molebny V V., Panagopoulou SI, Molebny S V., Wakil YS, Pallikaris IG. Principles of ray tracing aberrometry. J. Refract. Surg., vol. 16, 2000, p. S572–5. https://doi.org/10.3928/1081-597x-20000901-17.

[17] Liang J, Grimm B, Goelz S, Bille JF. Objective measurement of wave aberrations of the human eye with the use of a Hartmann–Shack wave-front sensor. J Opt Soc Am A 1994;11:1949. https://doi.org/10.1364/josaa.11.001949.

[18] Mrochen M, Kaemmerer M, Mierdel P, Krinke HE, Seiler T. Principles of Tscherning aberrometry. J. Refract. Surg., vol. 16, 2000. https://doi.org/10.3928/1081-597x-20000901-16.

[19] Thibos LN, Xin H, Bradley A, Applegate RA. Accuracy and precision of objective refraction from wavefront aberrations. J Vis 2004;4:329–51. https://doi.org/10.1167/4.4.9.

[20] Applegate R, Atchison D, Bradley A, Bruce A, Collins M, Marsack J, et al. Wavefront refraction and correction. Optom Vis Sci 2014;91:1154–5. https://doi.org/10.1097/OPX.0000000000000373.

[21] Carracedo G, Carpena-Torres C, Batres L, Serramito M, Gonzalez-Bergaz A. Comparison of Two Wavefront Autorefractors: Binocular Open-Field versus Monocular Closed-Field. J Ophthalmol 2020;2020. https://doi.org/10.1155/2020/8580471.

[22] Hung GK, Ciuffreda KJ, Rosenfield M. Proximal contribution to a linear static model of accommodation and vergence. Ophthalmic Physiol Opt 1996;16:31–41. https://doi.org/10.1016/0275-5408(95)00110-7.

[23] Sankaridurg P, He X, Naduvilath T, Lv M, Ho A, Smith E, et al. Comparison of noncycloplegic and cycloplegic autorefraction in categorizing refractive error data in children. Acta Ophthalmol 2017;95:e633–40. https://doi.org/10.1111/aos.13569.

[24] Domínguez-Vicent A, Al-Soboh L, Brautaset R, Venkataraman AP. Effect of instrument design and technique on the precision and accuracy of objective refraction measurement. J Clin Med 2020;9:1–9. https://doi.org/10.3390/jcm9103061.

[25] Salmon TO, West RW, Gasser W, Kenmore T. Measurement of refractive errors in young myopes using the COAS Shack-Hartmann aberrometer. Optom Vis Sci 2003;80:6–14. https://doi.org/10.1097/00006324-200301000-00003.

[26] Cooper J, Citek K, Feldman JM. Comparison of refractive error measurements in adults with Z-View aberrometer, Humphrey autorefractor, and subjective refraction. Optometry 2011;82. https://doi.org/10.1016/j.optm.2010.09.013.

[27] Gil A, Hernández C, Pérez-Merino P, Rubio M, Velarde G, Abellanas-Lodares M, et al.

Assesment of the QuickSee wavefront autorefractor for characterizing refractive errors in school-age children. PLoS One 2020;15:e0240933. https://doi.org/10.1371/journal.pone.0270449.

[28] Nissman SA, Tractenberg RE, Saba CM, Douglas JC, Lustbader JM. Accuracy, Repeatability, and Clinical Application of Spherocylindrical Automated Refraction Using Time-Based Wavefront Aberrometry Measurements. Ophthalmology 2006;113:570-577.e2. https://doi.org/10.1016/j.ophtha.2005.12.021.

[29] Mcginnigle S, Naroo SA, Eperjesi F. Evaluation of the auto-refraction function of the Nidek OPD-Scan III. Clin Exp Optom 2014;97:160–3. https://doi.org/10.1111/cxo.12109.

[30] Reinstein DZ, Archer TJ, Couch D. Accuracy of the WASCA aberrometer refraction compared to manifest refraction in myopia. J Refract Surg 2006;22:268–74. https://doi.org/10.3928/1081-597x-20060301-12.

[31] Zhu X, Dai J, Chu R, Lu Y, Zhou X, Wang L. Accuracy of WASCA aberrometer refraction compared to manifest refraction in Chinese adult myopes. J Refract Surg 2009;25:1026–33. https://doi.org/10.3928/1081597X-20091016-09.

[32] Bhatt UK, Sheppard AL, Shah S, Dua HS, Mihashi T, Yamaguchi T, et al. Design and validity of a miniaturized open-field aberrometer. J Cataract Refract Surg 2013;39:36–40. https://doi.org/10.1016/j.jcrs.2012.08.052.

[33] Harvey EM, Miller JM, Schwiegerling J. Utility of an open field Shack-Hartmann aberrometer for measurement of refractive error in infants and young children. J AAPOS 2013;17:494–500. https://doi.org/10.1016/j.jaapos.2013.05.015.

[34] Durr NJ, Dave SR, Vera-Diaz FA, Lim D, Dorronsoro C, Marcos S, et al. Design and clinical evaluation of a handheld wavefront autorefractor. Optom Vis Sci 2015;92:1140–7. https://doi.org/10.1097/OPX.0000000000000732.

[35] Rubio M, Hernández CS, Seco E, Perez-Merino P, Casares I, Dave SR, et al. Validation of an Affordable Handheld Wavefront Autorefractor. Optom Vis Sci 2019;96:726–32. https://doi.org/10.1097/OPX.0000000000001427.

[36] Demir P, Macedo AF, Chakraborty R, Baskaran K. Comparison of an open view autorefractor with an open view aberrometer in determining peripheral refraction in children. J Optom 2023;16:20–9. https://doi.org/10.1016/j.optom.2021.12.002.

[37] Nguyen MT, Berntsen DA. Aberrometry Repeatability and Agreement with Autorefraction. Optom Vis Sci 2017;94:886–93. https://doi.org/10.1097/OPX.0000000000001107.

[38] Plaza-Puche AB, Salerno LC, Versaci F, Romero D, Alio JL. Clinical evaluation of the repeatability of ocular aberrometry obtained with a new pyramid wavefront sensor. Eur J Ophthalmol 2019;29. https://doi.org/10.1177/1120672118816060.

[39] Singh NK, Jaskulski M, Ramasubramanian V, Meyer D, Reed O, Rickert ME, et al. Validation of a Clinical Aberrometer Using Pyramidal Wavefront Sensing. Optom Vis Sci 2019;96:733–44. https://doi.org/10.1097/OPX.0000000000001435.

[40] Yang Y, Rui N, Shuoyu X, Xiahou J, Li J, Savini G, et al. Evaluation of the Agreement

Between a New Pyramid Wavefront Sensor Aberrometer and Scheiner-Smirnov Aberrometers. J Refract Surg 2024;40:e218–28.

[41] Frings A, Hassan H, Allan BD. Pyramidal aberrometry in wavefront-guided myopic LASIK. J Refract Surg 2020;36:442–8. https://doi.org/10.3928/1081597X-20200519-03.

[42] Nti A., Dolce J., Berntsen DA. Validation of autorefraction and relative peripheral refraction with a pyramidal wavefront sensor. Invest Ophthalmol Vis Sci 2023;64.:3303–3303.

[43] Sheppard AL, Davies LN. Clinical evaluation of the Grand Seiko Auto Ref/Keratometer WAM-5500. Ophthalmic Physiol Opt 2010;30:143–51. https://doi.org/10.1111/j.1475-1313.2009.00701.x.

[44] Thibos LN, Wheeler W, Horner D. Power vectors: An application of fourier analysis to the description and statistical analysis of refractive error. Optom Vis Sci 1997;74:367–75. https://doi.org/10.1097/00006324-199706000-00019.

[45] Borish IM, Benjamin WJ. Monocular and binocular subjective refraction. In: Benjamin WJ, editor. Borish's Clin. Refract., Saunders; 1998, p. 790–872.

[46] Armstrong RA. Statistical guidelines for the analysis of data obtained from one or both eyes. Ophthalmic Physiol Opt 2013;33:7–14. https://doi.org/10.1111/opo.12009.

[47] Bland J, Altman D. Statistical methods for assessing agreement between two methods of clinical measurement. Int J Nurs Stud 2010;47:931–936.

[48] Holden BA, Fricke TR, Ho SM, Wong R, Schlenther G, Cronjé S, et al. Global vision impairment due to uncorrected presbyopia. Arch Ophthalmol 2008;126:1731–9. https://doi.org/10.1001/archopht.126.12.1731.

[49] Gwiazda J, Weber C. Comparison of Spherical Equivalent Refraction and Astigmatism Measured with Three Different Models of Autorefractors. Optom Vis Sci 2004;81:56–61. https://doi.org/10.1097/00006324-200401000-00011.

[50] SCHOBER HAW, DEHLER H, KASSEL R. ACCOMMODATION DURING OBSERVATIONS WITH OPTICAL INSTRUMENTS. J Opt Soc Amer 1970;60:103–7. https://doi.org/10.1364/josa.60.000103.

[51] Kingston AC, Cox IG. Population spherical aberration: Associations with ametropia, age, corneal curvature, and image quality. Clin Ophthalmol 2013;7:933–8. https://doi.org/10.2147/OPTH.S44056.

[52] Wang B, Ciuffreda KJ. Depth-of-focus of the human eye: Theory and clinical implications. Surv Ophthalmol 2006;51:75–85. https://doi.org/10.1016/j.survophthal.2005.11.003.

2.8 Supplementary Materials

2.8.1 Agreement among the different refraction procedures: J0 component

Descriptive statistics for the J0 are reported in Table S1 right eye and Table S2 left eye respectively.

The comparison between the instruments was performed on the J0 mean data of CFA, OFA monocular, OFAUTO monocular and Subjective procedure for right eye and left eye separately. On the right eye, the mean data sets for J0 resulted not normally distributed only in the case of the Young group for: all the OFA measures, all the OFAUTO measurements, and the subjective measure (Shapiro–Wilk test; $p < 0.005$). On the left eye, the mean data sets for J0 resulted not normally distributed in the case of Old group for all the CFA and OFA measures and Subjective refraction and in the Young group for Subjective refraction (Shapiro–Wilk test; $p < 0.005$).

The two-way ANOVA, run for J0 component (Figure S1) in the right eye, showed a main effect of procedure (within the subjects) ($F_{(3,144)}= 6.86$; $p = 0.01$), with a significant effect of group ($F_{(1,48)}= 12.7$; $p < 0.001$), whereas interaction resulted not significant; ($F_{(3,144)} = 3.1$; $p = 0.03$). Separate post-hoc analyses (Tukey test with Bonferroni correction) for the right eye showed a significant difference for comparisons between the CFA and OFA procedures both in the Old group ($p=0.008$ and $p=0.049$ respectively) and in the Young group. Also, a significant difference for comparisons was found between the CFA and Subjective procedures in the Young group ($p=0.002$).

A similar scenario was found in the case of J0 (Figure S2), for the left eye. The main effect of procedure (within the subjects) was present ($F_{(3,144)}= 8.32$; $p = <0.001$), with a significant effect of group ($F_{(1,48)}= 8.41$; $p = 0.006$), whereas interaction resulted not significant ($F_{(3,144)} = 0.42$; $p = 0.74$).

Separate post-hoc analyses (Tukey test with Bonferroni correction) for the left eye showed a significant difference for comparisons between the CFA and OFA in the Old group ($p=0.013$).

In Figure S3 a and b are reported the scatterplots between right eye J0 values achieved with subjective refraction versus objective procedures for the Old group and the Young group respectively. In Figure S4 a and b are reported the scatterplots between left eye J0 values achieved with subjective refraction versus objective procedures in the Old group and the Young group respectively.

The correlation analysis resulted exactly as the one achieved for the M vector component. In the right eye of the Old group, a significant correlation was found between the J0 value measured with subjective refraction and the objective methods: Spearman's Rho resulted 0.95, 0.90, and 0.87 ($p<0.001$), for the relations subjective-CFA, subjective-OFA, and subjective-OFAUTO respectively. Also, in the right eye of the Young group a significant correlation was found between the J0 value measured with subjective refraction and the objective methods: Spearman's Rho resulted 0.68 ($p<0.001$), 0.69 ($p<0.001$), and 0.60 ($p=0.001$), for the relations subjective-CFA, subjective-OFA, and subjective-OFAUTO respectively.

Similarly, in the left eye (Old group), a significant correlation was found between the J0 value measured with subjective refraction and the objective methods: Spearman's Rho resulted 0.66, 0.77, and 0.72 ($p<0.001$), for the relations subjective-CFA, subjective-OFA, and subjective-OFAUTO respectively. Also, for the Young group a significant correlation was found between the J0 value measured with subjective refraction and the objective methods: Spearman's Rho resulted 0.81, 0.70, and 0.80 (all $p<0.001$), for the relations subjective-CFA, subjective-OFA, and subjective-OFAUTO respectively.

In the right eye, Bland–Altman plots showed a proportional bias for the relationship between difference and mean of J0 values achieved by subjective refraction and CFA in the Old group (r of Pearson=0.60; p=0.003) (Figure S5a) and for the relationship between difference and mean of subjective refraction and OFA in the Young group (Spearman Rho=0.53; p=0.004) (Figure S6b). No proportional bias was found in the remaining comparisons (Figure S5b, c, S6a, and c).

In the left eye, no Bland–Altman plots for the relationship between difference and mean of J0 values achieved by subjective refraction and the objective procedures (CFA, OFA, and OFAUTO) showed a proportional bias both for the Old group and the Young group (Figure S7 and S8).

Table S1. Mean, standard deviation (SD), median, and interquartile range (IQR) of J0 values of the right eye achieved in the four procedures (for OFA and OFAUTO also in monocular and binocular conditions) for Old group (n = 23), and Young group (n = 27). The three repeated measurements and average are reported for CFA, OFA and OFAUTO whereas in the case of subjective refraction only the final measure is reported.

	Old group (n=23)				**Young Group (n=27)**			
	First Reading Mean ± SD; Median (IQ Range) (D)	**Second Reading Mean ± SD; Median (IQ Range) (D)**	**Third Reading Mean ± SD; Median (IQ Range) (D)**	**Average Reading Mean ± SD; Median (IQ Range) (D)**	**First Reading Mean ± SD; Median (IQ Range) (D)**	**Second Reading Mean ± SD; Median (IQ Range) (D)**	**Third Reading Mean ± SD; Median (IQ Range) (D)**	**Average Reading Mean ± SD; Median (IQ Range) (D)**
CFA	-0.02 ± 0.33; 0.00 (0.55)	-0.03 ± 0.32; 0.00 (0.53)	-0.02 ± 0.33; 0.00 (0.54)	-0.02 ± 0.32; 0.00 (0.52)	0.29 ± 0.30; 0.26 (0.41)	0.29 ± 0.34; 0.23 (0.38)	0.26 ± 0.32; 0.28 (0.43)	0.28 ± 0.30; 0.27 (0.39)
OFA (Mono)	-0.11 ± 0.29; -0.17 (0.41)	-0.12 ± 0.28; -0.17 (0.39)	-0.13 ± 0.29; -0.17 (0.34)	-0.12 ± 0.29; -0.17 (0.37)	0.20 ± 0.30; 0.15 (0.34)	0.20 ± 0.30; 0.17 (0.38)	0.20 ± 0.30; 0.16 (0.34)	0.20 ± 0.30; 0.16 (0.36)
OFA (Bino)	-0.13 ± 0.31; -0.17 (0.39)	-0.13 ± 0.30; -0.17 (0.35)	-0.13 ± 0.30; -0.17 (0.38)	-0.13 ± 0.29; -0.17 (0.38)	0.21 ± 0.30; 0.20 (0.40)	0.23 ± 0.31; 0.23 (0.36)	0.23 ± 0.30; 0.22 (0.43)	0.23 ± 0.30; 0.23 (0.38)
OFAUTO (Mono)	-0.02 ± 0.24; -0.03 (0.32)	-0.07 ± 0.24; -0.03 (0.29)	-0.06 ± 0.27; -0.07 (0.29)	-0.05 ± 0.24; -0.03 (0.31)	0.20 ± 0.30; 0.13 (0.37)	0.21 ± 0.29; 0.15 (0.37)	0.22 ± 0.31; 0.16 (0.31)	0.21 ± 0.30; 0.16 (0.36)
OFAUTO (Bino)	-0.07 ± 0.28; -0.06 (0.45)	-0.07 ± 0.29; -0.03 (0.47)	-0.06 ± 0.27; -0.02 (0.31)	-0.07 ± 0.28; -0.03 (0.36)	0.20 ± 0.29; 0.16 (0.29)	0.20 ± 0.27; 0.15 (0.36)	0.21 ± 0.28; 0.13 (0.32)	0.21 ± 0.28; 0.13 (0.30)
Subjective Procedure	_____	_____	_____	-0.05 ± 0.25; 0.00 (0.30)	_____	_____	_____	0.16 ± 0.26; 0.06 (0.25)

Table S2. Mean, standard deviation (SD), median, and interquartile range (IQR) of J0 values of the left eye achieved in the four procedures (for OFA and OFAUTO also in monocular and binocular conditions) for the Old group (n = 23), and the Young group (n = 27). The three repeated measurements and average are reported for CFA, OFA and OFAUTO whereas in the case of subjective refraction only the final measure is reported.

	Old group (n=23)				**Young Group (n=27)**			
	First Reading Mean ± SD; Median (IQ Range) (D)	**Second Reading Mean ± SD; Median (IQ Range) (D)**	**Third Reading Mean ± SD; Median (IQ Range) (D)**	**Average Reading Mean ± SD; Median (IQ Range) (D)**	**First Reading Mean ± SD; Median (IQ Range) (D)**	**Second Reading Mean ± SD; Median (IQ Range) (D)**	**Third Reading Mean ± SD; Median (IQ Range) (D)**	**Average Reading Mean ± SD; Median (IQ Range) (D)**
CFA	0.00 ± 0.30; 0.07 (0.26)	0.00 ± 0.28; 0.00 (0.27)	0.00 ± 0.28; 0.01 (0.27)	0.00 ± 0.29; 0.02 (0.29)	0.18 ± 0.27; 0.21 (0.37)	0.20 ± 0.27; 0.23 (0.36)	0.18 ± 0.27; 0.22 (0.36)	0.19 ± 0.27; 0.22 (0.36)
OFA (Mono)	-0.12 ± 0,30; -0.01 (0.26)	-0.11 ± 0,25; -0.05 (0.26)	-0.11 ± 0,27; -0.04 (0.29)	-0.11 ± 0,27; -0.04 (0.26)	0.10 ± 0,30; 0.00 (0.38)	0.12 ± 0,29; 0.13 (0.40)	0.12 ± 0,29; 0.13 (0.38)	0.11 ± 0,29; 0.11 (0.39)
OFA (Bino)	-0.08 ± 0,25; 0.00 (0.29)	-0.09 ± 0,26; 0.00 (0.30)	-0.09 ± 0,26; 0.00 (0.28)	-0.09 ± 0,26; 0.00 (0.29)	0.14 ± 0,31; 0.17 (0.48)	0.15 ± 0,31; 0.16 (0.39)	0.14 ± 0,30; 0.13 (0.45)	0.14 ± 0,30; 0.17 (0.44)
OFAUTO (Mono)	-0.02 ± 0.30; 0.02 (0.28)	-0.02 ± 0.25; 0.00 (0.23)	0.00 ± 0.22; 0.00 (0.30)	-0.01± 0.25; 0.02 (0.27)	0.18 ± 0.25; 0.16 (0.36)	0.18 ± 0.23; 0.14 (0.35)	0.21 ± 0.24; 0.18 (0.34)	0.19 ± 0.24; 0.15 (0.36)
OFAUTO (Bino)	-0.02 ± 0.31; 0.02 (0.34)	-0.02 ± 0.31; 0.01 (0.35)	-0.04 ± 0.30; 0.00 (0.38)	-0.03 ± 0.30; 0.01 (0.35)	0.21 ± 0.26; 0.17 (0.33)	0.20 ± 0.26; 0.18 (0.34)	0.20 ± 0.27; 0.16 (0.30)	0.21 ± 0.26; 0.17 (0.28)
Subjective Procedure	_____	_____	_____	0.00 ± 0.24; 0.02 (0.12)	_____	_____	_____	0.19 ± 0.24; 0.12 (0.35)

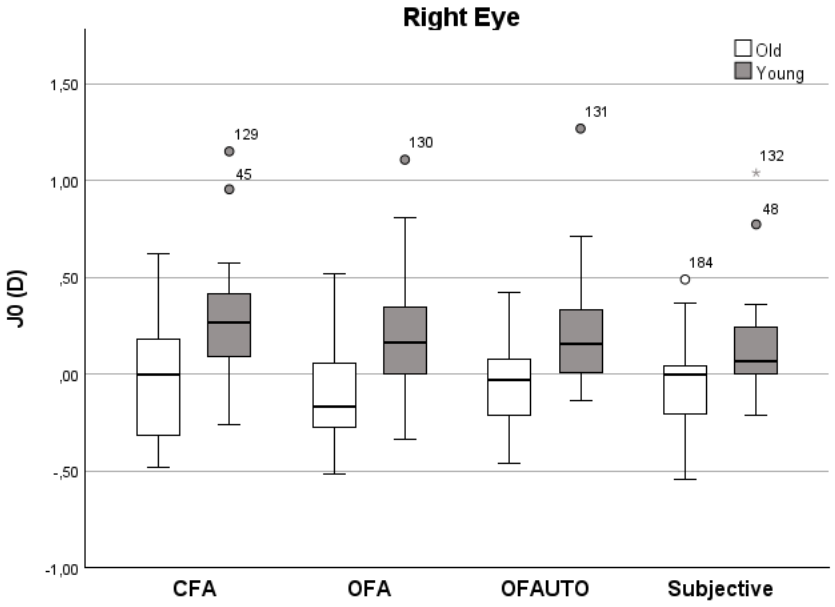

Figure S1: Box and whisker plot of the J0 values in the right eye achieved in the four procedures for the Old group (n = 23), and the Young group (n = 27) respectively. CFA: Closed-field aberrometer; OFA: Open-field aberrometer; OFAUTO: Open-field autorefractor; Subjective: subjective refraction.

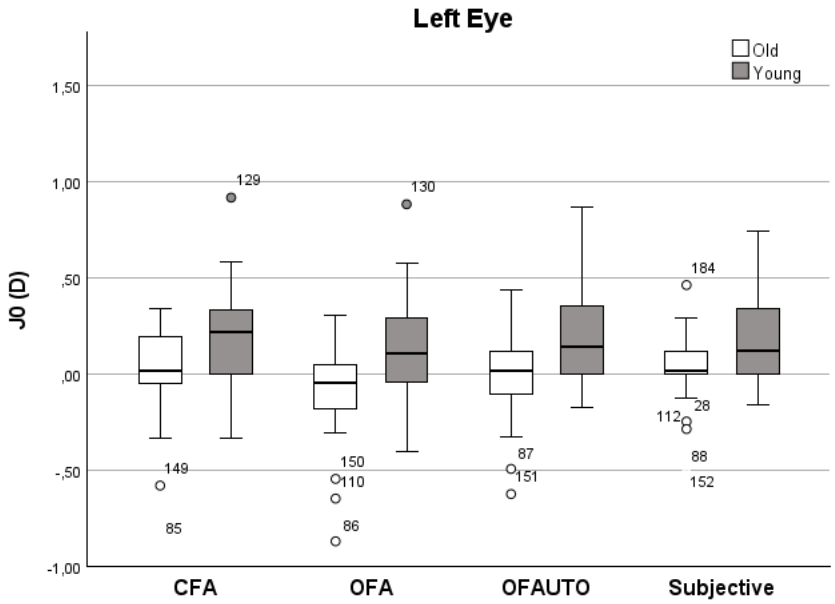

Figure S2: Box and whisker plot of the J0 values in the left eye achieved in the four procedures for the Old group (n = 23), and the Young group (n = 27) respectively. CFA: Closed-field aberrometer; OFA: Open-field aberrometer; OFAUTO: Open-field autorefractor; Subjective: subjective refraction.

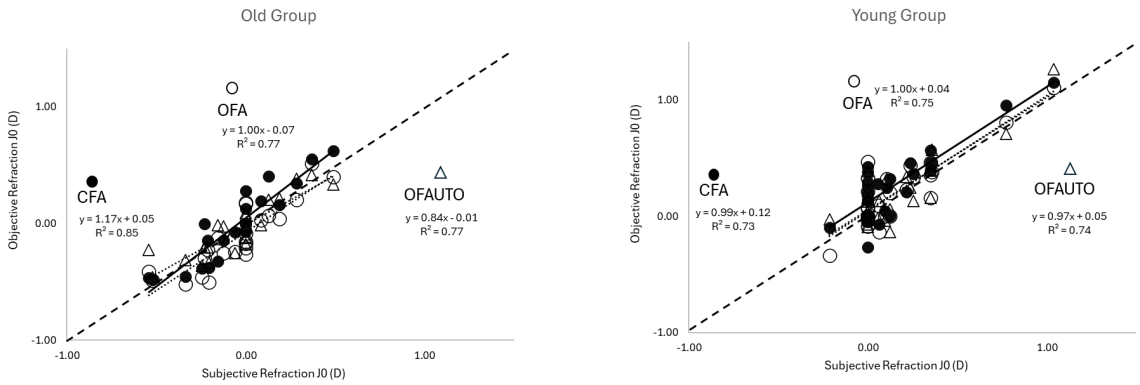

a) *b)*

Figure S3: scatterplot between J0 values achieved with Subjective refraction versus objective procedures in the right eye for the Old group (N=23) (a) and the Young group (N=27) (b) respectively.

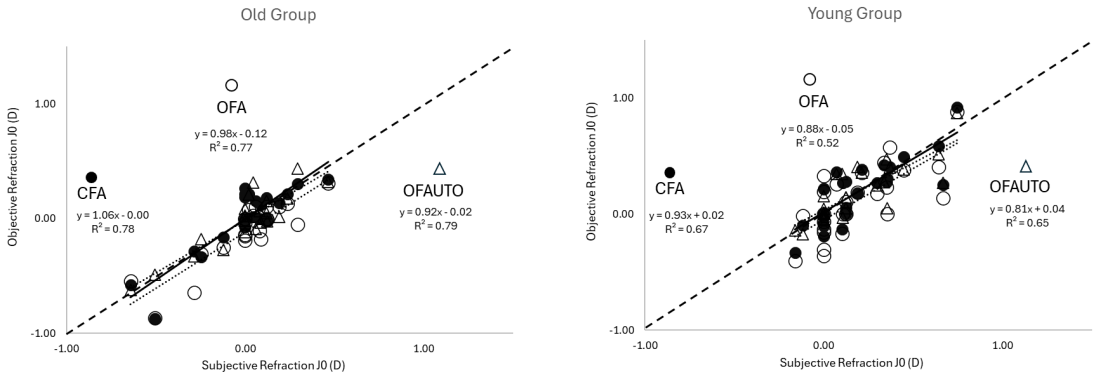

a) *b)*

Figure S4: scatterplot between J0 values achieved with Subjective refraction versus objective procedures in the left eye for the Old group (N=23) (a) and the Young group (N=27) (b) respectively.

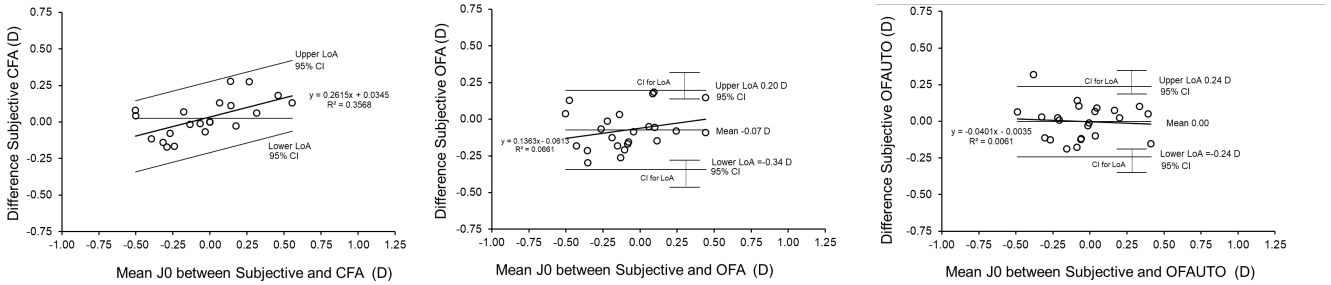

a) *b)* *c)*

Figure S5: Bland–Altman plot for the relationship between J0 values achieved with subjective refraction and objective procedure on the right eye of the Old group (N=23): CFA (a), OFA (b), and OFAUTO (c). Correlation between the difference of J0 values achieved with subjective refraction and CFA and their mean was significant (r of Pearson=0.60; p=0.03), whereas it was not significant in the case of OFA (r of Pearson=0.26; p=n.s.), and OFAUTO (r of Pearson=-0.08; p= n.s.). The limits of agreement (LoA) were calculated as mean of difference ± 1.96 SD of difference (D).

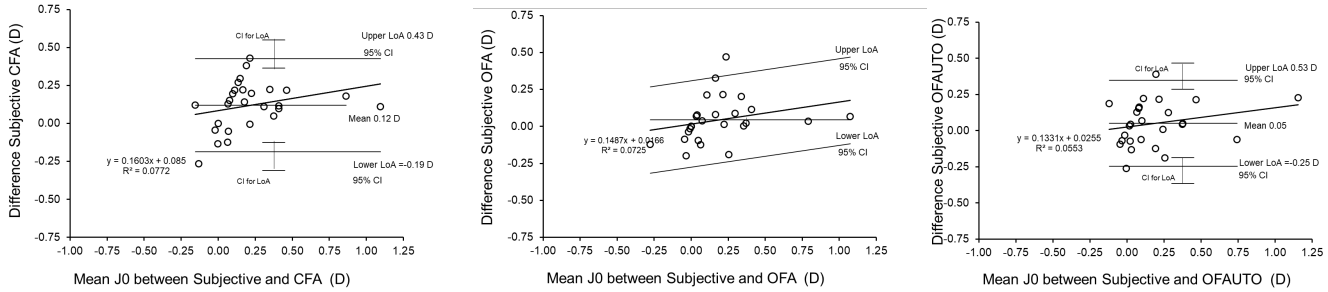

a) *b)* *c)*

Figure S6: Bland–Altman plot for the relationship between J0 values achieved with subjective refraction and objective procedure on the right eye of the Young group (N=27): CFA (a), OFA (b), and OFAUTO (c). Correlation between the difference and the mean of J0 values achieved with subjective refraction and CFA, and subjective refraction OFAUTO was not significant (Spearman Rho=0.36 and Spearman Rho =0.33 respectively). Correlation between the difference of J0 values achieved with subjective refraction and OFA and their mean was significant (Spearman Rho =0.53; p=0.004). The limits of agreement (LoA) were calculated as mean of difference ± 1.96 SD of difference (D).

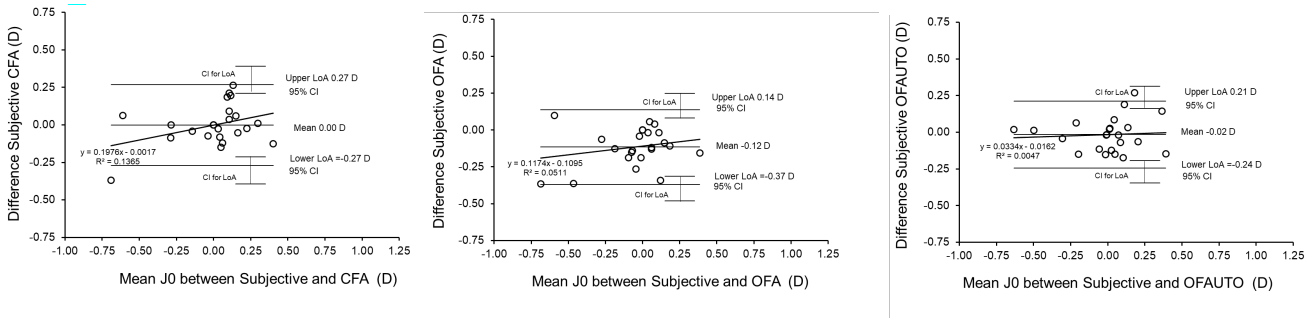

a) *b)* *c)*

Figure S7: Bland–Altman plot for the relationship between J0 values achieved with subjective refraction and objective procedure on the left eye of the Old group (N=23): CFA (a), OFA (b), and OFAUTO (c). Correlation (Spearman Rho) between the difference and the mean of J0 values achieved with subjective refraction and objective refraction resulted 0.30, 0.21, and 0.12 for CFA, OFA and OFAUTO respectively (all n.s.). The limits of agreement (LoA) were calculated as mean of difference ± 1.96 SD of difference (D).

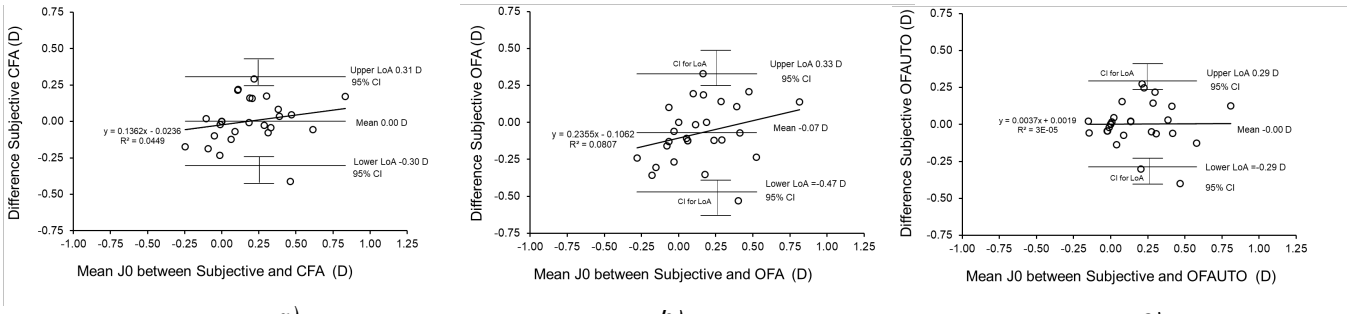

a) *b)* *c)*

Figure S8: Bland–Altman plot for the relationship between J0 values achieved with subjective refraction and objective procedure on the left eye of the Young group (N=27): CFA (a), OFA (b), and OFAUTO (c). The correlation (r of Pearson) between the difference and the mean of J0 values achieved with subjective refraction and objective refraction resulted 0.21, 0.28, and -0.01 for CFA, OFA and OFAUTO respectively (all n.s.). The limits of agreement (LoA) were calculated as mean of difference ± 1.96 SD of difference (D).

2.8.2. Mono vs Bino: J0 component

No statistically significant difference was found between monocular and binocular measurements of J0 component for OFA and OFAUTO in the right eye of Old group and the Young group (Wilcoxon test; all p= n.s.). The same results were found for the left eye (paired t test; all n.s.).

2.8.3 Reliability of the different refraction procedures: J0 component

In Tables S3 and S4 are shown the CP, CR, and ICC calculated for the value J0 achieved in the three repeated measures for each procedure, separately for Old and the Young group in the right and left eye respectively. All the reliability coefficients worked out for all procedures were extraordinarily high.

Table S3. CP, CR, and ICC calculated for the value J0 achieved in the right eye from the three repeated measures for each procedure separately for the Old group (n = 23), and Young (n = 27). * <0.001; **<0.01

	Old group (n=23)			Young Group (n=27)		
	CP	**CR**	**ICC (95% CI)**	**CP**	**CR**	**ICC (95% CI)**
CFA	0.04	0.06	0.995* (0.991-0.998)	0.11	0.16	0.966* (0.937-0.983)
OFA (Mono)	0.05	0.08	0.990* (0.981-0.996)	0.05	0.07	0.994* (0.988-0.997)
OFA (Bino)	0.03	0.05	0.997* (0.994-0.999)	0.07	0.11	0.984* (0.970-0.992)
OFAUTO (Mono)	0.14	0.20	0.914* (0.837-0.960)	0.11	0.16	0.962* (0.930-0.981)
OFAUTO (Bino)	0.10	0.14	0.965* (0.933-0.984)	0.10	0.15	0.964** (0.933-0.982)

Table S4. CP, CR, and ICC calculated for the value J0 achieved in the left eye from the three repeated measures for each procedure separately for the Old group (n = 23), and the Young group (n = 27). * <0.001

	Old group (n=23)			Young Group (n=27)		
	CP	**CR**	**ICC (95% CI)**	**CP**	**CR**	**ICC (95% CI)**
CFA	0.07	0.10	0.986* (0.972-0.994)	0.06	0.09	0.986* (0-974-0.993)
OFA (Mono)	0.13	0.19	0.938* (0.88-0.971)	0.07	0.10	0.986* (0.973-0.993)
OFA (Bino)	0.05	0.07	0-992* (0.983-0.996)	0.06	0.09	0.988* (0.978-0.994)
OFAUTO (Mono)	0.18	0.25	0.880* (0.778-0.943)	0.11	0.16	0-943* (0.986-0.972)
OFAUTO (Bino)	0.08	0.11	0-984* (0.968-0.993)	0.09	0.12	0.971* (0.947-0.986)

2.8.4 Agreement among the different refraction procedures: J45 component

Descriptive statistics for the J45 are reported in Table S5 right and S6 left eye respectively.

The comparison between the instruments was performed on the J45 mean data of CFA, OFA monocular, OFAUTO monocular and Subjective procedure for right eye and left eye separately.

On the right eye, the mean data sets for J45 resulted not normally distributed only in the case of Subjective refraction for the Old group and for CFA, OFA, and Subjective refraction and in the Young group (Shapiro–Wilk test; $p < 0.005$). On the left eye, the mean data sets for J45 resulted not normally distributed only in the case OFAUTO and Subjective refraction for Old groups (Shapiro–Wilk test; $p < 0.005$).

The two-way ANOVA, run for J45 component (Figure S9) in the right eye, showed a significant effect of procedure (within the subjects) ($F_{(3,144)}= 4.11$; Greenhouse-Geisser correction: $p = 0.01$) and interaction ($F_{(3,144)} = 3.13$; Greenhouse-Geisser correction: $p = 0.03$), without a significant effect of group. Separate post-hoc analyses (Tukey test with Bonferroni correction) for the right eye showed a significant difference for comparisons only between the CFA and Subjective and OFAUTO and Subjective in the Old group ($p=0.002$ and $p=0.009$).

In the case of J45 for the left eye (Figure S10), the main effect of procedure (within the subjects), the interaction and the effect of group were not significant.

In Figures S11 a and b are reported the scatterplots between right eye J45 values achieved with Subjective refraction versus objective procedures for the Old group and the Young group respectively. In Figures S12 a and b are reported the scatterplots between left eye J45 values achieved with Subjective refraction versus objective procedures in the Old group and the Young group respectively.

In the right eye, Bland–Altman plots showed a proportional bias for the relationship between difference and mean of J45 values achieved by subjective refraction and OFA in the Old group (r of Pearson=0.54; $p=0.008$) (Figure S13b) and for the relationship between difference and mean of subjective refraction and CFA (Spearman Rho=0.45; $p=0.02$), OFA (Spearman Rho=0.51; $p=0.006$), and OFAUTO (Spearman Rho=0.58; $p=0.002$) in the Young group (Figure S14). No proportional bias was found in the remaining comparisons (Figures S13a and c). In the left eye, Bland–Altman plots showed a proportional bias for the relationship between difference and mean of J45 values achieved by subjective refraction and CFA (Spearman Rho=0.50; $p=0.001$) and subjective refraction and OFA (Spearman Rho=0.45; $p=0.03$), both in the Old group (Figures S15a

and b). No proportional bias was found in the remaining comparisons (Figures S15c, S16a, b, and c).

Table S5. Mean, standard deviation (SD), median, and interquartile range (IQR) of J45 values of the right eye achieved in the four procedures (for OFA and OFAUTO also in monocular and binocular conditions) for Old group (n = 23), and the Young group (n = 27). The three repeated measurements and average are reported for CFA, OFA and OFAUTO whereas in the case of subjective refraction only the final measure is reported.

	Old group (n=23)				**Young Group (n=27)**			
	First Reading Mean ± SD; Median (IQ Range) (D)	**Second Reading Mean ± SD; Median (IQ Range) (D)**	**Third Reading Mean ± SD; Median (IQ Range) (D)**	**Average Reading Mean ± SD; Median (IQ Range) (D)**	**First Reading Mean ± SD; Median (IQ Range) (D)**	**Second Reading Mean ± SD; Median (IQ Range) (D)**	**Third Reading Mean ± SD; Median (IQ Range) (D)**	**Average Reading Mean ± SD; Median (IQ Range) (D)**
CFA	-0.07 ± 0.17; 0.00 (0.25)	-0.06 ± 0.17; -0.01 (0.31)	-0.07 ± 0.17; 0.00 (0.26)	-0.07 ± 0.17; -0.01 (0.28)	-0.01 ± 0.14; -0.01 (0.19)	-0.01 ± 0.13; -0.04 (0.17)	-0.01 ± 0.14; 0.00 (0.19)	-0.01 ± 0.13; -0.03 (0.19)
OFA (Mono)	-0.02 ± 0.20; -0.08 (0.34)	0.00 ± 0.21; -0.02 (0.35)	-0.01 ± 0.20; -0.04 (0.32)	-0.01 ± 0.21; -0.07 (0.32)	-0.03 ± 0.16; -0.02 (0.14)	-0.02 ± 0.15; -0.03 (0.12)	-0.03 ± 0.16; -0.03 (0.14)	-0.03 ± 0.16; -0.02 (0.12)
OFA (Bino)	-0.03 ± 0.19; -0.07 (0.31)	-0.02 ± 0.18; -0.01 (0.24)	-0.03 ± 0.19; -0.10 (0.27)	-0.03 ± 0.18; -0.10 (0.28)	-0.03 ± 0.17; -0.04 (0.13)	-0.04 ± 0.17; -0.03 (0.14)	-0.04 ± 0.16; -0.03 (0.17)	-0.04 ± 0.16; -0.05 (0.15)
OFAUTO (Mono)	-0.06 ± 0.18; -0.11 (0.18)	-0.05 ± 0.17; -0.11 (0.14)	-0.08 ± 0.18; -0.11 (0.20)	-0.06 ± 0.17; -0.12 (0.16)	0.01 ± 0.19; -0.03 (0.21)	0.00 ± 0.15; -0.02 (0.19)	-0.01 ± 0.14; -0.02 (0.17)	0.00 ± 0.16; -0.03 (0.19)
OFAUTO (Bino)	-0.11 ± 0.20; -0.13 (0.28)	-0.10 ± 0.19; -0.11 (0.24)	-0.09 ± 0.19; -0.07 (0.26)	-0.10 ± 0.19; -0.09 (0.24)	-0.02 ± 0.22; -0.03 (0.22)	-0.01 ± 0.17; -0.02 (0.14)	0.02 ± 0.18; -0.04 (0.21)	0.02 ± 0.18; -0.04 (0.16)
Subjective Procedure	_____	_____	_____	0.03 ± 0.15; 0.00 (0.07)	_____	_____	_____	0.01 ± 0.11; 0.00 (0.06)

Table S6. Mean, standard deviation (SD), median, and interquartile range (IQR) of J45 values of the left eye achieved in the four procedures (for OFA and OFAUTO also in monocular and binocular conditions) for Old group (n = 23), and the Young group (n = 27). The three repeated measurements and average are reported for CFA, OFA and OFAUTO whereas in the case of subjective refraction only the final measure is reported

	Old group (n=23)				**Young Group (n=27)**			
	First Reading Mean ± SD; Median (IQ Range) (D)	**Second Reading Mean ± SD; Median (IQ Range) (D)**	**Third Reading Mean ± SD; Median (IQ Range) (D)**	**Average Reading Mean ± SD; Median (IQ Range) (D)**	**First Reading Mean ± SD; Median (IQ Range) (D)**	**Second Reading Mean ± SD; Median (IQ Range) (D)**	**Third Reading Mean ± SD; Median (IQ Range) (D)**	**Average Reading Mean ± SD; Median (IQ Range) (D)**
CFA	-0.03 ± 0.22; 0.00 (0.19)	-0.03 ± 0.23; 0.00 (0.18)	-0.03 ± 0.23; 0.00 (0.23)	-0.03 ± 0.22; 0.00 (0.19)	-0.02 ± 0.14; 0.00 (0.17)	-0.01 ± 0.15; 0.00 (0.21)	-0.01 ± 0.13; 0.00 (0.18)	-0.01 ± 0.14; 0.00 (0.18)
OFA (Mono)	0.01 ± 0.19; 0.00 (0.24)	0.02 ± 0.18; 0.02 (0.20)	0.01 ± 0.19; 0.03 (0.28)	0.01 ± 0.19; 0.02 (0.24)	-0.01 ± 0.13; 0.00 (0.19)	-0.01 ± 0.13; 0.00 (0.20)	-0.01 ± 0.13; 0.00 (0.22)	-0.01 ± 0.13; 0.00 (0.20)
OFA (Bino)	0.03 ± 0.19; 0.04 (0.12)	0.03 ± 0.19; 0.05 (0.10)	0.03 ± 0.19; 0.05 (0.10)	0.03 ± 0.19; 0.04 (0.10)	0.03 ± 0.13; 0.00 (0.17)	0.02 ± 0.13; 0.00 (0.19)	0.03 ± 0.13; 0.00 (0.22)	0.03 ± 0.13; 0.01 (0.17)
OFAUTO (Mono)	-0.01 ± 0.19; 0.00 (0.26)	-0.03 ± 0.21; -0.04 (0.28)	-0.03 ± 0.20; -0.03 (0.28)	-0.03 ± 0.19; -0.06 (0.25)	-0.04 ± 0.16; -0.02 (0.13)	-0.05 ± 0.16; -0.02 (0.17)	-0.05 ± 0.17; -0.03 (0.12)	-0.05 ± 0.16; -0.02 (0.15)
OFAUTO (Bino)	0.02 ± 0.18; 0.01 (0.24)	0.02 ± 0.19; 0.00 (0.22)	0.00 ± 0.20; 0.00 (0.19)	0.01 ± 0.18; 0.01 (0.21)	-0.02 ± 0.18; -0.03 (0.18)	-0.01 ± 0.18; -0.02 (0.15)	-0.01 ± 0.18; 0.00 (0.17)	-0.01 ± 0.18; 0.00 (0.17)
Subjective Procedure	_____	_____	_____	-0.03 ± 0.13; 0.00 (0.09)	_____	_____	_____	-0.03 ± 0.15; 0.00 (0.13)

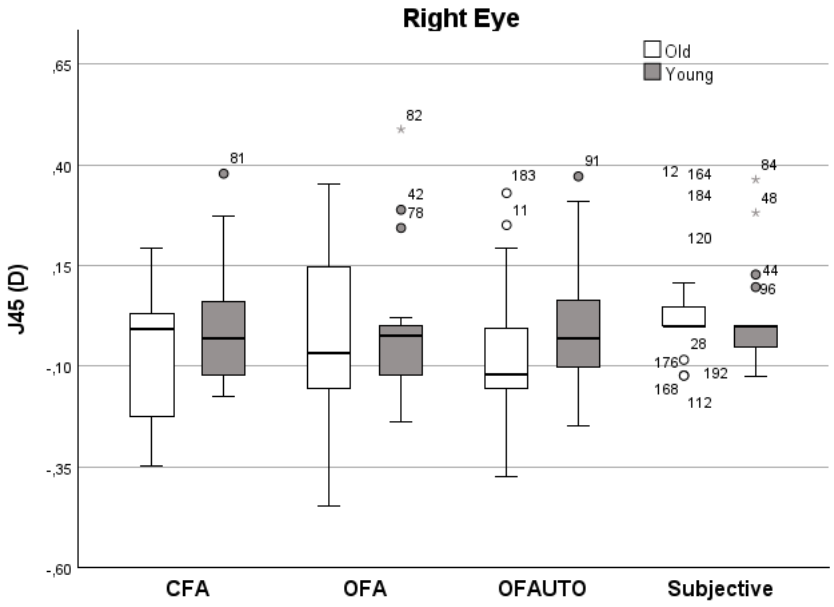

Figure S9: Box and whisker plot of the J45 values in the right eye achieved in the four procedures for the Old group (n = 23), and the Young group(n = 27) respectively. CFA: Closed-field aberrometer; OFA: Open-field aberrometer; OFAUTO: Open-field autorefractor; Subjective: subjective refraction.

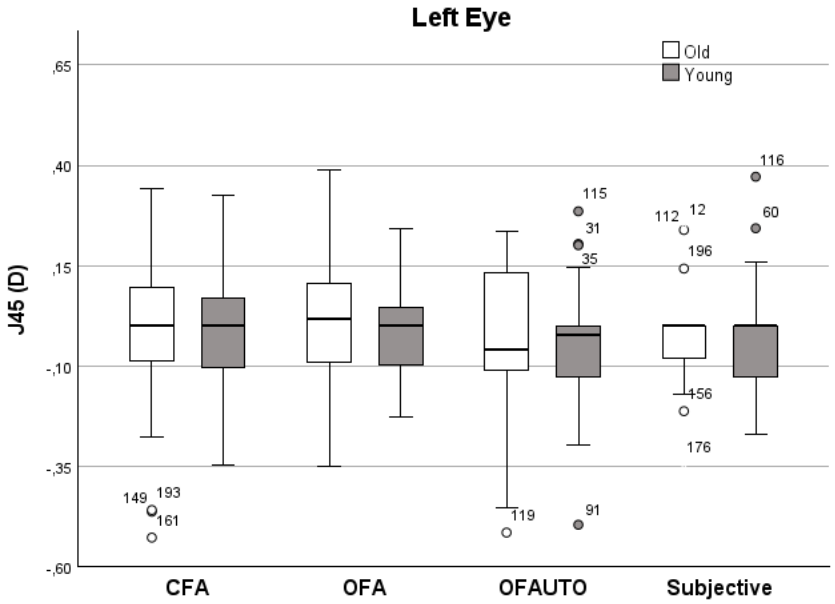

Figure S10: Box and whisker plot of the J45 values in the left eye achieved in the four procedures for the old group (n = 23), and the group (n = 27) respectively. CFA: Closed-field aberrometer; OFA: Open-field aberrometer; OFAUTO: Open-field autorefractor; Subjective: subjective refraction.

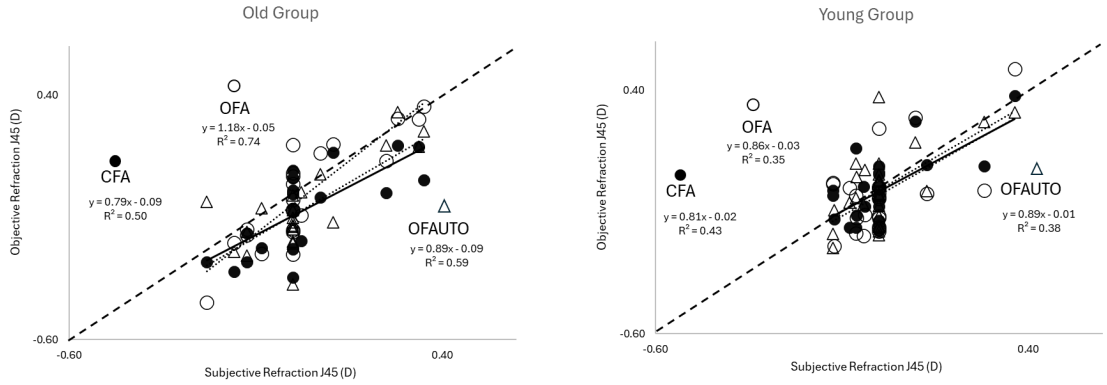

a) *b)*

Figure S11: Scatterplot between J45 values achieved with Subjective refraction versus objective procedures in the right eye for the Old group (N=23) (a) and the Young group (N=27) (b) respectively.

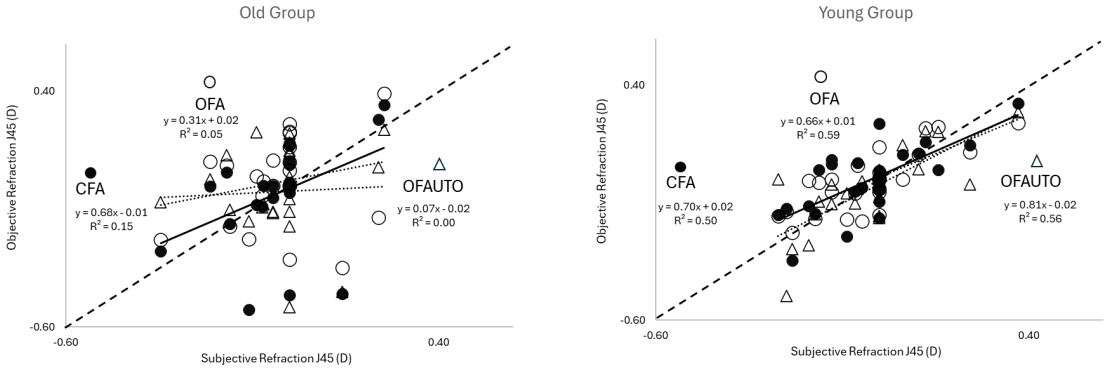

a) *b)*

Figure S12: Scatterplot between J45 values achieved with Subjective refraction versus objective procedures in the left eye for the old group (N=23) (a) and the Young group (N=27) (b) respectively.

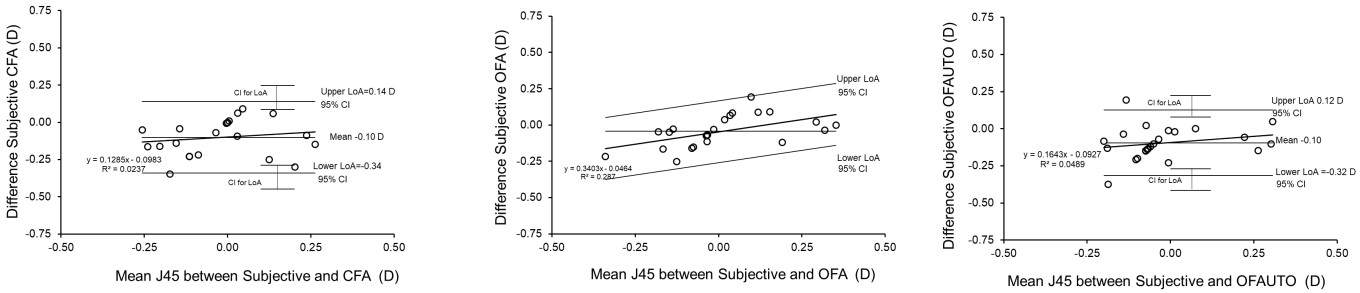

a) *b)* *c)*

Figure S13: Bland–Altman plot for the relationship between J45 values achieved with Subjective refraction and objective procedure on the right eye of the Old group (N=23): CFA (a), OFA (b), and OFAUTO (c). Correlation between the mean and the difference of J45 values achieved with Subjective refraction and OFA (b) was significant (r of Pearson = 0.54; p=0.008). Correlation was not significant for CFA (r of Pearson=0.15; n.s) and OFAUTO (Spearman Rho=0.30; n.s.). The limits of agreement (LoA) were calculated as mean of difference ± 1.96 SD of difference (D).

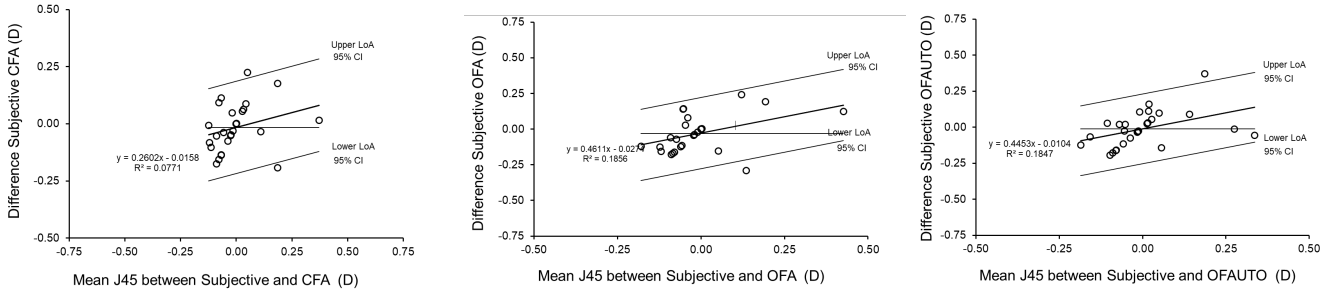

a) *b)* *c)*

Figure S14: Bland–Altman plot for the relationship between J45 values achieved with Subjective refraction and objective procedure on the right eye of the Young group (N=27): CFA (a), OFA (b), and OFAUTO (c). Correlation between the mean and the difference of J45 values achieved with Subjective refraction and objective procedure were all significant: Spearman rho coefficients were 0.45 (p=0.02), 0.51 (p=0.006), and 0.58 (p=0.002) for CFA, OFA and OFAUTO respectively. The limits of agreement (LoA) were calculated as mean of difference ± 1.96 SD of difference (D).

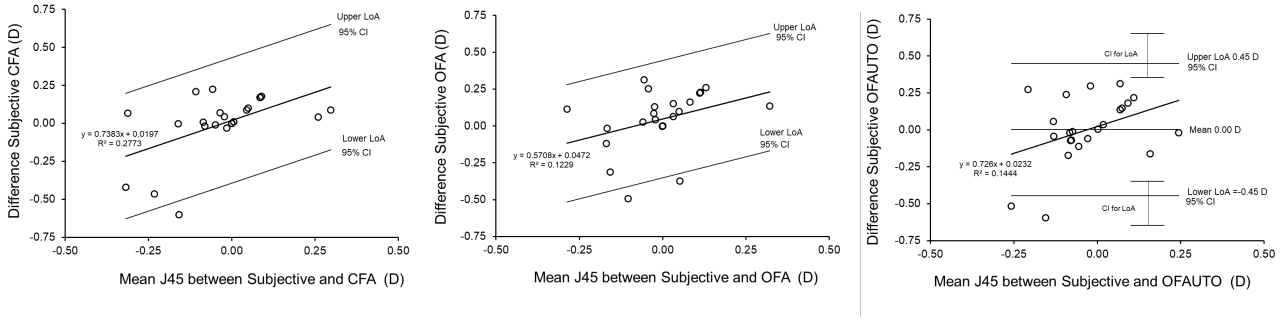

a) *b)* *c)*

Figure S15: Bland–Altman plot for the relationship between J45 values achieved with Subjective refraction and objective procedure on the left eye of the Old group (N=23): CFA (a), OFA (b), and OFAUTO (c). Correlation between the mean and the difference of J45 values achieved with Subjective refraction and objective procedure were significant for CFA (Spearman Rho=0.50; p=0.001) and OFA (0.45; p=0.03). In the case of OFAUTO correlation was not significant (Spearman Rho=0.31; n.s.). The limits of agreement (LoA) were calculated as mean of difference ± 1.96 SD of difference (D).

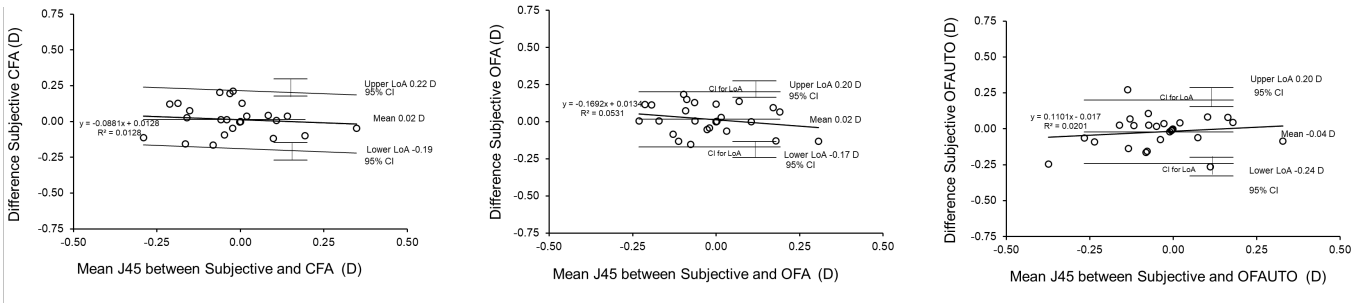

a) *b)* *c)*

Figure S16: Bland–Altman plot for the relationship between J45 values achieved with Subjective refraction and objective procedure on the left eye of the Young group (N=27): CFA (a), OFA (b), and OFAUTO (c). Correlation between the mean and the difference of J45 values achieved with Subjective and objective procedure was for all the comparisons not significant: Pearson correlation coefficient resulted -0.11, -0.23, and 0.14 for CFA, OFA and OFAUTO respectively (all p n.s). The limits of agreement (LoA) were calculated as mean of difference ± 1.96 SD of difference (D).

2.8.6 Mono vs Bino: J45 component

No statistical difference was found between monocular and binocular measurements of J45 for OFA and OFAUTO in both eyes of Old group and Young group (Wilcoxon test; all n.s.).

2.8.7 Reliability of the different refraction procedures: J45 component

In Tables S7 and S8 are shown the CP, CR, and ICC calculated for the value J45 achieved in the three repeated measures for each procedure, separately for Old and the Young group in the right and left eye respectively. All the reliability coefficients worked out for all procedures were extraordinarily high.

Table S7. CP, CR, and ICC calculated for the value J45 achieved in the right eye from the three repeated measures for each procedure separately for the Old group (n = 23), and the Young group (n = 27). * <0.001

	Old group (n=23)			**Young Group (n=27)**		
	CP	**CR**	**ICC (95% CI)**	**CP**	**CR**	**ICC (95% CI)**
CFA	0.05	0.07	0.980* (0.961-0.991)	0.06	0.09	0.948* (0.904-0.974)
OFA (Mono)	0.06	0.09	0.976* (0.952-0.989	0.04	0.05	0.987* (0.975-0.994)
OFA (Bino)	0.04	0.06	0.985* (0.970-0.993)	0.06	0.08	0.969* (0.943-0.985)
OFAUTO (Mono)	0.10	0.14	0.924* (0.854-0.964)	0.09	0.13	0.914* (0.846-0.957)
OFAUTO (Bino)	0.09	0.12	0.947* (0.898-0.975)	0.08	0.11	0.950* (0.909-0.975

Table S8. CP, CR, and ICC calculated for the value J45 achieved in the left eye from the three repeated measures for each procedure separately for the Old group (n = 23), and the Young group (n = 27). * <0.001

	Old group (n=23)			**Young Group (n=27)**		
	CP	**CR**	**ICC (95% CI)**	**CP**	**CR**	**ICC (95% CI)**
CFA	0.03	0.04	0.995* (0.990-0.998)	0.05	0.07	0.966* (0.938-0.983)
OFA (Mono)	0.03	0.04	0.994* (0.989-0.997)	0.04	0.05	0.976* (0.956-0.988)
OFA (Bino)	0.05	0.08	0.978* (0.958-0.990)	0.06	0.09	0.944* (0.898-0.972)
OFAUTO (Mono)	0.11	0.16	0.914* (0.839-0.959)	0.08	0.11	0.943* (0.896-0.972)
OFAUTO (Bino)	0.10	0.14	0.927* (0.861-0.966)	0.08	0.11	0.953* (0.914-0.977)

Chapter 3. Impact of Pupil Size on Defocus and Spherical Aberration Zernike Coefficients and on the Agreement with Subjective Refraction

3.1 Introduction

In the previous chapter, an analysis of the objective refraction agreement was done at 3 mm pupil of four different techniques: subjective refraction (SR), closed-field aberrometer (CFA), open-field aberrometer (OFA), and open-field autorefractor (OFAUTO), this approach allowed for a controlled assessment of the refractive error and minimized the influence of higher order aberrations (HOAs). However, a limitation that was addressed in that study was that the small pupil diameter did not represent real world viewing conditions, where natural pupil sizes often exceed 3 mm under mesopic or scotopic illumination [1], [2].

Since pupil size affects both the depth of focus and the impact of HOAs, it is reasonable that refractive outcomes from objective methods may vary as pupil size increases [3], [4], [5], [6]. In larger pupils, the effect of peripheral refraction becomes more noticeable, potentially strengthening the differences between methods that rely on different sampling zones and optical principles. For example, closed-field aberrometers, are particularly sensitive to HOAs that are magnified at larger pupils, while autorefractors often rely on paraxial or semi-paraxial rays that may not fully capture peripheral distortion [6], [7], [8], [9]. Moreover, in the previous analysis, a myopic shift was noticed in M with the CFA when compared to the OFA in young subjects, this shift was attributed to instrument myopia that could have resulted from the closed-field design and a possible failure of the fogging system efficacy [10]. As a result, it is worthy to investigate whether pupil size may also play a role.

Moreover, spherical aberration (SA), which is commonly represented by the Zernike coefficient C4,0, is expected to increase in magnitude when the pupil size increase under physiological conditions because peripheral rays contribute more strongly to the wavefront error. Several studies that were done under real pupil dilation showed an increase in positive spherical aberration [4],

[5], [8], [11], [12]. In standard ocular aberrometry measurements, data are acquired using the subject's natural pupil size under the measurement conditions. However, the subsequent wavefront analysis can be performed using a pupil diameter equal to, or smaller than, the pupil size at the time of measurement. When pupil size is reduced computationally, as is the case in aberrometer analysis, Zernike coefficients are mathematically rescaled rather than remeasured, this means that any changes reflect the numerical behavior of the reconstruction model rather than true modifications in the optical system [13], [14]. In this framework, the measured wavefront is reconstructed as a weighted sum of Zernike polynomials and the coefficients are then analytically transformed to a new pupil radius through exact scaling relations. The mathematical expression that describes this series expansion is the following:

$$W(r,\ \theta) = \sum_{n,m} a_{n,m} Z_n^m (r/r_1,\ \theta)$$

Equation 3. 1 Zernike polynomial expansion of the ocular wavefront, where the wavefront error W(r,θ) is expressed as a weighted sum of Zernike modes.

as already mentioned in Chapter 2. Interesting, the spherical aberration mode is the following

$$Z_4^0 = \sqrt{5}\,(6r^4 - 6r^2 + 1)$$

Equation 3. 2 Analytical form of the primary spherical aberration mode Z4,0. showing its mixed radial components (r^4, r^2)

It inherently contains lower-order radial terms, including a defocus component (r^2), implying that small changes in sampling or pupil geometry can theoretically influence both C4,0 and defocus estimates[15], [16].

For this reason, evaluating how C4,0 behaves across different analysis apertures is essential for determining whether pupil size meaningfully affects objective refraction or the agreement between different aberrometer systems.

Building on the findings of the 3 mm pupil analysis, this section extends the analysis to a larger pupil diameter by examining the same four refraction procedures under 4, 5, and 6 mm conditions in a subset of the previously studied young subjects. The selection of a subgroup of eyes depends on the lack of available data at larger diameters for all subjects, due to the smaller effective pupil size during the measurement. This approach allows for a more robust evaluation of each method under different optical conditions, where higher order aberrations are expected to play a greater role.

By directly comparing the results obtained at larger pupil sizes with those measured at 3 mm, the present analysis aims to determine whether the differences observed between procedures remain stable across pupil diameters or changed under more different pupil conditions. Enlarging the analyzed pupil increases the effective aperture of the system, making the measurement more sensitive to off-axis rays and higher-order aberrations, and therefore more dependent on how each instrument samples and reconstructs wavefront-based refraction.

3.2 Methods

This extended analysis was carried out using the same cohort and the same experimental procedures described in the previous 3 mm study chapter. The analyses at 4, 5, and 6 mm did not involve pharmacological dilation or a separate physiological pupil manipulation protocol. Instead, these pupil diameters were obtained through software-based wavefront analysis by recalculating the refraction and aberration outputs at larger analysis apertures, provided that the pupil recorded during measurement was sufficiently large to support reconstruction at that diameter. For this reason, only young subjects were included in the extended pupil-size analysis, as they were the only participants able to reach the larger natural pupil sizes required during acquisition. Consequently, the analyses at 4, 5, and 6 mm were performed on progressively smaller subsets of the young group. Specifically, 22 young participants had measurements suitable for analysis at 4 mm, 20 at 5 mm, and between 12 and 18 at 6 mm, depending on the instrument used (OFA or CFA), since not all subjects maintained a sufficiently large and stable pupil across all devices. These differences reflect natural inter-individual variability in pupil dynamics under the same measurement conditions rather than changes in protocol. The study design, order of measurements,

and procedures otherwise remained identical to those of the original 3 mm analysis. For refractive comparisons, differences smaller than 0.25 D were considered not clinically significant.

3.3 Data analysis

Data analysis at 4mm was carried out separately for the right eye (RE) and left eye (LE) to avoid statistical issues related to inter-eye correlation, [17] as well as for the three components of the power vector (M, J0, and J45). The differences between the four procedures of measurement (CFA, OFA, OFAUTO, and subjective refraction) were evaluated using repeated-measures tests. For components that met normality assumptions (J0), a one-way repeated-measures ANOVA was used, followed by pairwise t-tests with Bonferroni adjustment in case of significance. For components that did not meet normality assumptions (M and J45), the non-parametric Friedman test was applied, with post-hoc Wilcoxon signed-rank tests and Bonferroni correction for multiple comparisons. The Spearman correlation coefficient was calculated for each pair of measurements. Bland–Altman plots were used to assess the difference between each objective refraction procedure and subjective refraction and as a function of the mean of the two measurements.[18] The same approach was applied to the 5-mm dataset (n = 20) and both 6-mm datasets (n = 12 and n = 18), with paired comparisons generated for each pupil size against the corresponding 3-mm baseline. Per-subject comparisons across pupil sizes were evaluated using paired t-tests or Wilcoxon tests. Spherical aberration (C4,0) was analyzed using the same procedures: normality testing, followed by paired parametric or non-parametric tests for each pupil-size comparison. Bland–Altman plots were used to assess the difference between OFA and CFA and as a function of the mean of the two measurements. Proportional bias was tested by correlating the average and the difference of each pair of measurements. All analyses were performed with SPSS version 29.0.1 (IBM SPSS Statistics, USA).

3.4 Results

Although data analyses were carried out for the three components of the power vector (M, J0, J45) and for C4,0, the results presented below are limited to the M and C4,0 components. The results of J0 and J45 were analyzed at 4 mm, but they showed only small differences across procedures, with magnitudes below the threshold considered clinically significant in this thesis (0.25 D), and

no statistically significant effects, consistent with the 3 mm results. Because of this consistent lack of statistically and clinically meaningful variation, J0 and J45 analyses were not repeated at 5 or 6 mm, and the full 4 mm J0 and J45 results are reported only in the supplementary materials.

3.4.1- 4mm pupil size analysis

Agreement among the different refraction procedures at 4 mm

Descriptive statistics for M are reported in Table 3.1 (RE) and Table 3.2 (LE). The comparisons between the instruments were performed on the M mean data of CFA monocular, OFA monocular, OFAUTO monocular, and subjective procedure for right eye and left eye separately. These data set for both eyes did not result normally distributed (Shapiro–Wilk test, $p < 0.005$) except for the distribution of the subjective refraction in both eyes and the CFA in the right eye of that resulted normally distributed.

Table 3. 1 Mean, standard deviation (SD), median, and interquartile range (IQR) of M values of the right eye achieved in the four procedures for OFA and OFAUTO (monocular) for the young subsample (n = 22). The three repeated measurements and average for right eye are reported for CFA, OFA, and OFAUTO whereas in the case of subjective refraction only the final measure is reported. In the case of CFA and OFA, the pupil diameter is 4 mm.

	First Reading Mean ± SD; Median (IQ Range) (D)	**Second Reading Mean ± SD; Median (IQ Range) (D)**	**Third Reading Mean ± SD; Median (IQ Range) (D)**	**Average Reading Mean ± SD; Median (IQ Range) (D)**
CFA	-1.05 ± 1.51; -1.07 (2.66)	-1.00 ± 1.45; -0.88 (2.41)	-0.96 ± 1.49; -0.93 (2.62)	-1.01 ± 1.48; -0.96 (2.47)
OFA (Mono)	-0.64 ± 1.40; -0.05 (1.91)	-0.68 ± 1.38; -0.09 (1.88)	-0.66± 1.39; -0.07 (1.87)	-0.67 ± 1.39; -0.07 (1.86)
OFAUTO (Mono)	-0.83 ± 1.44; -0.12 (1.90)	-0.80 ± 1.48; -0.18 (1.90)	-0.82 ± 1.44; -0.19 (1.93)	-0.82 ± 1.45; -0.19 (1.94)
Subjective Procedure	_____	_____	_____	-1.33 ± 1.43; -0.79 (1.99)

Table 3.2 Mean, standard deviation (SD), median, and interquartile range (IQR) of M values of the left eye achieved in the four procedures for OFA and OFAUTO (monocular) for the young subsample (n = 22). The three repeated measurements and average for left eye are reported for CFA, OFA, and OFAUTO whereas in the case of subjective refraction only the final measure is reported. In the case of CFA and OFA, the pupil diameter is 4 mm.

	First Reading Mean ± SD; Median (IQ Range) (D)	**Second Reading Mean ± SD; Median (IQ Range) (D)**	**Third Reading Mean ± SD; Median (IQ Range) (D)**	**Average Reading Mean ± SD; Median (IQ Range) (D)**
CFA	-0.88 ± 1.64; -0.53 (1.98)	-0.85 ± 1.60; -0.45 (1.84)	-0.83 ± 1.59; -0.51 (1.91)	-0.85 ± 1.61; -0.54 (1.91)
OFA (Mono)	-0.60 ± 1.33; -0.19 (1.82)	-0.60 ± 1.32; -0.05 (1.83)	-0.61± 1.34; -0.08 (1.84)	-0.60 ± 1.33; -0.11 (1.83)
OFAUTO (Mono)	-0.83 ± 1.35; -0.24 (1.90)	-0.80 ± 1.34; -0.20 (1.90)	-0.77 ± 1.37; -0.17 (1.94)	-0.80 ± 1.36; -0.17 (1.93)
Subjective Procedure	_____	_____	_____	-1.19 ± 1.48; -0.67 (2.03)

Using a Friedman test, a significant effect of procedure was observed for the M component at 4 mm in both eyes, indicating that refractive outcomes differed across the four methods (Subjective, CFA, OFA, and OFAUTO). Pairwise post-hoc comparisons (Wilcoxon signed-rank tests with Bonferroni correction for six pairwise comparisons, $p < 0.0083$) showed that, in the right eye, OFA vs Subjective and OFAUTO vs Subjective were significant (both $p < 0.001$), while the remaining comparisons—including OFAUTO vs OFA ($p = 0.011$) and all comparisons involving CFA—were not significant after correction.

For the left eye, the same pattern was observed: OFA vs Subjective ($p = 0.001$) and OFAUTO vs Subjective ($p = 0.006$) were significant, whereas all other comparisons, including OFAUTO vs OFA ($p = 0.012$) and those involving CFA, were not significant after Bonferroni adjustment.

In Figure 3. 1 a and b the scatterplots between the right and left eye M values achieved with subjective refraction versus objective procedures are reported. In the right eye, a significant correlation was found between the M value measured with subjective refraction and the objective methods: Spearman's Rho resulted 0.85, 0.93, and 0.94 ($p < 0.001$), for the relations subjective-CFA, subjective-OFA, and subjective-OFAUTO, respectively. All correlations were strong and statistically significant, with 95% confidence intervals indicating high consistency across measurement methods. Similarly, in the left eye, a significant correlation was found between the M value measured with subjective refraction and the objective methods: Spearman's Rho resulted 0.79, 0.74, and 0.73 ($p < 0.001$), for the relations subjective-CFA, subjective-OFA, and subjective-OFAUTO, respectively. All correlations were statistically significant, though slightly weaker than those observed in the right eye.

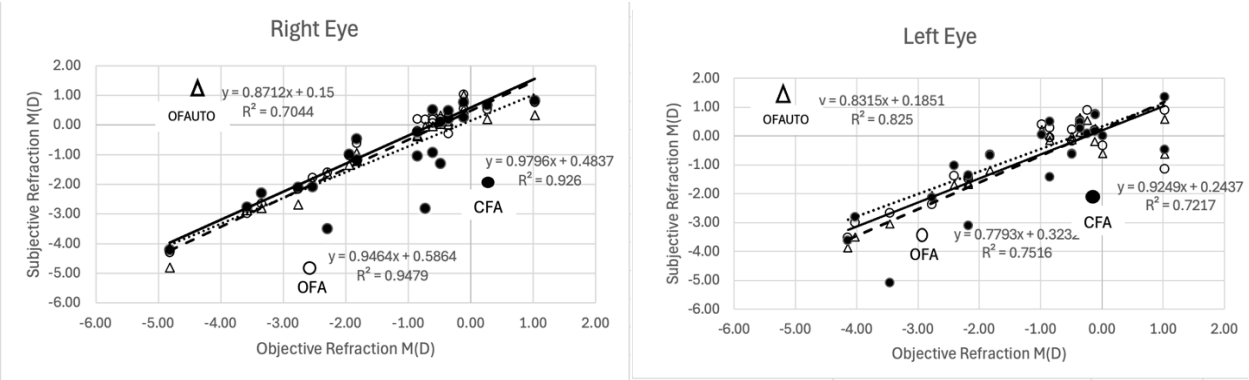

a) *b)*

Figure 3. 1 scatterplot between M values achieved with subjective refraction versus objective procedures in the right eye (a) and the left eye (b) respectively. In the case of CFA and OFA, the pupil diameter is 4 mm.

The Bland–Altman plots comparing M values obtained by subjective refraction and the objective procedures (CFA, OFA, and OFAUTO) showed no evidence of proportional bias in either the right eye (Figure 3.2a–c) or the left eye (Figure 3.3a–c)

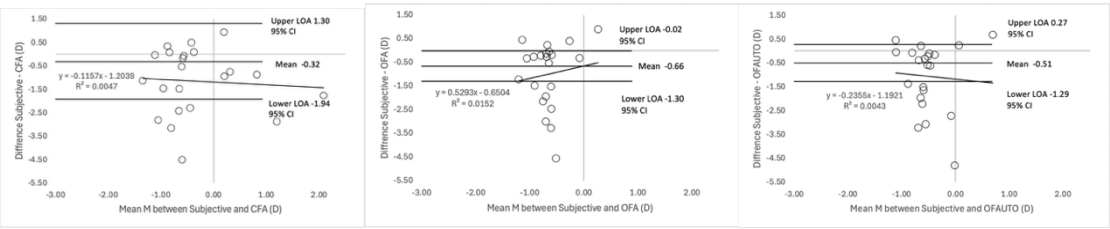

a) *b)* *c)*

Figure 3. 2 Bland–Altman plot for the relationship between M values achieved with subjective refraction and objective procedures on the right eye (N=22): CFA (a), OFA (b), and OFAUTO (c). Spearman Rho coefficients between the mean and the difference of M values achieved with subjective and objective refraction resulted 0.03, 0.05, and -0.02 for CFA, OFA and OFAUTO respectively (all n.s.). The limits of agreement (LoA) were calculated as mean of difference ± 1.96 SD of difference (D). In the case of CFA and OFA, the pupil diameter is 4 mm.

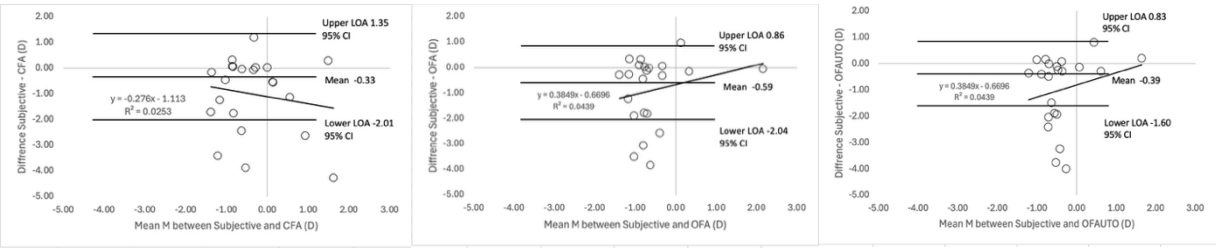

a) *b)* *c)*

Figure 3. 3 Bland–Altman plot for the relationship between M values achieved with subjective refraction and objective procedures on the left eye (N=22): CFA (a), OFA (b), and OFAUTO (c). Spearman Rho coefficients between the mean and the difference of M values achieved with subjective and objective refraction resulted -0.01, 0.12, and 0.17 for CFA, OFA and OFAUTO respectively (all n.s.). The limits of agreement (LoA) were calculated as mean of difference ± 1.96 SD of difference (D). In the case of CFA and OFA, the pupil diameter is 4 mm.

To enable a direct comparison, the same 22 young subjects who successfully reached a 4 mm pupil size were reevaluated under a 3 mm pupil condition (Table 3. 3 and Table 3. 4). This allowed the generation of matched datasets for both pupil diameters in the same individuals, ensuring that differences observed between techniques could be attributed to pupil size rather than sample variability. Analysis of these paired results allowed the construction of comparison tables (Table 3. 5 and Table 3. 6) that highlight how the agreement between subjective refraction and the three objective methods (CFA, OFA, OFAUTO) changes when moving from the 3 mm to the 4 mm pupil size.

Table 3. 3 Mean, standard deviation (SD), median, and interquartile range (IQR) of M values of the right eye achieved in the four procedures for OFA and OFAUTO (monocular) for the young subsample (n = 22). The three repeated measurements and average for right eye are reported for CFA, OFA, and OFAUTO whereas in the case of subjective refraction only the final measure is reported in the case of CFA and OFA, the pupil diameter is 3 mm.

	First Reading Mean ± SD; Median (IQ Range) (D)	**Second Reading Mean ± SD; Median (IQ Range) (D)**	**Third Reading Mean ± SD; Median (IQ Range) (D)**	**Average Reading Mean ± SD; Median (IQ Range) (D)**
CFA	-1.00 ± 1.50; -0.73 (2.71)	-0.96 ± 1.45; -0.64 (2.53)	-0.92 ± 1.49; -0.89 (2.68)	-0.96 ± 1.47; -0.71 (2.60)
OFA (Mono)	-0.68 ± 1.39; 0.00 (1.96)	-0.70 ± 1.37; -0.12 (1.91)	-0.69± 1.38; -0.06 (1.89)	-0.69 ± 1.38; -0.06 (1.92)
OFAUTO (Mono)	-0.83 ± 1.44; -0.12 (1.90)	-0.80 ± 1.48; -0.18 (1.90)	-0.82 ± 1.44; -0.19 (1.93)	-0.82 ± 1.45; -0.19 (1.94)
Subjective Procedure	_____	_____	_____	-1.33 ± 1.43; -0.79 (1.99)

Table 3. 4 Mean, standard deviation (SD), median, and interquartile range (IQR) of M values of the left eye achieved in the four procedures for OFA and OFAUTO (monocular) for the young subsample (n = 22). The three repeated measurements and average for left eye are reported for CFA, OFA, and OFAUTO whereas in the case of subjective refraction only the final measure is reported in the case of CFA and OFA, the pupil diameter is 3 mm.

	First Reading Mean ± SD; Median (IQ Range) (D)	**Second Reading Mean ± SD; Median (IQ Range) (D)**	**Third Reading Mean ± SD; Median (IQ Range) (D)**	**Average Reading Mean ± SD; Median (IQ Range) (D)**
CFA	-0.84 ± 1.67; -0.51 (1.77)	-0.82 ± 1.62; -0.51 (1.77)	-0.79 ± 1.60; -0.51 (1.75)	-0.82 ± 1.63; -0.51 (1.73)
OFA (Mono)	-0.54 ± 1.36; 0.07 (1.92)	-0.56 ± 1.33; -0.07 (1.90)	-0.56± 1.35; -0.02 (1.92)	-0.55 ± 1.35; -0.05 (1.91)
OFAUTO (Mono)	-0.83 ± 1.35; -0.24 (1.90)	-0.80 ± 1.34; -0.20 (1.90)	-0.77 ± 1.37; -0.17 (1.94)	-0.80 ± 1.36; -0.17 (1.93)
Subjective Procedure	_____	_____	_____	-1.19 ± 1.48; -0.67 (2.03)

The CFA–SR difference between the corresponding mean values was +0.37 D at 3 mm and +0.32 D at 4 mm, but for both diameters the CFA-SR was not statistically significant. The OFA–SR difference was similar across the same pupil sizes (+0.64 D to +0.66 D) and statistically significant in both cases. The OFA–OFAUTO difference remained stable (0.13 D at 3 mm and 0.15 D at 4 mm and significant in both cases). The CFA–OFA difference was –0.27 D at 3 mm and –0.34 D at 4 mm for the right eye, but the difference between the two techniques was not significant in both cases.

As for the left eye, the CFA–SR difference was not significant (+0.37 D at 3 mm and +0.34 D at 4 mm). The OFA–SR difference was +0.64 D and +0.59 D, respectively, and the OFA–OFAUTO difference was 0.25 D at 3 mm and 0.20 D at 4 mm, which all were significant. The CFA–OFA difference in the left eye was not significant (–0.27 D at 3 mm and –0.25 D at 4 mm).

Table 3. 5 Mean differences in refractive error (D) between objective techniques and subjective refraction (SR), and between objective techniques themselves, for young subjects measured at 3 mm and 4 mm pupil sizes in the right eye. Comparisons include CFA–SR, OFA–SR, OFA–OFAUTO, and CFA–OFA (monocular condition). Positive values indicate a relative hyperopic bias of the first method compared to the second, while negative values indicate a relative myopic bias. Δ represents the change in difference between 3 mm (N=22) and 4 mm (N=22) pupil sizes.

	3 mm (Mean ± SD)	**4 mm (Mean ± SD)**	**Δ (4–3 mm) (Mean ± SD)**
CFA-SR	+0.37 ± 0.83D	+0.32 ± 0.83D	–0.05 ± 0.15D
OFA-SR	+0.64 ± 0.36D	+0.66 ± 0.33D	+0.02 ± 0.11D
OFA-OFAUTO	+0.13 ± 0.31D	+0.15 ± 0.26D	+0.02 ± 0.11D
CFA-OFA	–0.27 ± 0.86D	–0.34 ± 0.84D	–0.07 ± 0.14D

Table 3. 6 Mean differences in refractive error (D) between objective techniques and subjective refraction (SR), and between objective techniques themselves, for young subjects measured at 3 mm and 4 mm pupil sizes in the left eye. Comparisons include CFA–SR, OFA–SR, OFA–OFAUTO, and CFA–OFA (monocular condition). Positive values indicate a relative hyperopic bias of the first method compared to the second, while negative values indicate a relative myopic bias. Δ represents the change in difference between 3 mm (N=22) and 4 mm (N=22) pupil sizes.

	3 mm (Mean ± SD)	**4 mm (Mean ± SD)**	**Δ (4–3 mm) (Mean ± SD)**
CFA-SR	+0.37 ± 0.87D	+0.34 ± 0.86D	–0.03 ± 0.12D
OFA-SR	+0.64 ± 0.74D	+0.59 ± 0.74D	–0.05 ± 0.11D
OFA-OFAUTO	+0.25 ± 0.27D	+0.20 ± 0.28D	–0.05 ± 0.11D
CFA-OFA	–0.27 ± 0.79D	–0.25 ± 0.76D	+0.02 ± 0.08D

Per-subject analysis using Wilcoxon signed-rank tests indicated that the 3 vs 4 mm differences were not statistically significant (after Bonferroni correction ($p < 0.0125$). For the right eye (RE), the comparisons were: OFA–SR ($Z = 0.52$, $p = 0.603$), OFA–OFAUTO ($Z = 0.52$, $p = 0.603$), CFA–SR ($Z = -1.43$, $p = 0.153$), and CFA–OFA ($Z = -2.11$, $p = 0.035$). For the left eye (LE), the results were: OFA–SR ($Z = -1.92$, $p = 0.055$), OFA–OFAUTO ($Z = -1.92$, $p = 0.055$), CFA–SR ($Z = -1.20$, $p = 0.230$), and CFA–OFA ($Z = 0.49$, $p = 0.626$).

3.4.2- 5 mm pupil size Analysis

Agreement among the different refraction procedures

Descriptive statistics for M are reported in (RE) Table 3.7 and (LE) Table 3.8. The comparisons between the instruments were performed on the M mean data of CFA monocular, OFA monocular, OFAUTO monocular, and subjective procedure for right eye and left eye separately. These data set for both eyes did not result normally distributed (Shapiro–Wilk test; $p < 0.005$) except for the distribution of the subjective refraction in both eyes and the CFA in the right eye of that resulted normally distributed.

Using a Friedman test, a significant effect of procedure was observed for the M component at 5 mm in both eyes, indicating that refractive outcomes differed across the four methods (Subjective, CFA, OFA, and OFAUTO). Pairwise post-hoc comparisons (Wilcoxon signed-rank tests with Bonferroni correction for six pairwise comparisons; $p < 0.0083$) showed that, in the right eye, OFA vs Subjective ($Z = -3.845$, $p < 0.001$) and OFAUTO vs Subjective ($Z = -3.285$, $p = 0.001$) were significant, while CFA vs Subjective ($Z = -1.792$, $p = 0.073$), CFA vs OFA ($Z = -1.456$, $p = 0.145$), OFA vs OFAUTO ($Z = -1.605$, $p = 0.108$), and CFA vs OFAUTO ($Z = -0.821$, $p = 0.411$) were not significant after correction.

For the left eye, post-hoc Wilcoxon tests with Bonferroni correction ($p < 0.0083$) indicated a significant difference between OFA vs Subjective ($Z = -2.987$, $p = 0.003$), whereas OFAUTO vs Subjective ($Z = -2.539$, $p = 0.011$), CFA vs Subjective ($Z = -1.419$, $p = 0.156$), CFA vs OFA ($Z = -0.859$, $p = 0.391$), OFA vs OFAUTO ($Z = -2.053$, $p = 0.040$), and CFA vs OFAUTO ($Z = 0.000$, $p = 1.000$) were not significant after Bonferroni adjustment.

Table 3. 7 Mean, standard deviation (SD), median, and interquartile range (IQR) of M values of the right eye achieved in the four procedures for OFA and OFAUTO (monocular) for the young subsample (n = 20). The three repeated measurements and average for right eye are reported for CFA, OFA, and OFAUTO whereas in the case of subjective refraction only the final measure is reported in the case of CFA and OFA; the pupil diameter is 5 mm.

	First Reading Mean ± SD; Median (IQ Range) (D)	**Second Reading Mean ± SD; Median (IQ Range) (D)**	**Third Reading Mean ± SD; Median (IQ Range) (D)**	**Average Reading Mean ± SD; Median (IQ Range) (D)**
CFA	-1.09 ± 1.51; -1.07 (2.77)	-1.05 ± 1.46; -0.89 (2.48)	-1.02 ± 1.49; -0.95 (2.48)	-1.05± 1.48; -0.97 (2.53)
OFA (Mono)	-0.66 ± 1.42; -0.03 (1.77)	-0.66 ± 1.40; -0.04 (1.79)	-0.67± 1.41; -0.04 (1.80)	-0.67 ± 1.41; -0.03 (1.79)
OFAUTO (Mono)	-0.78 ± 1.44; -0.12 (1.83)	-0.74 ± 1.49; -0.18 (1.83)	-0.77 ± 1.43; -0.19 (1.81)	-0.76 ± 1.45; -0.19 (1.86)
Subjective Procedure	_____	_____	_____	-1.30 ± 1.45; -0.79 (1.82)

Table 3. 8 Mean, standard deviation (SD), median, and interquartile range (IQR) of M values of the left eye achieved in the four procedures for OFA and OFAUTO (monocular) for the young subsample (n = 20). The three repeated measurements and average for left eye are reported for CFA, OFA, and OFAUTO whereas in the case of subjective refraction only the final measure is reported. In the case of CFA and OFA, the pupil diameter is 5 mm.

	First Reading Mean ± SD; Median (IQ Range) (D)	**Second Reading Mean ± SD; Median (IQ Range) (D)**	**Third Reading Mean ± SD; Median (IQ Range) (D)**	**Average Reading Mean ± SD; Median (IQ Range) (D)**
CFA	-0.88 ± 1.62; -0.52 (1.79)	-0.85 ± 1.58; -0.41 (1.65)	-0.83 ± 1.59; -0.46 (1.77)	-0.85± 1.60; -0.49 (1.74)
OFA (Mono)	-0.57 ± 1.27; -0.12 (1.85)	-0.58 ± 1.26; -0.08 (1.84)	-0.58± 1.27; -0.10 (1.84)	-0.57 ± 1.26; -0.10 (1.85)
OFAUTO (Mono)	-0.75 ± 1.26; -0.24 (1.88)	-0.71 ± 1.25; -0.20 (1.91)	-0.68 ± 1.29; -0.17 (1.93)	-0.71 ± 1.26; -0.17 (1.92)
Subjective Procedure	_____	_____	_____	-1.09 ± 1.40; -0.67 (2.03)

To enable a direct comparison, the same 20 young subjects who successfully reached a 5 mm pupil size were reevaluated under a 3 mm pupil condition (Table 3.9 and table 3.10). This allowed the generation of matched datasets for both pupil diameters in the same individuals, ensuring that differences observed between techniques could be attributed to pupil size rather than sample variability. Analysis of these paired results allowed the construction of comparison tables (Table 3.11 and Table 3.12) that highlight how the agreement between subjective refraction and the three objective methods (CFA, OFA, OFAUTO) changes when moving from the 3 mm to the 5 mm pupil size.

Table 3. 9 Mean, standard deviation (SD), median, and interquartile range (IQR) of M values of the right eye achieved in the four procedures for OFA and OFAUTO (monocular) for the young subsample (n = 20). The three repeated measurements and average for right eye are reported for CFA, OFA, and OFAUTO whereas in the case of subjective refraction only the final measure is reported. In the case of CFA and OFA, the pupil diameter is 3 mm.

	First Reading Mean ± SD; Median (IQ Range) (D)	**Second Reading Mean ± SD; Median (IQ Range) (D)**	**Third Reading Mean ± SD; Median (IQ Range) (D)**	**Average Reading Mean ± SD; Median (IQ Range) (D)**
CFA	-1.01 ± 1.51; -0.73 (2.72)	-0.97 ± 1.45; -0.64 (2.46)	-0.93 ± 1.50; -0.89 (2.42)	-0.97 ± 1.48; -0.71 (2.50)
OFA (Mono)	-0.64 ± 1.41; 0.00 (1.87)	-0.66 ± 1.37; -0.12 (1.79)	-0.65± 1.39; -0.06 (1.78)	-0.65 ± 1.39; -0.06 (1.80)
OFAUTO (Mono)	-0.78 ± 1.44; -0.12 (1.83)	-0.74 ± 1.49; -0.18 (1.83)	-0.77 ± 1.43; -0.19 (1.81)	-0.76 ± 1.45; -0.19 (1.86)
Subjective Procedure	_____	_____	_____	-1.30 ± 1.45; -0.79 (1.82)

Table 3. 10 Mean, standard deviation (SD), median, and interquartile range (IQR) of M values of the left eye achieved in the four procedures for OFA and OFAUTO (monocular) for the young subsample (n = 20). The three repeated measurements and average for left eye are reported for CFA, OFA, and OFAUTO whereas in the case of subjective refraction only the final measure is reported. In the case of CFA and OFA, the pupil diameter is 3 mm.

	First Reading Mean ± SD; Median (IQ Range) (D)	**Second Reading Mean ± SD; Median (IQ Range) (D)**	**Third Reading Mean ± SD; Median (IQ Range) (D)**	**Average Reading Mean ± SD; Median (IQ Range) (D)**
CFA	-0.80 ± 1.67; -0.51 (1.56)	-0.76 ± 1.62; -0.51 (1.54)	-0.73 ± 1.59; -0.51 (1.60)	-0.76 ± 1.62; -0.51 (1.57)
OFA (Mono)	-0.46 ± 1.29; -0.07 (1.96)	-0.49 ± 1.25; -0.07 (1.92)	-0.49± 1.27; -0.02 (1.92)	-0.48 ± 1.27; -0.05 (1.95)
OFAUTO (Mono)	-0.75 ± 1.26; -0.24 (1.88)	-0.71 ± 1.25; -0.20 (1.91)	-0.68 ± 1.29; -0.17 (1.93)	-0.71 ± 1.26; -0.17 (1.92)
Subjective Procedure	_____	_____	_____	-1.09 ± 1.40; -0.67 (2.03)

Mean difference analysis showed that the average changes (5–3 mm) were minimal across all methods, with mean absolute differences below 0.10 D. The CFA–SR difference was +0.33 D at 3 mm and +0.25 D at 5 mm (the difference between the two methods being unsignificant from the statistical point of view in both cases), while the OFA–SR difference was similar across the same pupil sizes (+0.65 D and +0.63 D, statistically significant in both cases). The OFA–OFAUTO difference remained stable (0.11 D at 3 mm and 0.09 D at 5 mm, with no statistical relevance). The CFA–OFA difference was –0.32 D at 3 mm and –0.38 D at 5 mm for the right eye with no statistical relevance in both cases.

As for the left eye, the CFA–SR difference was +0.33 D at 3 mm and +0.24 D at 5 mm with no statistical relevance in both cases), the OFA–SR difference was significant for both diameters and equal to +0.61 D and +0.52 D, respectively, and the OFA–OFAUTO difference was not statistically significant (0.23 D at 3 mm and 0.14 D at 5 mm). The CFA–OFA difference in the left eye was –0.28 D at 3 mm and –0.28 D at 5 mm but was not statistically significant.

Table 3. 11 Mean differences in refractive error (D) between objective techniques and subjective refraction (SR), and between objective techniques themselves, for young subjects measured at 3 mm and 5 mm pupil sizes in the right eye. Comparisons include CFA–SR, OFA–SR, OFA–OFAUTO, and CFA–OFA (monocular condition). Positive values indicate a relative hyperopic bias of the first method compared to the second, while negative values indicate a relative myopic bias. Δ represents the change in difference between 3 mm (N=20) and 5 mm (N=20) pupil sizes.

	3 mm (Mean ± SD)	**5 mm (Mean ± SD)**	**Δ (5–3 mm) (Mean ± SD)**
CFA-SR	+0.33± 0.86D	+0.25 ± 0.80D	–0.08± 0.20D
OFA-SR	+0.65± 0.37D	+0.63 ± 0.33D	–0.02± 0.21D
OFA-OFAUTO	+0.11± 0.32D	+0.09 ± 0.25D	–0.02± 0.21D
CFA-OFA	–0.32± 0.89D	–0.38 ± 0.81D	–0.06± 0.18D

Table 3,12 Mean differences in refractive error (D) between objective techniques and subjective refraction (SR), and between objective techniques themselves, for young subjects measured at 3 mm and 5 mm pupil sizes in the left eye. Comparisons include CFA–SR, OFA–SR, OFA–OFAUTO, and CFA–OFA (monocular condition). Positive values indicate a relative hyperopic bias of the first method compared to the second, while negative values indicate a relative myopic bias. Δ represents the change in difference between 3 mm (N=20) and 5 mm (N=20) pupil sizes.

	3 mm (Mean ± SD)	**5 mm (Mean ± SD)**	**Δ (5–3 mm) (Mean ± SD)**
CFA-SR	+0.33± 0.90D	+0.24 ± 0.84D	–0.09± 0.22D
OFA-SR	+0.61± 0.77D	+0.52 ± 0.77D	–0.09± 0.19D
OFA-OFAUTO	+0.23± 0.28D	+0.14 ± 0.27D	–0.09± 0.19D
CFA-OFA	–0.28± 0.82D	–0.28 ± 0.75D	0.00± 0.13D

Per-subject analysis using Wilcoxon signed-rank tests confirmed that these differences were not statistically significant (after Bonferroni correction ($p < 0.0125$). For the right eye, all comparisons revealed non-significant results: OFA–SR ($Z = –0.56$, $p = 0.575$), OFA–OFAUTO ($Z = –0.56$, $p = 0.575$), CFA–SR ($Z = –1.76$, $p = 0.079$), and CFA–OFA ($Z = –1.46$, $p = 0.145$). For the left eye, similar findings were observed: OFA–SR ($Z = –1.87$, $p = 0.062$), OFA–OFAUTO ($Z = –1.87$, $p = 0.062$), CFA–SR ($Z = –1.61$, $p = 0.108$), and CFA–OFA ($Z = –0.08$, $p = 0.940$). Although OFA–SR and OFA–OFAUTO showed weak trends toward more myopic outcomes at 5 mm ($p \approx 0.06$), these were not significant.

3.4.3- 6 mm pupil size Analysis (12 subjects)

Agreement among the different refraction procedures

Descriptive statistics for M are reported in Table 3.13 (RE) and Table 3.14 (LE). The comparisons between the instruments were performed on the M mean data of CFA monocular, OFA monocular, OFAUTO monocular, and subjective procedure for right eye and left eye separately. These data set for both eyes did not result normally distributed (Shapiro–Wilk test; $p < 0.005$) except for the distribution of the CFA in the right eye of that resulted normally distributed

Using a Friedman test, a significant effect of procedure was observed for the M component at 6 mm ($n = 12$) in the right eye, indicating that refractive outcomes differed across the four methods (Subjective, CFA, OFA, and OFAUTO). Pairwise post-hoc comparisons (Wilcoxon signed-rank tests with Bonferroni correction for six pairwise comparisons; $p < 0.0083$) showed significant differences between OFA and Subjective ($p = 0.002$) and between OFAUTO and Subjective ($p = 0.004$), while all remaining comparisons—including those involving CFA—were not significant after correction.

For the left eye, the Friedman test indicated that overall differences across procedures were not supported by post-hoc testing after correction. Accordingly, pairwise Wilcoxon comparisons with Bonferroni adjustment ($p < 0.0083$) showed no significant differences between any of the procedures at 6 mm (n = 12).

Table 3. 13 Mean, standard deviation (SD), median, and interquartile range (IQR) of M values of the right eye achieved in the four procedures for OFA and OFAUTO (monocular) for the young subsample (n = 12). The three repeated measurements and average for right eye are reported for CFA, OFA, and OFAUTO whereas in the case of subjective refraction only the final measure is reported. In the case of CFA and OFA, the pupil diameter is 6 mm.

	First Reading Mean ± SD; Median (IQ Range) (D)	**Second Reading Mean ± SD; Median (IQ Range) (D)**	**Third Reading Mean ± SD; Median (IQ Range) (D)**	**Average Reading Mean ± SD; Median (IQ Range) (D)**
CFA	-1.05 ± 1.50; -0.76 (2.25)	-1.07± 1.49; -0.69 (2.18)	-1.05 ± 1.50; -0.69 (2.22)	-1.06± 1.50; -0.71 (2.21)
OFA (Mono)	-0.88 ± 1.60; -0.13 (2.42)	-0.88 ± 1.59; -0.16 (2.38)	-0.89± 1.59; -0.17 (2.39)	-0.88 ± 1.59; -0.15 (2.40)
OFAUTO (Mono)	-1.01 ± 1.66; -0.11 (2.56)	-0.98 ± 1.72; -0.25 (2.58)	-1.01 ± 1.63; -0.28 (2.63)	-1.00 ± 1.66; -0.21 (2.61)
Subjective Procedure	_____	_____	_____	-1.55 ± 1.58; -0.73 (2.51)

Table 3.14 Mean, standard deviation (SD), median, and interquartile range (IQR) of M values of the left eye achieved in the four procedures for OFA and OFAUTO (monocular) for the young subsample (n = 12). The three repeated measurements and average for left eye are reported for CFA, OFA, and OFAUTO whereas in the case of subjective refraction only the final measure is reported. In the case of CFA and OFA, the pupil diameter is 6 mm.

	First Reading Mean ± SD; Median (IQ Range) (D)	**Second Reading Mean ± SD; Median (IQ Range) (D)**	**Third Reading Mean ± SD; Median (IQ Range) (D)**	**Average Reading Mean ± SD; Median (IQ Range) (D)**
CFA	-0.66 ± 1.30; -0.34 (1.42)	-0.65 ± 1.29; -0.21 (1.37)	-0.61 ± 1.27; -0.28 (1.32)	-0.64± 1.29; -0.31 (1.36)
OFA (Mono)	-0.59 ± 1.36; -0.14 (1.95)	-0.60 ± 1.37; -0.21 (1.96)	-0.60± 1.38; -0.18 (1.95)	-0.60 ± 1.37; -0.18 (1.95)
OFAUTO (Mono)	-0.74 ± 1.32; -0.36 (1.77)	-0.69 ± 1.31 -0.26 (1.83)	-0.67 ± 1.34; -0.30 (1.89)	-0.70 ± 1.33; -0.32 (1.83)
Subjective Procedure	_____	_____	_____	-1.09 ± 1.44; -0.67 (2.12)

To enable a direct comparison, the same 12 young subjects who successfully reached a 6 mm pupil size were reevaluated under a 3 mm pupil condition Table 3.15 and Table 3.16 . This allowed the generation of matched datasets for both pupil diameters in the same individuals, ensuring that differences observed between techniques could be attributed to pupil size rather than sample variability. Analysis of these paired results allowed the construction of comparison tables. Table 3.17 and Table 3.18. that highlight how the agreement between subjective refraction and the three objective methods (CFA, OFA, OFAUTO) changes when moving from the 3 mm to the 6 mm pupil size.

Table 3.15 Mean, standard deviation (SD), median, and interquartile range (IQR) of M values of the right eye achieved in the four procedures for OFA and OFAUTO (monocular) for the young subsample (n = 12). The three repeated measurements and average for right eye are reported for CFA, OFA, and OFAUTO whereas in the case of subjective refraction only the final measure is reported. In the case of CFA and OFA, the pupil diameter is 3 mm.

	First Reading Mean ± SD; Median (IQ Range) (D)	**Second Reading Mean ± SD; Median (IQ Range) (D)**	**Third Reading Mean ± SD; Median (IQ Range) (D)**	**Average Reading Mean ± SD; Median (IQ Range) (D)**
CFA	-0.96 ± 1.44; -0.73 (2.23)	-0.96 ± 1.43; -0.64 (2.20)	-0.92 ± 1.43; -0.67 (2.21)	-0.95± 1.43; -0.71 (2.21)
OFA (Mono)	-0.91 ± 1.56; -0.26 (2.56)	-0.93 ± 1.53; -0.29 (2.46)	-0.93± 1.54; -0.30 (2.51)	-0.92 ± 1.54; -0.29 (2.52)
OFAUTO (Mono)	-1.01 ± 1.66; -0.11 (2.56)	-0.98 ± 1.72; -0.25 (2.58)	-1.01 ± 1.63; -0.28 (2.63)	-1.00 ± 1.66; -0.21 (2.61)
Subjective Procedure	_____	_____	_____	-1.55 ± 1.58; -0.73 (2.51)

Table 3.16 Mean, standard deviation (SD), median, and interquartile range (IQR) of M values of the left eye achieved in the four procedures for OFA and OFAUTO (monocular) for the young subsample (n = 12). The three repeated measurements and average for left eye are reported for CFA, OFA, and OFAUTO whereas in the case of subjective refraction only the final measure is reported. In the case of CFA and OFA, the pupil diameter is 3 mm.

	First Reading Mean ± SD; Median (IQ Range) (D)	Second Reading Mean ± SD; Median (IQ Range) (D)	Third Reading Mean ± SD; Median (IQ Range) (D)	Average Reading Mean ± SD; Median (IQ Range) (D)
CFA	-0.54 ± 1.26; -0.17 (1.32)	-0.52 ± 1.23; -0.22 (1.12)	-0.48± 1.23; -0.16 (1.20)	-0.51± 1.24; -0.17 (1.16)
OFA (Mono)	-0.49± 1.37; -0.11 (1.90)	-0.55 ± 1.32; -0.16 (1.89)	-0.54± 1.34; -0.14 (1.91)	-0.53 ± 1.34; -0.14 (1.90)
OFAUTO (Mono)	-0.74 ± 1.32; -0.36 (1.77)	-0.69 ± 1.31 -0.26 (1.83)	-0.67 ± 1.34; -0.30 (1.89)	-0.70 ± 1.33; -0.32 (1.83)
Subjective Procedure	_____	_____	_____	-1.09 ± 1.44; -0.67 (2.12)

Mean difference analysis showed that the average changes (6–3 mm) were minimal across all methods, with mean absolute differences below 0.15 D. The CFA–SR difference was unsignificant from the statistical point of view and equal to +0.60 D at 3 mm and +0.49 D at 6 mm, while the OFA–SR difference was significant and similar for the two pupil diameters and equal to +0.63 D and +0.67 D. The OFA–OFAUTO difference was not significant and similar (+0.08 D at 3 mm and +0.12 D at 6 mm) for the two pupil sizes. The CFA–OFA difference was not significant (–0.03 D at 3 mm and –0.18 D at 6 mm) for the right eye.

As for the left eye, the comparison between two methods was never significant. The CFA–SR difference was +0.58 D at 3 mm and +0.45 D at 6 mm, the OFA–SR difference was +0.56 D and +0.49 D, respectively, and the OFA–OFAUTO difference was +0.17 D at 3 mm and +0.10 D at 6 mm. The CFA–OFA difference in the left eye was –0.02 D at 3 mm and –0.04 D at 6 mm.

Table 3. 17 Mean differences in refractive error (D) between objective techniques and subjective refraction (SR), and between objective techniques themselves, for young subjects measured at 3 mm and 6 mm pupil sizes in the right eye. Comparisons include CFA–SR, OFA–SR, OFA–OFAUTO, and CFA–OFA (monocular condition). Positive values indicate a relative hyperopic bias of the first method compared to the second, while negative values indicate a relative myopic bias. Δ represents the change in difference between 3 mm (N=12) and 6 mm (N=12) pupil sizes.

	3 mm (Mean ± SD)	**6 mm (Mean ± SD)**	**Δ (6–3 mm) (Mean ± SD)**
CFA-SR	+0.60± 0.65D	+0.49 ± 0.57D	–0.11± 0.30D
OFA-SR	+0.63 ± 0.39D	+0.67 ± 0.28D	+0.04± 0.34D
OFA-OFAUTO	+0.08± 0.39D	+0.12 ± 0.33D	+0.04± 0.34D
CFA-OFA	–0.03± 0.63D	–0.18 ± 0.49D	–0.15± 0.18D

Table 3. 18 Mean differences in refractive error (D) between objective techniques and subjective refraction (SR), and between objective techniques themselves, for young subjects measured at 3 mm and 6 mm pupil sizes in the left eye. Comparisons include CFA–SR, OFA–SR, OFA–OFAUTO, and CFA–OFA (monocular condition). Positive values indicate a relative hyperopic bias of the first method compared to the second, while negative values indicate a relative myopic bias. Δ represents the change in difference between 3 mm (N=12) and 6 mm (N=12) pupil sizes.

	3 mm (Mean ± SD)	**6 mm (Mean ± SD)**	**Δ (6–3 mm) (Mean ± SD)**
CFA-SR	+0.58 ± 0.84D	+0.45 ± 0.76D	–0.13± 0.32D
OFA-SR	+0.56± 0.97D	+0.49 ± 0.92D	–0.07± 0.30D
OFA-OFAUTO	+0.17± 0.31D	+0.10 ± 0.39D	–0.07± 0.30D
CFA-OFA	–0.02± 0.48D	–0.04 ± 0.39D	–0.02± 0.14D

Per-subject analysis using Wilcoxon signed-rank tests confirmed that these differences were not statistically significant (after Bonferroni correction ($p < 0.0125$). For the right eye, all comparisons between 3 and 6 mm revealed non-significant results: OFA–SR ($Z = –0.39$, $p = 0.695$), OFA–OFAUTO ($Z = –0.39$, $p = 0.695$), CFA–SR ($Z = –0.941$, $p = 0.347$), and CFA–OFA ($Z = –2.43$, $p = 0.015$). For the left eye, similar findings were observed: OFA–SR ($Z = –0.471$, $p = 0.638$), OFA–OFAUTO ($Z = –0.471$, $p = 0.638$), CFA–SR ($Z = –1.09$, $p = 0.272$), and CFA–OFA ($Z = 1.33$, $p = 0.182$). Although OFA–CFA in the right eye showed weak trends toward more myopic outcomes at 6 mm ($p = 0.01$), these were not significant.

3.4.4- 6 mm pupil size Analysis (18 subjects)

For the 6 mm pupil size, data were available for 18 young subjects who successfully reached this pupil diameter in the OFA, but because fewer subjects (n = 12) reached 6 mm in the CFA condition, another comparison at this pupil size were restricted to OFA against subjective refraction and OFAUTO. This allowed a consistent paired comparison of the same 18 subjects across these three methods.

Agreement among the different refraction procedures

Descriptive statistics for M are reported in Table 3.19 (RE) and Table 3.20 (LE). The comparisons between the instruments were performed on the M mean data of OFA monocular, OFAUTO monocular, and subjective procedure for right eye and left eye separately. These data set for both eyes resulted normal distribution (Shapiro–Wilk test; $p < 0.005$) except for the distribution of the OFA and OFAUTO in the right eye was not normally distributed.

Using a Friedman test, a significant effect of procedure was observed for the M component at 6 mm (n = 18) in the right eye, indicating that refractive outcomes differed across Subjective, OFA, and OFAUTO. Pairwise post-hoc comparisons (Wilcoxon signed-rank tests with Bonferroni correction for three pairwise comparisons; $p < 0.0167$) showed significant differences between OFA and Subjective ($p < 0.001$) and between OFAUTO and Subjective ($p = 0.002$), while OFA vs OFAUTO was not significant after correction ($p = 0.08$).

For the left eye, the Friedman test indicated an overall effect of procedure at 6 mm (n = 18); however, post-hoc Wilcoxon comparisons with Bonferroni adjustment ($p < 0.0167$) showed no significant pairwise differences between the procedures.

Table 3. 19 Mean, standard deviation (SD), median, and interquartile range (IQR) of M values of the right eye achieved in the three procedures for OFA and OFAUTO (monocular) for the young subsample (n = 18). The three repeated measurements and average for right eye are reported for OFA, and OFAUTO whereas in the case of subjective refraction only the final measure is reported. In the case of CFA and OFA, the pupil diameter is 6 mm.

	First Reading Mean ± SD; Median (IQ Range) (D)	**Second Reading Mean ± SD; Median (IQ Range) (D)**	**Third Reading Mean ± SD; Median (IQ Range) (D)**	**Average Reading Mean ± SD; Median (IQ Range) (D)**
OFA (Mono)	-0.74 ± 1.44; -0.07 (1.98)	-0.73 ± 1.43; -0.12 (2.02)	-0.74± 1.43; -0.10 (1.98)	-0.74 ± 1.43; -0.10 (1.99)
OFAUTO (Mono)	-0.85 ± 1.46; -0.12 (1.89)	-0.82 ± 1.51; -0.18 (1.90)	-0.85 ± 1.45; -0.19 (1.93)	-0.83 ± 1.47; -0.19 (1.94)
Subjective Procedure	_____	_____	_____	-1.34 ± 1.50; -0.79 (1.90)

Table 3. 20 Mean, standard deviation (SD), median, and interquartile range (IQR) of M values of the left eye achieved in the three procedures for OFA and OFAUTO (monocular) for the young subsample (n = 18). The three repeated measurements and average for left eye are reported for OFA, and OFAUTO whereas in the case of subjective refraction only the final measure is reported. In the case of CFA and OFA, the pupil diameter is 6 mm.

	First Reading Mean ± SD; Median (IQ Range) (D)	**Second Reading Mean ± SD; Median (IQ Range) (D)**	**Third Reading Mean ± SD; Median (IQ Range) (D)**	**Average Reading Mean ± SD; Median (IQ Range) (D)**
OFA (Mono)	-0.63± 1.29; -0.16 (1.90)	-0.63 ± 1.29; -0.15 (1.84)	-0.63± 1.30; -0.16 (1.85)	-0.63 ± 1.29; -0.16 (1.86)
OFAUTO (Mono)	-0.74 ± 1.82; -0.24 (1.80)	-0.72 ± 1.27 -0.20 (1.87)	-0.69 ± 1.32; -0.17 (1.94)	-0.72 ± 1.29; -0.17 (1.88)
Subjective Procedure	_____	_____	_____	-1.07 ± 1.44; -0.67 (2.12)

To enable a direct comparison, the same 18 young subjects who successfully reached a 6 mm pupil size were reevaluated under a 3 mm pupil condition Table 3.21 and Table 3.22. This allowed the generation of matched datasets for both pupil diameters in the same individuals, ensuring that differences observed between techniques could be attributed to pupil size rather than sample variability. Analysis of these paired results allowed the construction of comparison tables (Table 3.23 and Table 3.24) that highlight how the agreement between subjective refraction and the two objective methods (OFA, OFAUTO) changes when moving from the 3 mm to the 6 mm pupil size.

Table 3. 21 Mean, standard deviation (SD), median, and interquartile range (IQR) of M values of the right eye achieved in the three procedures for OFA and OFAUTO (monocular) for the young subsample (n = 18). The three repeated measurements and average for right eye are reported for OFA, and OFAUTO whereas in the case of subjective refraction only the final measure is reported. In the case of CFA and OFA, the pupil diameter is 3 mm.

	First Reading Mean ± SD; Median (IQ Range) (D)	**Second Reading Mean ± SD; Median (IQ Range) (D)**	**Third Reading Mean ± SD; Median (IQ Range) (D)**	**Average Reading Mean ± SD; Median (IQ Range) (D)**
OFA (Mono)	-0.70 ± 1.42; 0.00 (1.96)	-0.72 ± 1.40; -0.12 (1.91)	-0.72± 1.40; -0.06 (1.90)	-0.71 ± 1.41; -0.06 (1.92)
OFAUTO (Mono)	-0.85 ± 1.46; -0.12 (1.89)	-0.82 ± 1.51; -0.18 (1.90)	-0.85 ± 1.45; -0.19 (1.93)	-0.83 ± 1.47; -0.19 (1.94)
Subjective Procedure	_____	_____	_____	-1.34 ± 1.50; -0.79 (1.90)

Table 3. 22 Mean, standard deviation (SD), median, and interquartile range (IQR) of M values of the left eye achieved in the three procedures for OFA and OFAUTO (monocular) for the young subsample (n = 18). The three repeated measurements and average for left eye are reported for OFA, and OFAUTO whereas in the case of subjective refraction only the final measure is reported. In the case of CFA and OFA, the pupil diameter is 3 mm.

	First Reading Mean ± SD; Median (IQ Range) (D)	Second Reading Mean ± SD; Median (IQ Range) (D)	Third Reading Mean ± SD; Median (IQ Range) (D)	Average Reading Mean ± SD; Median (IQ Range) (D)
OFA (Mono)	-0.47± 1.32; -0.07 (1.92)	-0.51 ± 1.28; -0.07 (1.90)	-0.50± 1.30; -0.02 (1.91)	-0.49 ± 1.30; -0.05 (1.91)
OFAUTO (Mono)	-0.74 ± 1.82; -0.24 (1.80)	-0.72 ± 1.27 -0.20 (1.87)	-0.69 ± 1.32; -0.17 (1.94)	-0.72 ± 1.29; -0.17 (1.88)
Subjective Procedure	_____	_____	_____	-1.07 ± 1.44; -0.67 (2.12)

Mean difference analysis showed that the average changes (6–3 mm) were minimal across all methods, with mean absolute differences below 0.15 D. The OFA–SR difference was +0.63 D at 3 mm and +0.60 D at 6 mm (both significant), while the OFA–OFAUTO difference was +0.12 D at 3 mm and +0.09 D at 6 mm (not significant) for the right eye. Table 3.23 As for the left eye Table 3.24, the OFA–SR difference was +0.58 D at 3 mm and +0.44 D at 6 mm not significant), while the OFA–OFAUTO difference was +0.23 D at 3 mm and +0.09 D at 6 mm) for the left eye (not significant).

Table 3. 23 Mean differences in refractive error (D) between objective techniques and subjective refraction (SR), and between objective techniques themselves, for young subjects measured at 3 mm and 6 mm pupil sizes in the right eye. Comparisons include OFA–SR and OFA–OFAUTO (monocular condition). Positive values indicate a relative hyperopic bias of the first method compared to the second, while negative values indicate a relative myopic bias. Δ represents the change in difference between 3 mm (N=18) and 6 mm (N=18) pupil sizes.

	3 mm (Mean ± SD)	6 mm (Mean ± SD)	Δ (6–3 mm) (Mean ± SD)
OFA-SR	+0.63± 0.38D	+0.60 ± 0.36D	–0.03± 0.31D
OFA-OFAUTO	+0.12± 0.34D	+0.09 ± 0.29D	–0.03± 0.31D

Table 3. 24 Mean differences in refractive error (D) between objective techniques and subjective refraction (SR), and between objective techniques themselves, for young subjects measured at 3 mm and 6 mm pupil sizes in the left eye. Comparisons include OFA–SR and OFA–OFAUTO (monocular condition). Positive values indicate a relative hyperopic bias of the first method compared to the second, while negative values indicate a relative myopic bias. Δ represents the change in difference between 3 mm (N=18) and 6 mm (N=18) pupil sizes.

	3 mm (Mean ± SD)	**6 mm (Mean ± SD)**	**Δ (6–3 mm) (Mean ± SD)**
OFA-SR	+0.58± 0.81D	+0.44 ± 0.79D	–0.14± 0.29D
OFA-OFAUTO	+0.23 ± 0.29D	+0.09 ± 0.32D	–0.14± 0.29D

Per-subject analysis using Wilcoxon signed-rank tests confirmed that these differences were not statistically significant (after Bonferroni correction ($p < 0.025$). For the right eye, all comparisons between 3 and 6 mm were not statistically significant: OFA–SR ($Z = –0.370$, $p = 0.711$), OFA–OFAUTO ($Z = –0.370$, $p = 0.711$). For the left eye, similar findings were observed: OFA–SR ($Z = –1.59$, $p = 0.112$), OFA–OFAUTO ($Z = –1.59$, $p = 0.112$).

3.4.5- Summary of spherical Equivalent (M) Analysis Across All Pupil Sizes (3-6 mm)

Table 3.25 and Figure 3.4 report the averaged M outcomes obtained with the closed-field aberrometer (CFA), open-field aberrometer (OFA), open-field autorefractor (OFAUTO), and subjective refraction (SR) for the same subgroup of young subjects. Values from 3, 4, and 5 mm correspond to the same participants within each subgroup, 6-mm values are presented for subjects who reached this pupil diameter under each method. Across all procedures, M values remain relatively stable with increasing pupil size, consistent with the non-significant per-subject comparisons and the small mean differences reported in Table 3.5, Table 3.6, Table 3.11, Table 3.12, Table 3.17, Table 3.18, Table 3.23 and Table 3.24.

Table 3. 25 Summary of mean spherical equivalent (M) values (D) across pupil sizes (3–6 mm) for the right and left eyes. Mean ± SD are reported. SR and OFAUTO were not repeated across pupil sizes, so identical values across columns reflect the study protocol, not duplication.

Method / Eye (subgroup)	**3 mm** (same subgroup)	**4 mm** (22 subjects)	**5 mm** (20 subjects)	**6 mm** (12 subjects)	**6 mm** (18 subjects)
CFA Right (N=22)	-0.96 ± 1.47	-1.01 ± 1.48	—	—	—
CFA Right (N=20)	-0.97 ± 1.48	—	-1.05 ± 1.48	—	—
CFA Right (N=12)	-0.95 ± 1.43	—	—	-1.06 ± 1.50	—
CFA Right (N=18)	NA	—	—	—	NA
OFA Right (N=22)	-0.69 ± 1.38	-0.67 ± 1.39	—	—	—
OFA Right (N=20)	-0.65 ± 1.39	—	-0.67 ± 1.41	—	—
OFA Right (N=12)	-0.92 ± 1.54	—	—	-0.88 ± 1.59	—
OFA Right (N=18)	-0.71 ± 1.41	—	—	—	-0.74 ± 1.43
SR Right (N=22)	-1.33 ± 1.43	-1.33 ± 1.43	—	—	—
SR Right (N=20)	-1.30 ± 1.45	—	-1.30 ± 1.45	—	—
SR Right (N=12)	-1.55 ± 1.58	—	—	-1.55 ± 1.58	—
SR Right (N=18)	-1.34 ± 1.50	—	—	—	-1.34 ± 1.50
OFAUTO Right (N=22)	-0.82 ± 1.45	-0.82 ± 1.45	—	—	—
OFAUTO Right (N=20)	-0.76 ± 1.45	—	-0.76 ± 1.45	—	—
OFAUTO Right (N=12)	-1.00 ± 1.66	—	—	-1.00 ± 1.66	—
OFAUTO Right (N=18)	-0.83 ± 1.47	—	—	—	-0.83 ± 1.47
CFA Left (N=22)	-0.82 ± 1.63	-0.85 ± 1.61	—	—	—
CFA Left (N=20)	-0.76 ± 1.62	—	-0.85 ± 1.60	—	—
CFA Left (N=12)	-0.51 ± 1.24	—	—	-0.64 ± 1.29	—
CFA Left (N=18)	NA	—	—	—	NA
OFA Left (N=22)	-0.55 ± 1.35	-0.60 ± 1.33	—	—	—
OFA Left (N=20)	-0.48 ± 1.27	—	-0.57 ± 1.26	—	—
OFA Left (N=12)	-0.53 ± 1.34	—	—	-0.60 ± 1.37	—
OFA Left (N=18)	-0.49 ± 1.30	—	—	—	-0.63 ± 1.29
SR Left (N=22)	-1.19 ± 1.48	-1.19 ± 1.48	—	—	—
SR Left (N=20)	-1.09 ± 1.40	—	-1.09 ± 1.40	—	—
SR Left (N=12)	-1.09 ± 1.44	—	—	-1.09 ± 1.44	—
SR Left (N=18)	-1.07 ± 1.44	—	—	—	-1.07 ± 1.44
OFAUTO Left (N=22)	-0.80 ± 1.36	-0.80 ± 1.36	—	—	—
OFAUTO Left (N=20)	-0.71 ± 1.26	—	-0.71 ± 1.26	—	—
OFAUTO Left (N=12)	-0.70 ± 1.33	—	—	-0.70 ± 1.33	—
OFAUTO Left (N=18)	-0.72 ± 1.29	—	—	—	-0.72 ± 1.29

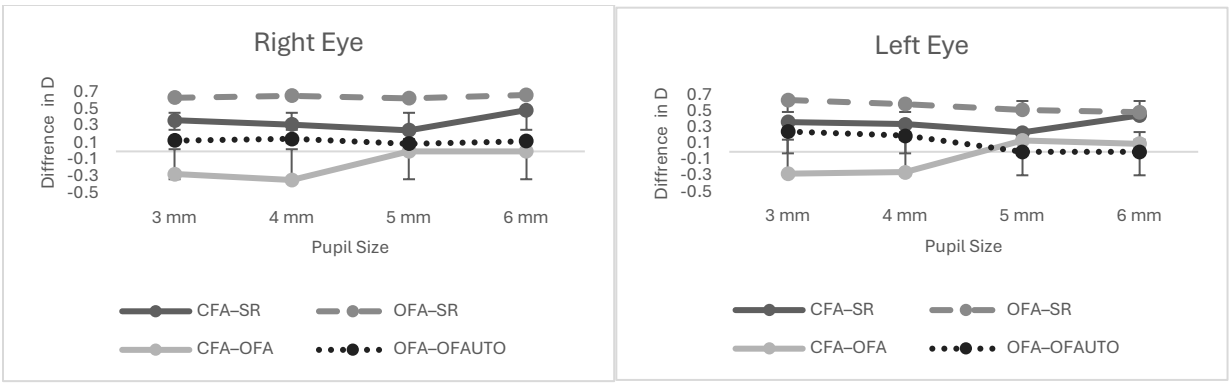

a) *b)*

Figure 3. 4 Differences in refractive error (D) between CFA–SR, OFA–SR, CFA–OFA, and OFA–OFAUTO at 3, 4, 5- and 6-mm pupil sizes. (a) Right eye. (b) Left eye. Positive values indicate a relative hyperopic bias, while negative values indicate a relative myopic bias. Differences remain small (<0.15 D) and show no clinically meaningful trend as pupil size increases.

Same method per-subject comparison

Per-subject analysis using Paired t-test or Wilcoxon signed-rank tests are reported in Table 3. 26 for the right eye and in Table 3. 27 for the left eye. After applying the Bonferroni-adjusted significance threshold ($p < 0.0167$), all comparisons within OFA and within CFA were confirmed to be non-significant, the corresponding trends are illustrated in Figure 3. 5 a and b.

Table 3. 26 Paired per-subject comparisons between 3 mm and larger pupil sizes for the right eye (RE). Mean ± SD differences in M are shown for OFA and CFA. Tests were paired t-test or Wilcoxon as appropriate.

Pupil Comparison	**Method**	**N**	**Mean ± SD**	**Test type (t / Z)**	**p - value**	**Significant?**
3 mm vs 4 mm	OFA	22	-0.19 ±0.11	t = -0.82	0.42	NO
3 mm vs 5 mm	OFA	20	0.01 ±0.20	t = 0.35	0.72	NO
3 mm vs 6 mm	OFA	18	0.20 ±0.30	t = 0.32	0.75	NO
3 mm vs 4 mm	CFA	22	0.04 ±0.14	Z=-1.49	0.13	NO
3 mm vs 5 mm	CFA	20	0.08 ±0.14	t = 1.90	0.72	NO
3 mm vs 6 mm	CFA	12	0.18 ±0.30	t = 1.24	0.23	NO

Table 3. 27 Paired per-subject comparisons between 3 mm and larger pupil sizes for the left eye (LE). Mean ± SD differences in M are shown for OFA and CFA. Tests were paired t-test or Wilcoxon as appropriate.

Pupil Comparison	Method	N	Mean ± SD	Test type (t / Z)	p - value	Significant?
3 mm vs 4 mm	OFA	22	0.04 ±0.11	t = 2.03	0.05	NO
3 mm vs 5 mm	OFA	20	0.09 ±0.18	t = 2.2	0.03	NO
3 mm vs 6 mm	OFA	18	0.13 ±0.29	t = 1.98	0.06	NO
3 mm vs 4 mm	CFA	22	0.03 ±0.12	t = 1.4	0.14	NO
3 mm vs 5 mm	CFA	20	0.09 ±0.22	t = 1.88	0.07	NO
3 mm vs 6 mm	CFA	12	0.12 ±0.32	t = 1.37	0.19	NO

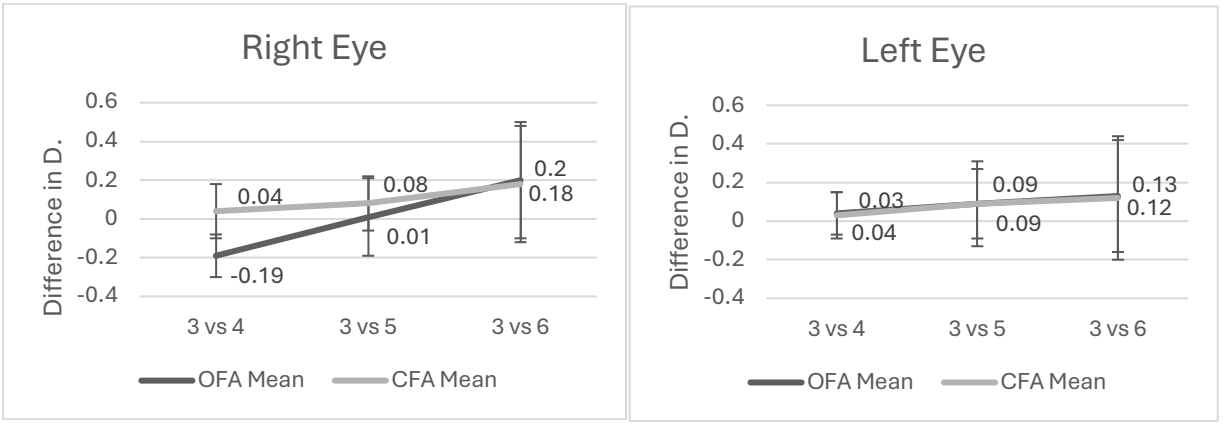

a) *b)*

Figure 3. 5 Mean differences (± SD) in spherical equivalent refraction across pupil-size comparisons (3 vs 4 mm, 3 vs 5 mm, and 3 vs 6 mm) for OFA and CFA methods in the right eye (a) and left eye (b). Error bars represent standard deviations. No statistically significant differences were found within either method across pupil sizes.

3.4.6_ Spherical Aberration (SA) Measurements Analysis Across Pupil Sizes (3–6 mm)- (C4,0).

In this section, the descriptive C4,0 outcomes (spherical aberration in µm) measured with OFA and CFA are first summarized across pupil sizes (3–6 mm) for the right and left eyes Table 2.28. To ensure consistency with the subsequent paired analyses, values are presented using the matched paired subsets available for each comparison (n=22 for 3–4 mm, n=20 for 3–5 mm, n=18 for 3–6 mm using OFA, and n=12 for 3–6 mm using CFA/OFA).

The following subsections then report within-method changes across pupil sizes and between-method differences to determine whether the observed numerical variations in C4,0 is statistically significant.

Table 3. 28 Mean ± SD of spherical aberration (C4,0 in µm) across pupil sizes (3–6 mm) for OFA and CFA in the right (RE) and left (LE) eyes. Values are reported to two decimal places for consistency with the measurement precision.

Procedure	3 mm (n=22)	4 mm (n=22)	3 mm (n=20)	5 mm (n=20)	3 mm (n=18)	6 mm (OFA n=18)	3 mm (n=12)	6 mm (OFA n=12)	6 mm (CFA n=12)
CFA (RE)	−0.01 ± 0.02	0.01 ± 0.03	−0.01 ± 0.02	−0.02 ± 0.07	—	—	−0.01 ± 0.02	—	−0.05 ± 0.14
OFA (RE)	0.01 ± 0.02	0.00 ± 0.04	0.00 ± 0.02	−0.01 ± 0.07	0.01 ± 0.03	−0.03 ± 0.12	0.01 ± 0.03	−0.01 ± 0.13	—
CFA (LE)	−0.01 ± 0.02	−0.01 ± 0.04	−0.01 ± 0.02	−0.03 ± 0.07	—	—	−0.01 ± 0.02	—	−0.06 ± 0.11
OFA (LE)	−0.01 ± 0.02	−0.01 ± 0.03	−0.01 ± 0.02	−0.03 ± 0.06	−0.01 ± 0.02	−0.06 ± 0.11	−0.00 ± 0.01	−0.04 ± 0.12	—

Same Method per-subject Comparison

Per-subject analysis using Paired t-test or Wilcoxon signed-rank for the right eye Table 3. 29. and left eye Table 3. 30. After applying the Bonferroni-adjusted significance threshold ($p < 0.0167$), all comparisons were confirmed to be non-significant. The corresponding trends are illustrated in Figure 3. 6 a and b.

Table 3. 29 Paired per-subject comparisons between 3 mm and larger pupil sizes for the right eye (RE). Mean ± SD differences in C4,0 (in micrometers) is shown for OFA and CFA.

Pupil Comparison	**Method**	**N**	**Mean ± SD**	**Test type (t / Z)**	**p - value**	**Significant?**
3 mm vs 4 mm	OFA	22	0.00 ±0.02	t = 0.16	0.87	NO
3 mm vs 5 mm	OFA	20	0.02 ±0.05	t=1.41	0.17	NO
3 mm vs 6 mm	OFA	18	0.03 ±0.11	t=1.18	0.25	NO
3 mm vs 4 mm	CFA	22	-0.00 ±0.02	t =-0.20	0.84	NO
3 mm vs 5 mm	CFA	20	0.01 ±0.07	t =0.83	0.41	NO
3 mm vs 6 mm	CFA	12	0.04 ±0.14	Z =-0.39	0.69	NO

Table 3. 30 Paired per-subject comparisons between 3 mm and larger pupil sizes for the left eye (LE). Mean ± SD differences in C4,0. are shown for OFA and CFA.

Pupil Comparison	Method	N	Mean ± SD	Test type (t / Z)	p - value	Significant?
3 mm vs 4 mm	OFA	22	0.00 ±0.02	t =0.44	0.66	NO
3 mm vs 5 mm	OFA	20	0.02 ±0.05	t=1.67	0.11	NO
3 mm vs 6 mm	OFA	18	0.05±0.11	t=1.94	0.07	NO
3 mm vs 4 mm	CFA	22	0.00 ±0.02	t=0.60	0.52	NO
3 mm vs 5 mm	CFA	20	0.01 ±0.06	t=1.23	0.23	NO
3 mm vs 6 mm	CFA	12	0.04 ±0.09	Z=-1.33	0.18	NO

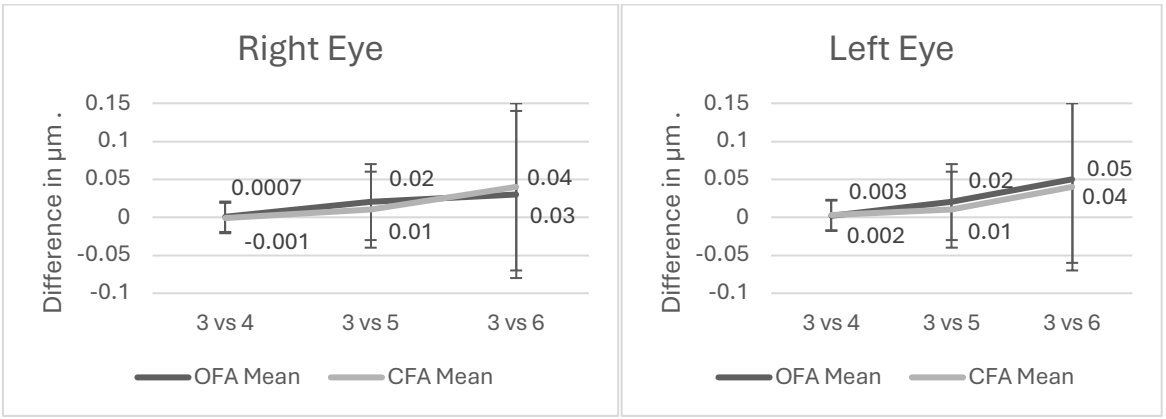

a) *b)*

Figure 3. 6 Mean differences (± SD) in spherical aberration across pupil-size comparisons (3 vs 4 mm, 3 vs 5 mm, and 3 vs 6 mm) for OFA and CFA methods in the right eye (a) and left eye (b). Error bars represent standard deviations. statistically significant differences were found within CFA in the RE across pupil sizes.

OFA-CFA per -subject comparison at the same pupil size

Per-subject analyses were conducted using Paired t-test for the right eye Table 3. 31. and the left eye Table 3. 32. After applying the Bonferroni-adjusted significance threshold ($p < 0.0125$), the OFA–CFA mean differences at all pupil sizes were confirmed to be non-significant.

Table 3.31 Paired per-subject comparisons between 3 mm and larger pupil sizes for the right eye (RE). Mean ± SD differences in C4,0. are shown for the difference between OFA and CFA.

Pupil size	**N**	**Mean Δ (OFA–CFA) ± SD**	**Test type (t / Z)**	**p - value**	**Significant?**
3mm	22	0.12 ±0.02	t = 2.60	0.015	NO
4mm	22	0.01 ±0.02	t = 1.79	0.04	NO
5mm	20	0.00±0.04	t = 0.65	0.52	NO
6mm	12	0.03 ±0.05	t = 2.25	0.04	NO

Table 3.32 Paired per-subject comparisons between 3 mm and larger pupil sizes for the right eye (RE). Mean ± SD differences in C4,0. are shown for the difference between OFA and CFA.

Pupil size	**N**	**Mean Δ (OFA–CFA) ± SD**	**Test type (t / Z)**	**p - value**	**Significant?**
3mm	22	0.00 ±0.02	t = 0.41	0.68	NO
4mm	22	0.00±0.02	t = 0.51	0.30	NO
5mm	20	0.00 ±0.04	t = 0.13	0.89	NO
6mm	12	0.01 ±0.05	t = 0.71	0.48	NO

OFA-CFA per -subject comparison across different pupil sizes.

Per-subject analysis using Paired t-test for the right eye Table 3. 33. and Left eye Table 3. 34. After applying the Bonferroni-adjusted significance threshold ($p < 0.0167$), all comparisons were confirmed to be non-significant.

Table 3.33 per-subject comparison of OFA–CFA difference across different pupil size in the RE.

Comparison (mm)	N	Mean Difference ±SD	Test type (t / Z)	p-value	Significant?
3mm vs 4mm	22	0.00 ± 0.02	t = 0.47	0.64	NO
3mm vs 5mm	20	0.01 ± 0.04	t = 0.59	0.56	NO
3mm vs 6mm	12	-0.02 ± 0.04	t = -1.77	0.10	NO

Table 3.34 per-subject comparison of OFA–CFA difference across different pupil size in the LE.

Comparison (mm)	N	Mean Difference ±SD	Test type (t / Z)	p-value	Significant?
3mm vs 4mm	22	-0.00 ± 0.02	t = -0.27	0.76	NO
3mm vs 5mm	20	0.00 ± 0.04	t = 0.15	0.87	NO
3mm vs 6mm	12	-0.00 ± 0.05	t = -0.19	0.84	NO

Bland–Altman Agreement Between CFA and OFA for C4,0

To show the agreement between the CFA and OFA in measuring C4,0, Bland–Altman analysis was used Figure 3.7 a and b at 3 mm pupil sizes because of its larger sample size. The mean differences were 0.01 µm and 0.002 µm, with limits of agreement ranging from -0.03 to +0.06 µm and -0.04 to +0.04 µm, for the RE and LE respectively. No proportional bias was detected.

Pearsons coefficients between the mean and the difference of C4,0. values achieved with OFA and CFA resulted 0.37 (p=0.08) for the RE and -0.17 for the LE (p=0.45) (both statistically not significant).

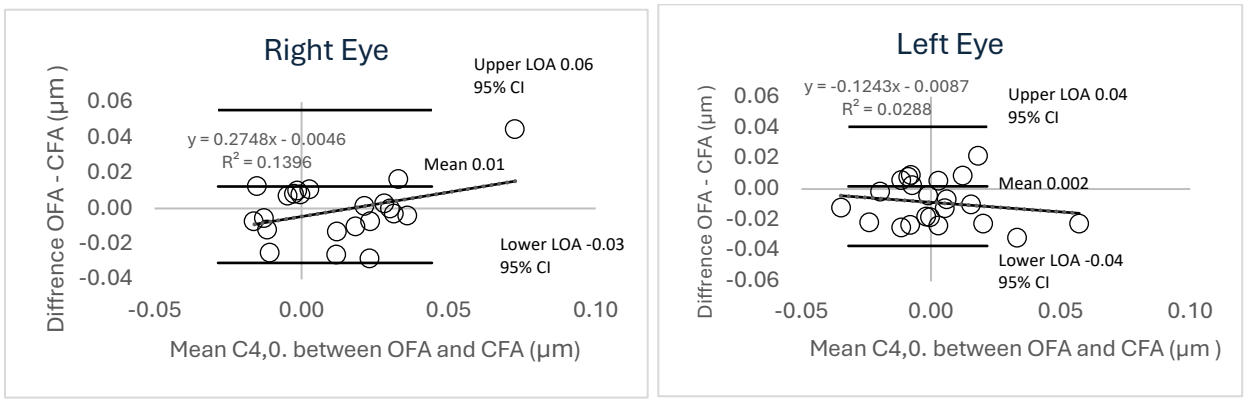

a) *b)*

Figure 3. 7 Bland–Altman plot for the relationship between C4,0. values achieved with OFA and CFA at 3mm pupil size data (N=22): Right eye (a), Left eye (b). The limits of agreement (LoA) were calculated as mean of difference ± 1.96 SD of difference (D).

3.5 Discussion

This analysis expands on the previous 3 mm pupil work. Subjective and objective refraction (CFA, OFA, OFAUTO, and subjective refraction) were evaluated at 4, 5, and 6 mm analysis pupil sizes, each with its own sample-size subset. In addition to refractive error, spherical aberration (C4,0), measured by both closed- and open-field aberrometers, was assessed across all available pupil sizes to determine whether higher-order aberrations contribute to method differences as pupil diameter increases. This made it possible to examine whether the stability observed in refraction measurements was maintained for higher-order aberration metrics across different pupil sizes.

In this study, the larger pupil diameters were not obtained through pharmacological or physiological dilation. Instead, the wavefront measured by the aberrometers was reconstructed by fitting the optical path differences within the pupil to a series of normalized Zernike polynomials and then mathematically rescaling the reconstruction to a larger analysis diameter by transforming the Zernike coefficients according to the ratio between the original and target pupil radii, without performing a new physiological measurement [13], [14], [16]. Therefore, any changes observed at larger analysis apertures reflect the behavior of the reconstruction algorithms rather than actual optical modifications within the eye.

3.5.1 Effect of Pupil Size on the behavior on objective refraction methods

Spherical Equivalent (M) Component – Defocus

Spherical equivalent values remained stable across all pupil sizes (from 3 to 6 mm), they showed minimal fluctuations with no statistical or clinical significance. Recently, several papers have been published by a research group to explain why and how Zernike polynomials (and also the M coefficient) are not always sufficiently accurate and to provide a solution through a new aberration basis that is better suited to describing an ocular wavefront [15] . On the contrary, other studies reported that defocus is dominated by central rays, where the wavefront is directly sampled. When the pupil diameter increases, the reconstruction algorithm extends to the periphery, but the central coefficients that determine M remain unchanged [8], [9]. Many wavefront modeling studies show

that lower order aberrations, including defocus, are largely unaffected by pupil size because they are managed by low frequency Zernike modes that are more resistant to peripheral noise and reconstruction artefacts [6], [7], [8], [9], [19], [20]. The results obtained here suggests that, for the subjects examined in this study, the problem highlighted by Gatinel et al. [15] did not arise.

This extended analysis resolves several limitations that was raised in the previous 3 mm analysis. First, the concern that defocus estimates might shift under more physiologic pupil sizes was not supported, M remained remarkably stable across all pupil sizes and all techniques, this confirms that defocus is dominated by central rays and insensitive to peripheral sampling[9], [21]. Second, the trend toward a more myopic shift with the closed-field aberrometer (relative to the open-field method) was observed across pupil sizes, although these differences were not statistically significant after correction, this suggests a possible accommodation-related 'instrument myopia' [22], [23] rather than a pupil-diameter interaction. Third, the small hyperopic bias of the OFA relative to subjective refraction also remained unchanged from 3 to 6 mm, suggesting that this difference is due to the outgoing wavefront aberrometry method rather than an artefact of the 3-mm aperture[24], [25]. Fourth, OFAUTO showed minimal change across all comparisons, confirming its stability as an open-field reference technique.

Spherical Aberration (C4,0) component

Although Fig. 3.6 shows a slight increase in the difference of the C4,0 coefficient as pupil size increases compared with the value measured at 3 mm, this work does not provide any statistical evidence of such a variation. Across all computational pupil sizes, spherical aberration (C4,0) remained statistically unchanged for both instruments, with no statistically significant differences within devices or between devices. Because these pupil sizes were not real physiological dilations, the absence of SA change likely reflects the mathematical nature of Zernike coefficient scaling rather than true alterations in the optical system. Earlier studies showed that Zernike-based spherical aberration is highly sensitive to the pupil margin under real optical dilation, and even small uncertainties at the edge can cause notable shifts when the pupil size increases [8], [9], [19]. In contrast, because the pupil enlargements in our study were computational rather than physiological, these theoretical sensitivities did not translate into measurable changes, and both the CFA and OFA produced stable C4,0 values across all pupil sizes.

The absence of significant changes in SA across all pupil sizes is consistent with the current understanding of Zernike reconstruction, despite the limitations highlighted by Gatinel [15], [16] Gatinel and colleagues (2020) demonstrated that Z4,0 is not a "pure" spherical aberration mode. Because defocus is dominated by central (paraxial) rays, computational enlargement of the analysis pupil may have limited impact on this component, which could contribute to minimal changes in the estimated C4,0 coefficient. Several studies [13], [14], [16] indicate that mathematical pupil scaling does not reproduce the true optical behavior of physiological dilation, especially in the peripheral region where spherical aberration originates. This may explain why the expected increase in SA at larger pupils, as reported in other studies [4], [5], [12] was not observed here.

Furthermore, the predicted change in SA is below the normal measurement variability of clinical aberrometers, according to optical modeling studies [26], [27] the intra-observer test–retest repeatability for Z(4,0) is approximately 0.06–0.07 μm, while inter-observer variability remains below 0.04 μm, with within-subject noise as low as 0.02 μm. This means that any scaling induced modification of C4,0 would fall within instrument noise and therefore remain undetectable. This provides an explanation for the stability of spherical aberration observed across all computational pupil sizes in the present study, despite the known tendency of SA to increase under real optical dilation.

Although minor numerical variation existed, the Bland–Altman analysis showed symmetrical limits of agreement, and absence of proportional bias. Also, the paired comparisons revealed that the CFA and the OFA still showed no significant difference in their measurement of SA (both at the same pupil size and across different pupil sizes). These results show that the two devices remain in good agreement when measuring spherical aberration at different pupil sizes.

To current knowledge, no prior study has directly examined agreement between open and closed field aberrometers for higher order aberrations. Existing comparisons are between open and closed field autorefractors [3], [28], [29], [30], [31], which focuses primarily on spherical equivalent (M), these studies showed small systematic differences but generally good agreement. Our findings extend this literature by demonstrating that, for SA (C4,0), both aberrometers also show strong agreement and minimal variation across pupil sizes.

3.5.2 Limitations

This study has some limitations that should be noted. Because the larger pupil sizes were generated computationally (assuming perfect centration and uniform pupil geometry [14]), the stability of the measurements observed at 3-6 mm reflect the devices' reconstruction behavior rather than true optical performance under real dilation. The sample size also decreased at the larger pupil diameters, which reduces statistical power and may limit the detection of smaller effects. Finally, all participants were young adults with healthy eyes, so the behavior of these aberrometers may differ in older individuals or in eyes with irregular optics, where peripheral sampling artefacts are more pronounced.

3.6 Conclusion

Across all analyses, spherical equivalent (M) remained remarkably stable, supporting the central-ray dominance of defocus, while the previously observed CFA myopic shift and OFA hyperopic bias persisted despite change in pupil size. Spherical aberration (C4,0) also remained statistically unchanged within and between devices, consistent with the limited peripheral information obtained from non-physiological pupil enlargement. This is in contrast with some other results reported in the literature, although from this point of view the literature is mixed. Despite inherent differences between open- and closed-field systems, the CFA and OFA showed strong agreement at all pupil sizes, indicating robust aberrometric performance across analysis apertures. Together, these findings extend the conclusions of the 3 mm analysis and demonstrate that, under computational pupil enlargement, both lower and higher order aberrations remain stable.

3.7 References:

[1] Winn B, Whitaker D, Elliott DB, Phillips NJ. Factors affecting light-adapted pupil size in normal human subjects. Vision Res 1994;34(18):2483–8. https://doi.org/10.1016/0042-6989(94)90208-9.

[2] Lara F, Bernal-Molina P, Fernández-Sánchez V, López-Gil N. Changes in the objective amplitude of accommodation with pupil size. Optom Vis Sci 2014;91(10):1215–21. https://doi.org/10.1097/OPX.0000000000000375.

[3] Noya-Padín V et al., Comparing close-field and open-field autorefractometry and subjective refraction. J Clin Med 2025;14(16):5680. https://doi.org/10.3390/jcm14165680.

[4] Zhu X, Ye H, Yang J, Lu Y. Effect of pupil size on higher-order aberrations in high-myopic pseudophakic eyes with posterior staphyloma. Eye 2015;29(1):98–105. https://doi.org/10.1038/eye.2014.242.

[5] Yan W, Zhang K, Jin Y, Ni Y, Zhou T. Changes of higher-order aberration with various pupil sizes in the myopic eye. J Refract Surg 2003;19(2 Suppl):S270–4. https://doi.org/10.3928/1081-597X-20030302-21.

[6] Nguyen MT, Berntsen DA. Aberrometry repeatability and agreement with autorefraction. Optom Vis Sci 2017;94(9):886–93. https://doi.org/10.1097/OPX.0000000000001107.

[7] Faria-Ribeiro M, Navarro R, González-Méijome JM. Effect of pupil size on axial and peripheral wavefront refraction during orthokeratology. J Optom 2016;9(3):164–71. https://doi.org/10.1016/j.optom.2015.11.001.

[8] Dai G. Comparison of wavefront reconstructions with Zernike polynomials and Fourier transforms. J Refract Surg 2006;22(9):943–8. https://doi.org/10.3928/1081-597X-20061101-21.

[9] Thibos LN, Xin H, Bradley A, Applegate RA. Accuracy and precision of objective refraction from wavefront aberrations. J Vis 2004;4(4):329–51. https://doi.org/10.1167/4.4.9.

[10] Schober HAW, Dehler H, Kassel R. Accommodation during observations with optical instruments. J Opt Soc Am 1970;60(1):103–6. https://doi.org/10.1364/JOSA.60.000103.

[11] Klyce SD, Karon MD, Smolek MK. Advantages and disadvantages of the Zernike expansion for representing wave aberration of the normal and aberrated eye. J Refract Surg 2004;20(5):537–41. https://doi.org/10.3928/1081-597X-20040901-25.

[12] Fernández de Castro LE, Sandoval HP, Bartholomew LR, Vroman DT, Solomon KD. High-order aberrations and preoperative associated factors. Acta Ophthalmol Scand 2007;85(1):106–10. https://doi.org/10.1111/j.1600-0420.2006.00757.x.

[13] Liang J, Williams DR. Aberrations and retinal image quality of the normal human eye. J Opt Soc Am A 1997;14(11):2873–83. https://doi.org/10.1364/JOSAA.14.002873.

[14] Schwiegerling J. Scaling Zernike expansion coefficients to different pupil sizes. J Opt Soc Am A 2002;19(10):1937–45. https://doi.org/10.1364/JOSAA.19.001937.

[15] Gatinel D, Rampat R, Dumas L, Malet J. An alternative wavefront reconstruction method for human eyes. J Refract Surg 2020;36(2):74–81. https://doi.org/10.3928/1081597X-20200113-01.

[16] Rampat R, Malet J, Dumas L, Gatinel D. Wavefront sensing, novel polynomial decomposition and its clinical applications. Indian J Ophthalmol 2020;68(12):2872–9. https://doi.org/10.4103/ijo.IJO_1760_20.

[17] Armstrong RA. Statistical guidelines for the analysis of data obtained from one or both eyes. Ophthalmic Physiol Opt 2013;33(1):7–14. https://doi.org/10.1111/opo.12009.

[18] Bland JM, Altman DG. Statistical methods for assessing agreement between two methods of clinical measurement. Lancet 1986;327(8476):307–10. https://doi.org/10.1016/S0140-6736(86)90837-8.

[19] Yoon G, Pantanelli S, MacRae S. Comparison of Zernike and Fourier wavefront reconstruction algorithms. J Refract Surg 2008;24(6):582–90. https://doi.org/10.3928/1081597X-20080601-06.

[20] Anderson HA, Ravikumar A, Benoit JS, Marsack JD. Impact of pupil diameter on objective refraction determination. Transl Vis Sci Technol 2019;8(6):32. https://doi.org/10.1167/tvst.8.6.32.

[21] Cheng X, Himebaugh NL, Kollbaum PS, Thibos LN, Bradley A. Validation of a clinical Shack–Hartmann aberrometer. Optom Vis Sci 2003;80(8):587–95. https://doi.org/10.1097/00006324-200308000-00010.

[22] Radhakrishnan H, Allen PM, Charman WN. Dynamics of accommodative facility in myopes. Invest Ophthalmol Vis Sci 2007;48(9):4375–82. https://doi.org/10.1167/iovs.07-0269.

[23] Ginis HS, Plainis S, Pallikaris A. Variability of wavefront aberration measurements in small pupil sizes. BMC Ophthalmol 2004;4:1. https://doi.org/10.1186/1471-2415-4-1.

[24] Navarro R. Refractive error sensing from wavefront slopes. J Vis 2010;10(13):3. https://doi.org/10.1167/10.13.3.

[25] Bennett JR, Stalboerger GM, Hodge DO, Schornack MM. Comparison of refractive assessment methods. J Optom 2015;8(2):109–15. https://doi.org/10.1016/j.optom.2014.11.001.

[26] Bayhan HA, Bayhan SA, Muhafiz E, Can I. Repeatability of aberrometric measurements in normal and keratoconus eyes. J Cataract Refract Surg 2014;40(2):269–75. https://doi.org/10.1016/j.jcrs.2013.07.046.

[27] Ning R et al., Repeatability and reproducibility of corneal higher-order aberrations after SMILE. Eye Vis 2022;9:4. https://doi.org/10.1186/s40662-021-00274-y.

[28] Kuo YC, Wang JH, Chiu CJ. Comparison of open-field autorefraction, closed-field autorefraction and retinoscopy. J Formos Med Assoc 2020;119(8):1251–8. https://doi.org/10.1016/j.jfma.2020.04.009.

[29] Nagra M, Akhtar A, Huntjens B, Campbell P. Open versus closed view autorefraction in young adults. J Optom 2021;14(1):86–91. https://doi.org/10.1016/j.optom.2020.06.007.

[30] Ruiss-Oliver MF et al., Agreement and variability of subjective refraction, autorefraction and wavefront aberrometry in pseudophakic patients. J Cataract Refract Surg 2021;47(8):1056–63. https://doi.org/10.1097/j.jcrs.0000000000000532.

[31] Carracedo G et al., Comparison of two wavefront autorefractors: binocular open-field versus monocular closed-field. J Ophthalmol 2020;2020:8580471. https://doi.org/10.1155/2020/8580471

3.8 Supplementary material

J0 and J45 Results (4 mm)

3.8.1 Agreement among the different refraction procedures: J0 Component

Descriptive statistics for J0 are reported in Table S1(RE) and Table S2 (LE). The comparisons between the instruments were performed on the J0 mean data of CFA monocular, OFA monocular, OFAUTO monocular, and subjective procedure for right eye and left eye separately. These data set for both eyes resulted normal distribution (Shapiro–Wilk test; $p > 0.005$).

Table S1 Mean, standard deviation (SD), median, and interquartile range (IQR) of J0 values of the right eye achieved in the four procedures for OFA and OFAUTO (monocular) for the young subsample (n = 22). The three repeated measurements and average for right eye are reported for CFA, OFA, and OFAUTO whereas in the case of subjective refraction only the final measure is reported.

	First Reading Mean ± SD; Median (IQ Range) (D)	**Second Reading Mean ± SD; Median (IQ Range) (D)**	**Third Reading Mean ± SD; Median (IQ Range) (D)**	**Average Reading Mean ± SD; Median (IQ Range) (D)**
CFA	0.25 ± 0.26; 0.25 (0.40)	0.25 ± 0.26 0.24 (0.40)	0.24 ± 0.26; 0.26 (0.39)	0.25 ± 0.26 0.25 (0.38)
OFA (Mono)	0.17 ± 0.23; 0.16 (0.34)	0.17 ± 0.24; 0.15 (0.34)	0.16± 0.23; 0.15 (0.29)	0.17 ± 0.24; 0.15 (0.33)
OFAUTO (Mono)	0.14 ± 0.24; 0.12 (0.29)	0.16 ± 0.21; 0.12 (0.27)	0.17 ± 0.21; 0.13 (0.24)	0.16 ± 0.21; 0.13 (0.29)
Subjective Procedure	_____	_____	_____	0.14 ± 0.20; 0.10 (0.28)

Table S2 Mean, standard deviation (SD), median, and interquartile range (IQR) of J0 values of the left eye achieved in the four procedures for OFA and OFAUTO (monocular) for the young subsample (n = 22). The three repeated measurements and average for left eye are reported for CFA, OFA, and OFAUTO whereas in the case of subjective refraction only the final measure is reported.

	First Reading Mean ± SD; Median (IQ Range) (D)	**Second Reading Mean ± SD; Median (IQ Range) (D)**	**Third Reading Mean ± SD; Median (IQ Range) (D)**	**Average Reading Mean ± SD; Median (IQ Range) (D)**
CFA	0.18 ± 0.21; 0.20 (0.32)	0.19 ± 0.21; 0.24 (0.33)	0.18 ± 0.22; 0.20 (0.32)	0.18 ± 0.21; 0.20 (0.32)
OFA (Mono)	0.10 ± 0.23; 0.10 (0.38)	0.11 ± 0.22; 0.12 (0.38)	0.11 ± 0.23; 0.11 (0.40)	0.11 ± 0.23; 0.11 (0.40)
OFAUTO (Mono)	0.15 ± 0.23; 0.12 (0.35)	0.16 ± 0.20; 0.15 (0.35)	0.18 ± 0.21; 0.20 (0.35)	0.16 ± 0.21; 0.15 (0.36)
Subjective Procedure	_____	_____	_____	0.17 ± 0.22; 0.11 (0.34)

The repeated-measures ANOVA conducted for the J0 component of the power vector in the right eye revealed no statistically significant effect of procedure ($F(3, 63) = 0.65$, $p = 0.586$), indicating that refractive outcomes did not vary significantly across the four measurement methods (Subjective, CFA, OFA, and OFAUTO). Separate post-hoc analyses (paired t-test with Bonferroni correction) for the right eye showed significant differences in two comparisons: between CFA and subjective ($p < 0.001$) and between the CFA and OFA ($p < 0.001$), where the CFA showed more positive results in both cases.

for the left eye. The main effect of procedure (within the subjects) was not present ($F(3, 63) = 1.62$, $p = 0.194$), indicating that the measured refractions did not significantly differ across the four

methods (Subjective, CFA, OFA, and OFAUTO). Separate post-hoc analyses (paired t-test with Bonferroni correction) for the left eye showed no significant differences between any of the procedures.

These findings are in line with the results from the original 3 mm pupil size data, supporting the conclusion that the method of refraction does not meaningfully affect the J0 component.

In Figure S1 a and b are reported the scatterplots between the right and left eye J0 values achieved with subjective refraction versus objective procedures. In the right eye, a significant correlation was found between the J0 value measured with subjective refraction and the objective methods: Pearson´s resulted 0.88, 0.89, and 0.80 ($p < 0.001$), for the relations subjective-CFA, subjective-OFA, and subjective-OFAUTO, respectively. All correlations were strong and statistically significant, with 95% confidence intervals indicating high consistency across measurement methods. Similarly, In the left eye, a significant correlation was found between the J0 value measured with subjective refraction and the objective methods: Spearman's Rho resulted 0.73, 0.65, and 0.71 ($p < 0.001$), for the relations subjective-CFA, subjective-OFA, and subjective-OFAUTO, respectively. All correlations were statistically significant, though slightly weaker than those observed in the right eye.

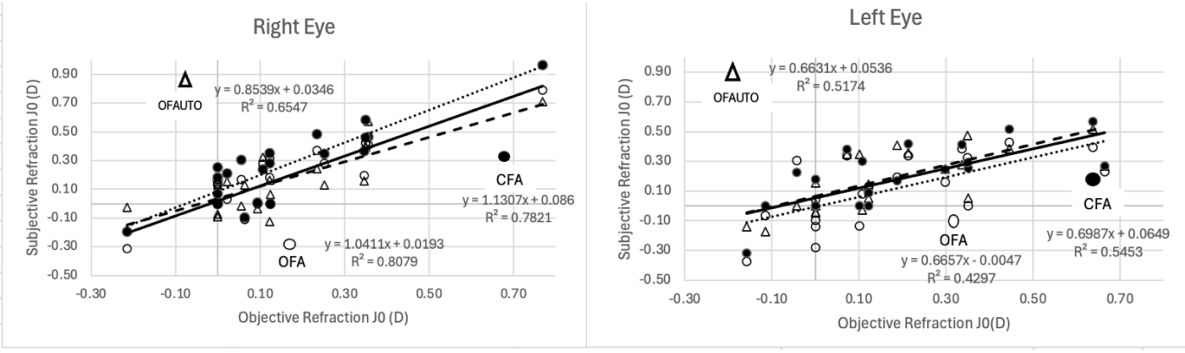

a) *b)*

Figure S1 scatterplot between J0 values achieved with subjective refraction versus objective procedures in the right eye (a) and the left eye (b) respectively

No Bland–Altman plots of the relationship between J0 values achieved by subjective refraction and the objective procedures (CFA, OFA, and OFAUTO) in right eye (Figure S2 a, b, and c) and the left eye (Figure S3 a, b, and c) showed any proportional bias.

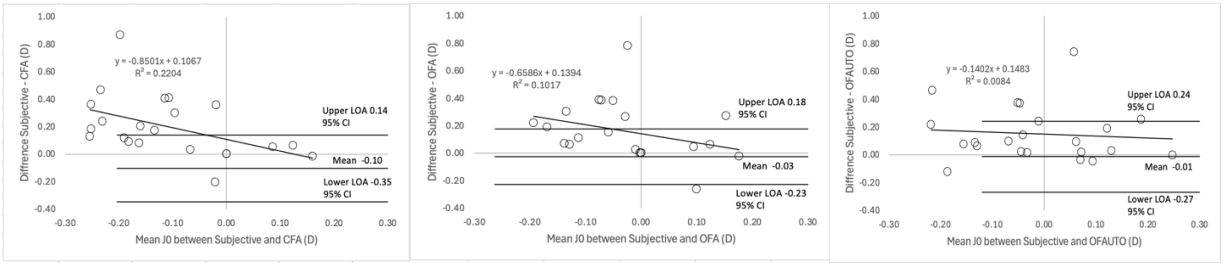

a) *b)* *c)*

Figure S2 Bland–Altman plot for the relationship between J0 values achieved with subjective refraction and objective procedures on the right eye (N=22): CFA (a), OFA (b), and OFAUTO (c). Pearson´s coefficients between the mean and the difference of J0 values achieved with subjective and objective refraction resulted -0.46, -0.31, and -0.09 for CFA, OFA and OFAUTO respectively (all n.s.). The limits of agreement (LoA) were calculated as mean of difference ± 1.96 SD of difference (D)

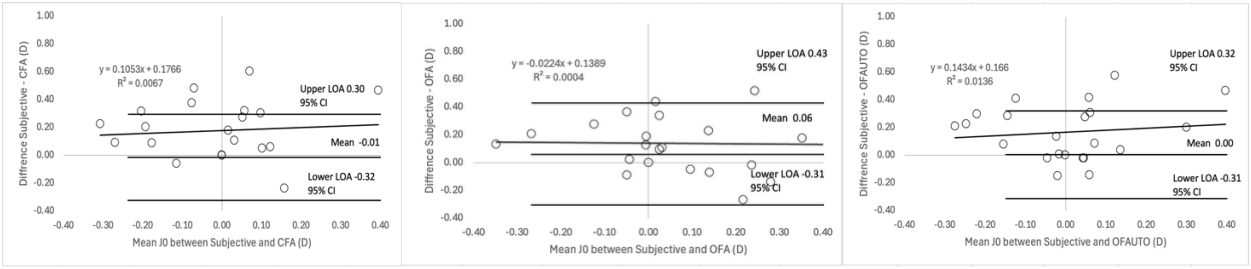

a) *b)* *c)*

Figure S3 Bland–Altman plot for the relationship between J0 values achieved with subjective refraction and objective procedures on the left eye (N=22): CFA (a), OFA (b), and OFAUTO (c). Pearson´s coefficients between the mean and the difference of J0 values achieved with subjective and objective refraction resulted 0.08, -0.02, and 0.11 for CFA, OFA and OFAUTO respectively (all n.s.). The limits of agreement (LoA) were calculated as mean of difference ± 1.96 SD of difference (D)

3.8.2 Agreement among the different refraction procedures: J45 Component

Descriptive statistics for J45 are reported in Table *S3* (RE) and Table S4 (LE). The comparisons between the instruments were performed on the J45 mean data of CFA monocular, OFA monocular, OFAUTO monocular, and subjective procedure for right eye and left eye separately. These data set for right eye did not result normal distribution (Shapiro–Wilk test; $p < 0.005$) except for the distribution of the OFAUTO which resulted normal distribution. As for the left eye, all data set resulted normal distribution (Shapiro–Wilk test; $p > 0.005$) except for the distribution of the CFA which resulted not normal distribution.

Table S3 Mean, standard deviation (SD), median, and interquartile range (IQR) of J45 values of the right eye achieved in the four procedures for OFA and OFAUTO (monocular) for the young subsample (n = 22). The three repeated measurements and average for right eye are reported for CFA, OFA, and OFAUTO whereas in the case of subjective refraction only the final measure is reported.

	First Reading Mean ± SD; Median (IQ Range) (D)	**Second Reading Mean ± SD; Median (IQ Range) (D)**	**Third Reading Mean ± SD; Median (IQ Range) (D)**	**Average Reading Mean ± SD; Median (IQ Range) (D)**
CFA	0.00 ± 0.14; -0.01 (0.19)	-0.01 ± 0.13; -0.01 (0.12)	-0.02 ± 0.14; -0.03 (0.14)	-0.01 ± 0.13; -0.02 (0.16)
OFA (Mono)	-0.01 ± 0.14; -0.01 (0.11)	-0.01 ± 0.14; -0.02 (0.11)	-0.01± 0.14; -0.02 (0.11)	-0.01± 0.14; -0.01 (0.11)
OFAUTO (Mono)	-0.01 ± 0.16; -0.01 (0.21)	0.00 ± 0.14; 0.00 (0.19)	0.01 ± 0.13; -0.01 (0.15)	0.00 ± 0.14; -0.02 (0.18)
Subjective Procedure	_____	_____	_____	0.01 ± 0.12; 0.00 (0.07)

Table S4 Mean, standard deviation (SD), median, and interquartile range (IQR) of J45 values of the left eye achieved in the four procedures for OFA and OFAUTO (monocular) for the young subsample (n = 22). The three repeated measurements and average for left eye are reported for CFA, OFA, and OFAUTO whereas in the case of subjective refraction only the final measure is reported.

	First Reading Mean ± SD; Median (IQ Range) (D)	**Second Reading Mean ± SD; Median (IQ Range) (D)**	**Third Reading Mean ± SD; Median (IQ Range) (D)**	**Average Reading Mean ± SD; Median (IQ Range) (D)**
CFA	-0.02 ± 0.12; 0.00 (0.11)	-0.03 ± 0.12; 0.00 (0.14)	-0.02 ± 0.11; 0.00 (0.13)	-0.02 ± 0.12; 0.00 (0.12)
OFA (Mono)	0.00 ± 0.10; 0.00 (0.10)	0.01 ± 0.12; 0.01 (0.16)	0.00 ± 0.10; 0.00 (0.13)	0.00 ± 0.10; 0.00 (0.13)
OFAUTO (Mono)	-0.03 ± 0.12; -0.01 (0.09)	-0.04 ± 0.13; -0.02 (0.13)	-0.03 ± 0.14; -0.03 (0.14)	-0.03 ± 0.13; -0.02 (0.11)
Subjective Procedure	_____	_____	_____	-0.03 ± 0.12; 0.00 (0.15)

The repeated-measures ANOVA conducted for the J45 component of the power vector in the right eye did not reveal a statistically significant main effect of procedure $F(3, 63) = 0.12$, $p = 0.947$, indicating that refractive outcomes did not vary significantly across the four measurement methods (Subjective, CFA, OFA, and OFAUTO).Separate post-hoc analyses (Wilcoxon Signed-Rank test with Bonferroni correction) for the right eye showed no significant differences between any of the procedures.

for the left eye. The main effect of procedure (within the subjects) was not present $F(3, 63) = 0.43$, $p = 0.729$), indicating that the measured refractions did not significantly differ across the four methods (Subjective, CFA, OFA, and OFAUTO). Separate post-hoc analyses (Wilcoxon Signed-Rank test with Bonferroni correction) for the left eye showed no significant differences between any of the procedures.

These findings are in line with the results from the original 3 mm pupil size data, supporting the conclusion that the method of refraction does not meaningfully affect the J45 component.

In Figure S4 a and b are reported the scatterplots between the right and left eye J45 values achieved with subjective refraction versus objective procedures. In the right eye, a significant correlation was found between the J45 value measured with subjective refraction and the CFA: Spearman's Rho resulted 0.64 ($p = 0.001$). No significant correlation was found between the J45 value measured with subjective refraction and the OFA or OFAUTO: Spearman's Rho resulted 0.48, 0.57, ($p = 0.02$,0.005) respectively, with 95% confidence intervals. In the left eye, a significant correlation was found between the J45 value measured with subjective refraction and the objective methods: Spearman's Rho resulted 0.70, 0.63, and 0.76 ($p < 0.001$), for the relations subjective-CFA, subjective-OFA, and subjective-OFAUTO, respectively. indicating high consistency across measurement methods.

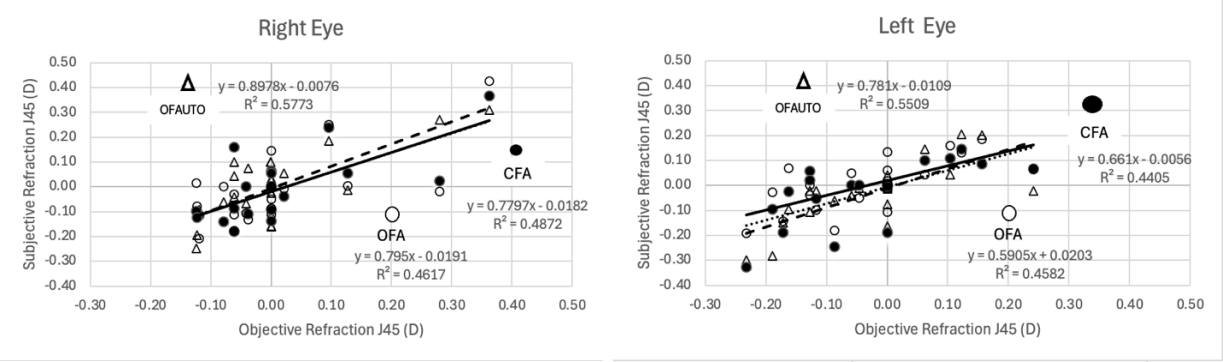

a) *b)*

Figure S4 scatterplot between J45 values achieved with subjective refraction versus objective procedures in the right eye (a) and the left eye (b) respectively.

No Bland–Altman plots of the relationship between J45 values achieved by subjective refraction and the objective procedures (CFA, OFA, and OFAUTO) in right eye (Figure S5 a, b, and c) and the left eye (Figure S6 a, b, and c) showed any proportional bias.

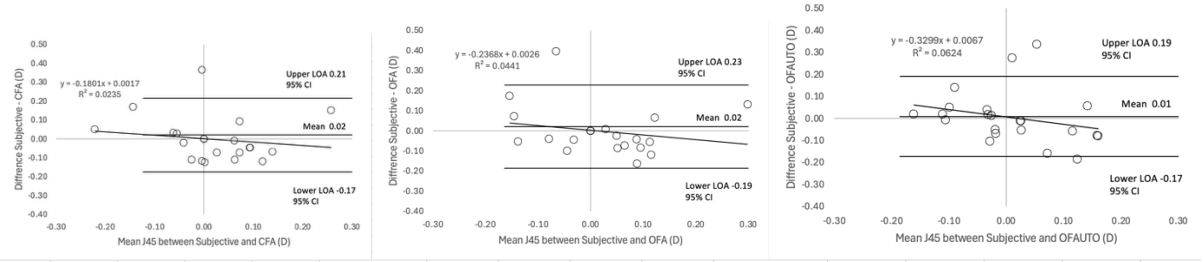

a) *b)* *c)*

Figure S5 Bland–Altman plot for the relationship between J45 values achieved with subjective refraction and objective procedures on the right eye (N=22): CFA (a), OFA (b), and OFAUTO (c). Spearmen rho coefficients between the mean and the difference of J45 values achieved with subjective and objective refraction resulted -0.32, -0.31, and -0.45 for CFA, OFA and OFAUTO respectively (all n.s.). The limits of agreement (LoA) were calculated as mean of difference ± 1.96 SD of difference (D)

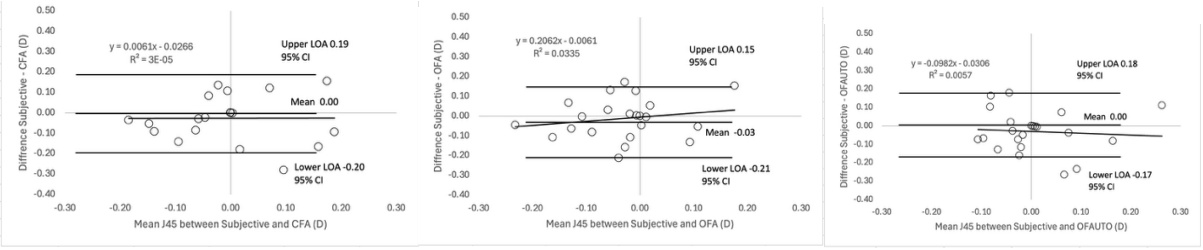

a) *b)* *c)*

Figure S6 Bland–Altman plot for the relationship between J45 values achieved with subjective refraction and objective procedures on the left eye (N=22): CFA (a), OFA (b), and OFAUTO (c). Spearmen rho coefficients between the mean and the difference of J45 values achieved with subjective and objective refraction resulted 0.07, 0.10, and -0.14 for CFA, OFA and OFAUTO respectively (all n.s.). The limits of agreement (LoA) were calculated as mean of difference ± 1.96 SD of difference (D)

Chapter 4. Study of myopia-related risk factors using longitudinal and a cross-sectional data

4.1 Introduction

Myopia progression is strongly linked to ocular growth and combining refractive outcomes with other structural measurements, particularly axial length (AL), provides a stronger way to monitor change over time [1]. While spherical equivalent refraction (SER) remains the standard clinical parameter [2], [3], longitudinal evidence shows that AL provides a more direct measure of eye growth and can reveal progression even when refractive change appears mild, especially in children [4], [5]. In addition to longer-term change, near work and accommodation have been proposed as functional factors related to myopia, and experimental studies suggest they may induce small, short-term shifts in ocular parameters, including transient AL changes and location-dependent choroidal thickness (CT) responses [6], [7]. This chapter examines these factors and their related structural parameters using both longitudinal follow-up and cross-sectional data to study myopia-related changes across age groups.

When studying structural or functional progression, even very small changes can be important, but only if they can be measured reliably. These estimations can be affected by the instrument used, acquisition conditions, and the analysis choices, especially when analyzing repeated measurements over time or across the peripheral field [8], [9]. The main limitations for choroidal thickness (CT) measurement reported are that manual caliper measurements are time-consuming and operator-dependent and the choroid–sclera interface is often difficult to delineate when image quality is poor [10], [11]. Automated and AI segmentation are promising but they can lose accuracy when boundaries are unclear [12] and most automated choroidal thickness methods rely on complex or proprietary algorithms that are difficult to reproduce across studies [13], [14], [15].

To reduce these sources of variability, a semi-automated method was adopted to keep segmentation consistent and reduce operator-related variability, A validation study was also performed against the manual OCT measurement to ensure the automated steps produced comparable results. Moreover, axial-length progression can be subtle as well [1], [16] and it is important to confirm that the measurement method is repeatable and agrees well with a reference

approach. We therefore validated axial-length measurements from the Myah biometer against OCT-derived axial length to ensure the device was reliable enough for monitoring progression and that observed changes were not driven by measurement error.

Recently, there has been an increasing emphasis on how AL is interpreted beyond simply measuring the absolute values. It is difficult to judge AL because eye size varies naturally with age, sex, and growth stage [5]. Several studies have developed AL growth curves and normative references using percentiles [4], [5], [17], [18], this allows clinicians and researchers to follow trajectories rather than single values and can help identify children who deviate from expected growth paths even over relatively short follow-up periods.

Moreover, AL and refraction change is often discussed in relation to near work and accommodation as functional factors related to myopia, even though the immediate effects of near work on ocular biometry can be subtle and timing dependent. Experimental studies have shown that accommodation or sustained near viewing can be accompanied by small, reversible increases in AL [19], [20], sometimes with refractive-group differences and a recovery phase after the task [6], [7], [21]. However, there remains uncertainty about how consistently these effects can be detected with shorter tasks or different measurement timing, especially in younger participants [7], [22].

Studies examining accommodation and near work have also reported short-term CT changes[6], [23]. Nevertheless, normative OCT studies have shown that CT is not uniform across the macula and is sensitive to measurement location and segmentation approach [24], this indicates that CT can provide additional biological context because it varies across retinal locations and may show location-dependent responses to visual demand. This supports the need for peripheral CT measurement rather than relying only on a single central point[6], [23].

Another factor that relates to myopia progression is peripheral refraction, it has gained great attention because it describes how the retinal image is formed away from the fovea and is frequently linked to the peripheral defocus hypothesis and optical myopia management strategies [3], [25]. Studies on peripheral refraction have reported relative peripheral hyperopia in myopic eyes, particularly along the horizontal meridian[26], [27], [28]. More recent work, however,

emphasizes that peripheral profiles are not uniform, and they can vary by meridian and eccentricity and between individuals with different refractive errors [29], [30]. A recent study by Antony et al. (2025)[29] reported that relative peripheral myopia was common even in hyperopes and emmetropes, while relative peripheral hyperopia appeared in only a subset of myopes. This variability suggests that a single relative peripheral hyperopia pattern may not be universal across individuals or refractive groups, and that interpretations based on this framework may not generalize to all retinal regions, particularly in non-myopic eyes.

Moreover, peripheral refraction profiles are method dependent, and studies differ in whether measurements are taken under cycloplegia or not [31], although some authors suggest accommodation has minimal influence on relative peripheral refraction[32], [33], [34], direct comparisons across protocols, especially beyond the horizontal meridian, remain limited[29], [35], [36]

This chapter evaluates axial length (AL) and spherical equivalent refraction (SER) longitudinally, describing absolute change over time, while additionally interpreting AL trajectories using age-referenced percentiles to better contextualize eye growth and progression risk across the study groups. It also examines the short-term response to a near task by assessing acute changes in AL and refraction, alongside choroidal thickness (CT), allowing structural and functional near-work effects to be interpreted together under the same protocol. Moreover, by characterizing baseline peripheral refraction in both children and adults, this chapter provides a foundation for interpreting peripheral profiles and for comparing findings across cohorts.

In addition to its clinical relevance, this chapter also frames ocular biometry and refraction measurements within physical optics. Parameters such as axial length, choroidal thickness, and peripheral refraction reflect how light is focused by the eye's geometry and how images form across central and peripheral retina [37]. Measurement outcomes can vary with instrument factors such as wavelength, alignment, and sampling setup, as well as fixation and accommodation during non-cycloplegic testing, which can affect resolution, repeatability, and sensitivity to small differences [38].

Overall, these analyses aim to give a clinically relevant picture of myopia-related risk across ages, and to highlight the influence of measurement conditions and retinal location on interpretation, acknowledging that the final values also depend on the optical measurement setup and processing choices.

4.2 Methods

4.2.1 Study design

Observational study with a longitudinal component and a cross-sectional component

4.2.2 Participants

Age groups

- Children (C) (7–17 years)
- Young adults (YA) (18–25 years)
- Adults (A) (40–45 years)

Inclusion criteria

- Age between 6 and 45 years.
- Monocular best corrected visual acuity (BCVA) ≥ 0.2 logMAR.
- Spherical refractive error between −6.00 D and +2.00 D
- Astigmatism ≤ 0.75 D
- Anisometropia (SER) less than 2.00 D
- No ocular or systemic known pathology, no eye surgery, not being pseudophakic.
- No history of ocular surgery
- Not being under any myopia control treatment
- Written informed consent obtained from adult participants and from parents/guardians of minors.

4.2.3 Devices and measurement techniques

- *Optical biometer (MYAH):* Axial length was measured using the MYAH optical biometer (Topcon Healthcare, Tokyo, Japan), a non-contact device based on optical low-coherence interferometry using an 820 nm super luminescent diode. The system provides axial length measurements over a range of 15.00–36.00 mm with a display resolution of 0.01 mm and an in-vivo repeatability of ±0.027 mm. The MYAH employs a guided-focus capture system and rapid acquisition to improve measurement stability and patient fixation during axial biometry.[39]
- *Optical coherence tomography (OCT):* Retinal imaging, axial length, and choroidal thickness measurements were obtained using the REVO FC spectral-domain optical coherence tomograph (Optopol Technology Sp. z o.o., Zawiercie, Poland). The system operates with a super luminescent diode light source at a central wavelength of 850 nm and provides an axial resolution of approximately 5 µm in tissue. The REVO FC includes an OCT-based biometry module enabling axial length measurements along the visual axis with visual verification of anatomical boundaries on B-scan images. High-resolution posterior segment scans were acquired for choroidal thickness assessment, supported by real-time eye-tracking to reduce motion artefacts during image acquisition[40]

- *Open-field aberrometer (OFA), open-field autorefractor (OFAUTO), and subjective refraction* were used to measure central and peripheral refractive error using the same instruments and standardized procedures described in Chapter 2. In this chapter, these methods were applied specifically for the assessment of central and peripheral refraction and for the evaluation of refractive changes during and after the near task.
- *Image analysis software (ImageJ/Fiji):* Choroidal thickness measurements were additionally analyzed using Fiji, an open-source distribution of ImageJ (National Institutes of Health, Bethesda, MD, USA). Fiji provides a platform for quantitative image analysis and allows manual and semi-automatic measurements on exported OCT B-scan images using calibrated distance tools. In the present study, vertical OCT scans were imported into Fiji and analyzed at predefined retinal locations to quantify choroidal thickness.[41]

4.3.4 Procedures

Axial length measurements

Axial length was measured in the right and left eye using the Myah biometry and in the right eye only using the OCT-based biometry. Myah biometry measurements were obtained at baseline (0 month), 9 months, and 18 months as part of the longitudinal follow-up, and additionally before and after the near task at baseline. At each session, three consecutive optical biometry measurements were acquired and averaged for analysis.

OCT-based axial length measurements were obtained for the right eye only at the 9-month visit and were used exclusively for method comparison analyses. For each OCT acquisition, a single scan provided ten axial length readings, which were automatically averaged by the system. OCT-derived axial length values were not included in the longitudinal or near-task analyses.

Manual choroidal thickness measurements using OCT

Manual choroidal thickness measurements were performed on posterior segment OCT images acquired using a crossline scan protocol (15 × 15 mm) centered on the fovea. Measurements were obtained from both vertical and horizontal B-scans, since comparable results were observed between orientations, vertical scans were used for analysis and reporting. Prior to measurement, OCT images were magnified using four consecutive zoom-in steps to improve visualization of choroidal boundaries.

Choroidal thickness was defined as the distance between the outer border of the retinal pigment epithelium/Bruch's membrane and the choroidal–scleral interface. As retinal thickness was automatically provided by the OCT software, a single vertical measurement line at Bruch's membrane was positioned at the point of minimum retinal thickness, corresponding to the foveal depression to the choroidal–scleral interface using the built-in caliper tool

Figure 4. 1. All measurements were performed following the same standardized procedure across subjects and time points.

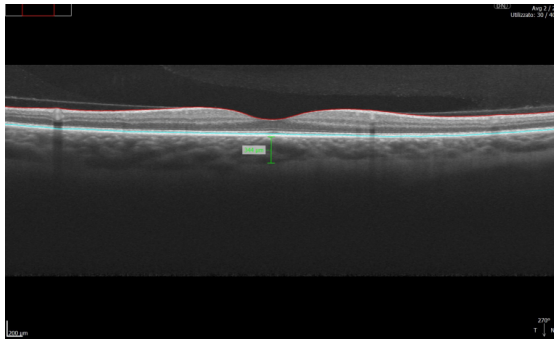

Figure 4. 1 Example of Manual CT Measurement from the Bruch's membrane to the Chorio-Scleral Interface on 4 times magnified Vertical OCT B-scan

Choroidal thickness analysis using Semi-automated (Fiji/ImageJ) method

Semi-automated choroidal thickness measurements were performed using Fiji (ImageJ) on exported vertical OCT B-scan images (tiff format). Only images with clearly visible choroidal boundaries were included in the analysis.

Step 1: Image preparation and scaling

OCT images were imported into ImageJ and converted to 8-bit grayscale format. The spatial scale was set using pixel units, based on the original OCT image dimensions (1566 pixels corresponding to 15 mm). Magnified images, four-click OCT magnification was applied prior to export, and the pixel-to-distance conversion was adjusted accordingly.

Step 2: Anatomical structure fitting

The foveal depression, Bruch's membrane, and choroidal–scleral interface were identified and fitted by manually tracing their visible boundaries using the multi points tool and then fitted using the Circle fit, placing multiple reference points along each structure to follow the anatomical contour Figure 4. 2

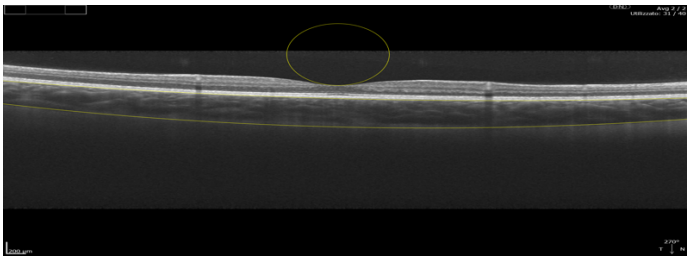

Figure 4. 2 Using the circle fit to align retinal center, Bruch's membrane, and choroidal-scleral interface

Step 3: Threshold adjustment and contrast enhancement

To improve boundary visibility, image thresholding was adjusted to white to obtain a uniform background, followed by contrast enhancement. The processed image was then saved in PNG format for further analysis Figure 4. 3.

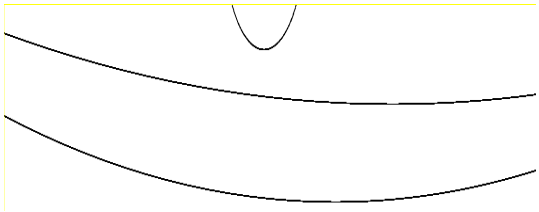

Figure 4. 3 Threshold adjustment and contrast enhancement .

Step 4: Line isolation and profile extraction

The saved image was reopened and cropped to retain only the three fitted anatomical lines. The image was then converted to 32-bit format to enhance contrast resolution. Choroidal thickness profiles were extracted using the Tools ▸ analyze line graph, allowing coordinate values to be obtained for each fitted line across the full scan width (Figure 4. 4).

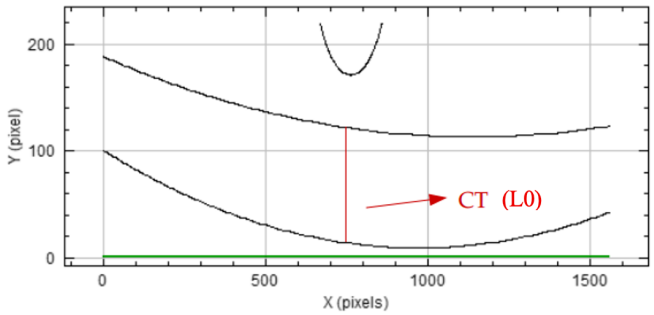

Figure 4. 4 Coordinate Extraction where the X-axis is Pixels (0-1566, 15 mm) and the Y-axis is the (CT)

Step 5: Coordinate extraction and thickness calculation

Coordinate values were extracted as an Excel sheet for the choroidal–scleral interface, Bruch's membrane, and foveal depression. Choroidal thickness was calculated as the vertical distance between Bruch's membrane and the choroidal–scleral interface at predefined central and peripheral retinal locations (the thinnest choroidal location, L0), sub-foveal superior at pixel 627 (L627) and sub-foveal inferior at pixel 939 (L939), and peripheral superior at pixel 101 (L101) and peripheral inferior at pixel 1466 (L1466). In this notation, L0 corresponds to the foveal depression identified for each subject, whereas Lxxx denotes the lateral pixel/A-scan index along the OCT B-scan. The selected indices were kept constant across participants to standardize sampling of parafoveal and more peripheral superior/inferior regions and to minimize edge-related artefacts (first 100 pixels excluded). The same procedure was applied consistently to pre- and post-near task images for each subject.

Near task procedure

The near task consisted of sustained near viewing at 33 cm. Participants watched a video displayed on a tablet mounted on the open field aberrometer (OFA). The total duration of the near task was 10 minutes.

Step 1: Pre- near task (Baseline) measurements (T0)

At the beginning of the protocol, before the video starts the participants were asked fixated on a central fixation target (cross/star (Figure 4. 5) displayed on the tablet for one minute to allow three repeated central refraction measurements, in the right eye only while the left eye is closed, using

the OFA. Three repeated axial length measurements were then obtained using optical biometry (MYAH), and one OCT (REVO) image was acquired independently using their respective devices.

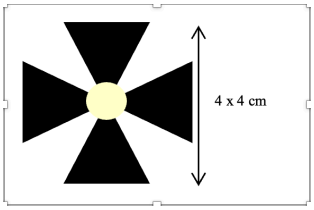

Figure 4. 5 central fixation target viewed by participants to stabilize fixation during OFA measurements

Step 2: Near viewing period

Participants continuously viewed the video on the tablet for the full duration of the near task while maintaining their habitual viewing posture.

Step 3: Intermediate measurement (T5)

After 5 minutes of near viewing, the video was paused and participants again fixated on the central fixation target for 1 minute. Central refraction measurements were repeated using the OFA only.

Step 4: Post–near task measurements (T10)

At the end of the 10-minute near task, the video was stopped and participants fixated on the central fixation target for 1 minute for three repeated central refraction assessment using the OFA. Three repeated axial length measurements were subsequently repeated using the MYAH, and one OCT image was acquired again using the OCT system.

The same near task protocol was applied consistently across all participants. Pre- and post-task measurements were used to evaluate acute changes associated with sustained near viewing.

Peripheral refraction measurement setup and targets

Peripheral refraction was measured at baseline in the right eye only, with the left eye occluded. Measurements were performed under non-cycloplegic conditions using the grand-Seiko open field autorefractor (OFAUTO) and a predefined fixation targets corresponding to visual eccentricities of 0°, 10°, 15°, 20°, and 30°, defined relative to the participant's primary gaze direction, rather than as a continuous spatial scale.

Participants were seated and instructed to maintain an upright head posture while moving only their eyes toward the fixation targets. Target positions were defined geometrically relative to the participant's eye position using the relationship, $\tan(\theta) = \text{offset}/\text{distance}$. Wall-mounted targets positioned at a distance of 4.40 m were used for 0° and superior eccentricities (10° and 15°), while freestanding vertical poles with a star fixation target at the top were used for 20° and 30° nasal and temporal eccentricities at a shorter viewing distance.

Measurements were obtained from two lateral seating positions to access nasal and temporal meridians. When seated on the right side, participants first fixated the wall target corresponding to 0°, followed by the superior targets (10° and 15°). In the same seating position, nasal peripheral refraction was measured by instructing participants to fixate the poles positioned to their left, corresponding to 20° and 30° nasal eccentricities along the horizontal meridian. Participants were then repositioned to the left side, where fixation of the wall target corresponded to 0° temporal, followed by fixation of poles positioned to their right, corresponding to 20° and 30° temporal eccentricities.

All angular target locations were pre-defined relative to the participant's eye position, ensuring that each fixation target subtended the intended visual eccentricity irrespective of the physical distance to the target.

provides a schematic representation of the fixation geometry and target arrangement used for peripheral refraction measurements

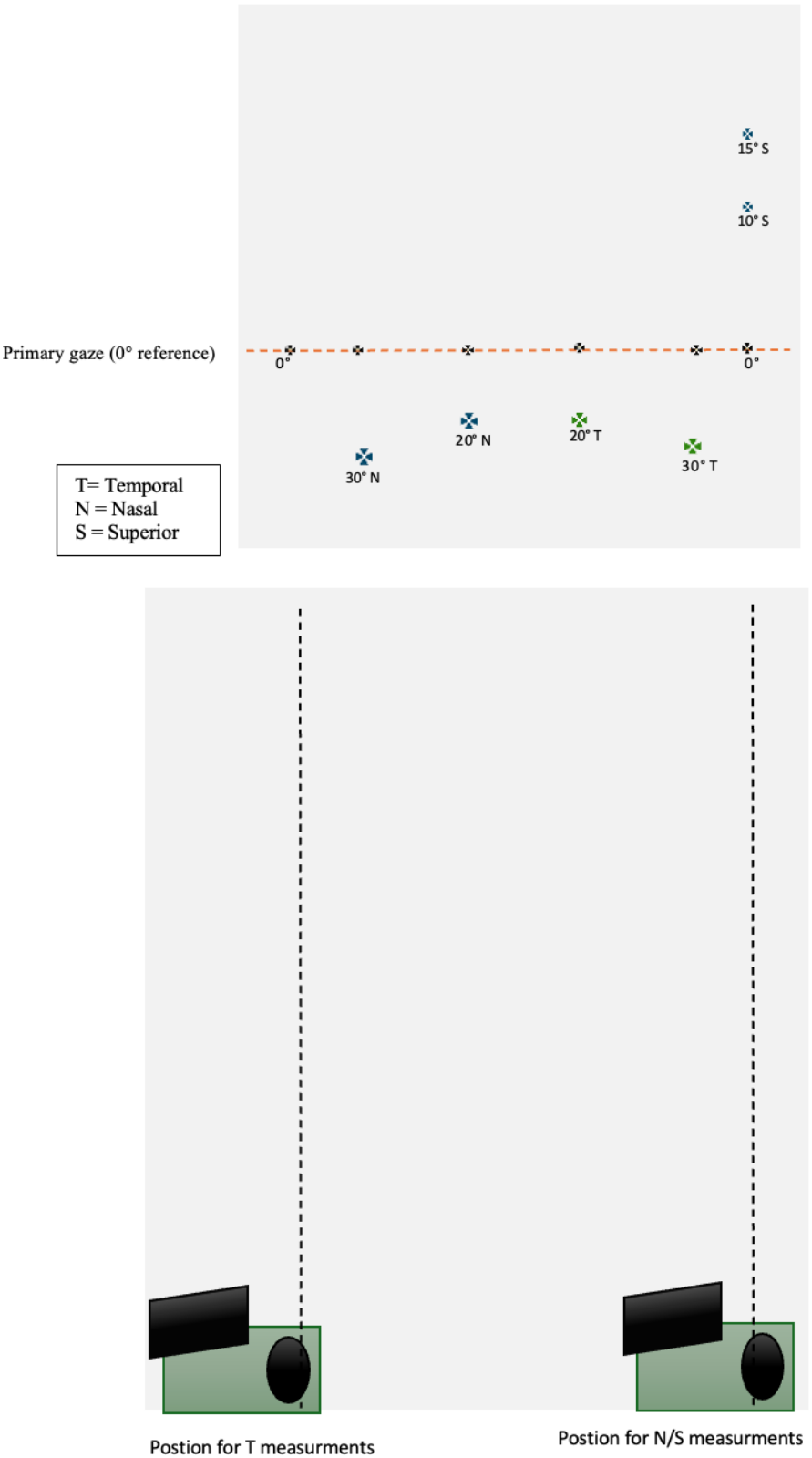

Figure 4. 6 Schematic representation of the peripheral refraction measurement setup and fixation geometry. Positions are schematic and not drawn to spatial scale

4.3 Data analysis

Statistical analyses were performed using IBM SPSS Statistics (version 29.0.1). Data were analyzed separately for children and adults and young adults when applicable. Normality of data distributions was assessed using the Shapiro–Wilk test.

For longitudinal and repeated-measures data (e.g., axial length and spherical equivalent progression across visits, and near task measurements at T0, T5, and T10), changes over time were analyzed using the Friedman test. When a significant effect of time was detected, post-hoc pairwise comparisons were performed with Bonferroni correction.

Pre–post comparisons (e.g., axial length and choroidal thickness before and after the near task) were assessed using paired t-tests for normally distributed data or Wilcoxon signed-rank tests for non-normally distributed data.

Peripheral refraction data were analyzed by comparing central (0°) and eccentric measurements using repeated-measures approaches, with eccentricity as a within-subject factor. Correlations between continuous variables (e.g., axial length and refractive error) were assessed using Pearson's or Spearman's correlation coefficients.

Agreement between measurement methods were evaluated using Bland–Altman analysis, including estimation of mean bias and 95% limits of agreement. The coefficients of variation (CV) and intraclass correlation coefficients (ICC) were calculated from the three repeated measurements for each instrument to assess repeatability. Statistical significance was set at $p < 0.05$. Where multiple comparisons were performed, Bonferroni-adjusted significance levels were applied accordingly.

4.4 Results

At the start of each results subsection, the sample size and key descriptive characteristics are reported, since they may differ depending on the specific analysis and data availability from the original participants listed in the methods section.

4.4.1 Measurement methods validation

Axial Length Measurement Methods: Myah vs REVO OCT Agreement

Axial length was measured using two instruments, the Myah biometer and the REVO OCT. Before analyzing axial length progression in the cohort, the agreement and repeatability of these two measurement methods were evaluated. A total of 143 paired measurements for the right eye were compared using the coefficient of variation (CV), intraclass correlation coefficient (ICC), Bland–Altman analysis and paired statistical testing.

Both devices showed similarly low CV values (Myah: 4.78%, REVO: 4.81%) and high ICC scores (Myah: 0.981, REVO: 0.989). Bland–Altman analysis demonstrated a mean difference of –0.02 ± 0.05 mm between devices, with the corresponding limits of agreement Figure 4.7. A statistically significant paired difference was found ($Z = -6.86$, $p < 0.001$) Figure 4.8 Spearman's Rho correlation coefficient indicated a strong association between Myah and REVO axial length measurements (0.99).

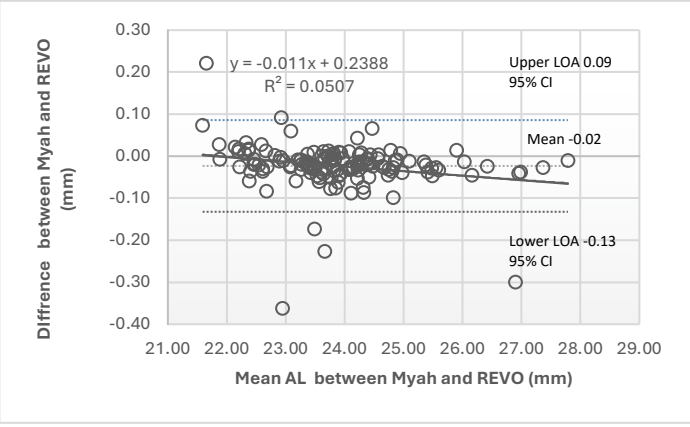

Figure 4. 7 Bland–Altman plot showing agreement between Myah and REVO axial length measurements.

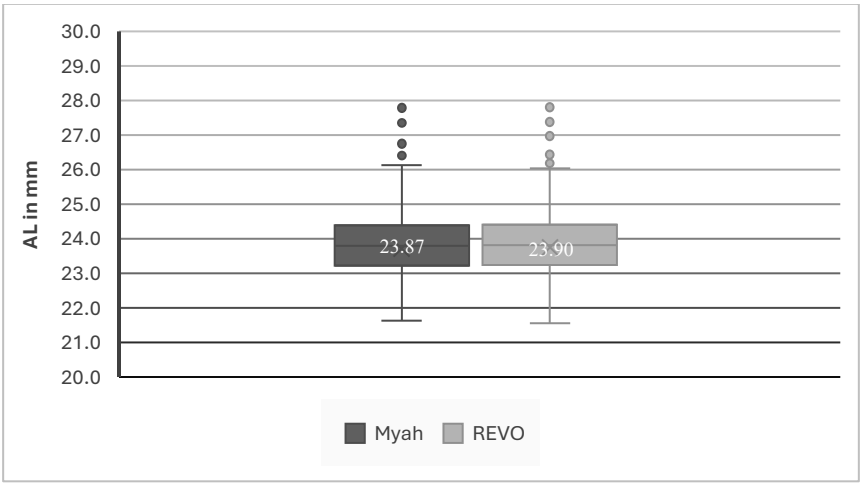

Figure 4 8 Comparison of mean axial length values between Myah and REVO OCT

Choroidal thickness Measurement Methods: Manual method vs ImageJ

Choroidal thickness (CT) was measured using both the manual measurement tool of the REVO-OCT software and a semi-automatic ImageJ-based method, and agreement between the two approaches were evaluated separately in the pre-near task and post-near task conditions in 28 subjects. In the pre–near task condition Figure 4. 9 a), the mean difference between manual and ImageJ measurements was −1.6 ± 12.8 µm, with Bland–Altman analysis showing narrow limits of agreement (upper limit: +23.3 µm, lower limit: −26.7 µm). After the near task Figure 4. 9 b), the mean difference between the two methods was 4.4 ± 13.0 µm, with similarly narrow limits of agreement (upper limit: +30.1 µm, lower limit: −21.1 µm). In both conditions, strong linear agreement was observed between methods, with high correlation coefficients ($r \geq 0.96$) Figure 4. 10 a) and Figure 4. 10 b).

Repeatability analysis further demonstrated comparable measurement stability for the two methods, with low coefficients of variation for both the manual (CV = 0.07) and semi-automatic

ImageJ method (CV = 0.06). Together, these findings indicate that the ImageJ-based method provides choroidal thickness measurements that are consistent with the manual REVO-OCT approach and sufficiently repeatable for CT analyses.

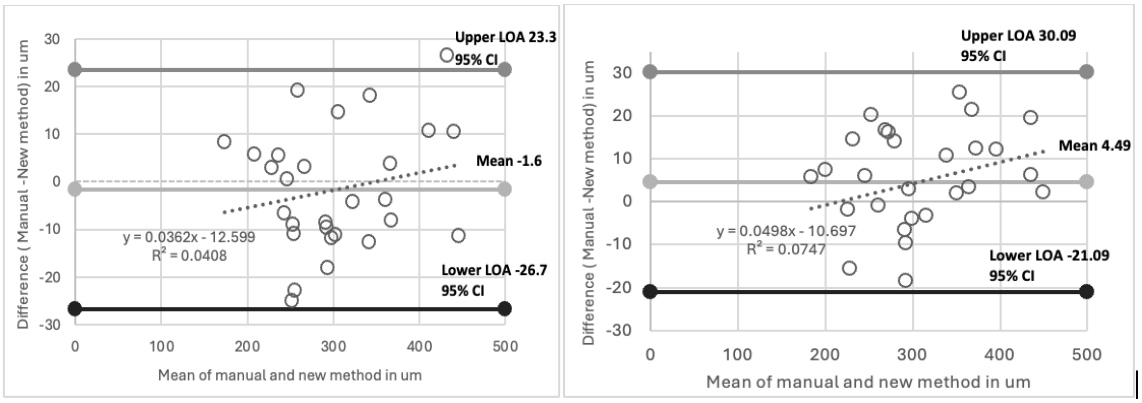

a) *b)*

Figure 4. 9 Bland–Altman analysis of agreement between manual REVO-OCT and semi-automatic ImageJ choroidal thickness measurements before (a) and after (b) the near task

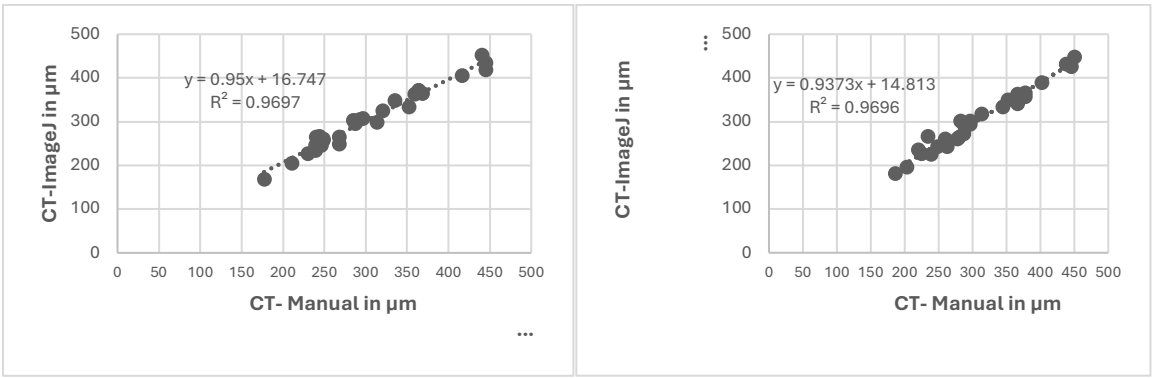

a) *b)*

Figure 4. 10 Correlation between manual REVO-OCT and semi-automatic ImageJ choroidal thickness measurements before (a) and after (b) the near task.

4.4.2 Biometric Progression of myopia related risk factors over the 18-Month Follow-Up

Participants were assessed across three measurement phases, baseline (0 months), 9 months (9m), and 18 months (18m). For each phase, axial length (AL) using Myah ocular biometry and spherical equivalent refraction (SER) using subjective refraction values were collected for the right (RE) and left (LE) eye in the three age groups (Children (C), young adults (YA), and adults (A)). The baseline data containing the full sample measured at each time point, including subjects who were present only at one or two visits, are reported in Table 4 1, Table 4 2 and Table 4 3.

In parallel, a longitudinal subsample was created consisting of the subjects who were successfully measured at all three phases, this matched dataset enables a true within-subject analysis of AL and SER progression.

Table 4 1 Baseline Axial Length (AL) and Spherical Equivalent Refraction (SER) at baseline for the RE and LE in (Children (C), young adults (YA), and adults (A).

Group	**Gender**	**N**	**AGE** Mean ± SD (years)	**AL_RE** Mean ± SD; Median (IQ Range) (mm)	**AL_LE** Mean ± SD; Median (IQ Range) (mm)	**SER_RE** Mean ± SD; Median (IQ Range) (D)	**SER_LE** Mean ± SD; Median (IQ Range) (D)
C	F	61	13.73 ± 3.60	23.21 ± 1.03; 23.10 (1.42)	23.17 ± 1.04; 23.07 (1.33)	-0.42 ± 1.47; 0.00 (1.31)	-0.34 ± 1.54; 0.00 (1.25)
C	M	44	12.57 ± 3.34	23.80 ± 0.83; 23.71 (0.99)	23.82± 0.86; 23.71 (0.92)	-0.62 ± 0.96; 0.13 (1.03)	-0.24 ± 1.05; 0.00 (0.63)
YA	F	30	22.32 ± 1.57	24.38 ± 1.95; 24.32 (1.14)	24.39 ± 0.99; 24.42 (1.28)	-2.19 ± 1.82; -2.19 (3.31)	-2.22 ± 1.81; -2.19 (3.34)
YA	M	26	22.66 ± 1.31	24.59 ± 1.03; 24.25 (0.85)	24.54 ± 1.07; 24.20 (1.15)	-1.21 ± 1.19; -1.19 (1.50)	-1.29 ± 1.45; -1.06 (1.75)
A	F	18	43.90 ± 1.42	23.95 ± 1.03; 23.87 (1.14)	24.03 ± 1.08; 23.84 (0.95)	-0.90 ± 1.57; -0.56 (1.50)	-1.12 ± 1.68; -0.56 (1.16)
A	M	24	43.72 ± 1.57	24.48 ± 1.24; 23.34 (1.73)	24.31 ± 1.23; 24.09 (1.68)	-1.35 ± 1.66; -0.81 (1.78)	-1.13 ± 1.87; -0.63 (2.22)

Table 4 2 Axial Length (AL) and Spherical Equivalent Refraction (SER) at 9 Months for the RE and LE.

Group	Gender	N	AL_RE Mean ± SD; Median (IQ Range) (mm)	AL_LE Mean ± SD; Median (IQ Range) (mm)	SER_RE Mean ± SD; Median (IQ Range) (D)	SER_LE Mean ± SD; Median (IQ Range) (D)
C	F	47	23.30 ± 1.03; 23.14 (1.62)	23.27 ± 1.05; 23.10 (1.50)	-0.66 ± 1.64; -0.13 (1.50)	-0.63 ± 1.62; -0.13 (1.13)
C	M	30	23.73 ± 0.86; 23.73 (0.65)	23.70± 0.77; 23.70 (0.67)	-0.29 ± 1.13; 0.00 (0.59)	-0.23 ± 0.95; -0.06 (0.56)
YA	F	21	24.41 ± 0.79; 24.56 (1.14)	24.43 ± 0.86; 24.62 (1.15)	-2.59 ± 1.85; -2.75 (3.69)	-2.67 ± 1.90; -3.25 (3.56)
YA	M	19	24.58 ± 1.19; 24.24 (0.62)	24.56 ± 1.17; 24.18 (0.89)	-1.42 ± 1.33; -1.25 (1.25)	-1.47 ± 1.57; -1.00 (1.75)
A	F	14	23.85 ± 1.14; 23.69 (1.27)	24.82 ± 1.15; 23.61 (1.17)	-0.90 ± 1.79; -0.44 (1.34)	-1.04 ± 1.73; -0.50 (1.16)
A	M	21	24.45 ± 1.29; 23.38 (1.93)	24.28 ± 1.29; 23.88 (1.74)	-1.15 ± 1.67; -0.50 (1.75)	-0.95 ± 1.84; -0.63 (1.69)

Table 4 3 Axial Length (AL) and Spherical Equivalent Refraction (SER) at 18 Months for the RE and LE.

Group	Gender	N	AL_RE Mean ± SD; Median (IQ Range) (mm)	AL_LE Mean ± SD; Median (IQ Range) (mm)	SER-RE Mean ± SD; Median (IQ Range) (D)	SER_LE Mean ± SD; Median (IQ Range) (D)
C	F	39	23.36 ± 1.12; 23.13 (1.72)	23.32 ± 1.09; 23.08 (1.70)	-0.56 ± 1.56; 0.00 (1.63)	-0.57 ± 1.51; 0.00 (1.63)
C	M	24	23.89 ± 0.79; 23.73 (0.74)	23.82± 0.71; 23.75 (0.69)	-0.31 ± 1.16; 0.00 (0.69)	-0.15 ± 0.96; 0.19 (0.59)
YA	F	16	24.60 ± 0.82; 24.79 (0.89)	24.63 ± 0.87; 24.77 (1.27)	-3.04 ± 1.82; -3.75 (3.66)	-3.20 ± 1.84; -3.88 (3.34)
YA	M	13	24.75 ± 1.35; 24.25 (0.83)	24.67 ± 1.30; 24.29 (1.03)	-1.20 ± 1.30; -1.00 (1.56)	-1.09 ± 1.35; -1.00 (1.94)
A	F	14	23.91 ± 1.13; 23.85 (1.29)	23.83 ± 1.14; 23.62 (1.18)	-0.84 ± 1.70; -0.25 (1.28)	-1.01 ± 1.81; -0.44 (1.28)
A	M	18	24.61 ± 1.29; 24.45 (1.91)	24.43 ± 1.31; 24.24 (1.83)	-1.17 ± 1.81; -0.69 (2.22)	-1.01 ± 1.98; -0.56 (1.91)

For the longitudinal progression analysis, axial length Table 4. 4 and Table 4. 5 and refractive changes Table 4.6 and Table 4. 7 were reported for 122 total subjects divided to three age categories, children (C), young adults (YA), and adults (A) for the RE and LE without separating males and females. This approach was selected because sex is not considered a determining factor in short-term axial length or refractive progression, and the primary aim of these tables is to describe within-group changes over time. Reporting the progression for the combined samples also maximizes statistical power and provides a clearer representation of the overall trends in each age category. A Bonferroni correction was applied to account for multiple comparisons, resulting in an adjusted significance threshold of $p < 0.016$. Bold p-values indicate statistically significant results.

Overall, the clearest pattern was observed in children, who showed consistent positive ΔAL across intervals, whereas young adults showed smaller changes and adults showed minimal change over follow-up. Children also showed the most noticeable refractive change over follow-up, while changes in young adults and adults were smaller and less consistently different across intervals.

Figure 4.11 and Figure 4 12 illustrate axial length (AL) and spherical equivalent refraction (SER) progression across the three time points. Data are presented as line charts for the right eye (A) and left eye (B).

Table 4. 4 Axial Length Progression (Matched Subjects) in the three groups in the RE

Group	**N**	**AL_0** **Mean ± SD; Median (IQ Range) (mm)**	**AL_9** **Mean ± SD; Median (IQ Range) (mm)**	**AL_18** **Mean ± SD; Median (IQ Range) (mm)**	**ΔAL_0–9** **Mean ± SD** **t-test/z (p-value)**	**ΔAL_9–18** **Mean ± SD** **t-test/z (p-value)**	**ΔAL_0–18** **Mean ± SD** **t-test/z (p-value)**
C	62	23.47 ± 1.04; 23.43 (1.29)	23.51 ± 1.02; 23.47 (1.31)	23.59 ± 1.02; 23.62 (1.43)	0.04 ± 0.08 Z=-4.25 **(<0.001)**	0.08 ± 0.10 Z=-5.69 **(<0.001)**	0.12 ± 0.14 Z=-5.85 **(<0.001)**
YA	28	24.63 ± 1.06; 24-36 (1.00)	24.63 ± 1.07; 24.40 (0.87)	24.67 ± 1.09; 24.49 (0.87)	0.00 ± 0.07 t =-0.17 (0.86)	0.04 ± 0.06 t =-3.48 **(0.002)**	0.04 ± 0.11 t =-1.91 (0.06)
A	32	24.32 ± 1.24; 24.04 (1.88)	24.28 ± 1.27; 24.01 (1.92)	24.30 ± 1.26; 24.15 (1.93)	-0.04 ± 0.19 Z=-0.86 (0.38)	0.02 ± 0.12 Z=-1.13 (0.25)	-0.01 ± 0.23 Z=-0.31 (0.75)

*** Bold p-values indicate statistically significant results**

Table 4. 5 Axial Length Progression (Matched Subjects) in the 3 groups in the LE

Group	N	AL_0 Mean ± SD; Median (IQ Range) (mm)	AL_9 Mean ± SD; Median (IQ Range) (mm)	AL_18 Mean ± SD; Median (IQ Range) (mm)	ΔAL_0–9 Mean ± SD t-test/z (p-value)	ΔAL_9–18 Mean ± SD t-test/z (p-value)	ΔAL_0–18 Mean ± SD t-test/z (p-value)
C	62	23.24 ± 0.99; 23.45 (1.23)	23.48 ± 1.00; 23.53 (1.30)	23.54 ± 0.97; 23.62 (1.44)	0.05 ± 0.07 Z=-5.48 **(<0.001)**	0.06 ± 0.11 Z=-4.86 **(<0.001)**	0.12 ± 0.13 Z=-6.22 **(<0.001)**
YA	28	24.60 ± 1.08; 24.55 (1.29)	24.65 ± 1.07; 24.55 (1.11)	24.67 ± 1.08; 24.56 (1.14)	0.05 ± 0.19 Z=-1.43 (0.15)	0.02 ± 0.07 t =1.18 (0.24)	0.07 ± 0.20 Z=-1.67 (0.09)
A	32	24.23 ± 1.22; 24.01 (1.41)	24.17 ± 1.26; 23.85 (1.92)	24.17 ± 1.26; 23.86 (1.58)	-0.06 ± 0.25 Z=-0.41 (0.68)	0.00 ± 0.03 t =0.22 (0.82)	-0.06 ± 0.24 Z=-0.54 (0.58)

*** Bold p-values indicate statistically significant results**

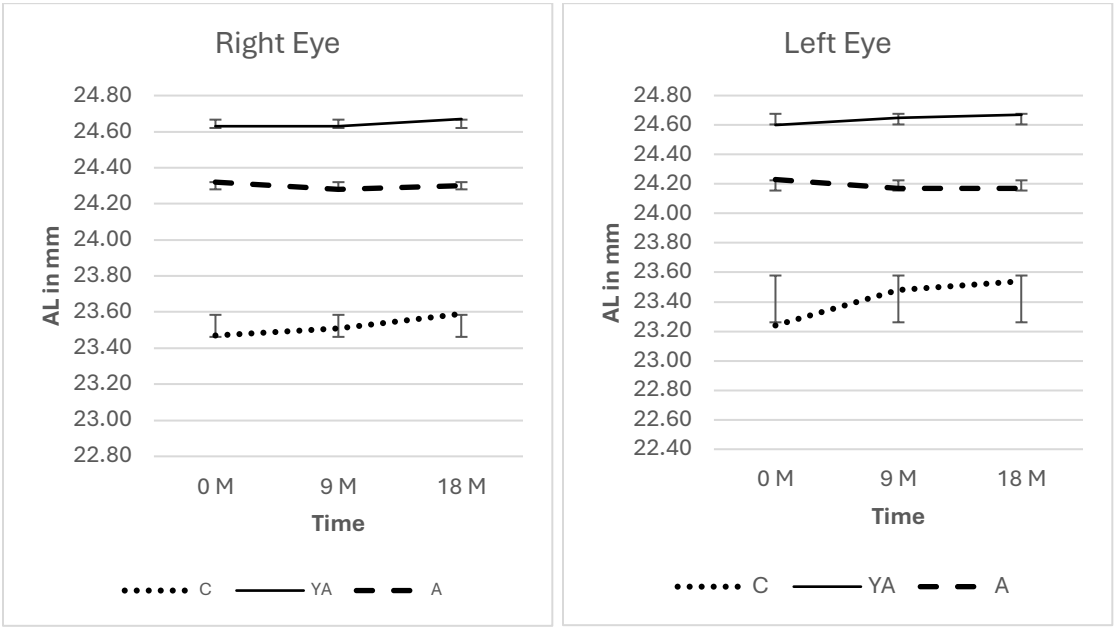

a) *b)*

Figure 4.11 Axial length progression in matched subjects measured at baseline, 9 months, and 18 months. in the right eye (a) and left eye (b).

Table 4.6 SER Progression (Matched Subjects) in the three groups in the RE

Group	N (122 Total)	SER_0 Mean ± SD; Median (IQ Range) (D)	SER_9 Mean ± SD; Median (IQ Range) (D)	SER_18 Mean ± SD; Median (IQ Range) (D)	ΔSER_0–9 Mean ± SD t-test/z (p-value)	ΔSER_9–18 Mean ± SD t-test/z (p-value)	ΔSER_0–18 Mean ± SD t-test/z (p-value)
C	62	-0.42 ± 1.37; 0.00 (1.13)	-0.51 ± 1.42; 0.00 (1.00)	-0.48 ± 1.42; 0.00 (1.16)	-0.09 ± 0.38 t =1.95 **(<0.001)**	0.03 ± 0.34 t =0.61 **(<0.001)**	-0.07 ± 0.41 Z=-1.30 **(<0.001)**
YA	28	-2.34 ± 1.73; -2.13 (3.34)	-2.39 ± 1.75; -2.00 (3.53)	-2.29 ± 1.82; -1.88 (3.56)	-0.04 ± 0.18 Z=1.23 (0.21)	0.10 ± 0.31 Z=-1.52 (0.12)	0.05 ± 0.35 t =-0.80 (0.42)
A	32	-1.14 ± 1.66; -0.63 (1.56)	-1.16 ± 1.74; -0.50 (1.59)	-1.02 ± 1.74; -0.50 (1.72)	-0.04 ± 0.18 Z=-0.65 (0.51)	0.10 ± 0.31 Z=-2.51 **(0.012)**	0.05 ± 0.35 t =-2.23 (0.03)

*** Bold p-values indicate statistically significant results**

Table 4. 7 SER Progression (Matched Subjects) in the three groups in the LE

Group	N (122 Total)	SER_0 Mean ± SD; Median (IQ Range) (D)	SER_9 Mean ± SD; Median (IQ Range) (D)	SER_18 Mean ± SD; Median (IQ Range) (D)	ΔSER_0–9 Mean ± SD t-test/z (p-value)	ΔSER_9–18 Mean ± SD t-test/z (p-value)	ΔSER_0–18 Mean ± SD t-test/z (p-value)
C	62	-0.34 ± 1.30; 0.00 (0.91)	-0.45 ± 1.34; -0.06 (0.88)	-0.42 ± 1.35; 0.00 (1.00)	-0.11 ± 0.30 t =2.95 **(<0.004)**	0.04 ± 0.34 t =-0.85 (0.39)	-0.08 ± 0.38 t =1.58 (0.12)
YA	28	-2.34 ± 1.81; -2.19 (3.13)	-2.42 ± 1.88; -2.19 (3.47)	-2.33 ± 1.92; -2.19 (3.41)	-0.08 ± 0.21 t =1.95 (0.06)	0.08 ± 0.21 t =-2.1 (0.04)	0.01 ± 0.27 Z=-0.43 (0.66)
A	32	-1.05 ± 1.78; -0.63 (1.34)	-1.08 ± 1.82; -0.63 (1.41)	-1.01 ± 1.88; -0.50 (1.47)	-0.03 ± 0.22 t =0.81 (0.42)	0.07 ± 0.17 t =2.46 (0.02)	0.04 ± 0.26 t =-0.94 (0.35)

*** Bold p-values indicate statistically significant results**

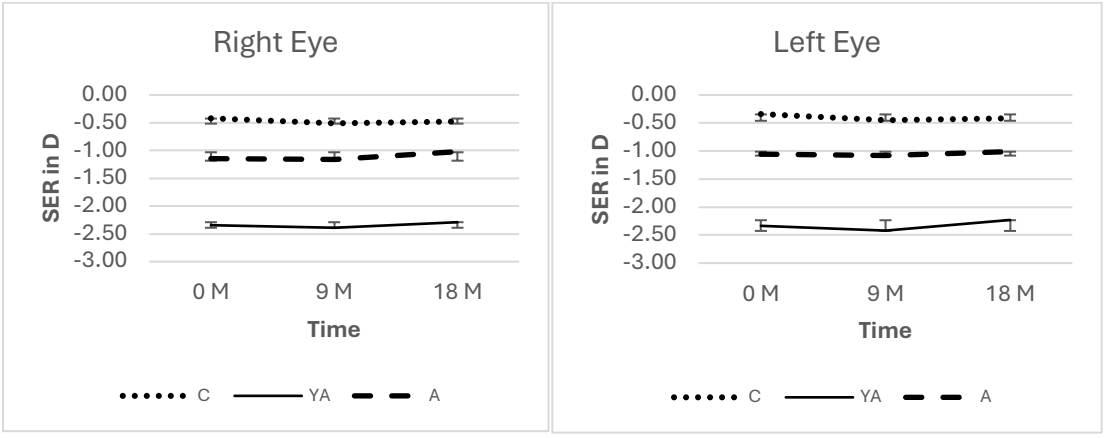

a) *b)*

Figure 4 12 Spherical equivalent refraction progression in matched subjects measured at baseline, 9 months, and 18 months. in the right eye (a) and left eye (b).

Spearman's rank correlation was performed to assess the association between axial elongation (ΔAL 0–18 months) and refractive error change (ΔSER 0–18 months) in children. For the right eye Figure 4. 13 a) significant negative correlation was found –0.33 (p -value = 0.008). For the left eye, Figure 4. 13 b) the correlation did not reach statistical significance = –0.24 (p = 0.051).

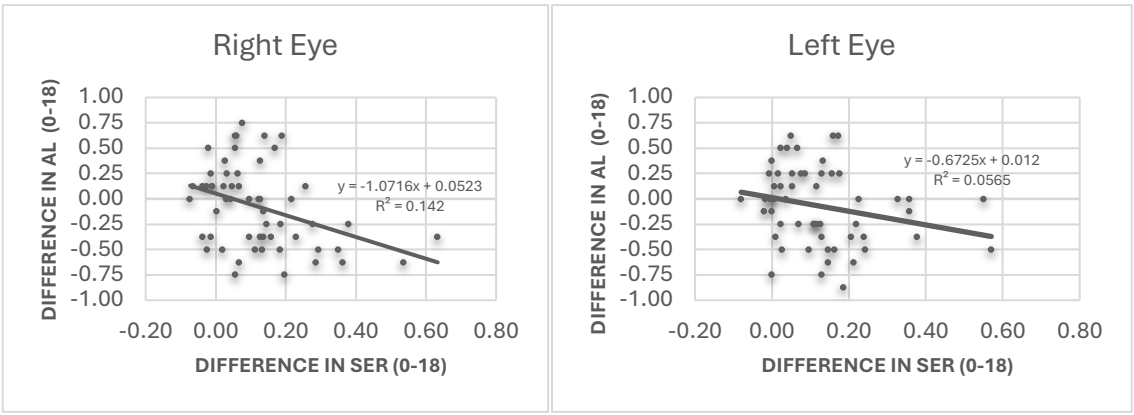

a) *b)*

Figure 4. 13 Correlation between axial elongation (ΔAL 0–18 months) and refractive error change (ΔSER 0–18 months) in children for the right eye (a) and left eye (b).

In the following analyses, males and females were separated when reporting percentile classifications and risk categories for the development of myopia at 0 M (Table 4. 8 RE and Table 4.9 LE), 9m (Table 4.10 RE and Table 4.11 LE) and at 18 m (Table 4. 12 RE and Table 4. 13 LE). This method was used in published normative axial length datasets, where percentile boundaries (e.g., P10, P50, P90, P98) are derived separately for girls and boys. Because axial length distributions differ slightly by sex at the population level, applying sex-specific thresholds is necessary to ensure accurate percentile assignment and valid interpretation of risk. Therefore, for all tables involving normative percentiles and percentile-based shifts, the data are presented separately for males and females, following the conventions established in previous large-scale studies [4], [5].

These tables highlight how many participants fall into higher-than-expected axial length ranges relative to normative references. Across visits, most subjects remained within the mid-percentile bands, while a smaller subset from the children group consistently fell at or above the ≥P90 and ≥P98.

Table 4. 8 Percentile Summary at 0 Months (Matched Subjects Only) RE

Group	Sex	N	% <P10	% P10–P50	% P50–P90	% ≥P90	% ≥P98 (subset of ≥P90)
C	F	38	10.5%	26.3%	39.5%	23.7%	7.9%
C	M	24	4.2%	37.5%	37.5%	20.8%	4.2%
YA	F	16	0%	12.5%	62.5%	25%	0%
YA	M	12	0%	25%	58.3%	16.7%	16.7%
A	F	14	0%	28.6%	57.1%	14.3%	0%
A	M	18	6%	27.8%	50%	16.7%	11.1%

Table 4.9 Percentile Summary at 0 Months (Matched Subjects Only) LE

Group	Sex	N	% <P10	% P10–P50	% P50–P90	% ≥P90	% ≥P98 (subset of ≥P90)
C	F	38	10.5%	31.6%	28.9%	28.9%	5.3%
C	M	24	4.2%	37.5%	41.7%	16.7%	4.2%
YA	F	16	0%	6.3%	62.5%	31.3%	0%
YA	M	12	0%	41.7%	41.7%	16.7%	16.7%
A	F	14	0%	21.4%	64.3%	14.3%	0%
A	M	18	6%	27.8%	50%	16.7%	0%

Table 4.10 Percentile Summary at 9 Months (Matched Subjects Only) RE

Group	Sex	N	% <P10	% P10–P50	% P50–P90	% ≥P90	% ≥P98 (subset of ≥P90)
C	F	38	10.5%	28.9%	36.8%	23.7%	7.9%
C	M	24	4.2%	33.3%	41.7%	20.3%	0%
YA	F	16	0%	12.5%	68.8%	18.8%	0%
YA	M	12	0%	25%	58.3%	16.7%	16.7%
A	F	14	0%	35.7%	50%	14.3%	0%
A	M	18	6%	33.3%	44.4%	16.7%	11.1%

Table 4.11 Percentile Summary at 9 Months (Matched Subjects Only) LE

Group	Sex	N	% <P10	% P10–P50	% P50–P90	% ≥P90	% ≥P98 (subset of ≥P90)
C	F	38	10.5%	28.9%	31.6%	28.9%	5.3%
C	M	24	4.2%	29.2%	45.8%	20.3%	4.2%
YA	F	16	0%	6.3%	62.5%	31.3%	0%
YA	M	12	0%	33.3%	50%	16.7%	16.7%
A	F	14	0%	28.6%	57.1%	14.3%	0%
A	M	18	6%	33.3%	44.4%	16.7%	5.6%

Table 4. 12 Percentile Summary at 18 Months (Matched Subjects Only) RE

Group	Sex	N	% <P10	% P10–P50	% P50–P90	% ≥P90	% ≥P98 (subset of ≥P90)
C	F	38	5.3%	34.2%	31.6%	28.9%	7.9%
C	M	24	0%	33.3%	41.7%	41.7%	8.3%
YA	F	16	0%	12.5%	62.5%	25%	0%
YA	M	12	0%	25%	58.3%	16.7%	16.7%
A	F	14	35.7%	50%	14.3%	0%	0%
A	M	18	6%	33.3%	44.4%	16.7%	11.1%

Table 4. 13 Percentile Summary at 18 Months (Matched Subjects Only) LE

Group	Sex	N	% <P10	% P10–P50	% P50–P90	% ≥P90	% ≥P98 (subset of ≥P90)
C	F	38	5.3%	34.2%	28.9%	31.6%	5.3%
C	M	24	0%	29.2%	50%	20.8%	8.3%
YA	F	16	0%	12.5%	50%	37.5%	0%
YA	M	12	0%	33.3%	50%	16.7%	16.7%
A	F	14	0%	28.6%	57.1%	14.3%	0%
A	M	18	6%	33.3%	44.4%	16.7%	0%

To further characterize longitudinal changes in axial length relative to normative growth, the risk of developing myopia was assessed based on shifts in axial length percentile position over time. summarize the distribution of subjects classified as stable (0–5 percentile shift), moderate risk (5–10 percentile shift), or high risk (≥10 percentile shift) for the right and left eyes across the three follow-up intervals (0–9 months, 9–18 months, and 0–18 months).

Results are reported separately by age group and sex, together with the mean ± standard deviation of the percentile shift for each interval. Table 4. 14 to Table 4. 19 provide a categorical overview of percentile-based progression in the RE and LE.

Table 4. 14 Risk of developing myopia Shift 0→9 in the RE

Group	Sex	N	Mean Shift ± SD 0→9 (Percentiles)	%Stable (0–5)	%Moderate risk (5–10)	%High risk (≥10)
C	F	38	0.95 ± 6.44	86.8%	7.9%	5.3%
C	M	24	3.21 ± 8.50	83.3%	4.2%	12.5%
YA	F	16	0.00 ± 0.00	100%	0%	0%
YA	M	12	0.00 ± 0.00	100%	0%	0%
A	F	14	-2.86 ± 10.69	100%	0%	0%
A	M	18	-1.39 ± 5.89	100%	0%	0%

Table 4. 15 Risk of developing myopia Shift 0→9 in the LE

Group	Sex	N	Mean Shift ± SD 0→9 (Percentiles)	%Stable (0–5)	%Moderate risk (5–10)	%High risk (≥10)
C	F	38	1.39 ± 4.74	89.5%	5.3%	5.3%
C	M	24	3.46 ± 7.86	83.3%	0%	16.7%
YA	F	16	-1.56 ± 6.25	100%	0%	0%
YA	M	12	2.08 ± 7.22	92%	0%	8%
A	F	14	-3.57 ± 0.08	100%	0%	0%
A	M	18	-1.22 ± 5.98	100%	0%	0%

Table 4. 16 Risk of developing myopia Shift 9→18 in the RE

Group	Sex	N	Mean Shift ± SD 9→18 (Percentiles)	%Stable (0–5)	%Moderate risk (5–10)	%High risk (≥10)
C	F	38	2.11 ± 5.77	81.6%	7.9%	10.5%
C	M	24	2.13 ± 9.41	83.3%	4.2%	12.5%
YA	F	16	-0.94 ± 3.75	100%	0%	0%
YA	M	12	0.00 ± 0.00	100%	0%	0%
A	F	14	-2.86 ± 7.52	86%	0%	14%
A	M	18	0.00 ± 0.00	100%	0%	0%

Table 4. 17 Risk of developing myopia Shift 9→18 in the LE

Group	Sex	N	Mean Shift ± SD 9→18 (Percentiles)	%Stable (0–5)	%Moderate risk (5–10)	%High risk (≥10)
C	F	38	1.45 ± 4.78	86.8%	7.9%	5.3%
C	M	24	3.67± 8.37	79.2%	8.3%	12.5%
YA	F	16	-0.63 ± 7.50	87.5%	0%	12.5%
YA	M	12	2.08 ± 7.22	92%	0%	8%
A	F	14	0.00 ± 0.00	100%	0%	0%
A	M	18	-0.17 ± 0.71	100%	0%	0%

Table 4. 18 Risk of developing myopia Shift 0→18 in the RE

Group	Sex	N	Mean Shift ± SD 0→18 (Percentiles)	%Stable (0–5)	%Moderate risk (5–10)	%High risk (≥10)
C	F	38	3.05 ± 8.32	71.1%	13.2%	15.8%
C	M	24	5.33 ± 9.63	70.8%	8.3%	20.8%
YA	F	16	-0.94 ± 3.75	100%	0%	0%
YA	M	12	0.00 ± 0.00	100%	0%	0%
A	F	14	0.00 ± 9.81	93%	0%	7%
A	M	18	-1.39 ± 5.89	100%	0%	0%

Table 4. 19 Risk of developing myopia Shift 0→18 LE

Group	Sex	N	Mean Shift ± SD 0→18 (Percentiles)	%Stable (0–5)	%Moderate risk (5–10)	%High risk (≥10)
C	F	38	2.84 ± 6.42	76.3%	13.2%	10.5%
C	M	24	7.13 ± 12.95	70.8%	4.2%	25%
YA	F	16	-2.19 ± 9.66	94%	0%	6%
YA	M	12	4.17 ± 9.73	83%	0%	17%
A	F	14	-3.57 ± 0.08	100%	0%	0%
A	M	18	-1.39 ± 5.89	100%	0%	0%

Axial length percentile positions remained largely stable across the follow-up period. Across all age groups and both eyes, the majority of subjects were classified as stable (0–5 percentile shift) at each interval, with only a small proportion exhibiting moderate (5–10 percentile shift) or high (≥10 percentile shift) risk.

In children, a limited subset showed moderate or high percentile shifts, particularly over the 0–18-month interval, whereas young adults and adults were predominantly classified as stable, with minimal mean percentile changes and no consistent upward shift. Mean percentile shifts were small relative to their associated variability, and no systematic differences were observed between sexes or between right and left eye.

4.4.3 Short-term near-work effects on myopia-related ocular parameters

Refractive Error

At baseline (0 M), central spherical equivalent refraction (SER) was measured for the right eye using an open field aberrometer (OFA) while participants viewed a video at 33 cm for 10 minutes. Measurements were obtained at 0, 5, and 10 minutes of near viewing in the right eye, and comparisons were performed between baseline (T0) and 10 minutes (T10). In children (n = 98), mean OFA remained stable across time points. Similarly, in adults (n = 72), OFA values showed minimal variation over time, and no significant differences were detected between measurement intervals (all $p > 0.05$), values are reported in Table 4.20

Table 4. 20. Central spherical equivalent refraction measured with an open field aberrometer (OFA) at baseline (T0), 5 minutes (T5), and 10 minutes (T10) of near viewing in children and adults

Group	**N**	Age Mean ± SD (years)	Subjective Refraction Mean ± SD; Median (IQ Range) (D)	OFA_T0 Mean ± SD; Median (IQ Range) (D)	OFA_T5 Mean ± SD; Median (IQ Range) (D)	OFA_T10 Mean ± SD Median (IQ Range) (D)	**ΔOFA_0–5 Mean ± SD t-test/z (p-value)**	**ΔOFA_5-10 Mean ± SD t-test/z (p-value)**	**ΔOFA_0–10 Mean ± SD t-test/z (p-value)**
C	98	13.63 ± 3.50	-0.39 ± 1.30; 0.00 (1.25)	-2.03 ± 0.55; -2.08 (0.55)	-2.09 ± 0.44; -2.08 (0.65)	-2.10 ± 0.53; -2.07 (0.59)	-0.06 ± 0.45 Z=-0.47 (0.63)	0.00 ± 0.39 Z=-1.70 (0.08)	0.06± 0.34 Z=-1.4 (0.15)
A	72	28.46 ± 9.55	-1.52 ± 1.55; -1.06 (2.25)	-1.90± 0.62; -1.90 (0.69)	-1.85 ± 0.56; -1.85 (0.69)	-1.84 ± 1.62; -1.90 (0.74)	0.04 ± 0.23 Z =-1.93 (0.05)	0.01 ± 0.38 Z =-0.89 (0.37)	-0.06 ± 0.50 Z =-0.38 (0.70)

The scatter plots compare OFA-derived spherical equivalent refraction at baseline (T0) and after 10 minutes of near viewing (T10) for each participant. In both children (Figure 4. 14 a) and adults (Figure 4. 14 b), points cluster closely along the diagonal, indicating that OFA values at T10 were generally similar to those measured at T0, with no evidence of a systematic shift following the near task. A strong positive correlation was observed between T0 and T10 values in both groups (children: $r = 0.802$, $p < 0.001$; adults: $r = 0.908$, $p < 0.001$). These plots support the statistical findings by illustrating the within-subject stability of OFA between T0 and T10.

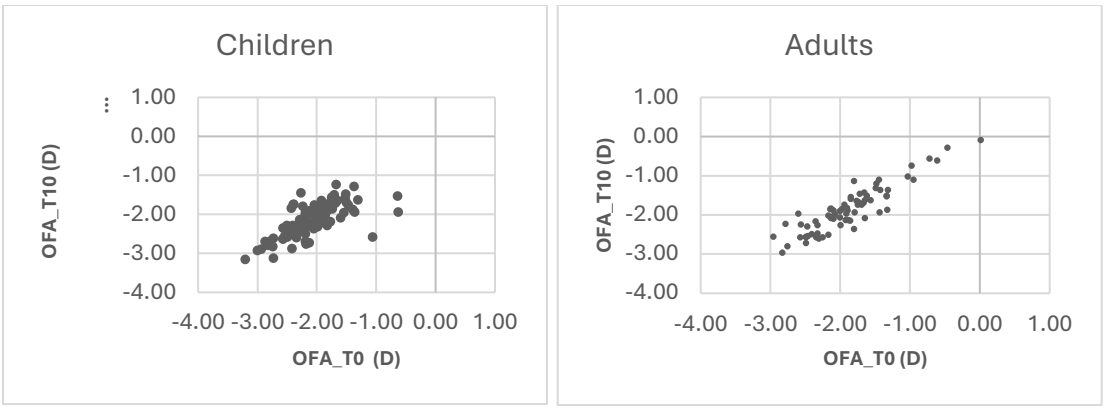

a) *b)*

Figure 4. 14 Scatter plot of OFA-derived spherical equivalent refraction (D) at baseline (T0) versus after 10 minutes of near viewing (T10) in (a) children and (b) adults, illustrating the stability of OFA following the near task.

Axial Length

Axial length (AL) was measured immediately before (T0) and after (T10) the near task in children (n = 85) and adults (n = 74). In children, mean AL values were 23.42 ± 0.89 mm at T0 and 23.41 ± 0.89 mm at T10, with no significant difference between time points (ΔAL_0–10 = −0.01 ± 0.06 mm, p = 0.16). Similarly, in adults, AL remained stable following the near task (T0: 24.41 ± 1.08 mm, T10: 24.40 ± 1.07 mm), with no significant change observed (ΔAL_0–10 = 0.01 ± 0.26 mm; p = 0.79) Table 4. 21.

In children, a strong positive correlation was found between AL at T0 and T10 (Spearman = 0.995, $p < 0.001$). In adults, AL showed a significant negative correlation with refractive error, with longer axial lengths associated with more myopic refraction (Spearman = −0.65, $p < 0.001$). Scatter plots Figure 4. 15 illustrates the relationship between refractive error and AL at T0 and T10 in both a) children and b) adults.

Pre–post differences were tested using the Wilcoxon signed-rank test (Z statistic) due to non-normal distribution of the paired differences in both children and adults.

Table 4. 21 Axial length measured before (T0) and after (T10) a 10-minute near task in children and adults.

Group	**N**	Age Mean ± SD (years)	Subjective Refraction Mean ± SD; Median (IQ Range) (D)	AL_T0 Mean ± SD; Median (IQ Range) mm)	AL_T10 Mean ± SD; Median (IQ Range) (mm)	**ΔAL_0–10 Mean ± SD t-test/z (p-value)**
C	85	13.60 ± 3.61	-0.24 ± 1.22; 0.00 (0.63)	23.42 ± 0.89; 23.36 (1.11)	23.41 ±0.89; 23.36 (1.08)	-0.01 ± 0.06 Z=-1.3 (0.16)
A	74	29.76 ± 10.20	-1.45 ± 1.56; -1.00 (2.25)	24.41 ± 1.08; 24-23 (1.13)	24.40 ± 1.07; 24.23 (1.12)	0.01 ± 0.26 Z =-0.25 (0.79)

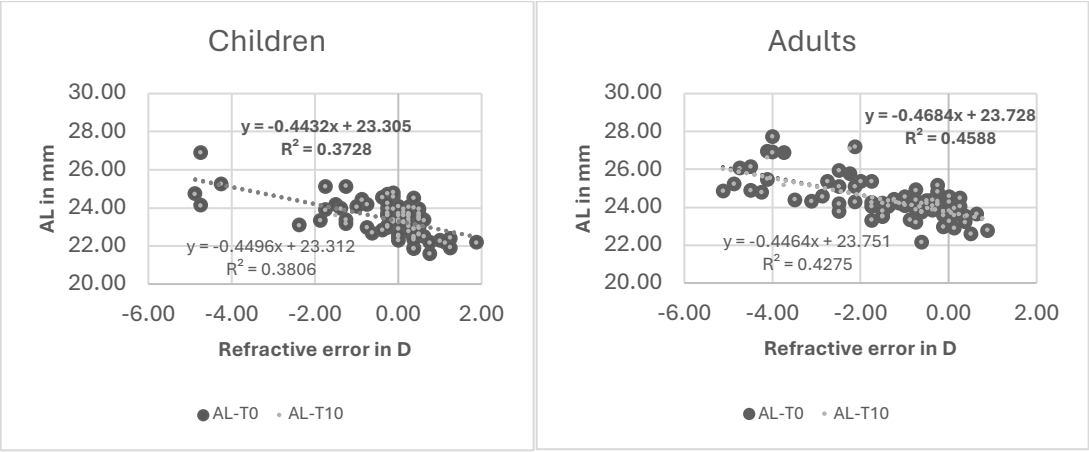

a) *b)*

Figure 4. 15 Relationship between Subjective refraction and axial length at baseline (T0) and after 10 minutes (T10) of near viewing in (a) children and (b) adults. Overlapping symbols indicate similar axial length values at T0 and T10

Choroidal Thickness change

Central and peripheral choroidal thickness (CT) changes following the near task were further assessed using the semi-automated ImageJ in a subsample of children (11.75 ± 3.29 years) (n = 33), and adults (26.85 ± 9.43 years) (n=33), based on vertical OCT scans. CT was evaluated across the full B-scan width, and we are reporting the CT at the thinnest choroidal location (L0), sub-foveal superior (L627) and sub-foveal inferior locations (L939), and peripheral superior (L101) and peripheral inferior regions (L1466). Baseline choroidal thickness (CT) values measured with the semi-automated ImageJ method are summarized in Table 4. 22.

In children, no significant differences were observed between pre- and post-near task measurements at any of the evaluated locations (Mean CT differences (post–pre) near task are listed in Table 4. 23. The distribution of location-specific ΔCT values in adults is illustrated in Figure 4. 16, showing greater variability at peripheral locations compared to central regions.

In adults, a similar spatial pattern was observed, however, a significant thinning was detected at the peripheral superior location (L101) following the near task (ΔCT = −10 ± 28 µm, p = 0.04), while changes at the sub-foveal superior, central (thinnest), sub-foveal inferior, and peripheral inferior locations were not statistically significant (Table 4. 24). The distribution of location-specific ΔCT values in adults is illustrated in Figure 4. 17, showing greater variability at peripheral locations compared to central regions.

However, It should be noted that if a strict Bonferroni correction were applied to account for multiple comparisons ($p < 0.01$), the peripheral superior result ($p = 0.04$) would no longer reach statistical significance.

Table 4. 22 Choroidal thickness (CT, µm) pre- and post-near task at each location (ImageJ). Values are Mean ± SD and Median.

Group	L101 Peripheral superior (Pre)	L101 (Post)	L627 Sub-foveal superior (Pre)	L627 (Post)	L0 Thinnest (Pre)	L0 (Post)	L939 Sub-foveal inferior (Pre)	L939 (Post)	L1466 Peripheral inferior (Pre)	L1466 (Post)
Children (n=33)	293.8 ± 68.8 282.5	301.4 ± 70.0 287.0	303.2 ± 63.37 301.5	309.8 ± 61.0 296.5	304.5 ± 60.0 294.5	308.8 ± 59.9 296.9	301.6 ± 60.2 298.5	305.2 ± 59.0 301.5	285.2 ± 57.2 287.0	279.5 ± 61.3 272.5
Adults (n=33)	287.8 ± 59.8 287.4	297.7 ± 58.9 287.4	290.8 ± 71.0 277.8	294.8 ± 69.5 284.9	290.1 ± 72.4 291.1	292.2 ± 72.2 287.0	287.7 ± 72.9 294.5	289.4 ± 72.3 282.6	272.0 ± 63.4 284.9	270.8 ± 68.4 275.4

Table 4. 23 Pre–post changes in choroidal thickness at central and peripheral locations in children.

Location	ΔCT (Post–Pre) Mean ± SD (µm)	t-test	p-value
L101 – Peripheral superior	−8 ± 32	−1.37	0.17
L627 – Sub-foveal superior	−7 ± 21	−1.83	0.07
L0 – Thinnest location	−4 ± 15	−1.63	0.11
L939 – Sub-foveal inferior	−4 ± 17	−1.19	0.24
L1466 – Peripheral inferior	6 ± 17	1.87	0.70

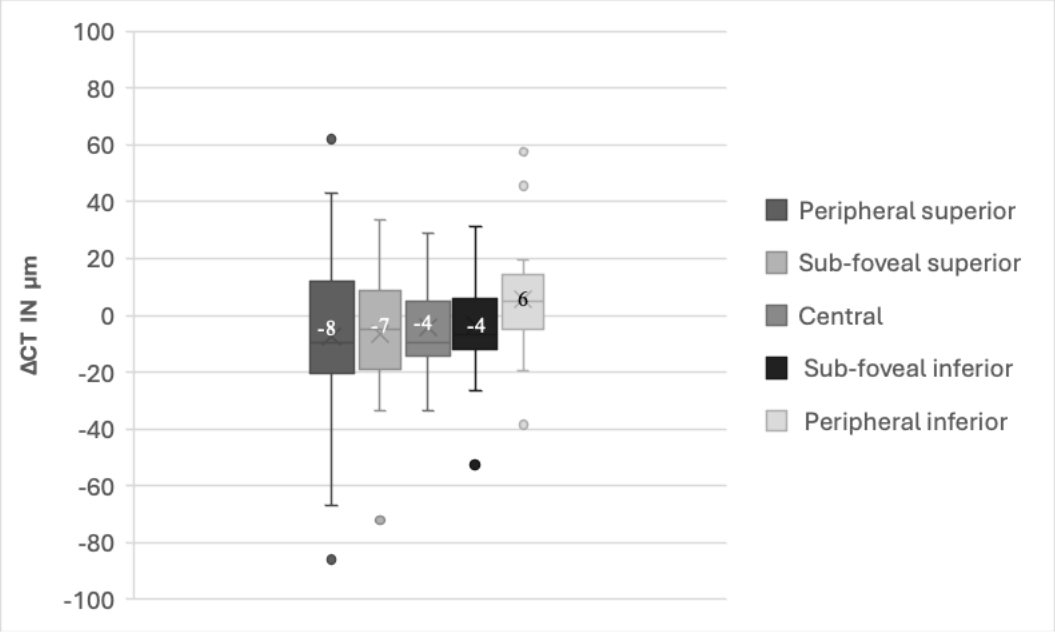

Figure 4. 16 Distribution of location-specific choroidal thickness changes (ΔCT = post–pre) following the near task in children.

Table 4. 24 Pre–post changes in choroidal thickness at central and peripheral locations in adults.

Location	ΔCT (Post–Pre) Mean ± SD (µm)	z/ t-test	p-value
L101 – Peripheral superior	−10 ± 28	−2.04	0.04
L627 – Sub-foveal superior	−4± 18	−1.25	0.22
L0 – Thinnest location	−2 ± 17	Z= −0.05	0.95
L939 – Sub-foveal inferior	−2 ± 17	Z= −0.05	0.95
L1466 – Peripheral inferior	1 ± 20	0.35	0.72

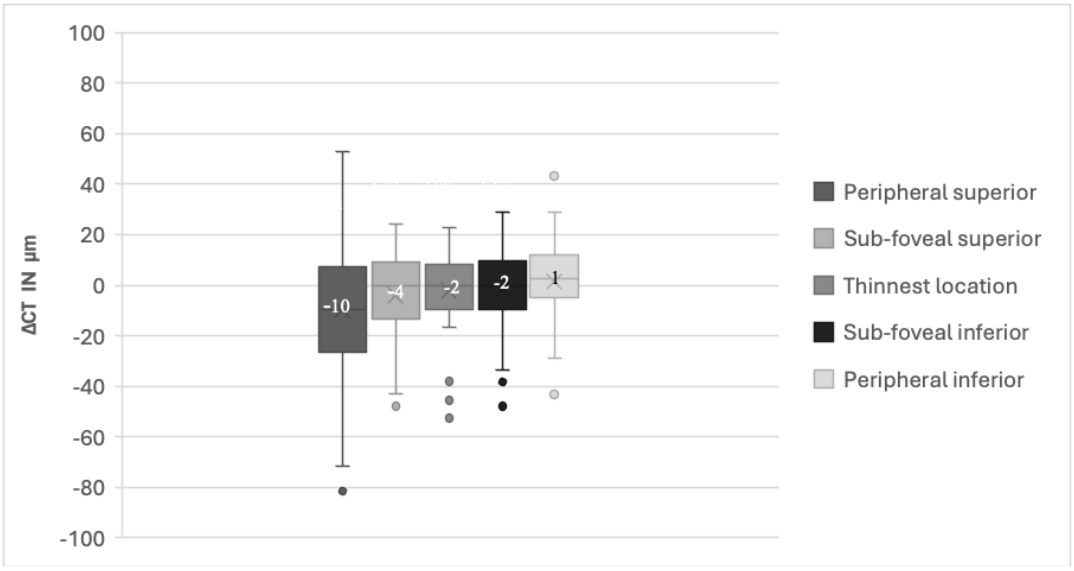

Figure 4. 17 Distribution of location-specific choroidal thickness changes (ΔCT = post–pre) following the near task in adults

The hypothesis test applied does not allow to conclude that statistically significant differences exist between pre- and post-task choroidal thickness on a point-by-point basis. Despite the absence of statistical significance, the mean pre–post difference is not uniform across retinal locations. The difference is almost consistently negative, however, some regions exhibit a relatively large mean

difference in absolute terms (also considering the typical measurement error of choroidal thickness, which is on the order of a few micrometers), whereas other regions show a relatively small mean difference, below the instrument's resolution. Across all regions, a large standard deviation of the difference values is observed, which may account for the lack of statistical evidence even in regions where the mean difference is relatively large. Therefore, an additional statistical analysis was conducted to compare the analyzed regions by directly contrasting the pre–post changes among them. The results show that the magnitude of the pre–post difference (ΔCT) varied across retinal locations.

In children (Table 4.25), pairwise comparisons of ΔCT revealed significant differences between peripheral regions, with the peripheral superior location showing a larger negative ΔCT compared to the peripheral inferior location ($p = 0.014$), as well as a significant difference between the central location and the peripheral inferior region ($p = 0.007$) and a significant difference was also found between the superior and inferior sub-foveal locations ($p = 0.023$). In contrast, no significant differences in ΔCT were found between central and parafoveal locations or between superior and inferior parafoveal regions (all $p > 0.05$).

In adults (Table 4.26) a similar spatial pattern was observed, although with fewer significant comparisons. The peripheral superior region exhibited a significantly larger negative ΔCT compared to the peripheral inferior region ($p = 0.007$), and a significant difference was also found between the superior and inferior sub-foveal locations ($p = 0.041$), Comparisons involving the central location did not reach statistical significance in adults, including central versus peripheral inferior ($p = 0.410$) and central versus sub-foveal inferior locations ($p = 0.303$).

Applying a conservative Bonferroni correction for the six pairwise comparisons ($p < 0.008$) would retain significance only for the strongest effects ($p = 0.007$), whereas the remaining borderline findings (e.g., $p = 0.014$, 0.023, and 0.041) would not meet the corrected threshold and should be interpreted cautiously.

Table 4. 25 Pairwise comparisons of location-specific choroidal thickness changes (ΔCT) following the near task in children

Comparison (ΔCT)	Mean Difference (µm)	SD (µm)	t-test	p-value
Peripheral superior (L101) − Peripheral inferior (L1466)	−13	29	−2.61	0.014
Sub-foveal superior (L627) − Sub-foveal inferior (L939)	−3	7	−2.38	0.023
Peripheral superior (L101) − Central (L0)	−3	29	−0.64	0.524
Sub-foveal superior (L627) − Central (L0)	−2	11	−1.20	0.240
Central (L0) − Sub-foveal inferior (L939)	−1	8	−0.65	0.520
Central (L0) − Peripheral inferior (L1466)	−10	20	−2.87	**0.007**

*** Bold p-values indicate statistically significant results**

Table 4. 26 Pairwise comparisons of location-specific choroidal thickness changes (ΔCT) following the near task in adults

Comparison (ΔCT)	Mean Difference (µm)	SD (µm)	t-test	p-value
Peripheral superior (L101) − Peripheral inferior (L1466)	−11	22	t = −2.87	**0.007**
Sub-foveal superior (L627) − Sub-foveal inferior (L939)	−2	6	t = −2.13	0.041
Peripheral superior (L101) − Central (L0)	−8	24	t = −1.85	0.073
Sub-foveal superior (L627) − Central (L0)	−2	7	t = −1.63	0.113
Central (L0) − Sub-foveal inferior (L939)	−1	6	Z =−1.031	0.303
Central (L0) − Peripheral inferior (L1466)	−3	23	t = −0.83	0.410

*** Bold p-values indicate statistically significant results.**

4.4.4 Cross-sectional evaluation of central and Peripheral Refraction profiles

Baseline peripheral refraction was assessed at month 0 in the right eye of children (13.41 ± 3.55 years, n = 104) and adults (31.77 ± 1.08 years, n = 97) using the WAM-5500 open-field autorefractor (OFAUTO). Peripheral refraction was measured objectively with OFAUTO at the central location (0°) and at multiple eccentricities along the superior, nasal, and temporal meridians (right eye only). To describe the participants' overall refractive status, distance subjective spherical equivalent refraction (Subjective SER) was also recorded (children: −0.34 ± 1.26 D and adults: −1.44 ± 1.62 D), these subjective values are reported only as baseline descriptors and are not used in the peripheral comparisons.

Mean OFAUTO refraction values by retinal location are summarized in (children) Table 4.27 and Table 4.28 (adults).

Table 4. 27 Baseline central and peripheral spherical equivalent refraction across retinal meridians in children.

Meridian	Location	SER (D) Mean ± SD
Superior	0°	−0.35 ± 1.20
	10°	−0.66 ± 1.20
	15°	−0.98 ± 1.16
Nasal	0°	−0.37 ± 1.20
	20°	−0.43 ± 1.21
	30°	−0.61 ± 1.17
Temporal	0°	−0.30 ± 1.18
	20°	−0.71 ± 1.11
	30°	−0.79 ± 1.22

*Central reference values correspond to the 0° measurement along each meridian.

Table 4. 28 Baseline central and peripheral spherical equivalent refraction across retinal meridians in adults

Meridian	Location	SER (D) Mean ± SD
Superior	0°	−1.21 ± 1.60
	10°	−1.45 ± 1.62
	15°	−1.70 ± 1.70
Nasal	0°	−1.28 ± 1.63
	20°	−1.35 ± 1.63
	30°	−1.49 ± 1.57
Temporal	0°	−1.15 ± 1.60
	20°	−1.50 ± 1.43
	30°	−1.67 ± 1.41

*Central reference values correspond to the 0° measurement along each meridian.

In children, direction-specific paired comparisons revealed significant myopic shifts relative to the corresponding 0° reference in the superior meridian at both 10° and 15°, in the nasal meridian at 30°, and in the temporal meridian at 20° and 30°. No significant difference was observed at 20° in the nasal meridian.

In adults, significant peripheral–central differences were detected in the superior meridian at 10° and 15°, in the nasal meridian at 30°, and in the temporal meridian at both 20° and 30°, while some inter-eccentricity comparisons did not reach statistical significance.

Mean differences, Z statistics, and p-values for all tested comparisons are reported in Table 4.29 for children and Table 4.30 adults.

To account for multiple paired comparisons within each meridian, Bonferroni correction was applied separately for the superior, nasal, and temporal meridians, resulting in an adjusted significance threshold of $p < 0.017$.

Table 4. 29 Direction-specific peripheral–central differences in spherical equivalent refraction in children.

Meridian	Comparison	Mean Difference ± SD (D)	Z	p-value
Superior	10° − 0°	−0.31 ± 0.31	−7.66	**<0.001**
	15° − 0°	−0.64 ± 0.45	−8.43	**<0.001**
	15° − 10°	−0.32 ± 0.29	−7.84	**<0.001**
Nasal	20° − 0°	−0.06 ± 0.69	−1.15	0.24
	30° − 0°	−0.24 ± 0.77	−3.60	**<0.001**
	30° − 20°	−0.18 ± 0.49	−3.59	**<0.001**
Temporal	20° − 0°	−0.41 ± 0.68	−5.61	**<0.001**
	30° − 0°	−0.48 ± 1.05	−4.39	**<0.001**
	30° − 20°	−0.08 ± 0.57	−1.69	0.09

*** Bold p-values indicate statistically significant results**

Table 4. 30. Direction-specific peripheral–central differences in spherical equivalent refraction in adults.

Meridian	Comparison	Mean Difference ± SD (D)	Z	p-value
Superior	10° − 0°	−0.24 ± 0.37	−5.71	**<0.001**
	15° − 0°	−0.49 ± 0.59	−6.56	**<0.001**
	15° − 10°	−0.25 ± 0.33	−6.22	**<0.001**
Nasal	20° − 0°	−0.07 ± 0.84	−1.70	0.08
	30° − 0°	−0.20 ± 0.96	−2.73	**0.006**
	30° − 20°	−0.13 ± 0.54	−2.19	0.03
Temporal	20° − 0°	−0.35 ± 0.69	−4.58	**<0.001**
	30° − 0°	−0.48 ± 1.05	−3.74	**<0.001**
	30° − 20°	−0.17 ± 0.63	−2.27	0.02

*** Bold p-values indicate statistically significant results**

Individual paired measurements are shown in Figure 4. 18 for children and in Figure 4. 19 for adults to illustrate how objective refraction varies between the central (0°) and most peripheral locations. In these plots, the x-axis shows subjective spherical equivalent refraction (subjective SER) to indicate each participant's clinical refractive status, while the y-axis shows spherical equivalent refraction measured objectively with OFAUTO at 0° (central) and at the corresponding peripheral location (15° superior, 30° nasal, or 30° temporal). Subjective SER is included only as a reference for refractive status; the peripheral comparisons are based on OFAUTO measurements.

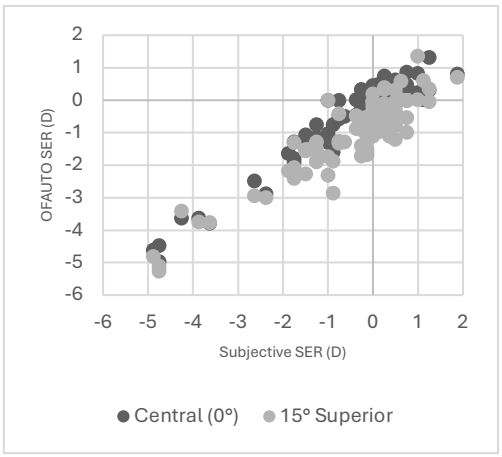

a)

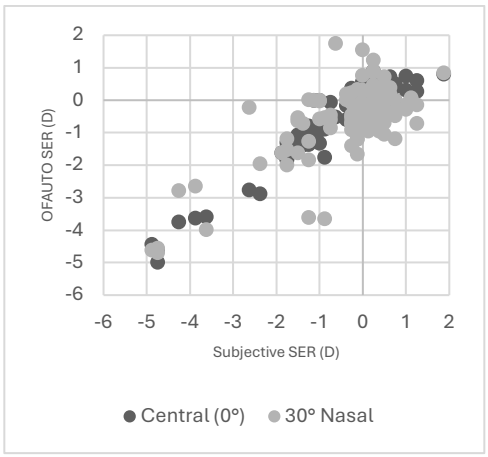

b)

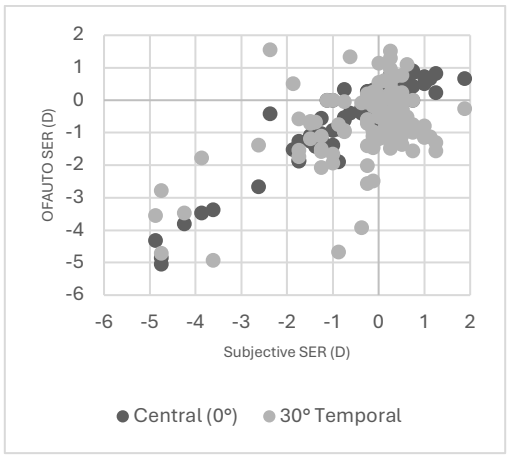

c)

Figure 4. 18 Individual peripheral–central comparisons of spherical equivalent refraction in children.

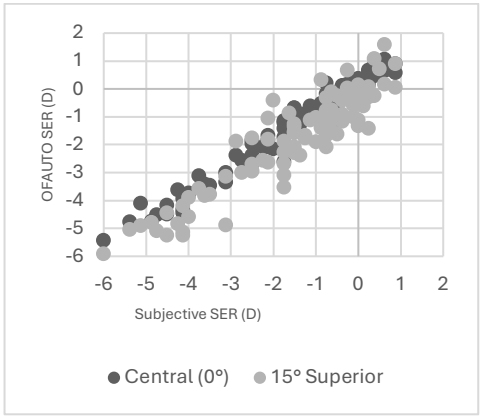

a)

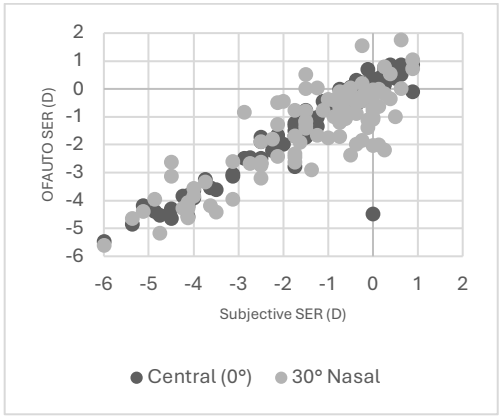

b)

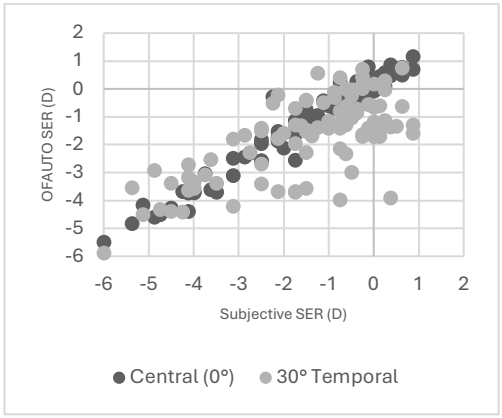

c)

Figure 4. 19 Individual peripheral–central comparisons of spherical equivalent refraction in adults.

4.5 Discussion

This chapter studies ocular parameters associated with myopia development and progression, with a focus on structural, refractive, and functional markers measured in children and adults. The analyses examined age-related patterns, longitudinal changes, and responses to near work to characterize factors linked to myopia risk and progression within the cohort. This was done by integrating refractive outcomes, axial length and choroidal thickness measurements, peripheral profiles, and near-task responses. It is important to understand the ocular parameters that are associated with myopia development and progression, as myopia prevalence continues to increase globally and is linked to a higher risk of sight-threatening complications later in life [42]. Longitudinal and age-related evaluations of these ocular parameter's changes provide insight into early markers of myopia risk beyond refractive status alone, this will help supporting earlier detection and more effective monitoring of individuals at risk of myopia [43], [44]. Investigating these factors across different stages contributes to a more comprehensive understanding of myopia as a dynamic and multifactorial process.

4.5.1 Method validation and measurement implications

Axial length measurement methods

Myah and REVO-OCT produced very similar axial length measurements across participants. There was a small systematic difference between the two devices, but it was minor (0.02 ± 0.05 mm) and unlikely to be clinically relevant.

These findings support the use of Myah as a reliable tool for longitudinal monitoring of axial length. This is also in line with previous studies showing that OCT-based biometry agrees with established axial length techniques (e.g. partial coherence interferometry or conventional optical biometry), with very small bias and narrow limits of agreement [45], [46], [47]. Although OCT systems offer advantages in imaging quality, the agreement observed in the results indicates that devices such as Myah remain well suited for clinical axial length change monitoring over time in myopia progression follow-up.

Choroidal thickness (CT) measurement methods

Choroidal thickness is usually measured using manual segmentation by drawing a line from the lower border of the retinal pigment epithelium (Bruch's membrane) to the choroid-scleral interface [24], [48]. The manual, single-point CT measurement is practical in clinic and research, but it can miss what is happening in other points in the choroid. For example, if the choroid has thickening or thinning in certain points or if the choroid-sclera interface is irregular, one measurement point may not reflect the thickness across the rest of the B-scan [49]. This is important when the question is not only central or sub-foveal CT, but how it varies across different regions, where the spatial pattern may change even if the overall mean change is small [50], [51]. Using the manual method in such cases can be a time-consuming process requires drawing multiple lines to measure thickness at different eccentricities from the foveal area to the periphery, relying on the operator's accuracy [49].

Studies show that the CT is typically thicker in the macular and supratemporal region and thinner inferior to the optic disc [51], [52], so one measurement location may not represent the rest of the scan. Also age-related differences can be region specific, Liu et al [51] showed that macular region may show a steeper age-related decline. Yet many studies still report CT at limited locations (often central or sub-foveal), which is sensitive for detecting a signal but can underestimate location-dependent effects[6], [53], [54]. Moreover, many of the existing semi-automated methods for measuring choroidal thickness are built around custom scripts (often MATLAB or similar) and several processing steps[15], [49], [55]. In practice, this makes these methods harder to implement outside the original lab and can limit repeatability when the workflow depends on specific code, settings, or technical expertise.

To address these challenges, a semi-automatic method was developed using external software (ImageJ). By uploading OCT images to ImageJ and fitting the retinal depression, Bruch's membrane, and choroid-scleral boundary, the coordinates were extracted between these three lines and calculate CT across the entire image (1566 pixels, or 15 millimeters), as described in the methods section. This method is teachable, time efficient and transparent, and it also addresses a common practical issue, the built-in OCT software does not provide automated choroid

segmentation in most devices [13], [14]. In the validation, ImageJ derived CT showed good agreement with manual REVO measurements (no significant systematic difference and strong correlations), mean differences around −1.6 µm pre-task and +4.4 µm post-task, $r \geq 0.96$) with low CV for both methods (0.06 and 0.07) (in both cases the p-value was not significant), based on this validation, the ImageJ based method was considered reliable and was used for choroidal thickness measurements in this study.

4.5.2 Interpretation of biometric progression and clinical relevance

Over the 18-month follow-up, both axial length (AL) and spherical equivalent refraction (SER) showed an age-related progression. Children had the most consistent change, with significant axial elongation accompanied by a tendency toward a more myopic refractive shift, whereas young adults and adults showed a more stable profile with only small or non-significant change over time. To place these longitudinal changes in a clinically meaningful context, we categorized the shift in axial length percentiles to help interpret the risk of myopia progression, based on the work established by Tideman et al. (2018) [4] and McCullough et al. (2020) [5] using a European children and adult cohorts. These studies introduced the idea that upward shifts in axial-length percentiles can serve as indicators of increased myopia risk. By applying a similar percentile-based approach in the present study, the analysis aimed to identify which children remained within expected growth lines and which showed shifts that might indicate a higher risk of developing myopia.

Other studies which developed a similar axial-length growth curves expressed as percentiles and Z-scores, emphasized that children in higher axial-length percentiles can show different growth dynamics over time [17], [56]. These studies concluded that axial-length percentiles provide a normative reference outline against which individual eye growth can be evaluated over time. Rather than focusing only on absolute or mean axial-length change, percentile-based tracking allows clinicians and researchers to assess whether a child is maintaining an expected growth trajectory or deviating toward higher percentiles associated with faster axial elongation. Several authors [18], [57], [58] further emphasized that changes in percentile position, or upward shifts across percentiles, may better reflect atypical growth dynamics and increased risk of myopia

development than raw axial-length change alone, supporting the clinical relevance of longitudinal percentile monitoring.

At the group level the percentile trajectories were generally stable, suggesting that much of the observed elongation in children revealed the expected growth, however, analyzing percentile shift and using the 0–18-month window as an example, the children group showed a high upward percentile shift, and this was slightly more frequent in males (20.8%) than females (15.8%) in the right eye, and 25% for males compared to 10.5% for females in the left eye. This finding may point to a sex-related difference in axial growth trajectories within our cohort, but it should be interpreted cautiously given the relatively short follow-up period and subgroup sizes.

Nevertheless, upward percentile shift is clinically relevant because it detects deviation from an expected growth track rather than absolute elongation alone. A high upward percentile shift was defined in this study as the increase of more than 10 axial-length percentiles, this criterion was adopted from the definition of accelerated growth used by Tideman et al. (2018) [4]. From a clinical perspective, these results highlight the value of using percentile tracking alongside absolute AL change to identify children who deviate from expected growth trajectories and may benefit from closer monitoring and intervention.

Moreover, longitudinal analyses in the children's populations have also found an association between axial elongation and refractive error (SER) progression, which supports the structural basis of myopia development. Studies show that greater increases in axial length over time are accompanied by more pronounced myopic shifts in spherical equivalent refraction, although the strength of this relationship was often found to be moderate rather than strong [4], [5], [57], [59]. This moderate association reflects that the nature of refractive development in childhood is depending on multiple factors, including changes in corneal curvature and crystalline lens power which partially may compensate for axial elongation, particularly during early or transitional stages of myopia [60], [61]. In line with these reports, the present data also showed a moderate negative association between axial elongation and refractive change over 18 months in children, reaching significance in the right eye (Spearman= -0.33, $p = 0.008$) and showing a similar but borderline trend in the left eye (Spearman= -0.24, $p = 0.051$). This supports the understanding that axial elongation is a major driver of refractive progression during childhood, while also

highlighting that refractive change alone does not fully reflect underlying structural growth. Overall, these findings reinforce the clinical value of combining refractive outcomes with axial length–based measurements when monitoring myopia progression.

4.5.3 Interpretation of short-term near-work effects

Refractive error (SER) and Axial length (AL)

In the present study, short-term near work did not induce significant short-term changes in either spherical equivalent refraction or axial length. SER remained stable during the 10-minute near task, with no significant differences over time at T0, T5, and T10, in either children or adults. Similarly, axial length showed no significant pre (T0) to post (T10) near-task change in either age group.

Several experimental studies found that near work can be associated with small, temporary changes in axial length, however these effects are most detected when measurements are taken during near work or after longer near tasks than the one used in this study. Studies that used prolonged near tasks of approximately 30 minutes have reported measurable axial elongation immediately after or during near viewing [6], [20], [21], even though the observed variations were often numerically very close to the resolution limit of the instrument used to measure them. They suggest that axial length can respond to accommodative demand, however, the magnitude of change is small and may partially recover over time, which indicates that the detection is highly dependent on task duration and measurement timing.

Based on our data, a 10-minute near task did not result in significant changes in both parameters, possibly because a relatively short near work exposure is less likely to produce detectable changes. Similar results have been reported in studies highlighting that accommodation related axial elongation may be transient and most evident during active accommodation rather than after task completion [19], [22]. However, refractive progression and long-term axial elongation are gradual processes best captured by longitudinal follow-up rather than brief acute exposures [5], [62] . Therefore, the absence of a sustained pre–post change in the present study does not exclude the possibility that near work contributes to long-term growth through cumulative effects. Assessing

whether larger transient axial-length responses predict later progression would require repeated measures and longer follow-up.

Choroidal Thickness

The choroidal thickness (CT) profiles were extracted at before (pre) and immediately after the near task (post). Overall, the pre–post measurements were very similar in both groups, showing no consistent change in CT across the scan. The only exception was a single localized site in adults, where CT showed a small but significant thinning in the superior peripheral region, all other locations were non-significant, and children showed no significant change at any sampled location. However, when looking at the magnitude of change (ΔCT) across the different locations, changes were not evenly distributed across locations. In both children and adults, ΔCT was not the same across the scan, the superior regions tended to show a more negative (thinning) ΔCT than the inferior regions. This might indicate that the near task response can depend on the location even when absolute pre–post CT differences at individual points are small or non-significant.

Other studies showed that near work and accommodation effects on choroidal thickness are usually small and not always the same across the posterior pole [6], [23], [63], which helps put the present peripheral CT findings into context. Short tasks can produce only small changes, and a 10-minute task may be less than the time needed to cause a clear global shift in CT [54]. Also, brief accommodative tasks have been reported to show detectable choroidal thinning mainly under specific viewing conditions (e.g. downward gaze) rather than a consistent whole scan change [64], whereas stronger accommodative demand makes thinning easier to detect and may be more evident in myopes[65].

Our results can also mean that the absence of central or sub-foveal change does not necessarily mean that there is no response, because accommodation-related thinning can vary depending on the choroid location, studies found regional differences across the posterior pole and measurable changes occurring at both central and peripheral locations [23], [66]. Longer duration near-work studies also suggest that the choroidal response can increase with exposure duration, and that longer near-work periods may make small changes easier to detect compared with short tasks. For

example, Liu et.al 2024 reported a significant reduction in sub-foveal CT by -5 ± 7 µm after 20 minutes of near work, indicating that duration and participant characteristics can influence whether a measurable effect is observed [67].

These results suggest that where CT is measured matters, even when there was no clear overall pre–post shift, the pattern of change varied by location, with the superior regions tending to show a more negative ΔCT than inferior regions. This supports the idea that short near tasks may produce subtle, non-uniform responses that can be missed by a single central measure. It is also likely that a longer exposure duration or stronger accommodative demand would make choroidal change easier to detect than the 10-minute task used here.

4.5.4 Baseline peripheral refraction profiles in children and adults (cross-sectional)

In the present study, baseline peripheral refraction was measured under non-cycloplegic conditions and showed a consistent pattern of relative peripheral myopia shift compared with the central (0°) reference in both children and adults, the magnitude of the shift varied by meridian and eccentricity. Children on average were emmetropic to mildly myopic centrally (OFAUTO = -0.3 to -0.4 D) and they demonstrated increasingly myopic peripheral refraction at superior and temporal eccentricities, whereas nasal differences were more evident at larger angles. Adults had a more myopic central profile (OFAUTO = -1.1 to -1.3 D), showed a similar pattern with stronger peripheral myopia shift superiorly and temporally.

These findings differ from many cross-sectional reports in which myopic eyes showed relative peripheral hyperopia, particularly along the horizontal meridian. This pattern is usually discussed in relation to the peripheral defocus hypothesis [26], [27], [68]. At the same time, other studies report that peripheral refraction is not uniform across meridians, and that vertical field behavior can differ from the horizontal one [29], [43]. Peripheral refraction also varies with refractive status and retinal sector [36] and may differ depending on the instrument used for peripheral assessment [8], [9].

Moreover, several studies that reported peripheral hyperopia measured refraction under cycloplegia [8], [27], [43], [69], which reduces direct comparability with non-cycloplegic refraction results. Under non-cycloplegic conditions accommodation may contribute to peripheral refraction measurement especially in younger subjects, this could lead to peripheral myopic shifts. In addition, the relatively low to moderate average central myopia in the study cohort (despite a small number of higher myopes) may partly explain why hyperopic periphery patterns are often seen in more highly myopic subjects. Non-cycloplegic studies suggest that peripheral refraction is direction-dependent [9], [30], [70], [71], [72], for example, Yelagondula et al. (2022) reported that myopes showed relative peripheral hyperopia temporally but relative peripheral myopia nasally at 30° along the horizontal field, while the vertical meridian tended toward relative peripheral myopia [28]. This asymmetry (horizontal vs vertical field behaving differently) has also been emphasized in foundational peripheral-optics work [37].This supports the idea that the sign and magnitude of peripheral–central differences can change depending on measurement conditions.

These findings suggest that peripheral refraction patterns may differ under habitual viewing conditions. Further work directly comparing cycloplegic and non-cycloplegic peripheral profiles across meridians would help clarify how measurement conditions influence interpretations of peripheral defocus in relation to myopia development and management.

4.5.5 limitations

Some limitations should be noted in this study. Although choroidal thickness extraction using the ImageJ-based method is semi-automatic, it still relies on manual identification of choroidal boundaries. As a result, accuracy depends on image quality and on how clearly the choroid–sclera interface can be visualized. In addition, the circular fitting model used in the current approach may not suit all choroidal profiles, in relatively flat or irregular scans, the fit may be less accurate, leading to fitting errors or exclusion of some images.

Another limitation relates to the near-task protocol, the task duration was limited to 10 minutes, mainly to maintain cooperation and reduce movement, especially in children. However, this short exposure may not have been sufficient to reveal larger or more consistent short-term changes,

particularly in axial length and choroidal thickness. Longer task durations may provide a clearer picture of the effects of sustained near work on ocular structure.

Finally, near-work responses can be small and transient, and axial length was assessed using a pre–post design, which may miss brief reversible changes occurring during active near viewing. These factors should be considered when interpreting the absence of significant acute effects in the present study.

4.6 Conclusions

This chapter includes device validation with longitudinal follow-up and baseline profiling of myopia-related parameters in children and adults. Children showed the most progression over 18 months, while adults were comparatively stable. The findings support the clinical value of axial length not merely as an absolute measurement, but when interpreted using axial-length percentiles, which provide a clearer method to track growth trajectories over time and help identify children who deviate from expected patterns. In this context, refractive change alone did not fully reflect underlying ocular growth.

Cross-sectional data at the baseline also highlighted that ocular responses are not uniform across the eye, choroidal thickness changes were location-dependent, with peripheral regions showing patterns that may differ from central measurements. Also, peripheral refraction showed direction-dependent differences from central refraction under non-cycloplegic (habitual) viewing conditions.

Finally, the near-work experiment suggests that acute effects on SER and axial length may be subtle and are not always detectable following short near-viewing periods with pre–post measurement timing, this highlights the importance of longer observation windows for capturing clinically meaningful change.

These results emphasize the need to monitor myopia progression using structural markers, particularly axial length interpreted through percentile tracking, while recognizing that both CT and refraction peripheral measures can vary by location and measurement conditions and may require a more targeted assessment in clinically representative settings.

Moreover, the results highlight that interpreting myopia-related parameters requires attention not only to biology but also to the optical measurement chain, device and protocol choice, alignment/fixation, and analysis method, which determines the practical resolution and repeatability of axial length, choroidal thickness, and peripheral refraction estimates.

4.7 References

[1] Gifford KL, et al. IMI – Clinical management guidelines report. Invest Ophthalmol Vis Sci. 2019;60(3):M184–M203. https://doi.org/10.1167/iovs.18-25977.

[2] Flitcroft DI, et al. IMI – Defining and classifying myopia: a proposed set of standards for clinical and epidemiologic studies. Invest Ophthalmol Vis Sci. 2019;60(3):M20–M30. https://doi.org/10.1167/iovs.18-25957.

[3] Wolffsohn JS, et al. IMI – Clinical myopia control trials and instrumentation report. Invest Ophthalmol Vis Sci. 2019;60(3):M132–M160. https://doi.org/10.1167/iovs.18-25955.

[4] Tideman JWL, et al. Axial length growth and the risk of developing myopia in European children. Acta Ophthalmol. 2018;96(3):301–309. https://doi.org/10.1111/aos.13603.

[5] McCullough S, Adamson G, Breslin KMM, McClelland JF, Doyle L, Saunders KJ. Axial growth and refractive change in white European children and young adults: predictive factors for myopia. Sci Rep. 2020;10(1). https://doi.org/10.1038/s41598-020-72240-y.

[6] Woodman EC, Read SA, Collins MJ. Axial length and choroidal thickness changes accompanying prolonged accommodation in myopes and emmetropes. Vision Res. 2012;72:34–41. https://doi.org/10.1016/j.visres.2012.09.009.

[7] Hughes RPJ, Read SA, Collins MJ, Vincent SJ. Axial elongation during short-term accommodation in myopic and nonmyopic children. Invest Ophthalmol Vis Sci. 2022;63(3):12. https://doi.org/10.1167/iovs.63.3.12.

[8] Fedtke C, Ehrmann K, Holden BA. A review of peripheral refraction techniques. Optom Vis Sci. 2009;86(5):429–446. https://doi.org/10.1097/OPX.0b013e31819fa727.

[9] Demir P, Macedo AF, Chakraborty R, Baskaran K. Comparison of an open view autorefractor with an open view aberrometer in determining peripheral refraction in children. J Optom. 2023;16(1):20–29. https://doi.org/10.1016/j.optom.2021.12.002.

[10] Hamzah F, Shinojima A, Mori R, Yuzawa M. Choroidal thickness measurement by enhanced depth imaging and swept-source optical coherence tomography in central serous chorioretinopathy. BMC Ophthalmol. 2014;14:145. https://doi.org/10.1186/1471-2415-14-145.

[11] Yamashita T, Yamashita T, Shirasawa M, Arimura N, Terasaki H, Sakamoto T. Repeatability and reproducibility of subfoveal choroidal thickness in normal eyes of Japanese using different SD-OCT devices. Invest Ophthalmol Vis Sci. 2012;53(3):1102–1107. https://doi.org/10.1167/iovs.11-8836.

[12] Branchini L, Regatieri CV, Flores-Moreno I, Baumann B, Fujimoto JG, Duker JS. Reproducibility of choroidal thickness measurements across three spectral domain optical coherence tomography systems. Ophthalmology. 2012;119(1):119–123. https://doi.org/10.1016/j.ophtha.2011.07.002.

[13] Mazzaferri J, Beaton L, Hounye G, Sayah DN, Costantino S. Open-source algorithm for automatic choroid segmentation of OCT volume reconstructions. Sci Rep. 2017;7:42112. https://doi.org/10.1038/srep42112.

[14] Eghtedar RA, Esmaeili M, Pey-Man A, Akhlaghi M, Rasta SH. An update on choroidal layer segmentation methods in optical coherence tomography images: a review. J Biomed Phys Eng. 2022;12(1):1–20. https://doi.org/10.31661/jbpe.v0i0.1234.

[15] Kugelman J, et al. Automatic choroidal segmentation in OCT images using supervised deep learning methods. Sci Rep. 2019;9(1). https://doi.org/10.1038/s41598-019-49816-4.

[16] Cheung SW, Cho P. Validity of axial length measurements for monitoring myopic progression in orthokeratology. Invest Ophthalmol Vis Sci. 2013;54(3):1613–1615. https://doi.org/10.1167/iovs.12-10434.

[17] Sanz Diez P, Yang LH, Lu MX, Kiess W, Wahl S. LMS parameters, percentile, and Z-score growth curves for axial length in Chinese schoolchildren in Wuhan. Sci Rep. 2022;12(1). https://doi.org/10.1038/s41598-022-08907-5.

[18] Gopalakrishnan A, et al. Ocular biometry percentile curves and their relation to myopia development in Indian children. J Clin Med. 2024;13(10):2867. https://doi.org/10.3390/jcm13102867.

[19] O'Donoghue L, Saunders KJ, Anderson RS. Effect of accommodation on axial length measurement in myopes and emmetropes. Invest Ophthalmol Vis Sci. 2005;46:5591. doi:10.1167/iovs.05-0123

[20] Read SA, Collins MJ, Woodman EC, Cheong S-H. Axial length changes during accommodation in myopes and emmetropes. Optom Vis Sci. 2010;87(9):656–662. https://doi.org/10.1097/OPX.0b013e3181e87dd3.

[21] Woodman EC, et al. Axial elongation following prolonged near work in myopes and emmetropes. Br J Ophthalmol. 2011;95(5):652–656. https://doi.org/10.1136/bjo.2010.180323.

[22] Laughton DS, Sheppard AL, Mallen EAH, Read SA, Davies LN. Does transient increase in axial length during accommodation attenuate with age? Clin Exp Optom. 2017;100(6):676–682. https://doi.org/10.1111/cxo.12533.

[23] Woodman-Pieterse EC, Read SA, Collins MJ, Alonso-Caneiro D. Regional changes in choroidal thickness associated with accommodation. Invest Ophthalmol Vis Sci. 2015;56(11):6414–6422. https://doi.org/10.1167/iovs.15-17102.

[24] Hirata M, et al. Macular choroidal thickness and volume in normal subjects measured by swept-source optical coherence tomography. Invest Ophthalmol Vis Sci. 2011;52(8):4971–4978. https://doi.org/10.1167/iovs.11-7729.

[25] Erdinest N, et al. Peripheral defocus and myopia management: a mini-review. Korean J Ophthalmol. 2023;37(1):70–81. https://doi.org/10.3341/kjo.2022.0125.

[26] Mutti DO, et al. Refractive error, axial length, and relative peripheral refractive error before and after the onset of myopia. Invest Ophthalmol Vis Sci. 2007;48(6):2510–2519. https://doi.org/10.1167/iovs.06-0562.

[27] Charman WN, Radhakrishnan H. Peripheral refraction and the development of refractive error: a review. Ophthalmic Physiol Opt. 2010;30(4):321–338. https://doi.org/10.1111/j.1475-1313.2010.00746.x.

[28] Yelagondula VK, Achanta DSR, Panigrahi S, Panthadi SK, Verkicharla PK. Asymmetric peripheral refraction profile in myopes along the horizontal meridian. Optom Vis Sci. 2022;99(4). doi:10.1097/OPX.0000000000001931

[29] Antony M, Maldoddi R, Atchison DA, Verkicharla PK. Diversity of peripheral refraction patterns—have these been oversimplified? Invest Ophthalmol Vis Sci. 2025;66(3):58. https://doi.org/10.1167/iovs.66.3.58.

[30] Xi X, et al. Two-dimensional peripheral refraction in adults. Biomed Opt Express. 2023;14(5):2375. https://doi.org/10.1364/BOE.488098.

[31] Lin Z, Lan W, Yang Z, Artal P. A review of peripheral refraction in myopia research. J Bio-optics. 2025;1(1):3. https://doi.org/10.53941/jbiop.2025.100003.

[32] Davies LN, Mallen EAH. Influence of accommodation and refractive status on the peripheral refractive profile. Br J Ophthalmol. 2009;93(9):1186. https://doi.org/10.1136/bjo.2009.159053.

[33] Mathur A, Atchison DA, Charman WN. Effect of accommodation on peripheral ocular aberrations. J Vis. 2009;9(12):20. https://doi.org/10.1167/9.12.20.

[34] Liu T, Sreenivasan V, Thibos LN. Uniformity of accommodation across the visual field. J Vis. 2016;16(3):6. https://doi.org/10.1167/16.3.6.

[35] Queirós A, Jorge J, González-Méijome JM. Influence of fogging lenses and cycloplegia on peripheral refraction. J Optom. 2009;2(2):83–89. https://doi.org/10.3921/joptom.2009.83.

[36] Lu W, et al. Agreement and repeatability of central and peripheral refraction by one novel multispectral-based refractor. Front Med (Lausanne). 2021;8. https://doi.org/10.3389/fmed.2021.777685.

[37] Atchison DA, Pritchard N, Schmid KL. Peripheral refraction along the horizontal and vertical visual fields in myopia. Vision Res. 2006;46(8–9):1450–1458. https://doi.org/10.1016/j.visres.2005.10.023.

[38] Wolffsohn JS, et al. IMI – Clinical myopia control trials and instrumentation report. Invest Ophthalmol Vis Sci. 2019;60(3):M132–M160. https://doi.org/10.1167/iovs.18-25955.

[39] Topcon Healthcare. MYAH optical biometry and corneal topography: technical specifications. Tokyo, Japan; 2024.

[40] Optopol Technology. REVO FC OCT and fundus camera: technical specifications. Zawiercie, Poland; 2023.

[41] Schindelin J, et al. Fiji: an open-source platform for biological-image analysis. Nat Methods. 2012;9(7):676–682. https://doi.org/10.1038/nmeth.2019.

[42] Holden BA, et al. Global prevalence of myopia and high myopia and temporal trends from 2000 through 2050. Ophthalmology. 2016;123(5):1036–1042. https://doi.org/10.1016/j.ophtha.2016.01.006.

[43] Berntsen DA, Mutti DO, Zadnik K, et al. Study of theories about myopia progression (STAMP) design and baseline data. Optom Vis Sci. 2010;87(11):823–832. https://doi.org/10.1097/OPX.0b013e3181f0fc4b.

[44] Chakraborty R, Read SA, Collins MJ. Monocular myopic defocus and daily changes in axial length and choroidal thickness of human eyes. Exp Eye Res. 2012;103:47–54. https://doi.org/10.1016/j.exer.2012.08.002.

[45] Kim KY, Choi GS, Kang MS, Kim US. Comparison study of the axial length measured using the swept-source OCT ANTERION and the partial coherence interferometry IOLMaster. PLoS One. 2020;15(12). https://doi.org/10.1371/journal.pone.0244590.

[46] Rizzieri N, Facchin A. Comparison of eye axial length measurements taken using partial coherence interferometry and OCT biometry. Vision (Basel). 2024;8(3):46. https://doi.org/10.3390/vision8030046.

[47] Gambra E, Ortiz S, Perez-Merino P, Gora M, Wojtkowski M, Marcos S. Static and dynamic crystalline lens accommodation evaluated using quantitative 3-D OCT. Biomed Opt Express. 2013;4(9):1595. https://doi.org/10.1364/BOE.4.001595.

[48] Tan CSH, Cheong KX. Macular choroidal thicknesses in healthy adults—relationship with ocular and demographic factors. Invest Ophthalmol Vis Sci. 2014;55(10):6452–6458. https://doi.org/10.1167/iovs.13-13771.

[49] Cheong KX, Lim LW, Li KZ, Tan CSH. A novel and faster method of manual grading to measure choroidal thickness using optical coherence tomography. Eye (Lond). 2018;32(2):433–438. https://doi.org/10.1038/eye.2017.210.

[50] Rasheed MA, et al. Wide-field choroidal thickness profile in healthy eyes. Sci Rep. 2018;8(1). https://doi.org/10.1038/s41598-018-35640-9.

[51] Liu X, et al. New findings on choroidal features in healthy people by ultra-widefield swept-source optical coherence tomography angiography. Sci Rep. 2023;13(1). https://doi.org/10.1038/s41598-023-36374-z.

[52] Tanabe H, Ito Y, Terasaki H. Choroid is thinner in inferior region of optic discs of normal eyes. Retina. 2012;32(1):134–139. https://doi.org/10.1097/IAE.0b013e318217ff87.

[53] Wang D, et al. Optical defocus rapidly changes choroidal thickness in schoolchildren. PLoS One. 2016;11(8). https://doi.org/10.1371/journal.pone.0161535.

[54] Ostrin LA, et al. IMI—The dynamic choroid: new insights, challenges, and potential significance for human myopia. Invest Ophthalmol Vis Sci. 2023;64(6):4. https://doi.org/10.1167/iovs.64.6.4.

[55] Li M, et al. Choroid automatic segmentation and thickness quantification on swept-source OCT images of highly myopic patients. Ann Transl Med. 2022;10(11):620. https://doi.org/10.21037/atm-21-6736.

[56] He X, et al. Normative data and percentile curves for axial length and axial length/corneal curvature in Chinese children and adolescents aged 4–18 years. Br J Ophthalmol. 2023;107(2):167–175. https://doi.org/10.1136/bjophthalmol-2021-319431.

[57] Chen Y, et al. Physiological growth of ocular axial length among Chinese children and teenagers: a 6-year cohort study. PLoS One. 2025;20(1). https://doi.org/10.1371/journal.pone.0317756.

[58] Truckenbrod C, et al. Longitudinal analysis of axial length growth in a German cohort of healthy children and adolescents. Ophthalmic Physiol Opt. 2021;41:532–540. https://doi.org/10.1111/opo.12817.

[59] Jiang F, Wang D, Yin Q, He M, Li Z. Longitudinal changes in axial length and spherical equivalent in children and adolescents with high myopia. Invest Ophthalmol Vis Sci. 2023;64(12):6. https://doi.org/10.1167/iovs.64.12.6.

[60] Mutti DO, et al. Axial growth and changes in lenticular and corneal power during emmetropization in infants. Invest Ophthalmol Vis Sci. 2005;46(9):3074–3080. https://doi.org/10.1167/iovs.04-1040.

[61] Mutti DO, Sinnott LT, Zadnik K. Compensation for vitreous chamber elongation in infancy and childhood. Optom Vis Sci. 2023;100(1):43–51. https://doi.org/10.1097/OPX.0000000000001970.

[62] Mutti DO, Mitchell GL, Moeschberger ML, Jones LA, Zadnik K. Parental myopia, near work, school achievement, and children's refractive error. Invest Ophthalmol Vis Sci. 2002;43(12):3633–3640. doi:10.1167/iovs.02-0193

[63] Ostrin LA, et al. Short-term myopic defocus and choroidal thickness in children and adults. Invest Ophthalmol Vis Sci. 2024;65(4):22. https://doi.org/10.1167/iovs.65.4.22.

[64] Ghosh A, Collins MJ, Read SA, Davis BA, Chatterjee P. Axial elongation associated with biomechanical factors during near work. Optom Vis Sci. 2014;91(3):322–329. https://doi.org/10.1097/OPX.0000000000000166.

[65] Hoseini-Yazdi H, Read SA, Alonso-Caneiro D, Collins MJ. Retinal OFF-pathway overstimulation leads to greater accommodation-induced choroidal thinning. Invest Ophthalmol Vis Sci. 2021;62(13):5. https://doi.org/10.1167/iovs.62.13.5.

[66] Kaphle D, Schmid KL, Suheimat M, Read SA, Atchison DA. Central and peripheral choroidal thickness and eye length changes during accommodation. Ophthalmic Physiol Opt. 2023;43(3):311–318. https://doi.org/10.1111/opo.13084.

[67] Liu M, et al. Differences in choroidal responses to near work between myopic children and young adults. Eye Vis (Lond). 2024;11(1). https://doi.org/10.1186/s40662-024-00382-5.

[68] Mutti DO, et al. AC/A ratio, age, and refractive error in children. Invest Ophthalmol Vis Sci. 2000;41(9):2469–2478. https://doi.org/10.1167/iovs.41.9.2469

[69] Bakaraju RC, Fedtke C, Ehrmann K, Ho A. Comparing the relative peripheral refraction effect of single vision and multifocal contact lenses measured using an autorefractor and an aberrometer: a pilot study. J Optom. 2015;8(3):206–218. https://doi.org/10.1016/j.optom.2015.01.005.

[70] Backhouse S, Fox S, Ibrahim B, Phillips JR. Peripheral refraction in myopia corrected with spectacles versus contact lenses. Ophthalmic Physiol Opt. 2012;32(4):294–303. https://doi.org/10.1111/j.1475-1313.2012.00912.x.

[71] Xiaoli L, et al. Comparative study of relative peripheral refraction in children with different degrees of myopia. Front Med (Lausanne). 2022;9. https://doi.org/10.3389/fmed.2022.800653.

[72] Xie F, Mao X, Jiang M, Li J, Zhang J. Alterations in peripheral refraction are most significant just before the onset of myopia: evidence from multispectral refraction topography. Ophthalmol Ther. 2025;14(9):2125–2139. https://doi.org/10.1007/s40123-025-01198-9.

Chapter 5. General Conclusions and Future Perspectives

5.1 General Conclusions

This thesis was developed with the aim of strengthening the evaluation of myopia and myopia-related change by combining objective optical measurements with clinically meaningful interpretation of both functional and structural ocular parameters. Across the three experimental chapters, the work addressed this aim in two complementary ways: first, by validating the agreement and reliability of objective refraction methods under different measurement conditions, and second, by applying these validated approaches to the study of myopia-related risk factors across time and across retinal location.

The first main contribution of this thesis lies in the validation of open-field and closed-field objective refraction methods against subjective refraction. The results showed that objective procedures, particularly open-field aberrometry and open-field autorefractors, were strongly correlated with subjective refraction, with no evidence of proportional bias across the tested refractive range. At the same time, the findings highlighted that measurement configuration is not neutral: in younger participants, the closed-field setup tended to produce more myopic results than the open-field configuration, most likely because accommodation was more difficult to control under closed-field conditions. The absence of clinically meaningful differences between monocular and binocular measurements in the open-field devices, together with the very high repeatability observed across repeated measures, supports the clinical relevance of open-field methods as robust tools for objective refraction under non-cycloplegic conditions.

The second contribution concerns the effect of pupil size on wavefront-derived refraction and spherical aberration. The analyses performed across 3 to 6 mm showed that spherical equivalent remained stable within methods and that the agreement between methods was maintained across the tested analysis diameters. Spherical aberration, represented by the C4,0 coefficient, also remained stable across the computationally enlarged pupil sizes. Taken together, these findings suggest that, under the tested reconstruction conditions, wavefront-derived lower- and higher-order metrics are relatively stable when the analysis pupil is mathematically expanded. At the same

time, the thesis also makes clear that these results should be interpreted within the limits of the methodology used, since computational pupil enlargement does not fully reproduce the optical behavior of real physiological dilation. In this sense, Chapter 3 not only adds a methodological result, but also clarifies an important interpretive boundary for wavefront-based optical measurements.

The third contribution of the thesis is the application of these measurement approaches to the study of myopia-related ocular change. In the longitudinal analysis, axial length proved to be particularly informative, especially when interpreted through age-referenced percentiles rather than as an isolated absolute value. This approach made it possible to identify variability in pediatric growth trajectories that would be less apparent from refractive error alone. The thesis therefore supports axial-length monitoring, particularly percentile-based monitoring, as a useful way to identify children whose eye growth is deviating from expected age-related patterns. This finding reinforces the idea that myopia progression is not only a refractive phenomenon, but also a structural one, and that structural monitoring can improve risk interpretation in clinical and research settings.

The near-work and spatial analyses further showed that myopia-related ocular responses are subtle, dynamic, and location-dependent. In the short-term near-work experiment, central spherical equivalent refraction and axial length did not show significant changes after 10 minutes of near viewing, suggesting that such effects may be small, transient, or strongly dependent on protocol duration and timing of acquisition. In contrast, choroidal thickness changes were not uniform across retinal locations, and peripheral refraction showed consistent peripheral-central differences that varied with meridian and eccentricity. These results indicate that ocular responses related to myopia cannot always be interpreted adequately from a single central or peripheral value. Instead, both retinal location and measurement protocol must be considered when drawing conclusions about peripheral and biometric parameters.

Taken together, the findings of this thesis show that the study of myopia requires both reliable measurement methods and careful interpretation of what those measurements represent. Instrument design, fixation conditions, analysis aperture, and retinal location can all influence the values obtained and the meaning attributed to them. The overall message emerging from the thesis is that: open-field objective refraction provides a reliable and clinically realistic approach for the

measurement of refractive error, and the interpretation of myopia-related change is strengthened when functional measurements are integrated with structural parameters such as axial length and choroidal thickness, with axial-length percentiles offering a particularly useful framework for monitoring myopia progression in children.

5.2 Overall Limitations

These conclusions should be interpreted considering the methodological boundaries of the individual studies. Across the thesis, the work was conducted mainly in healthy eyes and selected cohorts, which may limit direct generalization to broader clinical populations. In addition, the pupil-size analysis was based on computational enlargement rather than true physiological dilation, and the near-work protocol was relatively short, which may have reduced the detectability of transient structural changes. As a results, while the findings provide a consistent methodological and clinical framework, further studies in broader populations and under more natural physiological conditions are still needed.

5.3 Future Perspectives

The results of this thesis suggest several directions for future research. One important next step would be to compare computational pupil scaling with true physiological or pharmacological pupil enlargement, to better understand how peripheral optical behavior influences wavefront-derived refraction and higher-order aberrations. Another relevant extension would be the application of open-field objective refraction methods in broader and more heterogeneous clinical populations, including children with active myopia progression, eyes with higher refractive errors, and subjects undergoing myopia-control treatment. In addition, longer and repeated near-work protocols may help clarify whether transient structural responses, particularly in axial length and choroidal thickness, can predict longer-term progression risk. Finally, the integration of optical measurements with structural monitoring, especially axial-length percentile tracking and location-specific choroidal analysis, may contribute to more sensitive and clinically useful models of myopia progression in pediatric populations.